

Binary Communication Techniques in Locked-in and Completely Locked-in Patients

Dissertation

der Mathematisch-Naturwissenschaftlichen Fakultät
der Eberhard Karls Universität Tübingen
zur Erlangung des Grades eines

Doktors der Naturwissenschaften
(Dr. rer. nat.)

vorgelegt von
Alessandro Tonin
aus Venedig / Italien

Tübingen
2022

Gedruckt mit Genehmigung der Mathematisch-Naturwissenschaftlichen Fakultät
der Eberhard Karls Universität Tübingen.

Tag der mündlichen Qualifikation: 17.01.2023
Dekan: Prof. Dr. Thilo Stehle
1. Berichterstatter: Prof. Dr. Dr. Niels Birbaumer
2. Berichterstatter: Prof. Dr. Gerard Pons-Moll
3. Berichterstatterin: Assoc. Prof. Natsue Yoshimura

Contents

LIST OF ACRONYMS AND ABBREVIATIONS	v
ABSTRACT	vii
ZUSAMMENFASSUNG	ix
LIST OF PUBLICATIONS	xi
Accepted publications	xi
Manuscripts ready for submission	xii
Personal contribution	xiii
CONTRIBUTION DECLARATION	xv
1 INTRODUCTION	1
1.1 Amyotrophic lateral sclerosis	2
1.2 Augmentative and alternative communication devices	4
1.3 Neurophysiological signals for communication	5
1.4 Communication in Locked-in syndromes	10
1.5 Communication in Complete Locked-in syndromes	12
1.6 Overview	13
2 OBJECTIVES AND EXPECTED OUTCOME	17
3 RESULTS AND DISCUSSION	19
3.1 LIS and CLIS subjects	21
3.2 Signal acquisition and signal processing	24
3.2.1 Micro-ocular movements	24
3.2.2 EEG and fNIRS: the HybridBCI	28
3.2.3 EEG and galvanic vestibular stimulation	31
3.2.4 Intracortical BCI	33
3.3 Communication techniques	36
3.3.1 Basic yes-no communication	36
3.3.2 Spelling communication system	37

3.3.3	20-questions based communication system	43
4	CONCLUSIONS	49
	BIBLIOGRAPHY	53
	APPENDIX A ACCEPTED PUBLICATIONS	61
	Paper I: Auditory Electrooculogram-based Communication System for ALS Patients in Transition from Locked-in to Complete Locked-in State	63
	Paper II: A 20-questions-based binary spelling interface for communication systems.	73
	Paper III: Spelling interface using intracortical signals in a completely locked-in patient enabled via auditory neurofeedback training	87
	Paper IV: Binary Semantic Classification Using Cortical Activation with Pavlovian-Conditioned Vestibular Responses in Healthy and Locked-In Individuals	97
	Paper V: A dataset of EEG and EOG from an auditory EOG-based communication system for patients in locked-in state	111
	Paper VI: Neurophysiological aspects of the completely locked-in syndrome in patients with advanced amyotrophic lateral sclerosis	121
	Paper VII: Electroencephalography of completely locked-in state patients with amyotrophic lateral sclerosis	135
	Paper VIII: EEG power spectral density in locked-in and completely locked-in state patients: a longitudinal study	143
	Paper IX: Open Software/Hardware Platform for Human-Computer Interface Based on Electrooculography (EOG) Signal Classification	151
	Paper X: Sleep in the completely locked-in state (CLIS) in amyotrophic lateral sclerosis	165
	APPENDIX B MANUSCRIPTS READY FOR SUBMISSION	173
	Paper XI: A General-Purpose Framework for a Hybrid EEG-NIRS-BCI	175

List of Acronyms and Abbreviations

AAC	Augmentative and Alternative Communication
ALS	Amyotrophic Lateral Sclerosis
ANN	Artificial Neural Network
BCI	Brain-Computer Interface
CFD	Conditional Frequency Distribution
CLIS	Complete Locked-In Syndrome
ECoG	Electrocorticography
EEG	Electroencephalography
EMG	Electromyography
EOG	Electrooculography
ERP	Error Related Potential
fNIRS	Functional Near-Infrared Spectroscopy
GVS	Galvanic Vestibular Stimulation
HCI	Human-Computer Interface
LIS	Locked-In Syndrome
LMN	Low Motor Neuron
MEA	Microelectrode Array
SSVEP	Steady State Visual Evoked Potential
UMN	Upper Motor Neuron

Abstract

Neurodegenerative disease, such as amyotrophic lateral sclerosis (ALS), can lead to a partial or complete paralysis of the body, and patients in these conditions are considered to be in locked-in (LIS) or complete locked-in state (CLIS). Before reaching these advanced states, patients usually communicate by moving the eyes with the help of assistive and augmentative communication devices. With the progression of the disease these devices become useless due of ocular abnormalities that prevent the correct detection of the eye movements and gaze fixation. A valuable solution for these patients is the implementation of brain-computer interfaces (BCIs) which, by decoding neural signals directly acquired from the brain activity, can be used to develop communication paradigms without the need of relying on any muscular activity.

Several preliminary neurophysiological analyses have been conducted to assess possible pathological signs in the neural activity of ALS patients in LIS and CLIS. The published results included in the dissertation indicate heterogeneous conditions that, in most cases, highlight abnormal neural signals. Nevertheless, no result indicates significant cognitive problems that might affect the BCI performance.

The development of communications techniques has been implemented in a modular way by keeping the signal acquisition and signal processing phases separate from the implementation of the communication paradigms. Several acquired signals have been used to target different patient populations: electrooculography, electroencephalography, functional near-infrared spectroscopy, and intracortical neural activity. In each study, the signal was processed differently, but patients were always asked to modulate their brain activity in only two different ways; the signal was then decoded using a binary classifier. The output of the classifier has been used to control different developed communication paradigms: from simple yes/no questions, to a full speller that allowed the patient to form words and sentences.

The results show several combinations of different signal acquisition techniques with various communication paradigms, taking advantage of the modularity of the developed systems. Most of the communication paradigms have

also been successfully deployed to LIS or CLIS patients, including two cases in which the speller system has been used by patients with no other means of communication.

Zusammenfassung

Neurodegenerative Erkrankungen wie Amyotrophe Lateralsklerose (ALS) können zu teilweiser oder völliger Lähmung des Körpers führen, Patienten in diesem Zustand können dann als eingeschlossen (LIS) oder völlig eingeschlossen (CLIS) bezeichnet werden. Bevor Menschen diese Zustände erleiden, kommunizieren sie heutzutage meist mit Augenbewegungen, mit denen sie Kommunikationshilfen bedienen. Mit dem weiteren Fortschreiten der Erkrankung werden diese Geräte üblicherweise nutzlos, da man Augenbewegungen nicht mehr registrieren kann. Dann gibt es für diese Patienten nur noch die Lösung von Gehirn-Computer-Schnittstellen (BCI, brain-computer-interface), bei denen mit Hirnsignalen ohne Vermittlung von Muskelaktivität solche Kommunikationshilfen bedient werden können.

Obwohl die erfassten Hirnsignale bei solchen Patienten oft pathologisch sind, hatte dies bisher keinen nennenswerten Einfluss auf die Entschlüsselung ihrer Hirnsignale und ihre Kommunikationsleistungen mit einem BCI wie diese Dissertation zeigt.

Bei der Entwicklung solcher Kommunikationshilfen mit BCI ging man modular vor, indem man die Signalerfassung und -analyse getrennt von den Kommunikationsaufgaben und Kommunikationsleistungen hielt.

Verschiedene physiologische Parameter wurden für unterschiedliche Patientengruppen und Aufgaben verwendet: Elektrookulographie (EOG), Elektroenzephalographie (EEG), Nah-Infrarotspektroskopie (NIRS) und intrakortikale Hirnsignale. Obwohl die Signale unterschiedlich verarbeitet wurden, ist allen Versuchen, so auch unseren, gemeinsam, dass die Patienten lernen mussten, ihre Hirnsignale willentlich zu modulieren. Nach Klassifizierung des physiologischen Signals konnte der/die Patientin damit unterschiedliche Kommunikations-Paradigmen kontrollieren (z.B. ein „Ja“ oder „Nein“ auswählen). Wir haben hier verschiedenen Paradigmen bis hin zur hirngesteuerten Auswahl von Buchstaben und Bildung von Sätzen berichtet.

Wir stellen hier verschiedene Kombinationen von Signalaufnahmen und -verarbeitungen in unterschiedlichen Kommunikationssituationen vor. Die meisten davon wurden erfolgreich bei eingeschlossenen (LIS) und völlig eingeschlossenen Patienten (CLIS) erprobt. Es werden auch zwei Patienten berichtet, die über keine andere Kommunikationsmöglichkeit mehr verfügten.

List of publications

ACCEPTED PUBLICATIONS

The accepted publications are reported in Appendix A.

- I **Tonin, A.**, Jaramillo-Gonzalez, A., Rana, A., Khalili-Ardali, M., Birbaumer, N., & Chaudhary, U. (2020). Auditory Electrooculogram-based Communication System for ALS Patients in Transition from Locked-in to Complete Locked-in State. *Scientific Reports*, 10(1), 1–10.
<https://doi.org/10.1038/s41598-020-65333-1>
- II **Tonin, A.**, Birbaumer, N., & Chaudhary, U. (2018). A 20-questions-based binary spelling interface for communication systems. *Brain Sciences*, 8(7), 126.
<https://doi.org/10.3390/brainsci8070126>
- III Chaudhary, U., Vlachos, I., Zimmermann, J. B., Espinosa, A., **Tonin, A.**, Jaramillo-Gonzalez, A., Khalili-Ardali, M., Topka, H., Lehmsberg, J., Friehs, G. M., Woodtli, A., Donoghue, J. P., & Birbaumer, N. (2022). Spelling interface using intracortical signals in a completely locked-in patient enabled via auditory neurofeedback training. *Nature Communications*, 13(1), 1236.
<https://doi.org/10.1038/s41467-022-28859-8>
- IV Yoshimura, N., Umetsu, K., **Tonin, A.**, Maruyama, Y., Harada, K., Rana, A., Ganesh, G., Koike, Y., & Birbaumer, N. (2021). Binary Semantic Classification Using Cortical Activation with Pavlovian-Conditioned Vestibular Responses in Healthy and Locked-In Individuals. *Cerebral Cortex Communications*, 2(3), 1–13.
<https://doi.org/10.1093/TEXCOM/TGAB046>
- V Jaramillo-Gonzalez, A., Wu, S., **Tonin, A.**, Rana, A., Khalili-Ardali, M., Birbaumer, N., & Chaudhary, U. (2021). A dataset of EEG and

EOG from an auditory EOG-based communication system for patients in locked-in state. *Scientific Data*, 8(1), 1–10.
<https://doi.org/10.1038/s41597-020-00789-4> o

VI Khalili-Ardali, M., Wu, S., **Tonin, A.**, Birbaumer, N., & Chaudhary, U. (2021). Neurophysiological aspects of the completely locked-in syndrome in patients with advanced amyotrophic lateral sclerosis. *Clinical Neurophysiology*, 132(5), 1064–1076.
<https://doi.org/10.1016/j.clinph.2021.01.013>

VII Maruyama, Y., Yoshimura, N., Rana, A., Malekshahi, A., **Tonin, A.**, Jaramillo-Gonzalez, A., Birbaumer, N., & Chaudhary, U. (2021). Electroencephalography of completely locked-in state patients with amyotrophic lateral sclerosis. *Neuroscience Research*, 162, 45–51.
<https://doi.org/10.1016/j.neures.2020.01.013>

VIII Secco, A., **Tonin, A.**, Rana, A., Jaramillo-Gonzalez, A., Khalili-Ardali, M., Birbaumer, N., & Chaudhary, U. (2021). EEG power spectral density in locked-in and completely locked-in state patients: a longitudinal study. *Cognitive Neurodynamics*, 15(3), 473–480.
<https://doi.org/10.1007/s11571-020-09639-w>

IX Martínez-Cerveró, J., Khalili-Ardali, M., Jaramillo-Gonzalez, A., Wu, S., **Tonin, A.**, Birbaumer, N., & Chaudhary, U. (2020). Open Software/Hardware Platform for Human-Computer Interface Based on Electrooculography (EOG) Signal Classification. *Sensors*, 20(9), 2443.
<https://doi.org/10.3390/s20092443>

X Malekshahi, A., Chaudhary, U., Jaramillo-Gonzalez, A., Lucas Luna, A., Rana, A., **Tonin, A.**, Birbaumer, N., & Gais, S. (2019). Sleep in the completely locked-in state (CLIS) in amyotrophic lateral sclerosis. *Sleep*, 42(12), 1–8.
<https://doi.org/10.1093/sleep/zsz185>

MANUSCRIPTS READY FOR SUBMISSION

XI Khalili-Ardali, M., Martínez-Cerveró, J., **Tonin, A.**, Jaramillo-Gonzalez, A., Wu, S., Zanella, G., Corniani, G., Montoya-Soderberg, A., Birbaumer, N., & Chaudhary, U. A General-Purpose Framework for a Hybrid EEG-NIRS-BCI

PERSONAL CONTRIBUTION

Nr.	Accepted	Position of candidate in list of authors *	Candidate's contribution **
I	Yes	1 st	Performed 35% of the BCI sessions and data collection; Data analysis; Manuscript writing.
II	Yes	1 st	Conceptualization; Methodology; Software; Validation; Formal analysis; Investigation; Data curation; Original draft preparation; Visualization.
III	Yes	5 th	Speller software development; Performed 30% of sessions before implantation and 20% of the sessions after implantation; EEG/EOG analysis; Figures.
IV	Yes	3 rd	† Data collection; Help in the software implementation.
V	Yes	3 rd	Performed 35% of the auditory communication system sessions and data collection.
VI	Yes	3 rd	Help in the implementation of the experimental paradigms.
VII	Yes	5 th	Data collection.
VIII	Yes	2 nd	Performed 40% of data collection; Data analysis discussion.
IX	Yes	5 th	Review and editing.
X	Yes	6 th	† Data collection.
XI	No	3 rd	Implemented NIRS pipeline, presenting paradigm and classification methods; Implemented speller; Writing of NIRS section.

* Full list of authors is presented in the list of publications.

** As specified in the manuscripts.

† Manuscript does not report author contributions.

Contribution declaration

I hereby declare that the thesis I submit for my doctorate with the title *Binary Communication Techniques in Locked-in and Completely Locked-in Patients* is my own independent work, that I used only the sources and resources cited and have clearly indicated all content adopted either word-for-word or in substance. I declare that the University of Tübingen's guidelines to ensure good academic practice (Senate decision of 25.5.2000) have been observed. I solemnly swear that this information is true and that I have not concealed any relevant information. I am aware that making a false declaration is punishable by a fine or by a prison term of up to three years.

M. Noirtier, immobile comme un cadavre, regardait avec des yeux intelligents et vifs ses enfants, dont la cérémonieuse révérence lui annonçait quelque démarche officielle inattendue.

La vue et l'ouïe étaient les deux seuls sens qui animassent encore, comme deux étincelles, cette matière humaine déjà aux trois quarts façonnée pour la tombe; encore, de ces deux sens, un seul pouvait-il révéler au dehors la vie intérieure qui animait la statue: et le regard qui dénonçait cette vie intérieure était semblable à une de ces lumières lointaines qui, durant la nuit, apprennent au voyageur perdu dans un désert qu'il y a encore un être existant qui veille dans ce silence et cette obscurité.

Alexandre Dumas, *Le Comte de Monte-Cristo*

1

Introduction

Alexandre Dumas, in *The Count of Monte Cristo*, describes the character of Noirtier de Villefort as an old man completely paralyzed whose only mean of communication is the movement of the eyes. The condition well portrayed in the novel is the locked-in syndrome (LIS) and can be caused by several neuronal disorder, such as brain stem stroke, or amyotrophic lateral sclerosis (ALS), among others (Birbaumer, 2006). For persons in this state, communication is one of the biggest challenges: while for the early stage of the paralysis

commercial tools are available and provide reliable communication, there is no device available for patients affected by advanced paralysis of the body. For this reason, many research groups focus their attention on brain-computer interfaces (BCIs), in order to acquire and decode signals directly from the brain activity and thus, to avoid using the unreliable muscles activity.

This dissertation focuses on techniques to decode two different signals from the brain and translate them into a binary classification used for communication purposes.

1.1 AMYOTROPHIC LATERAL SCLEROSIS

Amyotrophic lateral sclerosis (ALS) is a neurodegenerative disease with no available treatment that affects motor neurons, whose incidence in Europe is 2.16 per 100 000 person-years (95% CI 2.0-2.3) (Logroscino et al., 2010). The etiology of the disease is still unclear, but the scientific community is reaching a consensus on identifying a multifactorial mechanism underlying the development of ALS with interactions between genetic and molecular pathways (Chou & Norris, 1993). Although the underlying reasons for the development of the disease remain uncertain, it is well known that ALS might affect both upper and lower motor neurons (UMN and LMN). In case of UMN the degradation affects the neural pathways between the cerebral cortex and the spinal cord and leads to spasticity and weakness; on the contrary, when LMN are involved, the degeneration alters the communication between the UMN and the associated muscles and results in fasciculations, wasting, and

weakness (Kiernan et al., 2011); often both UMN and LMN are affected and therefore all these symptoms are present. In either UMN- or LMN-predominant ALS, the neuromuscular disease is relentlessly progressive and leads to a loss of the entire motor control: starting from the limbs, it advances up to a total paralysis of the body, involving also respiratory failure that are the cause of death in 60% of those patients that do not accept artificial ventilation (Wolf et al., 2017).

In general, the progress of ALS is not related with a decrease in cognitive functions (Schnakers et al., 2008), although it is often reported a development of frontotemporal dementia (Lomen-Hoerth et al., 2003; Stanton et al., 2007). The exact rate of ALS patients affected by dementia is unclear: different studies reported rates varying between 5% and 50% (Lomen-Hoerth et al., 2003; Ringholz et al., 2005). Nonetheless, at least half of ALS population (but probably more) has no symptoms indicating frontotemporal dementia or cognitive dysfunction, and it has been suggested that sensory perception and cognitive abilities remain intact even in the late stage of the disease (Kübler & Birbaumer, 2008).

With the progression of the disease, the paralysis proceeds leading the patients to a locked-in syndrome (LIS), defined as a state of total immobility except for eye movements that, usually, are the least muscles affected by ALS. Some studies report the voluntary movement of other muscles, such as sphincter muscles, even after the complete loss of eye control (Murguialday et al., 2011). When all the remaining volitive movements are lost, the patients

are said to be in complete locked-in syndrome (CLIS) (Bauer et al., 1979).

Persons with no cognitive impairment in these very advanced conditions are the patients object of this dissertation.

1.2 AUGMENTATIVE AND ALTERNATIVE COMMUNICATION DEVICES

Most of the patients in LIS that are not able to speak continue to communicate using an augmentative and alternative communication (AAC) device (Ball et al., 2004), i.e., a device that displays an interface with letters and/or words and allows to select them using some remaining movement, for example by using a mouse, a keyboard, a joystick, or by tracking the line of gaze on the screen using an eye tracker device (Beukelman & Light, 2020). When communication is restored through any AAC tool, the will to live for the patients increase significantly (Linse et al., 2018).

In most cases, ALS patients in LIS are completely paralyzed except for the control of ocular muscles; hence, once patients lose speech capabilities, the primary channel for communication is eye movement, that is converted to speech through an eye tracker device (Beukelman et al., 2011). These systems are formed by two parts: one screen that is placed in front of the patient and shows a grid of letters and words, and one or multiple cameras, usually placed below or above the screen, that track the eye movement, and detect the gaze point by analyzing the pupil position. The usage of these commercial products is fast and very reliable and allows a patient to communicate by naturally looking at the screen and selecting letters and words by fixating the gaze.

The main problems with eye trackers are intrinsic to the nature of the technology: they are based on visual feedback, eye movement and gaze fixation, therefore if just one of these three is missing or become pathological, the system will no longer function properly.

Even if ocular muscles are one of the last muscles lasting in ALS, with the progression of the disease ocular abnormalities and dysfunctions appear frequently in all the stages of disease (Jacobs et al., 1981; Donaghy et al., 2011; Kang et al., 2018; Cozza et al., 2021) and involve among others saccadic movements (Donaghy et al., 2010), smooth pursuit (Abel et al., 1995), and blink suppression (Byrne et al., 2013). Moreover, ALS patients show slow eye movement, inability on gaze fixation, blurred vision, and dryness of cornea (Jacobs et al., 1981; Palmowski et al., 1995; Spataro et al., 2014; Cozza et al., 2021). With the advancement of these ocular dysfunctions, the usability of eye trackers declines to such an extent that the precision of the tracking software becomes useless for communication purpose.

1.3 NEUROPHYSIOLOGICAL SIGNALS FOR COMMUNICATION

Once a patient loses the ability to use eye tracker devices there is no commercial tool that can be used to restore communication. Nevertheless, many research groups have conducted studies to provide communication by using different neurophysiological signals (Chaudhary et al., 2016). The systems that use such signals are generally called Human-Computer Interfaces (HCIs), but in the specific case of neural signals usually people refer to them

as Brain-Computer Interfaces (BCIs).

One of the main signals used in HCI is the electromyography (EMG), i.e., the electrical potential generated by the activation of muscle cells. EMG is usually recorded by placing some electrodes on the monitored muscles and observing the changes in the electrical activity when the muscles are contracted or relaxed. The electrical signal generated by the muscles' activation is orders of magnitude bigger than the underlying electrical activity of the brain, and therefore it is a valid tool for detecting even micromovements that cannot be directly observed. In patients affected by LIS the monitor of muscular activity is overall useless due to the general paralysis of the body, nevertheless this same technique can be used to inspect the movement of the eye balls by measuring the change in the electrical potential between the cornea and the retina, and, in this specific case, the recording is called electrooculography (EOG). In normal conditions EOG can be used to record both horizontal and vertical eye movement, and, in absence of abnormalities or ocular dysfunction, the signal can be used to completely reconstruct the ocular movements of the recorded subject.

Brain signals acquisition systems can be divided in two categories: non-invasive and invasive systems (Figure 1.1). The first category includes all signals that can be recorded externally from the scalp by placing some specific sensors, while invasive systems require a surgery to place the recording electrodes below the scalp.

The vast majority of BCIs are based on electroencephalographic (EEG)

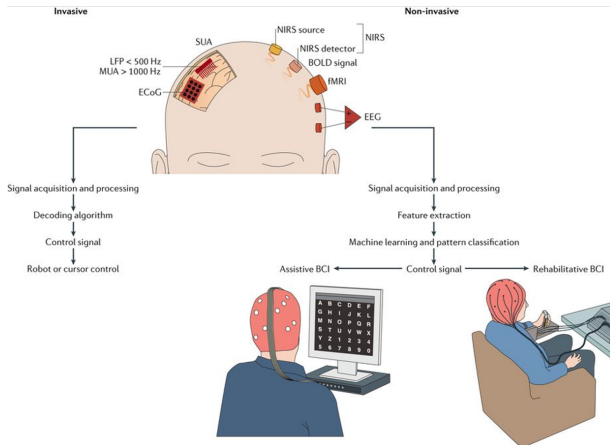


Figure 1.1 – General framework of brain–computer interface (BCI) systems. Invasive BCI approaches (left) include the measurement of local field potentials (LFPs), single-unit activity (SUA), multi-unit activity (MUA), and electrocortico- graphy (ECoG). Noninvasive BCI approaches (right) include EEG, blood oxygenation level-dependent (BOLD) functional MRI, and near-infrared spectroscopy (NIRS). Brain signals are processed to extract features relevant to the aim of the BCI (for example, communication) and then classified using a translational algorithm to construct a control signal that drives the BCI. BCIs can be classified as assistive to help patients with communication or movement, or as rehabilitative to help recover neural function. Reprinted from Chaudhary et al. (2016).

signals which represent the electrical activity generated by the neurons of the brain, firstly recorded in humans in 1924 (Berger, 1929). EEG recording is performed by placing electrodes on the scalp, using one electrode as ground (usually placed on the forehead) and one as reference (usually placed at the center of the head or below the ear), and measuring the potential difference between each electrode and the reference. The acquisition is done through an amplifier that usually works with a sampling rate between 250 and 2000 Hz. The location of each electrode usually follows a standard called 10-20 system (indicating the distance of each adjacent electrode); the position is very impor-

Name	Frequency
Delta	0.5 – 3 Hz
Theta	4 – 7 Hz
Alpha	8 – 12 Hz
Beta	15 – 30 Hz
Gamma	> 30 Hz

Table 1.1 - List of the EEG frequency bands commonly used.

tant since each electrode records the neural activity generated by the underlying brain section, and every brain region is mainly activated by specific tasks and maps different parts of the body. Brain activity is composed by neural oscillations at different frequencies (more details can be found in Jackson & Bolger (2014)), for this reason one of the features often analyzed is the power spectrum restricted to some specific bands: the bands usually analyzed are listed in Table 1.1.

Another widely used system to record brain activity is functional near-infrared spectroscopy (fNIRS): a neuroimaging technique that estimates hemodynamic activity of the brain with optical sensors placed on the surface of the scalp. The use of near-infrared light to detect changes of cortical oxygenation was firstly demonstrated in adults in 1977 (Jöbsis, 1977). fNIRS setup includes a couple of sensors that work at specific wavelengths between 650 and 900 nm, the sensors are a light emitter and a light detector. The principle behind this technique is that near-infrared light can penetrate the tissues of the head and it is absorbed by hemoglobin, therefore, knowing the amount of light emitted and detected, is possible to estimate the level of concentration

of oxy- or deoxy-hemoglobin in the blood flow, and consequently to estimate the neural activation. One of the main pros in using *f*NIRS-BCI is the low sensitivity to motion artifacts, that are one of the biggest problems in EEG systems; moreover, *f*NIRS has also a better spatial resolution than EEG (Wilcox & Biondi, 2015). Nevertheless, the hemodynamic change reaches the peak only after 5 s, therefore, in contrast to EEG, *f*NIRS have very low temporal resolution.

The noninvasive systems usually require long setup procedures and are in general prone to environmental noise. These two drawbacks can be overcome by using invasive acquisition systems like electrocorticography (ECoG) or microelectrode arrays (MEAs). The principle of ECoG is the same of EEG and the signal is also very similar since it records the electrical potential of the underlying neurons. The main difference is that in ECoG electrodes larger 2-3 mm are placed directly on the cortex giving the possibility to acquire an electrical signals that are not attenuated by the skull (Buzsáki et al., 2012). Finally, with a more invasive procedure, is possible to place MEA directly in the cortex. These microelectrodes systems can record extracellular action potentials from single neurons. The action potentials (or spikes) are events fired by the neurons when they are activated, and each single electrode, depending on its position, can record the activity from a single neuron (or single-unit activity) or from multiple neurons (multi-unit activity). Spikes events last for approximately 2 ms, therefore the time resolution of MEA is extremely high, and BCI systems based on this signal can provide an immediate feedback of

the recorded neural activity.

1.4 COMMUNICATION IN LOCKED-IN SYNDROMES

BCI communication systems for ALS person in LIS can be based on visual feedback, auditory feedback or on both. The very first BCI system for patients in LIS was developed by Birbaumer et al. (1999) and used slow cortical potentials of EEG signal to binary select letters from a screen. After this study many other researches focused on developing faster and more reliable systems. Patients that still have voluntary eye control can benefit from EOG-based BCI systems, and a system that uses involuntary ocular activity has been tested in two ALS patients for binary communication (Kim et al., 2018). Most BCI systems use EEG signals, and the most used technique to decode patient's intention is by analyzing the evoked responses generated in the EEG after the presentation of a stimulus. Each stimulus, either auditory or visually presented, induces a positive or negative event-related potential (ERP) in the brain whose shape appears constant over time. One of the most used ERP components is P300: a positive potential with peak approximately 300 ms after a stimulus onset elicited during decision making process by infrequent stimuli. This EEG feature has been used in multiple studies with LIS participants by showing a keyboard on a screen and highlighting different groups of letters: by analyzing the P300 component during multiple trials it is possible to determine if the letter thought by the participant is included in the group of highlighted letters (Sellers et al., 2010; McCane et al., 2014;

Ryan et al., 2018). P300 system can also be used with a combination of visual and auditory feedback (Kübler et al., 2009). Some of these systems provided good spelling performance, but all of them have been tested with patients with some residual movements. Other BCI systems used auditory evoked potentials by presenting sequences of different sounds and detecting on which the patient was focusing by analyzing the negative potentials at 100 ms and 200 ms after the stimulus onset (N1 and N2) and P300 component (Hill et al., 2014). The proposed auditory paradigm shows single sessions performance above chance for a basic “yes” / “no” communication, nevertheless the performance decreased when classifier weights are transferred from session to session. Another widely used BCI paradigm is based on steady state visual evoked potential (SSVEP): when a visual stimulation at specific blinking frequency is presented, the brain naturally responds generating electrical activity at the same frequency. The generated brain response is greater for the stimuli to which the patient pays attention, therefore presenting multiple visual stimulations at the same time at different frequencies, the EEG power spectrum shows peaks corresponding to the frequency attended by the patient and to its harmonics. This signal has been used in different communication paradigms: binary questions (Lim et al., 2013; Lesenfants et al., 2014), multiple choice selection (Hwang et al., 2017) and by implementing a full speller system (Peters et al., 2020). Some of the results look promising, however SSVEP has some drawbacks (e.g., it might provoke epileptic seizures, and it causes eye and mental fatigue) that do not allow paradigms to last for very

long, and therefore such systems are not suitable for long communication sessions. Invasive BCI systems have also been used for communication with ALS, in particular ECoG signal has been used with a LIS patient (Vansteensel et al., 2016). The patient was trained to imagine moving the hand and the decoded signal was used to select letters from a screen. Another study involving two ALS patients classified local field potentials from intracortical MEAs, and both patients were able to modulate the brain signal to compose messages (Milekovic et al., 2018).

Despite all the promising results, all the reported studies target patients in LIS that still have other channel of communication, for example eye trackers.

1.5 COMMUNICATION IN COMPLETE LOCKED-IN SYNDROMES

Performing experiments with patients in CLIS is extremely more challenging than targeting LIS population, mainly because researchers cannot receive any feedback from the patient and, therefore, the reasons of low decoding in a given session can vary from patient being sleeping or tired to patient not able to perform the requested task. A study shows that BCI performance are not affected by the progression of ALS and there is no significant difference between neurophysiological signals of patient before and after entering CLIS (Silvoni et al., 2013), nevertheless a patient implanted with ECoG system shows that after the transition between LIS and CLIS the usual BCIs do not succeed (Murguialday et al., 2011). Kübler & Birbaumer (2008) tried to explain the reasons by theorizing an extinction of goal-directed thinking in

CLIS patients, but, at least for one case, this theory has been proved wrong in the single-case study reported in Paper III. A first NIRS-based BCI system used different imagery techniques to get a binary classification (Fuchino et al., 2008), results were not sufficient to provide communication, but most of the tasks were successfully performed and suggested the potential of NIRS-BCI systems in CLIS patients. A first successful NIRS-BCI was implemented by decoding different modulations corresponding to “yes” and “no” responses of the patient (Gallegos-Ayala et al., 2014; Borgheai et al., 2020). The hemodynamic response shows significant difference in the deoxygenation levels for positive and negative answers and half of the sessions show better-than-chance accuracy using a support vector machine trained with data from calibration session. EEG-BCI have been proven to work in one CLIS patient using SSVEP signal (Okahara et al., 2018), but in this study the patient was trained to use the BCI paradigm when he still had voluntary eye movement. Like in the NIRS-BCI studies, the performed communication was limited to binary yes/no answers.

1.6 OVERVIEW

In this dissertation, I propose several communication systems that can be used by LIS and CLIS patients, analyzing both the signal acquisition step and the communication interface.

The first problem that I had to address was to define the CLIS condition and to quantify when the condition was affecting the cognitive capabilities of

the patients. In Paper VI (*Neurophysiological aspects of the completely locked-in syndrome in patients with advanced amyotrophic lateral sclerosis*) our research group studied some EEG features acquired from CLIS patients, while in Paper X (*Sleep in the completely locked-in state (CLIS) in amyotrophic lateral sclerosis*) the sleep pattern of those patients is more deeply analyzed. Longitudinal studies of the EEG in LIS and CLIS patients are reported in Paper VII (*Electroencephalography of completely locked-in state patients with amyotrophic lateral sclerosis*) and Paper VIII (*EEG power spectral density in locked-in and completely locked-in state patients: a longitudinal study*), with the first one focused on differences between healthy subjects and CLIS patients, while the second one analyzes the evolution over time of LIS and CLIS patients.

After this neurophysiological analysis of patients in LIS and CLIS, I report different developed communication systems based on binary input signal, each of them built in a modular way so the acquired signal and its processing can be independent from the communication program. In Paper I (*Auditory Electrooculogram-based Communication System for ALS Patients in Transition from Locked-in to Complete Locked-in State*) we proposed a system based on residual ocular movement, and its valuable dataset has been published in Paper V (*A dataset of EEG and EOG from an auditory EOG-based communication system for patients in locked-in state*). The underlying experimental software, designed to acquire simultaneously EEG and NIRS signals in a user-friendly interface, is presented in Paper XI (*A General-Purpose Framework for a Hybrid EEG-NIRS-BCI*). The speller communication interface has later

been reused in Paper III (*Spelling interface using intracortical signals in a completely locked-in patient enabled via auditory neurofeedback training*), a single-case study that reports for the first time full communication with an ALS patient in CLIS using MEAs. Noninvasive BCI in CLIS has been studied also in Paper IV (*Binary Semantic Classification Using Cortical Activation with Pavlovian-Conditioned Vestibular Responses in Healthy and Locked-In Individuals*) with a novel EEG system based on vestibular stimulation. Finally, the acquisition of EOG signal using open-source device has been investigated in Paper IX (*Open Software/Hardware Platform for Human-Computer Interface Based on Electrooculography (EOG) Signal Classification*), and a new paradigm for communication with a binary signal is proposed in Paper II (*A 20-questions-based binary spelling interface for communication systems*).

2

Objectives and expected outcome

The main objective of this thesis is the development of a system to restore communication for patients in LIS and CLIS. The work is focused on ALS patients in an advanced stage of the disease, when usual AAC systems do not work due to the progressive paralysis that affects all the muscles of the body. For this reason, a system has been developed to work both with minimal ocular movements, in case of patients still able to generate recordable muscular activity, and directly with brain signals, for the patients completely paralyzed

in the late stage of the disease. Therefore, the development of the communication system is split in two phases: the first one is focused on the signal analysis and it aims to retrieve features useful for classification from the acquired neurophysiological signals; the second one is the implementation of techniques that can use these signals to select letters and words or, more in general, to communicate.

The most obvious result expected from such system is the restoration of the communication in ALS patients in the latest stage of the disease. But, due to the progressive nature of the disease, it is not possible to expect that a system based on one specific signal can be successfully used for a long period of time. Therefore, the more general expected outcome is a customized HCI or BCI that follows the course of the disease. For this reason, the acquired signal will be categorized with a general binary classifier and the implemented system will use this signal-agnostic classification to allow communication.

3

Results and discussion

The following paragraphs describe the methods and the techniques developed to achieve communication in late-stage ALS patients. The chapter is divided in two sections: the first is a description of the signal acquisition and signal processing techniques that have been applied, and the second depicts the methods that have been developed to achieve the actual communication.

It is important to keep in mind that these two sections are tightly related, and often they have been developed in parallel. Nonetheless, in the discus-

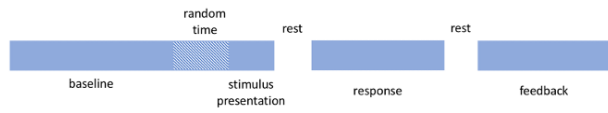


Figure 3.1 – The general trial structure includes a baseline period of a fixed plus random time; the auditory presentation of the stimulus; a rest period; the response period during which the patient is asked to perform the task; a second rest period; and a feedback of the classified response given to the patient auditory.

sion I preferred to keep the two topics separate, because all the communication techniques can be independently applied with respect to the acquisition method that the experimental paradigm requires.

Since all developed communication methods are based on a binary input, the final step of the signal processing will always be related to the extraction of features to feed a binary classifier, while the pipeline followed always the same schema: calibration, validation, and finally the communication application. Both calibration and validation phases are based on the trial structure reported in Figure 3.1: it starts with few seconds of baseline, followed by the instruction of the trial (i.e., the stimulus presentation), then a response time where the patient is asked to perform the required task and finally a feedback that indicates the end of the trial. The paradigms are always binary (e.g., “yes” or “no”, “up” or “down”), and during the response time the patient is asked to modulate the acquired signal in two different ways, for example to move the eyes to reply “yes” and not to move to reply “no”. The data acquired in these binary trials is used to build the classifier.

Even if the communication methods shared the same trial structure, each

Publication	Signal	Feature	Instructions	Classification method
Paper I	EOG	Amplitude	Move the eyes in two different ways	Support Vector Machine
Paper III	Intracortical	Spikes, Spike band power	Modulate neural activity in two different ways	Threshold crossing, Logistic regression
Paper IV	EEG	EEG cortical current source	Think “yes” or “no”	Offline classification

Table 3.1 - List of the different paradigms developed for communications. All the paradigms have been tested in LIS or CLIS patients. The table reports the signal that has been used, the feature of the signal used for classification, the instructions given to the patient and the classification method.

experimental paradigm was developed in a specific way. The data acquisition systems and communication methods are detailed described in Sections 3.2 and 3.3, but a summary of the different paradigms that have been designed is reported in Table 3.1 listing signals, features, instructions and classification methods that have been used.

3.1 LIS AND CLIS SUBJECTS

All performed studies are focused on ALS patients in LIS or CLIS showing no significant cognitive impairments. This assumption is difficult to be done for person who do not communicate, therefore in case of complete paralyzed patients we included only patients that were cognitively intact before transitioning to CLIS. The findings on LIS and CLIS states are summarized in Table 3.2.

Publication	Findings in LIS	Findings in CLIS
Paper VI	-	Slowing in EEG and attenuation of α wave activity. Altered somatosensory and auditory evoked potentials.
Paper VII	-	Power reduction in high α , β and γ bands.
Paper VIII	Healthy EEG pattern.	Slowing in EEG, α peak between 4 and 5 Hz.
Paper X	-	Healthy sleep pattern with preserved circadian rhythm.

Table 3.2 – Findings for LIS and CLIS patients. The papers listed here are the ones included in the dissertation.

In order to find a metric for impairment, Paper VI analyzes the neurophysiological signals in four of these patients and it shows altered metrics in all of them, even if it was not possible to determine a unique and common pattern. Nevertheless, similarities among all the patients were found in a general slowing of EEG and attenuation of alpha wave activities. The other neurophysiological metrics analyzed include auditory and somatosensory evoked potentials and show absence or altered responses in the patients compared to healthy population, but without a general pattern that could be applied to all the subjects.

The study also analyzes the sleep signals of these patients and replicates the results achieved in Paper X where it has been shown that CLIS patients have, despite some irregularities, a healthy sleep pattern. For cognitive assessment it was very important to prove that these patients conserve a day-night self-regulation and, in particular, a clear circadian rhythm. These findings,

even if they do not guarantee any level of cognitive capabilities, are important because the absence of these markers would have meant serious cognitive decline.

The resting state EEG traces of CLIS patients have been compared to healthy EEG in Paper VII, and results confirm a significant power reduction in high alpha, beta and gamma bands indicating dominance of slower EEG frequencies in the oscillatory activity. Nevertheless, any conclusion about a relationship between these pathological signals and cognitive abilities was not possible, since a clear metric of consciousness is still undefined. However, the study suggests that the slowness of the EEG spectrum might be associated with the complete immobility of CLIS subjects and the consequent deprivation of the environmental stimuli, including the communication.

This thesis is reinforced by Paper VIII where EEG signals is compared between CLIS and LIS patients in a longitudinal study. The study, performed across multiple sessions, shows a significant difference in the power spectrum of CLIS patients without any means of communication with respect to LIS patient that was using an AAC device. In general, the EEG power spectrum of CLIS patients, as highlighted in Papers VI, VII, and X, appears with dominant slow waves and a pathological alpha frequency between 4 and 5 Hz. Moreover, the recordings performed over one year show a general slowness of the EEG traces in CLIS patients. On the contrary, the patient in LIS during the same time showed no degradation in the EEG components and in general a healthy EEG pattern with an alpha peak constantly at 9 Hz.

The analyses performed in these papers were fundamental to develop the communication paradigms with LIS and CLIS patients.

3.2 SIGNAL ACQUISITION AND SIGNAL PROCESSING

During the experiments, four signals have been used: EOG, EEG, NIRS, and intracortical signal. In the following paragraphs the acquisition process used for all these signals will be described, highlighting the pro and cons, and the patient population that can be targeted.

3.2.1 MICRO-OCULAR MOVEMENTS

Eye movement is usually the last remnant voluntary movement in ALS patients, and it is widely used to communicate thanks to eye-tracking AAC devices that allow patients to select letters and words by fixating them on a screen. During the transitional state from LIS to CLIS, patients become unable to maintain gaze-fixation and, therefore, unable to use eye-tracking AAC technologies. Nonetheless, some remaining controllable muscles of the eyes continue to function, and it is therefore possible to use this muscular signal to provide a means of communication during this transition.

In Paper I, we recorded EOG signals from four ALS patients unable to use eye-tracking devices. Signals were recorded with Ag/AgCl active electrodes placed on the standard EOG positions SO₁, IO₁ (vertical EOG) and LO₁, LO₂ (horizontal EOG), as depicted in Figure 3.2. The amplitude of the acquired signal was very small compared to ocular activity of healthy subjects:

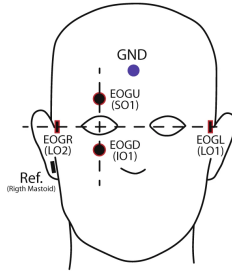


Figure 3.2 - Montage for the minimum number of EOG channels for each recorded session, using the locations LO1 (left cantus) and LO2 (right cantus) for horizontal eye movement, and SO1 (above superior orbit) and IO1 (below inferior orbit) for vertical eye movement. Modified from Paper V.

while in normal conditions the amplitude of the EOG signal varies from 50 to 3500 μV , the patients were able to generate a signal six times smaller, in the best case. In particular one patient was able to move the eyes in a range of $\pm 300 \mu\text{V}$, while the other patients were generating an ocular movement in an approximate range of $\pm 100 \mu\text{V}$.

Figure 3.3 shows the horizontal eye movement for a paradigm with two different conditions, in which each patient was asked to generate two different movements for “yes” and “no” trials. The amplitude values clearly indicate a pathological condition in all patients, but they also show that even in presence of these micro-ocular movements, the traces are clearly separable between two conditions. In order to extract the features, the signals were first filtered between 0.1 Hz and 35 Hz, and then normalized against a baseline signal. The choice of the actual feature to use for classification was data-driven: for the two patients with a highly separable signal (P15 and P16) we used the range of signal amplitude (i.e., the difference between the maximum and

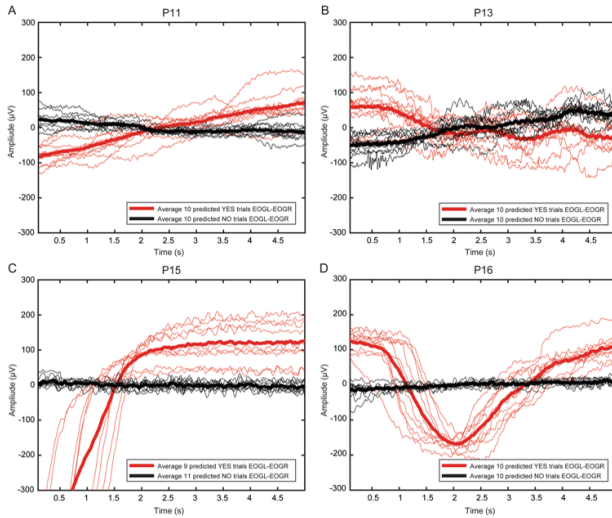


Figure 3.3 – Horizontal eye movement during feedback sessions for all patients. Differential channel EOGL - EOGR for a particular feedback session performed by (A) P11, (B) P13, (C) P15, and (D) P16 during the first visit. In each subfigure, the x-axis is the response time in seconds, and the y-axis is the amplitude of the eye- movement in microvolts (μV). The thin and thick red trace corresponds to a single “yes” response and average of all the “yes” responses, respectively. The black thin and thick trace corresponds to a single “no” response and average of all the “no” response. The box at the bottom right of each subfigure lists the number of trials classified as “yes” and “no” by the Support Vector Machine classifier for that particular session. Reprinted from Paper I.

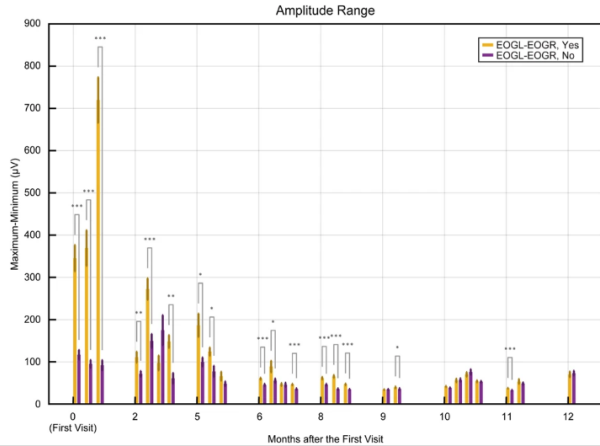


Figure 3.4 - Progressive decline of the eye-movement amplitude along the visits for P11. Depicts the trend of decline in the range of the amplitude of the EOG signal for yes/no questions answered by the patient during the period March 2018 to March 2019. The figure shows the mean and the standard error of the mean of the extracted range of the amplitude of the horizontal EOG signal across each day for yes and no trials. The x-axis represents the month of the sessions, and the y-axis represents the amplitude in microvolts. The asterisk (* - p-value less than 0.05; ** - p-value less than 0.01; *** - p-value less than 0.001) in the figure represents the results of the significance test performed between yes and no for horizontal EOG employing the Mann-Whitney U-test. Reprinted from Paper 1.

minimum values), while for the other two patients we took into account also the dynamic of the response by extracting the maximum and minimum values of the signal together with the respective occurrence time. The features obtained during the training sessions were used to train a support vector machine classifier that was validated through 5-fold cross-validation.

It is important to highlight that the ocular signal might be used only for a short period of time, because the degeneration of the disease will lead to a complete paralysis of the ocular muscles. This decline can be seen in Figure 3.4: the amplitude of the EOG signal recorded from P11 decreases over time,

up to the point to be indistinguishable among the two conditions. These valuable datasets have been published in Paper V with the aim to help redefine the course of the progression in ALS.

Moreover, following this study, a prototype of an open-source hardware for communication with EOG has been developed. The prototype has never been tested with patients, but it is a proof of concept that such system can also be built using non expensive components and, therefore, it might be widely used by patients. The whole software/hardware platform is described in detail in Paper IX.

3.2.2 EEG AND fNIRS: THE HYBRIDBCI

When a patient completes the transition from LIS to CLIS all residual movements of the eyes are lost, and the patient becomes completely paralyzed. This condition obviously implies that the recording of muscular activity (even from the eyes) becomes useless for the purpose of communication. Therefore, the only signal that can be acquired and used for this purpose is the electrical signal coming directly from the brain. In particular, we focused on two types of signals that are suitable for home use experiments: EEG and fNIRS. Several systems have been already proposed for BCI applications with non-invasive signals, such as BCI2000, BioSig, OpenVibe, and Mushu, but none of them was suitable to be easily used with ALS-CLIS patients. For example, most of these platforms are focused only on the paradigm design or on the signal acquisition, but it is difficult to design a full experiment that is completely

auditory; moreover, in these patients EEG and NIRS signals are significantly altered and change with the progression of the disease, therefore the analysis pipeline should be highly customizable for each patient individually.

To overcome these problems in Paper XI we have proposed HybridBCI: a new framework for BCI experiments completely focused on the need of ALS-CLIS patients. HybridBCI has been designed following the object-oriented programming principles in order to be flexible and extendable. The framework is written in Matlab with a file-based structure (Figure 3.5) and a graphic user interface is used to change the settings that can be necessary to run the experiment at patient's bedside, giving the flexibility to adapt the configuration of the experiment at every single run. The platform provides an easy-to-use software to conduct experiments (focused on the communication) with ALS patients in LIS or CLIS, starting from the signal acquisition phase, implementing the signal processing and features extraction algorithms, up to the communication paradigm.

HybridBCI is designed to work with both EEG and NIRS signals, and the synchronization of the two is done via hardware triggers. A basic preprocessing pipeline has been implemented for both signals (Figure 3.6), and it can be easily extended by just adding a new function in the proper directory of the Matlab code. The default preprocessing pipeline for EEG includes a filter that can be wideband or automatically set to any of the specific EEG band, while for NIRS it converts the signal acquired as pair of wavelengths belonging to the near-infrared spectral range directly to hemodynamic concentrations

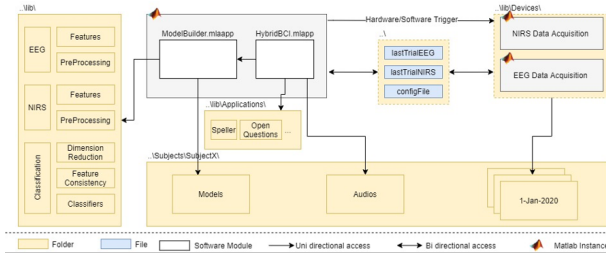


Figure 3.5 - HybridBCI System Design and file organization. Two main software modules, ModelBuilder.mlapp and HybridBCI.mlapp (white boxes), and three Matlab instances (Matlab icons) control the experimental procedure and online data acquisitions. For each functionality of the system, a folder is dedicated (yellow boxes) and the HybridBCI automatically recognizes new .m files in these folders and extends its' functionality accordingly. Reprinted from Paper XI.

of oxyhemoglobin (HbO), deoxyhemoglobin (HbR) and total hemoglobin (HbT), and it filters the signal to provide the hemodynamic response. After the preprocessing phase, the signal can be normalized with respect to a baseline, a common average reference can be applied, and features are extracted from it. A subset of more than twenty common processing algorithms is already implemented (e.g., mean, kurtosis, standard deviation, mean of the envelope, and more), but the modularity of the system allows to add any specific feature by just including a new file with the corresponding function. Finally, the framework provides classification algorithms, such as support vector machine, to build a model that can provide a binary classification of the trials.

For the experimental applications the classification provides a binary input that can be used in different communication techniques. The framework already includes a basic yes-no communication and a spelling communication system, that will be discussed in the Sections 3.3.1 and 3.3.2.

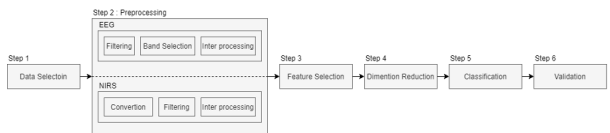


Figure 3.6 – Six steps of the analysis pipeline used in ModelBuilder. Step 1 is for loading the data and select/deselect channels. Step 2 is designed for the preprocessing of the NIRS and EEG signals based. Step 3 is used to select the desired features to be extracted from NIRS and EEG. In step 4 before passing the features to classifiers in step 5, the dimension of the feature space is reduced. Finally, in step 6 the acquired model is validated on the data that has not been used for training the classifier. Reprinted from Paper XI.

3.2.3 EEG AND GALVANIC VESTIBULAR STIMULATION

One of the most famous experiment in neuroscience shows that if a dog repeatedly listens to the sound of a bell preceding feeding, then the animal will associate the ring of the bell to the idea of food and it will start salivating in anticipation of food. This salivation is unconscious and involuntary, hence it will appear also if the dog is not fed anymore, and the sound of the bell can be used to make the dog salivating (Pavlov, 1927). This important finding, called Pavlovian conditioning, can be directly translated to human and can be used to train the brain to unconsciously respond to a stimulus. Using this principle, in Paper IV we developed a conditioning paradigm that associate the answers “yes” and “no” to a small electrical current applied on the left or right vestibular labyrinth behind the ears, i.e., galvanic vestibular stimulation (GVS). GVS is nonpainful and safe, however the stimulation applied to the vestibular system causes an equilibrium distortion sensation and reflexive responses such as visual rotation and tilt of the body. These automatic reflexes have been used to condition the patient with a long sequence of known bi-

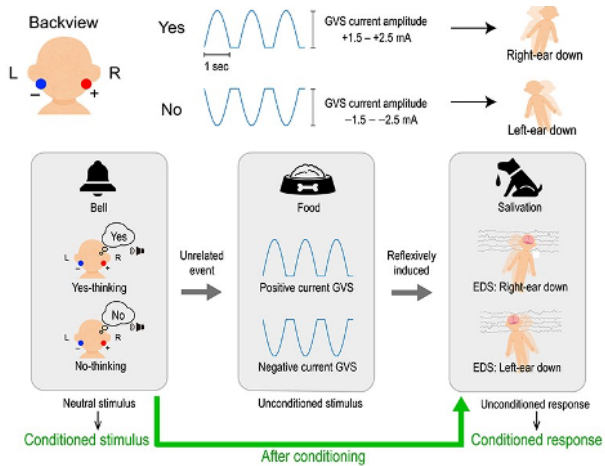


Figure 3.7 – Experimental concept and paradigm. Upper panel: Two GVS electrodes were placed behind the ears, an anode (red) electrode behind the right ear, and a cathode (blue) behind the left ear. Three positive half cycles of 0.5 Hz sine waves were provided for thought of “yes” which resulted in right-ear-down tilt sensation. In the case of thought of “no” 3 negative half cycles of 0.5 Hz sine waves were given to induce left-ear-down tilt sensation. Lower panel: Conceptual diagram of the thought of yes/no, GVS, and brain activity caused by EDS aligned with examples of Pavlovian conditioning. Modified from Paper IV.

nary questions: when the expected answer was positive a left stimulation was applied, when negative the stimulation was applied on the right side (Figure 3.7).

After many trials of conditioning sessions, we performed trials with the same structure but without any stimulation. In 85.3% of the validation trials the effect of the conditioning was reflected in the EEG and it was possible to correctly distinguish “yes” and “no” patterns for trials respectively with expected positive or negative answer.

3.2.4 INTRACORTICAL BCI

The use of non-invasive BCI systems is extremely wide and powerful, but when applied in ALS patients in CLIS it often failed, and, even in the few positive case reported, it was never accurate enough to provide full communication to the patient (Chaudhary et al., 2016). For these reasons, in Paper III a single-case study of an ALS patient in CLIS is reported: the patient has been implanted with two 64 microelectrode arrays in the supplementary and primary motor cortex and was able to use an intracortical BCI system to communicate. The patient was not new to BCI: before the implantation he was communicating with his residual eye movement in an experimental setup involving HybridBCI framework. The patient of this single-case study is P11 of Paper I.

The intracortical BCI setup and a schema of the communication paradigm is shown in Figure 3.8. The raw neural signal was acquired at 30 kHz from 128 channels, it was bandpass filtered with a window of 250-7500 Hz, and action potentials (i.e., spikes) from single- and multi-unit were extracted. The feature that has been used to get a binary classification was the firing rate, calculated as the number of spikes generated in a time window of one second. On the 86th day after implantation the patient was finally able to modulate his neural activity, using an auditory feedback that was directly mapping the firing rate to a sound. At that time the patient had a good control over the signal, and we decided not to apply any further machine learning algorithm, but to use directly the normalized firing rate: a trial was classified

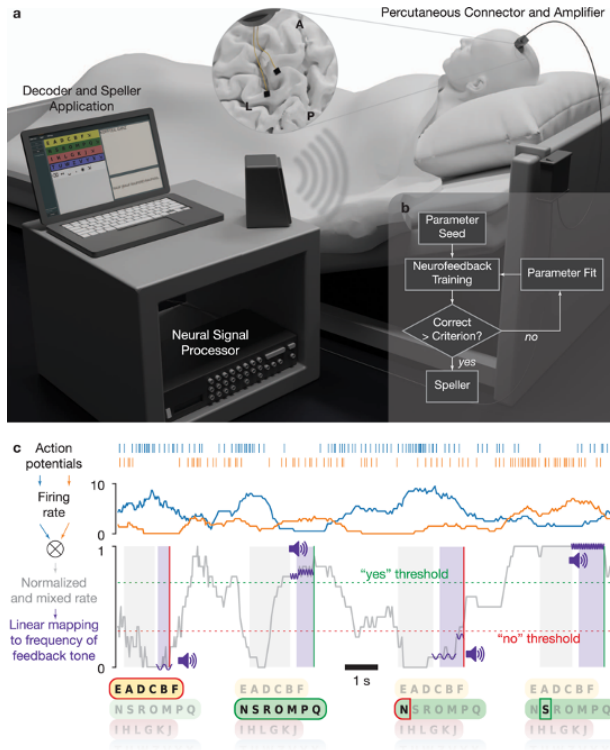


Figure 3.8 – Setup and neurofeedback paradigm. **a** Experimental setup. Two microelectrode arrays were placed in the precentral gyrus and superior frontal gyrus (insert, L: left central sulcus, A-P: midline from anterior to posterior). An amplifying and digitizing headstage recorded signals through a percutaneous pedestal connector. Neural signals were pre-processed on a Neural Signal Processor and further processed and decoded on a laptop computer. **b** Daily sessions began with Neurofeedback training. If the performance criterion was reached, the patient proceeded to speller use. If the criterion was not reached, parameters were re-estimated on neurofeedback data, and further training was performed. **c** Schematic representation of auditory neurofeedback and speller. Action potentials were detected and used to estimate neural firing rates. One or several channels were selected, their firing rates normalized and mixed (two channels shown here for illustration; see Online Methods). Options such as letter groups and letters were presented by a synthesized voice, followed by a response period during which the patient was asked to modulate the normalized and mixed firing rate up for a positive response and down for a negative response. The normalized rate was linearly mapped to the frequency of short tones that were played during the response period to give feedback to the patient. The patient had to hold the firing rate above (below) a certain threshold for typically 500 ms to evoke a “Yes” (“No”) response. Control over the neural firing rates was trained in neurofeedback blocks, in which the patient was instructed to match the frequency of target tones. Reprinted from Paper III.

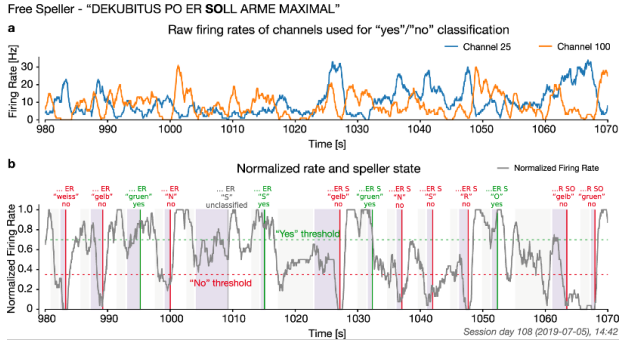


Figure 3.9 – Example of letter selection during a free spelling block. a Firing rate of the channels 25 and 100 used for “yes”/“no” classification on day 108. **b** Normalized firing rate and the speller state during the same 90 s period of a speller block. “Yes”/“no”/ timeout decisions are marked by vertical lines and the option selected in green and not selected in red. This example is part of the phrase “dekubitus po er soll arme maximal”, referring to bedside and instructing the aide to change arm position. Reprinted from Paper III.

as “yes” if the modulation was kept above a certain threshold, and as “no” if it was below another threshold. This direct mapping of the spike activity is shown in Figure 3.9.

Paper III reports the evolution of the BCI performance up to 470 days after the implantation, but the case study continued afterwards. After approximately two years the firing rate started to decline, the electrodes’ impedance started to decrease, and, in general, the intracortical signal started to degrade. It was then decided to change the acquisition software to a custom one and, instead of using the spike rate as feature for classification, we started to use the spike band power. Moreover, the binary classification value has been changed from the simple thresholding method described above, to a more sophisticated logistic regression classifier. It is important to highlight that the output

of the classification was always a binary value independently of the processing pipeline, this allowed us to keep in place the same communication applications that were used before, and the patient was able to communicate for one more year.

3.3 COMMUNICATION TECHNIQUES

In the following paragraphs I will analyze the techniques that have been developed to allow communication in LIS and CLIS patients once that a binary classifier was built. The first two paragraphs will describe actual communication methods that have been used directly with patients, while the last one describes a proof of concept for an innovative system that could overcome some of the problem that an auditory binary communication intrinsically has, for example the slowness of the selections and the dealing with false classifications. All paradigms will be discussed independently of the nature of the acquired signal.

3.3.1 BASIC YES-NO COMMUNICATION

The most basic technique that can be applied to a binary system is to directly ask yes and no questions to a patient. After the model has been built its output is a binary classification value, therefore one simple way to achieve communication with a patient is to use the same trial structure depicted in Figure 3.1 where now the stimulus presentation is a yes/no question with unknown answer, for example “Do you have pain?”. It is clear that such a system, not

only provides just a very small communication freedom, but also – more important – needs to have a very accurate classification in order to reduce the number of wrong yes/no answers. For this reason, the system has been used only when the cross-validation accuracy of the selected classifier was at least 80%, than chance level for a 2-class BCI with 20 trials (Müller-Putz et al., 2008), moreover, all questions were repeated multiple times to confirm the result.

This basic communication system has been implemented in HybridBCI (Paper XI), and it was used with the acquisition methods described in Papers I, III, and IV.

In the continuation of the study described in Paper III, the reliability of the yes/no communication was slightly improved by asking the patient to reply five consecutive times to the question and other five times to reply the opposite of the correct answer. For example, if the question was “Do you have pain?” and the patient wanted to reply “no”, then he had to reply “no” for five trials and “yes” for the following five trials. As mentioned before, the paradigm is completely auditory since it is not possible to rely on the sight of LIS/CLIS patients. This implies that each trial lasts for about 10 seconds, therefore, to receive a simple binary answer, it takes around 2 minutes: in order to be reliable this system is very slow.

3.3.2 SPELLING COMMUNICATION SYSTEM

A more advanced communication can be achieved using a speller system,

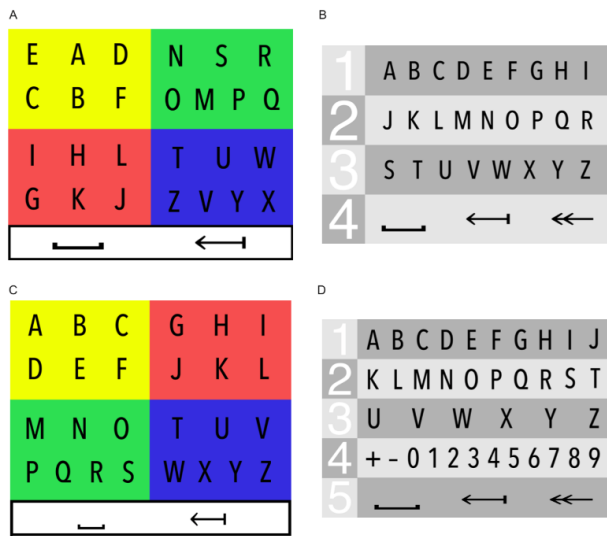


Figure 3.10 – Schema of the speller designed for the four patients. Speller schemas used for (A) P11, (B) P13, (C) P15, and (D) P16. In each schema the letters are grouped in sectors proposed to the patient: in (A) and (B) “yellow”, “red”, “green”, “blue” and “white”, in (C) “1”, “2”, “3” and “4”, and in (D) “1”, “2”, “3”, “4” and “5”. The special characters represent in (A) and (B) “space” and “backspace”, and in (C) and (D) “space”, “backspace” and “delete word”. Reprinted from supplementary material of Paper I.

where a subject can form entire sentences by selecting single letters or words. The speller system has originally been developed in Paper I, and continued to be successfully in Paper III.

The speller layout was implemented by optimizing a design previously developed by patients’ caretakers, in order to avoid unnecessary new learning phases for the patients. The speller consists of letters grouped in different sectors, plus one sector containing special characters as space and delete. The layout of the spellers used by the four patients of Paper I is reported in Figure 3.10.

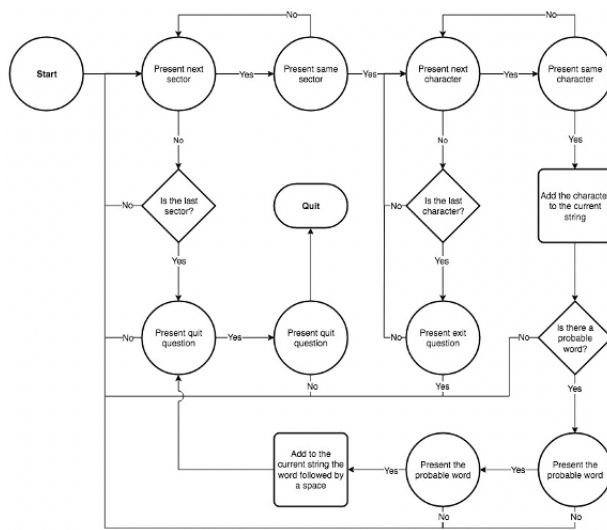


Figure 3.11 - Flow chart of the letter selection algorithm. Circles indicate questions presented by the computer, diamonds decisions done by the algorithm, and squares internal process of the algorithm. Reprinted from supplementary material of Paper I.

In order to customize the BCI schema for every individual, the previous patients' communication systems were investigated and the BCI was adapted accordingly: for two of them the groups were indexed as colors, while for the other two patients the groups were indexed as sequential numbers. In one case (Figure 3.10A) the letters were originally ordered alphabetically, but in order to improve the BCI performance, the letters inside each sector have been ordered based on the letters frequency distribution of german language. The communication algorithm obviously works indifferently of the convention that is used, but this simplifies the usability of the speller for the patients since they have to know by hard to which sector each letter belongs.

Keeping in mind that the output of the classifier (or the input of the speller) is always binary, it becomes clear that a patient will have to select a sector first, and only afterwards he will be asked to select a letter. In particular the selection of each letter proceeds with the following algorithm (Figure 3.11):

1. The first sector is presented to the patient;
2. The patient will reply “yes” to select it, or “no” to skip it;
 - (a) If the sector is skipped, the next sector is presented (back to 1.);
3. Once the patient selects a sector the first letter of that sector is presented;
4. The patient will reply “yes” to select it, or “no” to skip it;
 - (a) If the letter is skipped, the next letter is presented (back to 3.);
5. Once a letter is presented, go back to the selection of sector to start the next letter selection.

By replying just “yes” or “no” to confirm or skip a selection, a patient will be able to form words and sentences by selecting each single letter.

One drawback of this layout is that with a single wrong “yes” classification a patient might end in a wrong sector. For this reason, if the patient skips all the letter of a sector he will be asked if he wants to exit from that sector, and if the answer is affirmative the program will present the following sector, otherwise it will restart the presentation of the letters of that same sector. A second precaution to avoid wrong selection was added: each time a “yes” answer is decoded, the same sector or letter is presented to confirm the answer. The rationale behind this choice of double confirmation is that it is better to miss one

selection, rather than selecting a wrong sector or letter. Assuming a classifier accuracy of 80% using a double confirmation strategy the rate of correct selections decreases from 80% to 64%, but the rate of wrong selections is reduced from 20% to 4%.

The typing speed of the speller has been improved by adding a word prediction algorithm that, after each letter selection, would suggest a full word based on the context and on the incomplete word selected up to that point. In order to predict a word a conditional frequency distribution (CFD) is computed based on the n-gram (sequence of n words) analysis of a corpus of 10000 sentences (Goldhahn et al., 2012). The CFD is computed for all the sequences of one, two or three consecutive words (unigrams, bigrams and trigrams), and whenever a letter is selected the program returns the CFD of all the words starting with the current non-completed word, giving priority to one belonging to trigrams, then to bigrams and unigrams. If one word is highly probable, that word is presented to the patient and, as usual, he can select it or skip it. In this implementation, a word is defined to be highly probable if its CFD is higher than 50% the CFDs of all the other possible words. A more complete explanation of the word prediction algorithm can be found in Paper I.

This spelling algorithm has been used by LIS patients using EOG signal (Paper I) and more extensively by the patient that, after the transition to CLIS, has been implanted with microelectrodes and was able to continue using the speller through the modulation of his neural activity, becoming the first per-

Signal	Patient	# Sessions	# Characters	Speed (char/min)
EOG	P11	5/9	11.60 ± 8.79	0.57 ± 0.29
EOG	P13	10/11	13.00 ± 10.34	0.48 ± 0.24
EOG	P15	4/5	26.27 ± 19.14	0.68 ± 0.13
EOG	P16	3/3	14.00 ± 4.36	0.64 ± 0.13
Spikes	K01 (P11)	44/107	46.31 ± 57.30	1.07 ± 0.66

Table 3.3 – Results of the spelling sessions performed by the four patients of Paper I and by the patient of Paper III. The first column indicates the signal used for classification; the second the identifier of the patient as reported in the publications; in the third column is reported the number of intelligible sessions and the total number of performed sessions; the fourth and fifth columns report the number of spelled characters in the included sessions and the typing speed calculated in characters per minute, both values are reported as mean ± standard deviation. Modified from Paper I.

son in CLIS able to communicate (Paper III). In particular this patient used the developed speller for 107 days producing intelligible output on 44 of them. The intelligible sessions were performed over 5338 min, and during these sessions the patient also gave suggestions to improve his performance by spelling for example “TURN ON WORD RECOGNITION”, “IS IT EASY BACK ONCE CONFIRMATION”, and “TELL ALESSANDRO I NEED TO SAVE EDIT AND DELETE WHOLE PHRASES AND ALL OF THAT INTO THE LIST”. Usually, when he was communicating with non-German speakers the patient spelled in English.

It is important to notice that, due to the binary nature of the algorithm, the speller algorithm is very slow in comparison to other communication programs: the average typing speed is lower than 1 character/min (see Table 3.3).

Nevertheless, the developed paradigm is fully auditory and, since it works

with a binary signal, is easy to learn and to use. These two characteristics make the system a valid (if not the only) option for patients in LIS and CLIS to communicate.

3.3.3 20-QUESTIONS BASED COMMUNICATION SYSTEM

As mentioned in the previous paragraph, the main two drawbacks of the speller are the low typing speed and the wrong selections in case of low classification accuracy. To overcome these problems, in Paper II I have proposed a communication system that is not based on the selections of letters or words, but on the guess of the final sentence based on twenty yes/no questions.

The idea behind this paradigm comes from the popular 20 questions game, where a subject (or a software) is allowed to ask up to twenty yes/no questions in order to guess a word. In the usual game, the guesser will initially ask more general questions (e.g. if the target is a person one typical initial question is whether it is male or female), and it will proceed with always more specific questions. What makes the game interesting for communication purpose is that it works with just a binary input and often is possible to guess the correct word even in presence of some wrong answers, therefore, if applied to a BCI system, it might allow to form a word or a sentence in twenty trials even if some of the trials gets misclassified.

The algorithm of the paradigm has been developed as an artificial neural network (ANN) that links two databases: in the first one all the possible final statements are stored, while in the second one all the possible yes/no ques-

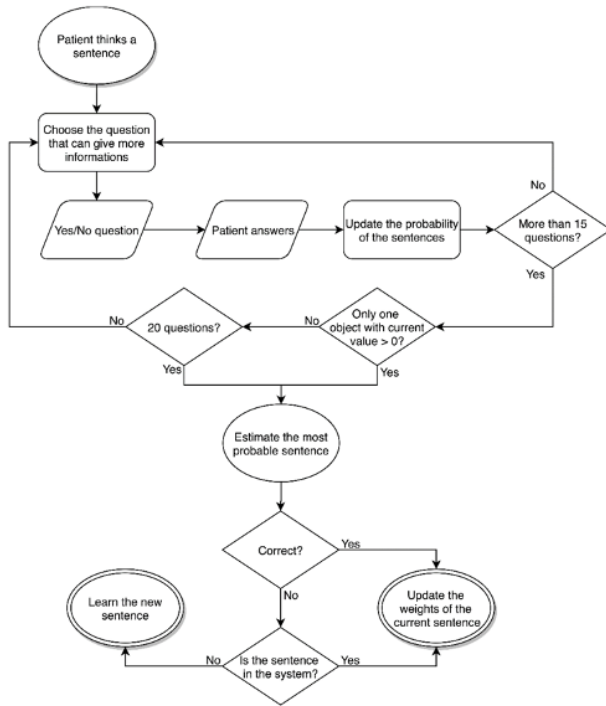


Figure 3.12 - Flow chart of the proposed 20-questions-based communication system. Reprinted from Paper II.

tions are stored. The two databases are linked through a weight matrix that assigns to each target statement the probability of the answer to each question. The ANN presents the questions stored in the database, choosing each question based on the weight matrix and on the previous answers. After a question is made, the ANN updates an internal probability matrix using the weights of the received answer and uses this probability matrix to compute which target statement is the most probable and which question should be ask next in order to maximize the probability of one or another statement. Finally, after twenty questions, the ANN estimation is the target statement with highest probability, and if the estimation is correct it will update the general weight matrix using the new received answers, allowing a learning process that refines and improves the stored probabilities. The schema of the proposed algorithm is reported in Figure 3.12.

The proposed 20-questions based communication system has been tested using a web-based implementation and it has been validated with offline simulations, but it has not been deployed in a real BCI environment, due to the limited available time during experiments with patients.

In the web-based implementation participants were asked to think a sentence and to answer to the proposed questions with “yes”, “no”, or “unsure”. After twenty questions the program proposed the most probable sentence and the participant was asked to mark if it was correct or not and, if it was not present at all in the databases, to add it into the system. Moreover, the participants were also allowed to add new questions to the system. This im-

plementation was available on the internet and it has been used 92 times, out of which 45 times the target was not present in the system. For the remaining 47 times, the system estimated the correct statement 65.95% of the time (31 correct estimation).

Using the databases updated by the online attempts, in order to emulate a non-optimal BCI classification, the system has been validated programmatically simulating different classification accuracies: given a target statement, each answer had a certain probability of being wrong. The results of the simulation, reported in Figure 3.13, show that in presence of a binary classification with accuracy of 80%, most of the time the program correctly estimates the target sentence (as first, second or third estimation).

The results of the simulation are not sufficient to allow a patient in CLIS to communicate reliably, and for this reason the system has not been tested in a real environment. Nevertheless, the results are promising and suggest that this communication system could reliably work by restricting the possible target statements to more specific topics and/or to single words, and by fine-tuning the probability matrix. Moreover, the typing speed reached by such a system is vastly superior to the typing speed of a binary letter-based speller, since it can form full sentences by using just twenty binary trials.

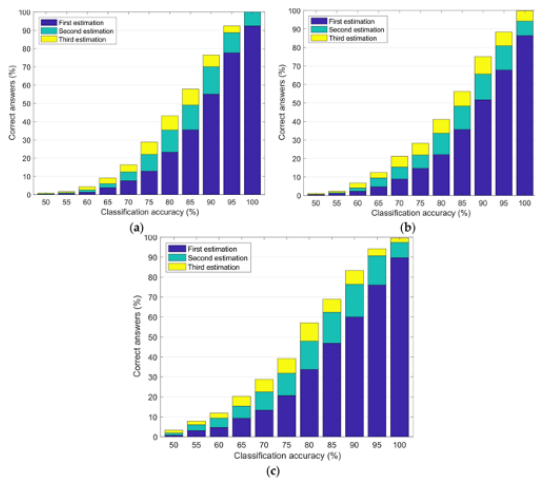


Figure 3.13 – Results of the offline simulation in the three different cases. Blue, green, and yellow represent the percentage of statements correctly estimated as most, second most, and third most probable statement, respectively. **(a)** Simulated results using “yes”, “no”, and “unsure” answers, with the questions answered as “unsure” excluded from the total number of questions; **(b)** simulated results using “yes”, “no”, and “unsure” answers, with the questions answered as “unsure” included in the total number of questions; and **(c)** simulated results using “yes” and “no” answers only. Reprinted from Paper II.

4

Conclusions

In this dissertation I have described different techniques used to build binary communication systems for patients in LIS and CLIS. The most important achieved results are published in Papers I and III where the developed software has been successfully tested to restore communication in four LIS patients by decoding ocular movements and in one CLIS patient by classifying his intracortical activity. In particular, Paper III is the first study ever that es-

established communication with a patient completely paralyzed allowing him to form words and sentences.

The developed software have been structured in a modular way, by separating the signal acquisition part from the proper communication interface. Due to the challenge in acquiring signals from paralyzed patients, my research group decided to reduce the number of variables by focusing on binary classification techniques asking the patients to modulate their activity in just two different ways (or even one single modulation that was classified against no modulation). On one side this decision simplified the development of paradigms for calibration and validation, and it allowed us to use basic binary classification methods, but, on the opposite, it drastically reduced the degrees of freedom that could be used to communicate. Nevertheless, a speller system controlled by binary signal has been designed by optimizing the letter order, making more robust the letter selection, and introducing word suggestion, but at the same time keeping the interface as simple as possible due to the difficulties that the condition of these patients introduces in teaching new paradigms. The modularity of the developed system allowed to use the same speller algorithm with EEG and fNIRS signals (Paper XI), EOG signal (Paper I), and intracortical signal (Paper III). Moreover, these different signals, including also EEG response induced by classical conditioning (Paper IV), have also been used for a more basic binary yes/no communication.

Therefore, the novelty of the findings should not be searched in very advanced and theoretically perfect techniques, but in the translational impact

of efficient interfaces simple enough to be learned by patients that have no means to give any feedback, and flexible enough to be used with several neurophysiological signals of different nature that can be acquired from patients in different conditions.

The positive results of this thesis show that is possible to build a communication system for ALS patients in advanced stage of the disease, nevertheless they also suggest limitations in using just a binary input to command such a system. The most obvious perspective is introducing paradigms that allow a multiclass classification, in order to allow a more natural communication at a higher speed. Some studies (Herff & Schultz, 2016; Rabbani et al., 2019) have already tried to directly decode speech from the brain signals, but these techniques are in very early research stage. Any improvement in communication techniques will become a breakthrough when it will be finally deployed for home-use for the large public outside the scientific community, since, at the moment, the vast majority of LIS and CLIS patients are left unable to communicate once commercial AAC devices stop working. As stated by philosopher Ludwig Hohl: “The Human being lives according to its capacity to communicate, losing communication means losing life”.

Bibliography

- Abel, L. A., Williams, I. M., Gibson, K. L., & Levi, L. (1995). Effects of stimulus velocity and acceleration on smooth pursuit in motor neuron disease. *J. Neurol.*, 242(7), 419–424, doi:10.1007/BF00873543.
- Ball, L. J., Beukelman, D. R., & Pattee, G. L. (2004). Acceptance of Augmentative and Alternative Communication Technology by Persons with Amyotrophic Lateral Sclerosis. *Augment. Altern. Commun.*, 20(2), 113–122, doi:10.1080/0743461042000216596.
- Bauer, G., Gerstenbrand, F., & Rimpl, E. (1979). Varieties of the locked-in syndrome. *J. Neurol.*, doi:10.1007/BF00313105.
- Berger, H. (1929). Über das Elektrenkephalogramm des Menschen. *Arch. Psychiatr. Nervenkr.*, 87(1), 527–570, doi:10.1007/BF01797193.
- Beukelman, D., Fager, S., & Nordness, A. (2011). Communication Support for People with ALS. *Neurol. Res. Int.*, 2011, 1–6, doi:10.1155/2011/714693.
- Beukelman, D. R. & Light, J. C. (2020). *Augmentative and alternative communication*. Baltimore: Paul H. Brookes, 5th edition.
- Birbaumer, N. (2006). Breaking the silence: Brain-computer interfaces (BCI) for communication and motor control. *Psychophysiology*, 43(6), 517–532, doi:10.1111/j.1469-8986.2006.00456.x.
- Birbaumer, N., Ghanayim, N., Hinterberger, T., Iversen, I., Kotchoubey, B., Kübler, A., Perelmouter, J., Taub, E., & Flor, H. (1999). A spelling device for the paralysed. *Nature*, 398(6725), 297–298, doi:10.1038/18581.
- Borghesai, S. B., Mclinden, J., Zisk, A. H., Hosni, S. I., Deligani, R. J., Abtahi, M., Mankodiya, K., & Shahriari, Y. (2020). Enhancing Communication for People in Late-Stage ALS Using an fNIRS-Based BCI System. *IEEE Trans. Neural Syst. Rehabil. Eng.*, 28(5), 1198–1207, doi:10.1109/TNSRE.2020.2980772.

- Buzsáki, G., Anastassiou, C. A., & Koch, C. (2012). The origin of extracellular fields and currents-EEG, ECoG, LFP and spikes. *Nat. Rev. Neurosci.*, 13(6), 407–420, doi:10.1038/nrn3241.
- Byrne, S., Pradhan, F., Dhubhghaill, S. N., Treacy, M., Cassidy, L., & Hardiman, O. (2013). Blink rate in ALS. *Amyotroph. Lateral Scler. Front. Degener.*, 14(4), 291–293, doi:10.3109/21678421.2012.729217.
- Chaudhary, U., Birbaumer, N., & Ramos-Murguialday, A. (2016). Brain-computer interfaces for communication and rehabilitation. *Nat. Rev. Neurol.*, 12(9), 513–525, doi:10.1038/nrneurol.2016.113.
- Chou, S. M. & Norris, F. H. (1993). Amyotrophic lateral sclerosis: Lower motor neuron disease spreading to upper motor neurons. *Muscle Nerve*, 16(8), 864–869, doi:10.1002/mus.880160810.
- Cozza, F., Lizio, A., Greco, L. C., Bona, S., Donvito, G., Carraro, E., Tavazzi, S., Ticozzi, N., Poletti, B., Sansone, V. A., & Lunetta, C. (2021). Ocular involvement occurs frequently at all stages of amyotrophic lateral sclerosis: Preliminary experience in a large Italian cohort. *J. Clin. Neurol.*, 17(1), 96–105, doi:10.3988/jcn.2021.17.1.96.
- Donaghy, C., Pinnock, R., Abrahams, S., Cardwell, C., Hardiman, O., Patterson, V., McGivern, R. C., & Gibson, J. M. (2010). Slow saccades in bulbar-onset motor neurone disease. *J. Neurol.*, 257(7), 1134–1140, doi:10.1007/s00415-010-5478-7.
- Donaghy, C., Thurtell, M. J., Pioro, E. P., Gibson, J. M., & Leigh, R. J. (2011). Eye movements in amyotrophic lateral sclerosis and its mimics: a review with illustrative cases. *J. Neurol. Neurosurg. Psychiatry*, 82(1), 110–116, doi:10.1136/jnnp.2010.212407.
- Fuchino, Y., Nagao, M., Katura, T., Bando, M., Naito, M., Maki, A., Nakamura, K., Hayashi, H., Koizumi, H., & Yoro, T. (2008). High cognitive function of an ALS patient in the totally locked-in state. *Neurosci. Lett.*, 435(2), 85–89, doi:10.1016/j.neulet.2008.01.046.
- Gallegos-Ayala, G., Furdea, A., Takano, K., Ruf, C. A., Flor, H., & Birbaumer, N. (2014). Brain communication in a completely locked-in patient using bedside near-infrared spectroscopy. *Neurology*, 82(21), 1930–1932, doi:10.1212/WNL.000000000000449.

- Goldhahn, D., Eckart, T., & Quasthoff, U. (2012). Building large monolingual dictionaries at the leipzig corpora collection: From 100 to 200 languages. In *Proc. 8th Int. Conf. Lang. Resour. Eval. Lr. 2012* (pp. 759–765). Istanbul, Turkey: European Language Resources Association (ELRA).
- Herff, C. & Schultz, T. (2016). Automatic Speech Recognition from Neural Signals: A Focused Review. *Front. Neurosci.*, 10, doi:10.3389/fnins.2016.00429.
- Hill, N. J., Ricci, E., Haider, S., McCane, L. M., Heckman, S., Wolpaw, J. R., & Vaughan, T. M. (2014). A practical, intuitive brain-computer interface for communicating 'yes' or 'no' by listening. *J. Neural Eng.*, 11(3), doi:10.1088/1741-2560/11/3/035003.
- Hwang, H. J., Han, C. H., Lim, J. H., Kim, Y. W., Choi, S. I., An, K. O., Lee, J. H., Cha, H. S., Hyun Kim, S., & Im, C. H. (2017). Clinical feasibility of brain-computer interface based on steady-state visual evoked potential in patients with locked-in syndrome: Case studies. *Psychophysiology*, 54(3), 444–451, doi:10.1111/psyp.12793.
- Jackson, A. F. & Bolger, D. J. (2014). The neurophysiological bases of EEG and EEG measurement: A review for the rest of us. *Psychophysiology*, 51(11), 1061–1071, doi:10.1111/psyp.12283.
- Jacobs, L., Bozian, D., Heffner, R. R., & Barron, S. A. (1981). An eye movement disorder in amyotrophic lateral sclerosis. *Neurology*, 31(10), 1282–1287, doi:10.1212/wnl.31.10.1282.
- Jöbsis, F. F. (1977). Noninvasive, Infrared Monitoring of Cerebral and Myocardial Oxygen Sufficiency and Circulatory Parameters. *Science (80-)*, 198(4323), 1264–1267, doi:10.1126/science.929199.
- Kang, B. H., Kim, J. I., Lim, Y. M., & Kim, K. K. (2018). Abnormal oculomotor functions in amyotrophic lateral sclerosis. *J. Clin. Neurol.*, 14(4), 464–471, doi:10.3988/jcn.2018.14.4.464.
- Kiernan, M. C., Vucic, S., Cheah, B. C., Turner, M. R., Eisen, A., Hardiman, O., Burrell, J. R., & Zoing, M. C. (2011). Amyotrophic lateral sclerosis. *Lancet*, 377(9769), 942–955, doi:10.1016/S0140-6736(10)61156-7.
- Kim, D. Y., Han, C. H., & Im, C. H. (2018). Development of an

electrooculogram-based human-computer interface using involuntary eye movement by spatially rotating sound for communication of locked-in patients. *Sci. Rep.*, 8(1), 1–10, doi:10.1038/s41598-018-27865-5.

Kübler, A. & Birbaumer, N. (2008). Brain-computer interfaces and communication in paralysis: Extinction of goal directed thinking in completely paralysed patients? *Clin. Neurophysiol.*, 119(11), 2658–2666, doi:10.1016/j.clinph.2008.06.019.

Kübler, A., Furdea, A., Halder, S., Hammer, E. M., Nijboer, F., & Kotchoubey, B. (2009). A brain-computer interface controlled auditory event-related potential (p300) spelling system for locked-in patients. *Ann. N. Y. Acad. Sci.*, 1157, 90–100, doi:10.1111/j.1749-6632.2008.04122.x.

Lesenfants, D., Habbal, D., Lugo, Z., Lebeau, M., Horki, P., Amico, E., Pokorny, C., Gómez, F., Soddu, A., Müller-Putz, G., Laureys, S., & Noirhomme, Q. (2014). An independent SSVEP-based brain-computer interface in locked-in syndrome. *J. Neural Eng.*, 11(3), 035002, doi:10.1088/1741-2560/11/3/035002.

Lim, J. H., Hwang, H. J., Han, C. H., Jung, K. Y., & Im, C. H. (2013). Classification of binary intentions for individuals with impaired oculomotor function: 'eyes-closed' SSVEP-based brain-computer interface. *J. Neural Eng.*, 10(3), doi:10.1088/1741-2560/10/3/039501.

Linse, K., Rüger, W., Joos, M., Schmitz-Peiffer, H., Storch, A., & Hermann, A. (2018). Usability of eyetracking computer systems and impact on psychological wellbeing in patients with advanced amyotrophic lateral sclerosis. *Amyotroph. Lateral Scler. Front. Degener.*, 19(3-4), 212–219, doi:10.1080/21678421.2017.1392576.

Logroscino, G., Traynor, B. J., Hardiman, O., Chió, A., Mitchell, D., Swingler, R. J., Millul, A., Benn, E., & Beghi, E. (2010). Incidence of amyotrophic lateral sclerosis in Europe. *J. Neurol. Neurosurg. Psychiatry*, 81(4), 385–390, doi:10.1136/jnnp.2009.183525.

Lomen-Hoerth, C., Murphy, J., Langmore, S., Kramer, J. H., Olney, R. K., & Miller, B. (2003). Are amyotrophic lateral sclerosis patients cognitively normal? *Neurology*, 60(7), 1094–1097, doi:10.1212/01.WNL.0000055861.95202.8D.

McCane, L. M., Sellers, E. W., McFarland, D. J., Mak, J. N., Carmack, C. S., Zeitlin, D., Wolpaw, J. R., & Vaughan, T. M. (2014). Brain-computer interface (BCI) evaluation in people with amyotrophic lateral sclerosis. *Amyotroph. Lateral Scler. Front. Degener.*, 15(3-4), 207-215, doi:10.3109/21678421.2013.865750.

Milekovic, T., Sarma, A. A., Bacher, D., Simeral, J. D., Saab, J., Pandarinath, C., Sorice, B. L., Blabe, C., Oakley, E. M., Tringale, K. R., Eskandar, E., Cash, S. S., Henderson, J. M., Shenoy, K. V., Donoghue, J. P., & Hochberg, L. R. (2018). Stable long-term BCI-enabled communication in ALS and locked-in syndrome using LFP signals. *J. Neurophysiol.*, 120(1), 343-360, doi:10.1152/jn.00493.2017.

Müller-Putz, G. R., Scherer, R., Brunner, C., Leeb, R., & Pfurtscheller, G. (2008). Better than random? A closer look on BCI results. *Int. J. Bioelectromagn.*, 10(1), 52-55.

Murguialday, A. R., Hill, J., Bensch, M., Martens, S., Halder, S., Nijboer, F., Schoelkopf, B., Birbaumer, N., & Gharabaghi, A. (2011). Transition from the locked in to the completely locked-in state: A physiological analysis. *Clin. Neurophysiol.*, 122(5), 925-933, doi:10.1016/j.clinph.2010.08.019.

Okahara, Y., Takano, K., Nagao, M., Kondo, K., Iwadate, Y., Birbaumer, N., & Kansaku, K. (2018). Long-term use of a neural prosthesis in progressive paralysis. *Sci. Rep.*, 8(1), 1-8, doi:10.1038/s41598-018-35211-y.

Palmowski, A., Jost, W. H., Prudlo, J., Osterhage, J., Käsmann, B., Schimrigk, K., & Ruprecht, K. W. (1995). Eye movement in amyotrophic lateral sclerosis: a longitudinal study. *Ger. J. Ophthalmol.*, 4(6), 355-62.

Pavlov, I. P. (1927). *Conditioned reflexes: An investigation of the physiological activity of the cerebral cortex*. Oxford University Press.

Peters, B., Bedrick, S., Dudy, S., Eddy, B., Higger, M., Kinsella, M., McLaughlin, D., Memmott, T., Oken, B., Quivira, F., Spaulding, S., Erdogmus, D., & Fried-Oken, M. (2020). SSVEP BCI and Eye Tracking Use by Individuals With Late-Stage ALS and Visual Impairments. *Front. Hum. Neurosci.*, 14(November), 1-15, doi:10.3389/fnhum.2020.595890.

Rabbani, Q., Milsap, G., & Crone, N. E. (2019). The Potential for a Speech Brain-Computer Interface Using Chronic Electrocorticography. *Neurotherapeutics*, 16(1), 144-165, doi:10.1007/s13311-018-00692-2.

Ringholz, G. M., Appel, S. H., Bradshaw, M., Cooke, N. A., Mosnik, D. M., & Schulz, P. E. (2005). Prevalence and patterns of cognitive impairment in sporadic ALS. *Neurology*, doi:10.1212/01.wnl.0000172911.39167.b6.

Ryan, D. B., Colwell, K. A., Throckmorton, C. S., Collins, L. M., Caves, K., & Sellers, E. W. (2018). Evaluating Brain-Computer Interface Performance in an ALS Population: Checkerboard and Color Paradigms. *Clin. EEG Neurosci.*, 49(2), 114–121, doi:10.1177/1550059417737443.

Schnakers, C., Majerus, S., Goldman, S., Boly, M., Eeckhout, P., Gay, S., Pellas, F., Bartsch, V., Peigneux, P., Moonen, G., & Laureys, S. (2008). Cognitive function in the locked-in syndrome. *J. Neurol.*, 255(3), 323–330, doi:10.1007/s00415-008-0544-0.

Sellers, E. W., Vaughan, T. M., & Wolpaw, J. R. (2010). A brain-computer interface for long-term independent home use. *Amyotroph. Lateral Scler.*, 11(5), 449–455, doi:10.3109/17482961003777470.

Silvoni, S., Cavinato, M., Volpato, C., Ruf, C. A., Birbaumer, N., & Piccione, F. (2013). Amyotrophic lateral sclerosis progression and stability of brain-computer interface communication. *Amyotroph. Lateral Scler. Front. Degener.*, 14(5-6), 390–396, doi:10.3109/21678421.2013.770029.

Spataro, R., Ciriacocono, M., Manno, C., & La Bella, V. (2014). The eye-tracking computer device for communication in amyotrophic lateral sclerosis. *Acta Neurol. Scand.*, 130(1), 40–45, doi:10.1111/ane.12214.

Stanton, B. R., Williams, V. C., Leigh, P. N., Williams, S. C. R., Blain, C. R. V., Jarosz, J. M., & Simmons, A. (2007). Altered cortical activation during a motor task in ALS. *J. Neurol.*, 254(9), 1260–1267, doi:10.1007/s00415-006-0513-4.

Vansteensel, M. J., Pels, E. G., Bleichner, M. G., Branco, M. P., Denison, T., Freudenburg, Z. V., Gosselaar, P., Leinders, S., Ottens, T. H., Van Den Boom, M. A., Van Rijen, P. C., Aarnoutse, E. J., & Ramsey, N. F. (2016). Fully Implanted Brain-Computer Interface in a Locked-In Patient with ALS. *N. Engl. J. Med.*, doi:10.1056/nejmoa1608085.

Wilcox, T. & Biondi, M. (2015). fNIRS in the developmental sciences. *Wiley Interdiscip. Rev. Cogn. Sci.*, 6(3), 263–283, doi:10.1002/wcs.1343.

Wolf, J., Safer, A., Wöhrle, J. C., Palm, F., Nix, W. A., Maschke, M., & Grau, A. J. (2017). Todesursachen bei amyotropher Lateralsklerose. *Nervenarzt*, 88(8), 911–918, doi:10.1007/s00115-017-0293-3.



Accepted publications

In this appendix are reported all the accepted publications included in the dissertation.



OPEN

Auditory Electrooculogram-based Communication System for ALS Patients in Transition from Locked-in to Complete Locked-in State

Alessandro Tonin^{1,3}, Andres Jaramillo-Gonzalez^{1,3}, Aygul Rana¹, Majid Khalili-Ardali¹, Niels Birbaumer¹ & Ujwal Chaudhary^{1,2,3✉}

Patients in the transition from locked-in (i.e., a state of almost complete paralysis with voluntary eye movement control, eye blinks or twitches of face muscles, and preserved consciousness) to complete locked-in state (i.e., total paralysis including paralysis of eye-muscles and loss of gaze-fixation, combined with preserved consciousness) are left without any means of communication. An auditory communication system based on electrooculogram (EOG) was developed to enable such patients to communicate. Four amyotrophic lateral sclerosis patients in transition from locked-in state to completely locked-in state, with ALSFRS-R score of 0, unable to use eye trackers for communication, learned to use an auditory EOG-based communication system. The patients, with eye-movement amplitude between the range of $\pm 200\mu\text{V}$ and $\pm 40\mu\text{V}$, were able to form complete sentences and communicate independently and freely, selecting letters from an auditory speller system. A follow-up of one year with one patient shows the feasibility of the proposed system in long-term use and the correlation between speller performance and eye-movement decay. The results of the auditory speller system have the potential to provide a means of communication to patient populations without gaze fixation ability and with low eye-movement amplitude range.

Swiss philosopher Ludwig Hohl stated that “The Human being lives according to its capacity to communicate, losing communication means losing life”¹. Our ability to communicate ideas, thoughts, desires, and emotions shapes and ensures our existence in a social environment. There are several neuronal disorders, such as amyotrophic lateral sclerosis (ALS), or brain stem stroke, among others, which paralyzes the affected individuals severely impairing their communication capacity^{2–5}. The affected paralyzed individuals with intact consciousness, voluntary eye movement control, eye blinks, or twitches of other muscles are said to be in locked-in state (LIS)^{6–11}.

Early and modern descriptions of ALS disease emphasize that oculomotor functions are either spared or resistant to the progression of the disease⁶, and consequently, eye-tracking devices can be used to enable patients in the advanced state of ALS to communicate^{12,13}. Besides, longitudinal studies evaluating eye-tracking as a tool for cognitive assessment report that the progression of the disease does not affect eye-tracking performance⁹. Nevertheless, a subset of the literature reports a wide range of oculomotor dysfunctions in these patients^{14–17} that might prevent the use of eye-tracking devices¹⁸. The most used metric to evaluate the patient's degree of functional impairment is the revised ALS functional rating scale (ALSFRS-R)¹⁹, which is not a precise measure of the ability to communicate. A patient with an ALSFRS-R score of zero can still have eye-movement capability or control over some other muscles of the body, which can be used for communication⁴.

CLIS is an extreme type of LIS, which leads to complete body paralysis, including paralysis of eye-muscles combined with preserved consciousness^{6,20}; therefore, even if the individuals are incapable of voluntary control of any muscular channels of the body, they might remain cognitively intact⁶. Several systemic or traumatic

¹Institute of Medical Psychology and Behavioral Neurobiology, University of Tübingen, Tübingen, Germany. ²Wyss-Center for Bio- and Neuro-Engineering, Geneva, Switzerland. ³These authors contributed equally: Alessandro Tonin and Andres Jaramillo-Gonzalez. ✉e-mail: chaudharyujwal@gmail.com

neurological diseases may result in a LIS with the potential to progress towards CLIS, such as ALS, Guillain-Barré, pontine stroke, end-stage Parkinson disease, multiple sclerosis, traumatic brain injury and others with different etiological and neuropathological features^{47,48}. In the case of ALS patients in LIS who survive longer attached to life-support systems, the disease progression might ultimately destroy the oculomotor control in many patients, leading to the loss of gaze-fixation⁴⁷. Thus, patients become unable to use eye-tracker-based communication technologies and are therefore left without any means of communication. This raises the question, what happens with those ALS patients in transition from LIS to CLIS with highly compromised oculomotor skills unable to retain gaze-fixation, and therefore unable to use eye-tracking systems to communicate?

There is a considerable amount of research related to patients in the early stages of ALS who can successfully achieve communication by using gaze-fixation-based assistive and augmentative communication (AAC) technologies or brain-computer interfaces (BCIs). These patients have intact cognitive skills, residual voluntary movements, intact or partial vision with complete gaze-fixation capabilities. Several examples of communication technologies for ALS patients in LIS can be found in the literature. Concerning BCI-based communication, different types of systems have been developed to provide a means of communication to LIS patients^{43,49,11}, among the most recognized are the ones based in features of the EEG, as the slow cortical potential⁴⁹, or evoked potentials, mainly the P300^{32–26} or SSVEP³⁷; or the BCIs based in metabolic features, as NIRS^{38–34}. Concerning the use of eye-tracking systems, as long as the patients have intact vision and control gaze fixation, commercial systems are an accessible and reliable option to allow them limited communication³⁹. Other types of eye-tracking technologies as the scleral search coils, infrared reflection oculography, or video-oculography (or video-based eye-tracking)³⁴, have not yet been tested on LIS patients to our knowledge. Except for two studies^{38,39}, all the developed BCIs for ALS patients describe patients with remnant muscular activity, remnant eye movement control, or even without assisted ventilation, and in general with ALSFRS-R score above 15.

The progress of ALS often, if not always, diminishes the general capabilities of the patients making BCI-based communication impossible^{7–24}. On the other hand, even though eye movement might be the last remnant voluntary movement before CLIS⁵⁴, during this transitional state from LIS to CLIS, patients become unable to maintain gaze-fixation and, unable to use eye-tracking AAC technologies.

Some electrooculogram (EOG)-based systems have been presented to overcome the limitations of other AAC technologies. However, most of the studies were performed on healthy participants or tested in LIS patients in the early stages of ALS, reporting results of single sessions or sessions performed closely in time, allowing the patients in advanced LIS to reply yes/no questions, but without the feasibility of freely communicate spelling sentences^{35,36}. To our knowledge, no studies report on the long-term use of EOG or eye-tracking for patients on the transition from LIS to CLIS, and how this progression affects communication capabilities using these AAC technologies. Either in clinical descriptions or technical applications, very little is known about how this LIS to CLIS progression affects the oculomotor capabilities precluding the patient's communication.

Considering ALS patients in an advanced state, a first meta-analysis has shown that there is a correlation between the progression of physical impairment and BCI performance³, and a recent one has suggested that the performance of CLIS patients using BCI cannot be differentiated from chance³⁷. The only available long-term studies are either single cases for patients able to perform with a P300-based BCI^{38,39} or a thoroughly home-based BCI longitudinal study⁴⁰ that shows favorable results. However, these studies do not provide details on how the progression affected the performance, particularly for the patients with the lowest ALSFRS-R score.

It has been shown in a single case report³⁴, that during the transition from LIS to CLIS, despite compromised vision due to the dryness and necrosis of the cornea and inability to fixate, some remaining controllable muscles of the eyes continue to function. Hence, there is an opportunity to develop a technology to provide a means of communication in this critical transition. Such a technology would extend these patients' communication capacities until the point the disease progression destroys any volitional motor control. Pursuing that goal, an EOG-based auditory communication system was developed, which enabled patients to communicate independent of their gaze fixation ability and independent of intact vision. This study was performed with four ALS patients in transition from the locked-in state to the completely locked-in state, with ALSFRS-R score of 0, and unable to use eye-trackers effectively for communication, i.e., without any other means of communication. The patients, with eye-movement amplitude between the range of $\pm 200\mu\text{V}$ and $\pm 40\mu\text{V}$, were able to form complete sentences and communicate independently and freely, selecting letters from an auditory speller system. Moreover, the study shows the possibility of using the proposed system for a long-term period, and, for one patient, it shows the decay in the oculomotor control, as reflected in EOG signals, until the complete loss of eye control. Such a communication device will have a significant positive effect on the quality of life of completely paralyzed patients and improve mandatory 24-hours-care.

Results

Four advanced ALS patients (P11, P13, P15, and P16) in the transition from LIS to CLIS, all native German speakers (Table 1), used the developed auditory communication system to select letters to form words and hence sentences. All the patients attended to four different types of auditory sessions: training, feedback, copy spelling, and free spelling session. Each training and feedback sessions consisted of 20 questions with known answers (10 questions with "yes" answer and 10 questions with "no" answer, presented in random order), for example, "Berlin is the capital of Germany" vs. "Paris is the capital of Germany". All the questions were presented auditorily. While in the copy and free spelling sessions, the patients were presented the group of characters and each character auditorily (see "Methods" section for the details). Patients were instructed to move the eyes ("eye-movement") to say "yes" and not to move the eyes ("no eye-movement") to say "no". Features of the EOG signal corresponding to "eye-movement" and "no eye-movement" or "yes" and "no" were extracted to train a binary support vector machine (SVM) to identify "yes" and "no" response. This "yes" and "no" response was then used by the patient to auditorily select letters to form words and hence sentences during the feedback and spelling sessions. Due

Patient	Gender/ Age	ALS type	Medical history	Visits
P11	M/33	Non-bulbar	Aug 2015: Diagnosis	10 visits over 13 months from March 2018 onwards
			Aug 2017: Last use of AAC	
P13	M/58	Bulbar	Jan 2011: Diagnosis	4 visits over 12 months from Jun 2018 onwards
			Jan 2018: Last use of AAC	
P15	F/63	Lower motor neuron predominant (ICD-10: G12.2)	Feb 2017: Diagnosis	2 visits over 5 months from Feb 2019 onwards
			Nov 2018: Last use of AAC	
P16	M/56	Lower motor neuron	Dec 2012: Diagnosis	2 visits over 3 months from March 2019 onwards
			Jun 2018: Last use of AAC	

Table 1. List of participants. The table lists the patient's number, the gender and the age at the time of the first visit, the type of diagnosed ALS, year of diagnosis, and the last use of assistive and augmentative communication (AAC) technologies, and the number of performed visits and their time range.

to the degradation of vision in ALS patients^{14,16,17}, the system was designed to work only in the auditory mode without any video support. We frequently traveled to the patient's home to perform the communication sessions. Each visit (V) lasted for a few days (D), during which the patient performed different session (S) as listed in Supplementary Tables S1–S4.

Eye movement. According to the literature, in healthy subjects, the amplitude of the EOG signal varies from 50 to 3500 μV , and its behavior is practically linear for gaze angles of ± 30 degrees and changes approximately 20 μV for each degree of eye movement^{18,19}. Nevertheless, like any other biopotential, EOG is rarely deterministic; its behavior might vary due to physiological and instrumental factors²⁰. For LIS patients in the transition to CLIS, the range and angle of movement are affected by the progress of the ALS disease, affecting the range of voltage amplitude as well. Figure 1 depicts the horizontal eye movement of P11, P13, P15, and P16 during one of the feedback sessions of their first visit (V01). In each plot, for a particular feedback session, all the questions' responses classified as "yes" or "no" by the SVM models were grouped and averaged. Figure 1 elucidates the differences in the dynamics of the signals corresponding to the "yes" and "no" responses, and it can be observed that each patient used different dynamics to control the auditory communication system.

Figure 2 depicts a decrease in horizontal eye-movement amplitude of P11 over 13 months. During the 12 months period, from March 2018 (V01) to February 2019 (V09), P11 performed feedback sessions with a prediction accuracy above chance level, in which small eye-movements recorded with EOG allow classification of "yes" and "no" signals. Employing the same eye-movement dynamics with an approximate amplitude range smaller than ± 40 μV over 4 months, from V06 (November 2018) to V09 (February 2019), P11 was able to select letters, words and form sentences using the speller. The eye-movement amplitude range decreased to ± 30 μV during V10, i.e., 12 months after the first BCI sessions, because of the progressive paralysis typical of ALS. During V10, model-building for prediction during feedback and spelling sessions was unsuccessful. Thus, V10 was the last visit for a communication attempt by P11 using this paradigm. During this visit, even if this training session allowed to build a model of 80% of cross-validation accuracy (Supplementary Table S1), it proved unsuccessful for predicting any classes from the data (50% accuracy).

In the case of P13, the progression of the disorder has been slower, which can be ascertained by the relatively high and constant amplitude of EOG, in an approximate range of ± 300 μV , but still, he was unable to communicate with the commercial eye-tracker technology. Employing the eye-movement strategy, as shown in Fig. 1B, P13 was able to maintain a constant dynamic to control the auditory communication system for feedback and spelling sessions (see Supplementary Table S2). Similar observations can be drawn for P15 and P16 EOG plots in Fig. 1C,D. During two visits each, they achieved successful performance for feedback and spelling sessions (see Supplementary Tables S3 and S4), with stable eye-movement dynamics.

Speller results. The performance of the SVM during all the feedback sessions by each patient is reported in Fig. 3 as a Receiver-Operating Characteristic (ROC) space. The ROC space of P11, who was followed for one year from March 2018 to March 2019, shows a trend in the performance of the feedback sessions. As shown in Fig. 3A, during the initial visits P11 exhibited a successful feedback performance (markers located in the upper-left corner in the ROC space), while during the later visits, particularly V08 and V09, P11 exhibited a decrease in feedback performance and ultimately by V10, it was impossible to perform a successful feedback session. This negative trend is due to the progressive neurodegeneration associated with ALS¹, which leads to the complete paralysis of all muscles, including eyes muscles. For each of the three patients P13, P15, and P16, the feedback sessions' performances are located mostly in the upper-left region of the ROC space, which means successful feedback performance. Nevertheless, for each of these three patients, a few feedback sessions also fall in the lower-right region of the ROC space. This might be due to a learning process of the patients in which they improved or adjusted their eye-movement strategy or due to the suboptimal performance of the SVM classifier during the first few feedback sessions.

The patients were asked to attempt a spelling session when a model was validated with a successful feedback session, i.e., results above random⁴¹. After the feedback session, patients performed two different types of spelling sessions: copy spelling and free spelling, i.e., sessions in which the patient was asked to spell a predetermined phrase, and sessions in which the patient spelled the sentence she/he desired.

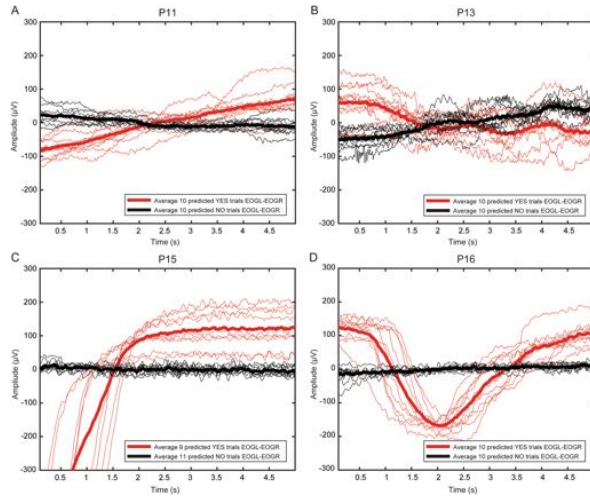


Figure 1. Horizontal eye movement during feedback sessions for all patients. Differential channel EOGL-EOGR for a particular feedback session performed by (A) P11, (B) P13, (C) P15, and (D) P16 during the first visit. In each subfigure, the x-axis is the response time in seconds, and the y-axis is the amplitude of the eye-movement in microvolts (μV). The thin and thick red trace corresponds to a single “yes” response and average of all the “yes” responses, respectively. The black thin and thick trace corresponds to a single “no” response and average of all the “no” response. The box at the bottom right of each subfigure lists the number of trials classified as “yes” and “no” by the SVM classifier for that particular session.

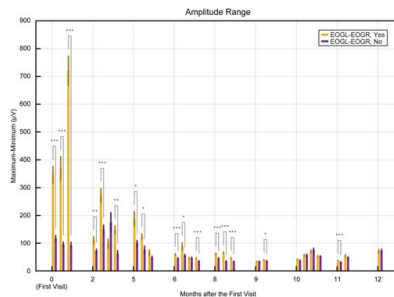


Figure 2. Progressive decline of the eye-movement amplitude along the visits for P11. Depicts the trend of decline in the range of the amplitude of the EOG signal for yes/no questions answered by the patient during the period March 2018 to March 2019. The figure shows the mean and the standard error of the mean of the extracted range of the amplitude of the horizontal EOG signal across each day for yes and no trials. The x-axis represents the month of the sessions, and the y-axis represents the amplitude in microvolts. The asterisk (* - p-value less than 0.05; ** - p-value less than 0.01; *** - p-value less than 0.001) in the figure represents the results of the significance test performed between yes and no for horizontal EOG employing the Mann-Whitney U-test.

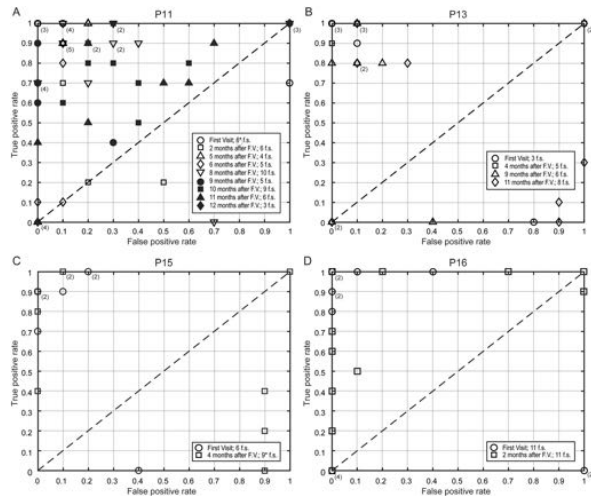


Figure 3. ROC space of feedback sessions for the four patients. Receiver operating characteristic (ROC) space for the performance of the binary support vector machine (SVM) classifier during the total number of feedback sessions performed by (A) P11, (B) P13, (C) P15, and (D) P16. In the figures, the x-axis is the false positive rate (FPR), and the y-axis is the true positive rate (TPR). The diagonal line dividing the ROC space represents a 50% level. Points above the diagonal represent good classification results (accuracy better than 50%), points below the line represent poor classification results (accuracy worse than 50%). In each subfigure, FPR vs. TPR for the feedback sessions are indicated by different arbitrary symbols according to the visit (V) they belong and the date, as defined in the legend at the bottom right side of each subfigure. The rectangular box at the bottom right of each subfigure lists the visit's month and the number of feedback sessions performed during each visit. Some feedback sessions have the same coordinate values in the ROC space, and their symbols overlapped; in these cases, the number of overlapped symbols is specified in parenthesis close to the symbols.

In the developed auditory communication system, the letters have been grouped in different sectors in a layout that was personalized for each patient to match the paper-based layout developed independently by each family (Supplementary Fig. S1). To select one letter, every sector was sequentially presented to the patient and the patient auditorily selected or skipped a sector, once a sector was selected the letters inside the sector were presented auditorily. This select/skip paradigm (i.e., yes/no answer to auditory stimuli) allows the system to work using just a binary yes/no response. The patient could form words by selecting every single letter, but the speed of the system was improved by a word predictor, which, based on the previous selections, suggested the completion of a word whenever it was probable. The speller algorithm is described in detail in the section Speller algorithm.

The results of the copy spelling sessions performed by all the patients are reported in Supplementary Table S5. As shown in Table 2, P11 performed 14 copy-spelling sessions out of which 7 times he correctly copy-spelled the target phrase. Moreover, in one of the other cases, he just miss-selected one letter, and in another one, he selected only one of the two requested words. P13 over 8 sessions copy spelled correctly the target word 6 times. P15 selected correctly the target phrase 3 times out of 5 sessions. Finally, P16 was able to correctly copy spell a target phrase 3 out of 5 sessions. The typing speed achieved by each patient is shown in Table 2.

The system can present one question every 9 seconds, which implies an information transfer rate of 6.7 bits/min. The optimal speed of the speller, along with the user accuracy, depends on the two factors mentioned: first, the speller design for the letter selection (Supplementary Fig. S1); second, the collection of stored sentences (i.e., corpus) needed for the word prediction. In order to describe and evaluate the performance, the sentence "Ich bin" (German for "I am") followed by the name of the patient was considered as a standard example for P11 and P13, while the name of the spouse was considered for P15 and P16. These standard example sentences are composed of 13, 11, 5, and 6 characters for P11, P13, P15, and P16, respectively. Therefore, considering no errors in the answers' classification, the average typing speed for the sentence mentioned above is 1.14 char/min for P11, 1.19 char/min for P13, 1.08 char/min for P15, and 0.87 char/min for P16. These theoretical results show that, due

Type	Patient	Number of sessions	Characters selected	Speed (char/min)
Copy	P11	7/14	5,28 ± 3,59	0,54 ± 0,30
	P13	6/8	4,00 ± 1,67	0,50 ± 0,35
	P15	3/5	5,00 ± 0,00	0,49 ± 0,30
	P16	3/5	5,00 ± 1,73	0,69 ± 0,14
Free	P11	5/9	11,60 ± 8,79	0,57 ± 0,29
	P13	10/11	13,00 ± 10,34	0,48 ± 0,24
	P15	4/5	26,67 ± 19,14	0,68 ± 0,13
	P16	3/3	14,00 ± 4,36	0,64 ± 0,13

Table 2. Results of the spelling sessions performed by the four patients. The columns indicate the type of sessions, the patient, the number of considered sessions over the total number of sessions, the number of characters selected (mean ± standard deviation), and the typing speed in characters per minute (mean ± standard deviation). For the copy and free spelling sessions, only the sessions in which the target was spelled correctly, and the spelled sentence was meaningful, respectively, have been considered. Sessions have been excluded a priori if an error in the code occurred, if the signal was noisy, if they terminated before 15 trials, if the patient did not select any letter, or if all the answers have been classified only as “yes” or only as “no”: in total 6 sessions from P11, 2 sessions from P13, 10 sessions from P15, and 3 sessions from P16 were excluded.

to the word prediction, the performance of the speller improves when the patient auditorily spells a complete sentence rather than a single word. The difference between the theoretical and the real typing speed is due to the nature of the speller that requires many inputs to correct a mistake, e.g., if a sector is wrongly skipped, to select that sector again the patient must first skip all the other sectors.

After successful copy spelling sessions, the patients were free to form words and sentences of their choice. The results of these free spelling sessions performed by all the patients are reported in Supplementary Table S6. The typing speed in these sessions is similar to the speed achieved by each patient during the copy spelling; one exception is P13 who due to the low number of errors and to better words' prediction reached the speed of 1.02 char/min during one of the sessions shown in Supplementary Table S6. In most of the sessions, the patients were able to form complete sentences communicating their feelings and their needs. Nonetheless, some of the performed sessions were not successful. Videos of selected spelling sessions are available in Supplementary Videos S1–S3.

Discussion

The auditory communication system enabled four ALS patients, with ALSFRS-R score of 0, on the verge to CLIS to select letters and words to form sentences. Three out of the four patients (P13, P15, and P16) showed, during all the sessions, a preserved eye movement. One patient (P11), followed over one year from March 2018 to March 2019, demonstrated an effective eye-movement control until the penultimate visit (V09 in February 2019), despite August 2017 being the last successful communication with a commercial AAC device. However, the progression of the disease varies from patient to patient.

Nonetheless, P11's successful results of V09, even if not perfect, are very encouraging since they show the possibility of communicating even with an eye-movement amplitude range of $\pm 30 \mu\text{V}$. Even if the developed auditory communication system was used only from V06, the evolution of eye movements of P11 (Fig. 2) indicates that the eye signal was clear enough to be used for communication purposes since the first visit in March 2018. The results of the feedback sessions confirm this during the initial five visits (Fig. 3A). Speed is the main limitation of the developed system since the spelling of one single word could take up to 10 minutes. In the literature, other spelling systems have been successfully tested with ALS patients, and they achieved an information transfer rate of 16.2 bits/min⁴⁴ and 19.95 bits/min⁴⁵. However, since all of them are based on visual paradigms, except a single study where the patients communicated just “yes” or “no” using an auditory system⁴⁶, comparison with the here proposed system is difficult. The slow speed of our system is an intrinsic characteristic of its auditory nature, even though the spelling time can be reduced by optimizing the speller schema and improving the word prediction with the creation of a corpus of words personalized for each patient. Even though the user experience was not assessed with a questionnaire, it is vital to notice that the patients showed no frustration for this slow speed, which they indicated by moving their eyes when questioned, “Would you like to continue?”. The patient formed sentences like, “I am Happy”, “I am happy to see my grandchildren growing up”, and “I look forward to a vacation” indicating their willingness to communicate. From these, we infer speculatively that the slow speed did not frustrate the patients, probably because even this slow communication is preferred and valued in comparison to the isolation experienced without a functioning eye-tracker. It is essential to employ such a paradigm and follow these patients regularly to elucidate their eye-movement dynamics further and provide them a means of communication.

In conclusion, the long-term viability of an EOG based auditory speller system in ALS patients on the verge of CLIS (with ALSFRS-R score of 0) unable to use eye-tracking based AAC technologies were explored. For one of the patients, it was possible to perform a long-term recording, capturing the changes in the EOG signal, evidencing a correlation between speller performance and progressive degeneration of the oculomotor control. After a follow-up of one year, the patient was unable to take advantage of the spelling system proposed because of the complete loss of oculomotor control. Although the reported system cannot be considered as the ultimate communication solution for these patients according to the best of the authors' knowledge, this is the only system

that, during the period of transition from LIS to CLIS, might offer a means of communication that otherwise is not possible. Nevertheless, whether this can be generalized to other patient populations or not is an empirical question.

Methods

The Internal Review Board of the Medical Faculty of the University of Tübingen approved the experiment reported in this study. The study was performed per the guideline established by the Medical Faculty of the University of Tübingen. The patient or the patients' legal representative gave informed consent with permission to publish the results and to publish videos and pictures of patients. The clinical trial registration number is ClinicalTrials.gov Identifier: NCT02980380.

Instrumentation. During all the sessions, EOG channels were recorded with a 16 channel EEG amplifier (V-Amp DC, Brain Products, Germany) with Ag/AgCl active electrodes. A total of four EOG electrodes were recorded (positions SO1 and IO1 for vertical eye movement, and LO1 and LO2 for horizontal eye movement). During some sessions, a minimum of seven EEG channels were recorded for analysis, not directly related to the purpose of this paper. All the channels were referenced to an electrode on the right mastoid and grounded to the electrode placed at the FPz location on the scalp. For the montage, electrode impedances were kept below 10 k Ω . The sampling frequency was 500 Hz.

Patients. Four ALS patients with ALSFRS-R score of 0 participated in this study. Table 1 summarizes the clinical history of each patient and lists the number of visits (V). After the last successful use of AAC, all the four patients were still communicating with the relatives saying "yes" and "no" by moving and not moving the eyes. Using this technique, patients P11, P13, and P15 were forming words by selecting letters from a paper-based layout (Supplementary Fig. S1A–C) developed, independently, by each family. These same layouts were integrated into our developed system to provide each patient with a personalized schema for selecting letters. For patient P16, based on the feedback and suggestions of the family members, we proposed and tested the spelling schema shown in Supplementary Fig. S1D.

Paradigm. The developed paradigm is based on a binary system, in which a patient is asked to reply to an auditorily presented question by moving the eyes to say "yes" and by not moving the eyes to say "no". The paradigm includes four different types of sessions: training, feedback, copy spelling, and free spelling session. Each training and feedback session consists of 10 questions with a "yes" answer and 10 questions with a "no" answer well known by the patient. Each question represents a trial. Copy and free spelling sessions consist of yes/no questions (i.e., trial) in which a patient is asked whether he wants to select a particular letter or group of letters (see the below paragraph Speller algorithm). Each of these trials consists of the baseline (i.e., no sound presented), the stimulus (i.e., auditory presentation of the question and the speller options), the response time (i.e., time for the patient to move or not move the eyes), and feedback (i.e., auditory feedback to the patient to indicate the end of the response time). The training sessions differ from the feedback sessions in terms of the feedback that is provided to the patient. During the training sessions, the feedback is a neutral stimulus ("Danke" – "Thank you" in English) to indicate the end of the response time, while during the feedback sessions, the feedback is the answer that the program classifies (see Online analysis for details). Copy and free spelling sessions differ in terms of the instruction given to the patient. During the copy spelling sessions, the patient was asked to spell a specific sentence, while during the free spelling sessions, the patient was asked to spell whatever he desired.

The length of the response time-window was determined according to the progress and performance of the patient as described in the Supplementary Tables S1–S4 and varies between 3 and 10 seconds. The duration of each trial varies accordingly between 9 and 20 seconds. Therefore, each training and feedback session lasted for 3–7 minutes. The spelling sessions were usually longer (up to 57 minutes), but no fixed time can be indicated since the number of trials is different from session to session; on average, the copy and free spelling sessions lasted respectively for 10 and 27 minutes.

Speller algorithm. After the patients were unable to communicate with the commercial eye-tracker based AACs devices, the primary caretakers developed a speller design/layout. The auditory speller layouts used here were developed by optimizing and automatizing the schematics already used by the primary caretakers. The spellers used by the patients are shown in Supplementary Fig. S1. The spellers consist of letters grouped in different sectors, plus one sector with some special characters ("space", "backspace" for P11 and P15, and for P13 and P16 along with these the additional option, "delete the word"). Despite the different layouts, the same algorithm, as described below, drives all the spellers. The spellers enable the patients to auditorily select letters and compose words. To increase the speed of the sentence completion, the speller predicts and proposes words based on the letters previously chosen. The auditory speller developed to enable patients without any means of communication to spell letters, words freely, and form sentences auditorily have two main components called "Letter selection" and "Word prediction", which are described below.

Letter selection. The patient, in order to select a letter, first must select the corresponding sector, and only once he is inside the sector, he can select the letter. The selection is made, answering "yes" or "no" to the auditory presentation of a sector or a letter. As schematized in the diagram in Supplementary Fig. S2, to avoid false positives, the speller uses a single-no/double-yes strategy. If the recognized answer is "no" the sector is not selected, and the following sector will be asked, if the answer is "yes" the same sector is asked a second time as a confirmation: the sector is selected if the patient replies "yes" also the second time. If the last sector is not selected, the program asks the patient whether he wants to quit the program. If he replies "yes", and confirms the answer, the program is quit.

Otherwise, the algorithm restarts from the first sector. Once a sector is selected, the paradigm for selecting a letter (or a special character) uses the same single-no/double-yes strategy as described above. If none of the letters in a sector is selected, the patient is asked to exit the sector. If he replies a confirmed “yes” the speller goes back asking the sectors starting from the one after the current, otherwise, if he replies “no”, the algorithm asks the letters of the current sector again starting from the first one. Whenever a letter or a special character is selected, the speller updates the current string and gives auditory feedback reading the words already completed (i.e., followed by a space) and spelling the last one if it is not complete. After every selected letter, the speller searches for probable words based on the current string (the details are explained in the paragraph below). If a word is probable, the program presents that word auditorily. Otherwise, it starts the letter selection algorithm from the first sector again.

Word prediction. To speed up the formulation of sentences, the speller is provided with a word predictor that compares the current string with a language corpus to find if there is any word that has a high probability of being the desired one. To have a complete and reliable vocabulary, the German general corpus of 10000 sentences compiled by the Leipzig University⁴⁷ was used. Since the developed speller contains only English letters, firstly the corpus is normalized converting the special German graphemes (ä, ö, ü, ß) with their usual substitutions (ae, oe, ue, ss). Thus, a conditional frequency distribution (CFD) is created based on the n-gram analysis of the normalized corpus; for word prediction, we considered the frequencies of the single words (i.e., unigrams), of two consecutive words (i.e., bigrams), and three consecutive words (i.e., trigrams). Whenever a letter is added to the current string, the program returns the CFD of all the words starting with the current non-completed word (if the last word is complete, it considers all the possible words). For these words first, the frequency value is considered concerning the two previous words, i.e., trigram frequency. Then, if for the current string, there is any stored trigram in the corpus, the program considers only the last complete word and checks the bigram frequency. Finally, if it is not possible to find any bigram, it considers the overall frequency value of the single word, i.e., unigram frequency. Once all the frequency values of the words are stored, considered as trigrams, bigrams, or unigrams, the program establishes if any of these words are highly probable comparing their values to a predefined threshold. To predict words, we considered a word as probable if its frequency value is more significant than half of the sum of all the frequency values of the possible words. If a word is detected as probable, the speller, after a letter is selected, instead of restarting the algorithm from the first sector, proposes that word to the patient, and if a confirmed “yes” is answered it adds the word followed by a space to the current string.

Online analysis. The EOG data were acquired online in real-time throughout all the sessions. During all the trials belonging to a session (except for the training sessions), the signal of the response time was processed in real-time to extract features to be fed to a classification algorithm for classifying the “yes” and “no” answers. Features computed from the trials of the training sessions were used to train an SVM classifier that was validated through 5-fold cross-validation. The obtained SVM classifier was used to classify feedback and speller sessions only if its accuracy was higher than the upper threshold of chance-level⁴⁵.

To extract the features from the signal during the response time, the time-series were first preprocessed with a digital finite impulse response (FIR) filter in the passband of 0.1 to 35 Hz and with a notch filter at 50 Hz. The first 50 data points were removed to eliminate filtering-related transitory border effects at the beginning of the signal. Then all the channels were standardized to have a mean of zero and a standard deviation of one. Subsequently, features were extracted from all the data series from the “yes” and “no” answer for all the channels.

Different features were extracted for the different patients: for P11 and P13 the maximum and minimum amplitude and their respective value of time occurrence feature were used; while for P15 and P16 the range of the amplitude (i.e., the difference between the values of maximum and minimum amplitude) feature was used.

The code was developed and run in Matlab_R2017a. For the SVM classification, the library LibSVM⁴⁸ was used. The detailed list of sessions used for building the model and, therefore, perform feedback and spelling sessions are described in the Supplementary Tables S1–S4.

Receiver-operating characteristic space. For binary classifiers in which the result is only positive or negative, there are four possible outcomes. When the outcome of the prediction of the answer is yes (positive), and the actual value is positive, it is called True Positive (TP); however, if the actual answer to a positive question response is negative, then it is a False Negative (FN). Complementarily, when the predicted answer is negative, and the actual answer is also negative, this is a True Negative (TN), and if the prediction outcome is negative and the actual answer is positive, it is a False Negative (FN). With these values, it is possible to formulate a confusion or contingency matrix, which is useful to describe the performance of the classifier employing its tradeoffs between sensitivity and specificity. The contingency matrix can be used to derive several evaluation metrics, but it is particularly useful for describing and visualizing the performance of classifiers via the Receiver-Operating Characteristic (ROC) space⁴⁹. A ROC space depicts the relationship between the True Positive Rate (TPR) and the False Positive Rate (FPR). TPR and FPR were calculated for each feedback session, and they were then used to draw ROC space, as shown in Fig. 3.

Data availability

The data and the scripts are available without any restrictions. The correspondence between sessions and the corresponding raw files are listed in Supplementary Table S7. Data link <https://doi.org/10.5281/zenodo.3605395>.

Received: 2 October 2019; Accepted: 30 April 2020;

Published online: 21 May 2020

References

- Hohl, L. Die Notizen oder Von der unvoreiligen Versöhnung. (Suhrkamp, 1981).
- Birbaumer, N. & Chaudhary, U. Learning from brain control: clinical application of brain-computer interfaces. *e-Neuroforum*. <https://doi.org/10.1515/s13295-015-0015-x> (2015).
- Birbaumer, N. Breaking the silence: Brain-computer interfaces (BCI) for communication and motor control. in *Psychophysiology* <https://doi.org/10.1111/1469-8986.2006.00456.x> (2006).
- Chaudhary, U., Birbaumer, N. & Ramos-Murguialday, A. Brain-computer interfaces for communication and rehabilitation. *Nat. Rev. Neurol.* **12**, 513–525 (2016).
- Brownlee, A. & Bruneing, L. M. Methods of communication at end of life for the person with amyotrophic lateral sclerosis. *Topics in Language Disorders* <https://doi.org/10.1097/TLD.0b013e31825616ef> (2012).
- Bauer, G., Gerstenbrand, F. & Rumpel, E. Varieties of the locked-in syndrome. *J. Neurol.* <https://doi.org/10.1007/BF00313105> (1979).
- Kübler, A. & Birbaumer, N. Brain-computer interfaces and communication in paralysis: Extinction of goal directed thinking in completely paralysed patients? *Clin. Neurophysiol.* **119**, 2658–2666 (2008).
- Chaudhary, U., Mrachacz-Kersing, N. & Birbaumer, N. Neuropsychological and neurophysiological aspects of brain-computer interface (BCI)-control in paralysis. *J. Physiol.* <https://doi.org/10.1113/jp278775> (2020).
- Beedman, E. et al. The cognitive profile of ALS: A systematic review and meta-analysis update. *Journal of Neurology, Neurosurgery and Psychiatry* **87**, 611–619 (2016).
- Chaudhary, U., Birbaumer, N. & Ramos-Murguialday, A. Brain-computer interfaces in the completely locked-in state and chronic stroke. in *Progress in Brain Research* <https://doi.org/10.1016/bs.pbr.2016.04.019> (2016).
- Chaudhary, U., Birbaumer, N. & Curado, M. R. Brain-Machine Interface (BMI) in paralysis. *Ann. Phys. Rehabil. Med.* <https://doi.org/10.1016/j.rehab.2014.11.002> (2015).
- Calvo, A. et al. Eye tracking impact on quality-of-life of ALS patients. in *International Conference on Computers for Handicapped Persons 70-77* (2008). Springer, Berlin, Heidelberg.
- Hwang, C. S., Weng, H. H., Wang, L. F., Tsai, C. H. & Chang, H. T. An eye-tracking assistive device improves the quality of life for ALS patients and reduces the caregivers' burden. *Journal of motor behavior* **46**, 233–238 (2014).
- Jacobs, L., Bozian, D., Hefner, R. R. & Barron, S. A. An eye movement disorder in amyotrophic lateral sclerosis. *Neurology* **31**, 1282–1282 (1981).
- Hayashi, H. & Oppenheimer, E. A. ALS patients on TPPV: totally locked-in state, neurologic findings and ethical implications. *Neurology* **61**, 135–137 (2003).
- Leveille, A., Klerman, J., Goodwin, J. A. & Antel, J. Eye movements in amyotrophic lateral sclerosis. *Archives of Neurology* **39**, 684–686 (1982).
- Gorges, M. et al. Eye movement deficits are consistent with a staging model of pTDP-43 pathology in amyotrophic lateral sclerosis. *PLoS one*, **10** (2015).
- Spataro, R., Ciriaco, M., Manno, C. & La Bella, V. The eye-tracking computer device for communication in amyotrophic lateral sclerosis. *Acta Neurologica Scandinavica* **130**, 40–45 (2014).
- Cedarbaum, J. M. et al. The ALSFRS-R: a revised ALS functional rating scale that incorporates assessments of respiratory function. *Journal of the neurological sciences* **169**, 13–21 (1999).
- Tachino, Y. et al. High cognitive function of an ALS patient in the totally locked-in state. *Neuroscience letters* **435**, 85–89 (2008).
- Birbaumer, N. et al. A spelling device for the paralysed. *Nature* <https://doi.org/10.1038/18581> (1999).
- Spier, W., Chandradavala, N., Roberts, D., Pendekanti, S. & Pouratian, N. Online BCI typing using language model classifiers by ALS patients in their homes. *Brain-Computer Interfaces* **4**, 114–121 (2017).
- McCane, L. M. et al. P300-based brain-computer interface (BCI) event-related potentials (ERPs): People with amyotrophic lateral sclerosis (ALS) vs. age-matched controls. *Clin. Neurophysiol.* <https://doi.org/10.1016/j.clinph.2015.01.013> (2015).
- Cipresso, P. et al. The use of P300-based BCIs in amyotrophic lateral sclerosis: From augmentative and alternative communication to cognitive assessment. *Brain and Behavior* **2**, 479–498 (2012).
- Guy, V. et al. Brain computer interface with the P300 speller: Usability for disabled people with amyotrophic lateral sclerosis. *Ann. Phys. Rehabil. Med.* **61**, 5–11 (2018).
- Krusienski, D. J., Sellers, E. W., McFarland, D. J., Vaughan, T. M. & Wolpaw, J. R. Toward enhanced P300 speller performance. *J. Neurosci. Methods* **167**, 15–21 (2008).
- Lim, J. H. et al. An emergency call system for patients in locked-in state using an SSVEP-based brain switch. *Psychophysiology* **54**, 1632–1643 (2017).
- Gallegos-Ayala, G. et al. Brain communication in a completely locked-in patient using bedside near-infrared spectroscopy. *Neurology* **82**, 1930–1932 (2014).
- Naito, M. et al. A communication means for totally locked-in ALS patients based on changes in cerebral blood volume measured with near-infrared light. *IEICE Trans. Inf. Syst.* <https://doi.org/10.1093/ietisy/e90-d.7.1028> (2007).
- Chaudhary, U., Xia, B., Silvoni, S., Cohen, L. G. & Birbaumer, N. Brain-computer interface-based communication in the completely locked-in state. *PLoS biology* **15**, e1002593 (2017).
- Khalili Ardali, M., Rana, A., Purmohammad, M., Birbaumer, N. & Chaudhary, U. Semantic and BCI-performance in completely paralyzed patients: Possibility of language attrition in completely locked in syndrome. *Brain Lang.* <https://doi.org/10.1016/j.bandl.2019.05.004> (2019).
- Beukelman, D., Fieger, S. & Nordness, A. Communication support for people with ALS. *Neurology Research International* <https://doi.org/10.1155/2011/714693> (2011).
- Duchowski, A. *Eye tracking methodology: Theory and practice*. *Eye Tracking Methodology: Theory and Practice* <https://doi.org/10.1007/978-1-84628-609-4> (2007).
- Murguialday, A. R. et al. Transition from the locked in to the completely locked-in state: A physiological analysis. *Clin. Neurophysiol.* <https://doi.org/10.1016/j.clinph.2010.08.019> (2011).
- Chang, W. D. U., Cha, H. S., Kim, D. Y., Kim, S. H. & Im, C. H. Development of an electrooculogram-based eye-computer interface for communication in amyotrophic lateral sclerosis. *J. Neuroeng. Rehabil.* **14**, 7–9 (2017).
- Kim, D. Y., Han, C. H. & Im, C. H. Development of an electrooculogram-based human-computer interface using involuntary eye movement by spatially rotating sound for communication of locked-in patients. *Sci. Rep.* **8**, 1–10 (2018).
- Marchetti, M. & Priftis, K. Brain-computer interfaces in amyotrophic lateral sclerosis: A metanalysis. *Clin. Neurophysiol.* **126**, 1255–1263 (2015).
- Holz, E. M., Botrel, L., Kaufmann, T. & Kübler, A. Long-term independent brain-computer interface home use improves quality of life of a patient in the locked-in state: A case study. *Arch. Phys. Med. Rehabil.* **96**, S16–S26 (2015).
- Sellers, E. W., Vaughan, T. M. & Wolpaw, J. R. A brain-computer interface for long-term independent home use. *Amyotroph. Lateral Scler.* **11**, 449–455 (2010).
- Wolpaw, J. R. et al. Independent home use of a brain-computer interface by people with amyotrophic lateral sclerosis. *Neurology* <https://doi.org/10.1212/wnl.0000000000005812> (2018).
- Schomer, D. L. & Lopes Da Silva, F. *Basic Principles, Clinical Applications, and Related Fields. Niedermeyer's Electroencephalography: Basic Principles, Clinical Applications, and Related Fields* (2010).

42. Barea Navarro, R., Boquete Vázquez, L. & López Guillén, E. EOG-based wheelchair control. in *Smart Wheelchairs and Brain-Computer Interfaces* 381–403 <https://doi.org/10.1016/b978-0-12-812892-3.00016-9> (Elsevier, 2018).
43. Müller-Putz, G. R., Scherer, R., Brunner, C., Leeb, R. & Pfurtscheller, G. Better than random? A closer look on BCI results. *Int. J. Bioelectromagn* **10**, 52–55 (2008).
44. Käthner, I., Kübler, A. & Halder, S. Rapid P300 brain-computer interface communication with a head-mounted display. *Front. Neurosci.* <https://doi.org/10.3389/fnins.2015.00207> (2015).
45. Pires, G., Nunes, U. & Castelo-Branco, M. Comparison of a row-column speller vs. a novel lateral single-character speller: Assessment of BCI for severe motor disabled patients. *Clin. Neurophysiol.* <https://doi.org/10.1016/j.clinph.2011.10.040> (2012).
46. Hill, N. J. et al. A practical, intuitive brain-computer interface for communicating 'yes' or 'no' by listening. *J. Neural Eng.* **11**, (2014).
47. Goldhahn, D., Eckart, T. & Quasthoff, U. Building large monolingual dictionaries at the leipzig corpora collection: From 100 to 200 languages. in *Proceedings of the 8th International Conference on Language Resources and Evaluation, LREC 2012* (2012).
48. Chang, C.-C. & Lin, C.-J. LIBSVM: A Library for Support Vector Machines. *ACM Trans. Intell. Syst. Technol.* **2**, 1–27 (2011).
49. Fawcett, T. An introduction to ROC analysis. *Pattern Recognit. Lett.* <https://doi.org/10.1016/j.patrec.2005.10.010>.

Acknowledgements

Deutsche Forschungsgemeinschaft (DFG) DFG BI 195/77-1, BMBF (German Ministry of Education and Research) 16SV7701 CoMiCon, LUMINOUS-H2020-FETOPEN-2014-2015-RIA (686764), and Wyss Center for Bio and Neuroengineering, Geneva.

Author contributions

Alessandro Tonin – Performed 35% of the BCI sessions and data collection; Data analysis; Manuscript writing. Andres Jaramillo-Gonzalez – Performed 35% of the BCI sessions and data collection; Data analysis; Manuscript writing. Aygul Rana – Performed 35% of the BCI sessions and data collection. Majid Khalili Ardali – Data analysis. Niels Birbaumer – Study design and conceptualization; Manuscript correction. Ujwal Chaudhary – Study design and conceptualization; Performed 65% of the BCI sessions and data collection; Data analysis supervision; Manuscript writing.

Competing interests

The authors declare no competing interests.

Additional information

Supplementary information is available for this paper at <https://doi.org/10.1038/s41598-020-65333-1>.

Correspondence and requests for materials should be addressed to U.C.

Reprints and permissions information is available at www.nature.com/reprints.

Publisher's note Springer Nature remains neutral with regard to jurisdictional claims in published maps and institutional affiliations.



Open Access This article is licensed under a Creative Commons Attribution 4.0 International License, which permits use, sharing, adaptation, distribution and reproduction in any medium or format, as long as you give appropriate credit to the original author(s) and the source, provide a link to the Creative Commons license, and indicate if changes were made. The images or other third party material in this article are included in the article's Creative Commons license, unless indicated otherwise in a credit line to the material. If material is not included in the article's Creative Commons license and your intended use is not permitted by statutory regulation or exceeds the permitted use, you will need to obtain permission directly from the copyright holder. To view a copy of this license, visit <http://creativecommons.org/licenses/by/4.0/>.

© The Author(s) 2020

Article

A 20-Questions-Based Binary Spelling Interface for Communication Systems

Alessandro Tonin¹, Niels Birbaumer^{1,2} and Ujwal Chaudhary^{1,2,*}

¹ Institute of Medical Psychology and Behavioral Neurobiology, University of Tübingen, 72076 Tübingen, Germany; alessandro.tonin@uni-tuebingen.de (A.T.); niels.birbaumer@uni-tuebingen.de (N.B.)

² Wyss-Center for Bio- and Neuro-Engineering, 1202 Geneva, Switzerland

* Correspondence: chaudharyujwal@gmail.com; Tel.: +49-707-129-73254

Received: 11 June 2018; Accepted: 30 June 2018; Published: 2 July 2018



Abstract: Brain computer interfaces (BCIs) enables people with motor impairments to communicate using their brain signals by selecting letters and words from a screen. However, these spellers do not work for people in a complete locked-in state (CLIS). For these patients, a near infrared spectroscopy-based BCI has been developed, allowing them to reply to “yes”/“no” questions with a classification accuracy of 70%. Because of the non-optimal accuracy, a usual character-based speller for selecting letters or words cannot be used. In this paper, a novel spelling interface based on the popular 20-questions-game has been presented, which will allow patients to communicate using only “yes”/“no” answers, even in the presence of poor classification accuracy. The communication system is based on an artificial neural network (ANN) that estimates a statement thought by the patient asking less than 20 questions. The ANN has been tested in a web-based version with healthy participants and in offline simulations. Both results indicate that the proposed system can estimate a patient’s imagined sentence with an accuracy that varies from 40%, in the case of a “yes”/“no” classification accuracy of 70%, and up to 100% in the best case. These results show that the proposed spelling interface could allow patients in CLIS to express their own thoughts, instead of only answer to “yes”/“no” questions.

Keywords: brain computer interface; complete locked-in state; communication; Artificial Neural Network; 20-questions-game

1. Introduction

In the past decades, many alternative communication systems have been developed for people with speech, language, or motor impairments. Brain computer interfaces (BCI) were developed to provide a means of communication for people with severe motor disabilities (for review see Chaudhary et al., 2016) [1–3]. The most commonly used non-invasive BCI spelling application is based on the electroencephalography (EEG) based P300 event-related brain potential, where a patient can select letters from a matrix in which each character is transiently illuminated [4]. Another BCI system commonly used to select letters from a screen is based on steady state visually evoked potential (SSEVP) [5,6]. Other BCI communication systems are based on slow cortical potential [7], and on the sensorimotor rhythm of the EEG [8,9] to control cursors or keyboards on a screen. These systems, even using different signals and different interfaces, are all based on the same general paradigm, namely, that patients communicate by selecting letters or words from a screen. Different features and classification techniques are used to decode the intention of patients [10–12]. Independently from the signal type, all of these BCI systems are based on the control of a neuroelectric brain response, and the learning process is based on feedback and reward. Despite the good results achievable using

these systems with patients suffering from disorders leading to loss of communication, none of these techniques were able to provide a means of communication to amyotrophic lateral sclerosis (ALS) patients in a completely locked-in state (CLIS). An explanation of the non-applicability of the standard BCI in complete paralysis with otherwise intact cognitive processing, Kübler and Birbaumer suggested the theoretical psychophysiological notion of “extinction of goal directed cognition and thought” in CLIS [13]. Following this idea, a BCI based on functional near-infrared spectroscopy (fNIRS) was developed for ‘reflexive’ communication in CLIS. Unlike the other communication systems, it allows the patient to answer short questions affirmatively (“yes”) and negatively (“no”), using the blood oxygenation change of their fronto-central brain regions. The best accuracy reported for correctly classified “yes”/“no” answers is 70% in CLIS [14,15]. The low classification accuracy and the only binary “yes”/“no” answers do not allow the patients to express their own thoughts using a classic character-selection-based speller, but only to answer prerecorded questions.

The limitations of the fNIRS-BCI, especially the restriction to a binary “yes”/“no” signal and a substantial error rate, are common not only to all non-invasive BCI systems, but also to all the telecommunication systems. Using telecommunication words, the BCI problem involves the correct detection of a communication between two agents through a noisy channel. The communication, both in the general case of telecommunication or in the particular case of the “yes”/“no”-BCI, is a binary message sent from the sender (or the brain) to the receiver (the computer), whose information may be distorted in the transmission due to the noise in the channel (wrong classification), and the task of the receiver is to recover the message reconstructing the corrupted signal [16].

The BCI-spellers usually solve the problem of the wrong signal classification with a redundant number of inputs (e.g., flashing each letter multiple times in order to be sure that the selection was not due to a false positive). With the fNIRS-BCI, this technique is because of the characteristic of the fNIRS signal; the fNIRS-BCI system is slow and allows the patient to answer approximately only one question every 20 s. The solution for this kind of BCI would be a speller capable of correcting the errors in the classification of the answers, allowing a patient to communicate using minimum number of inputs.

A solution can be found in a popular game, the 20-questions-game. In this game, a player has to guess what the other player is thinking within 20 “yes”/“no” questions. An electronic version of the game, which has been played more than 88 millions times, can correctly guess what someone is thinking with 80% precision, by asking 20 questions (95% of the time with 25 questions) [17]. The game was mathematically formalized by Alfred Rényi [18] and it was later proposed in a different version by Stanislaw Ulam [19]. The Rényi–Ulam game and its variations have been used to solve many different problems [20–22], in this paper we propose to use the game as a spelling interface for a binary BCI, like the fNIRS-based BCI described in Chaudhary et al. (2017). This kind of communication system may allow patients in CLIS to express their own thoughts and not just to reply to prerecorded questions.

The rest of the paper is structured as follows: in Section 2, the method used to design the communication system is described, and in particular, in Sections 2.1 and 2.2 describe the algorithm of the Rényi–Ulam game and its application to the popular 20-questions-game using an artificial neural network, and in Section 2.3, the implementation as an interface for a BCI system is described. In Section 3, the proposed algorithm is explained in detail. Then, in Section 4, we present the results of the algorithm, both for an online version of the game played by real persons (Section 4.1) and for an offline version with computer simulations (Section 4.2). The results are discussed and followed by the conclusion in Section 5. While the databases used for the results are described in Appendix A.

2. Materials and Methods

2.1. Rényi–Ulam Game

The 20-questions-game is a popular game played by two players. The rules of the game are as follows: the first player (player *A*, the Responder) imagines a famous person, while the second (player *B*, the Questioner) must guess the person by asking twenty “yes”/“no” questions (e.g., “Is the person alive?”).

The game has been mathematically described by Rényi and Ulam, as follows: the Responder can imagine any target statement that is contained in a fixed search space (i.e., the topic, e.g., famous people), while the Questioner has to guess the statement using less than n (e.g., 20) “yes”/“no” questions. Moreover, the Responder is allowed to lie up to e times on the answers given to the “yes”/“no” questions (i.e., they can give wrong answers). The lies are a formalization of the wrong answer that a player can give if their knowledge about the statement is different from the knowledge of the other player (e.g., the Responder thinks that a person is alive, but instead it is dead).

The complete description of the game is outlined below:

1. The game is played by two players: *A* (the Responder) and *B* (the Questioner).
2. A set S of target statements (the search space) is fixed.
3. A number $n > 0$ of questions is fixed.
4. An upper bound $e \geq 0$ of number of lies is fixed.
5. *B* can ask questions in the form of “Is x in T ?”, where T is a subset of S .
6. *A* must reply “yes” or “no”, and he can lie up to e times.
7. *B* wins if he can correctly guess x after n questions.

The number of questions n to solve the Rényi–Ulam game depends linearly on the cardinality of S and on the maximum number of lies e , but for the general case of an arbitrary number of lies, there is no general solution and only heuristic methods have been proposed [23].

2.2. Artificial Neural Network

A heuristic solution of the Rényi–Ulam game with arbitrary number of lies can be found using an artificial neural network (ANN). This method was first developed by Robin Burgener [24] for 20q, an electronic version of the 20-question-game. This version is slightly different from the Rényi–Ulam game; for instance, the allowed answers are not only “yes” and “no”, but also “unknown”, “irrelevant”, “sometimes”, “depends”, etc. Here, we propose an ANN for the original Rényi–Ulam game with binary answers only.

The ANN will play the role of the Questioner, that is, it will ask questions, and it will estimate a particular target statement (e.g., a person) imagined by a Responder. Therefore, in order to work, the ANN needs two databases, one with the target statements belonging to the search space (e.g., all of the possible famous people), and one with the possible “yes”/“no” questions (e.g., “Is it alive?”, “Is it a woman?”, etc.).

The main core of the ANN is the relation between the statements and questions. Each target statement is connected to each question, and the strength of this connection is indicated by a weight. The weights can be negative if the statement and question are not related (i.e., the expected answer is “no”) and positive if they are related (i.e., the expected answer is “yes”). All of the weights are stored in a matrix called a weight matrix.

The ANN will present to the Responder the questions stored in the database. The choice of the question is based on the weight table and on the previous questions.

The final estimation of the ANN is the statement that, based on the received answers, is the most probable. In order to calculate this probability, after each question, the ANN will penalize or reward, based on the answer, the target statements (e.g., if the answer to “Is she a woman?” is “yes”, all male persons will be penalized).

Finally, after each correct final estimation, the weight matrix is updated based on the received answer, allowing a learning process.

Using ANN has two advantages. First, if the Responder occasionally lies, the ANN will not exclude any possible target statement, based on that single answer, but it will only change the probability for the final estimation. Second, the estimation of the target statement will improve with frequent usage of ANN, because the learning process improves the reliability of the weight table.

2.3. 20-Questions-Based Interface for Communication Systems

2.3.1. Proposed BCI Implementation

We endeavor to use the 20-questions-game as a communication system for patients that do not have a reliable means of communication, like patients in a complete locked-in state (CLIS). This system is based on an ANN that interacts with the patient in a 20-questions-based paradigm, in order to estimate their thoughts.

For this purpose, the ANN can be developed as part of a brain-computer interface; the computer proposes auditorily the questions to the patient, and it records a brain signal (e.g., fNIRS). The BCI classifies the brain signal in a binary answer (“yes” or “no”), which will be the answer required by the ANN. In this implementation, the patient will play the role of the Responder, while the ANN will be the Questioner. The patient can think of any word or sentence that is stored in the database of the ANN, and the ANN will ask questions, also stored in the database, in order to estimate the patient’s thought. The “yes”/“no” classification accuracy achieved using BCI systems with CLIS patients is around 70% [14,15]. Using the 20-questions-based system, the errors on the “yes”/“no” classification will be considered as the lies of the Rényi–Ulam game, therefore, they will not automatically lead to a wrong estimation of the sentence.

The proposed 20-questions-based communication system is depicted in Figure 1. The system has been tested as a communication system, independently from the brain signal records, with healthy participants, using a web interface, and with computer simulations.

2.3.2. Web-Based Implementation

The web-based version of the algorithm (www.alsbci.eu) was written in Python and it has been translated into three languages, English, German, and Italian.

In the website, the user is asked to put himself in a complete locked-in patient’s shoes, playing the 20-questions-game by thinking a sentence that could be asked by a patient in such conditions. The search space was intentionally left ambiguous and not bound to a specific topic, in order to check the performance of the system in a not optimal scenario. The user had also the option to check the list of target statements already stored in the database.

During the game, the ANN presented the questions to the user, who had the opportunity to reply “yes”, “no”, or “unsure”. In the case of an “unsure” answer, the ANN ignored the answer and, instead, it was asking a different question. At the end of each game, the ANN tried to estimate the thought sentence three times, proposing to the users the three most probable targets (i.e., the three statements with the highest current value). Finally, if none of the proposed target statements was the correct one, the user could select (or, if not present, insert) the thought sentence directly from the database.

From the website, the users had also the opportunity to improve the databases of the ANN by adding new statements and questions.

The web-based version was initialized with an initial database manually populated with a set of 41 target statements and 25 questions. The website has been online, accessible to everyone since November 2017. Since then, the game has been played 92 times, and 50 new statements and 113 new questions have been added to the system, bringing the total number to 91 statements and 138 questions, respectively (see Appendix A).

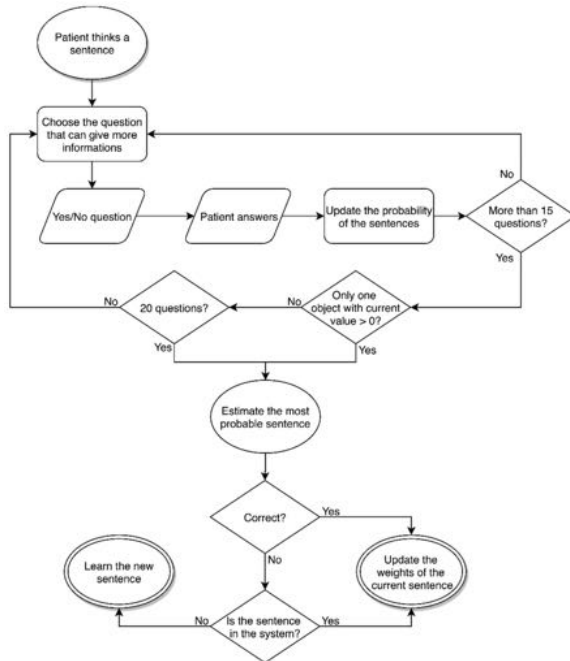


Figure 1. Flow chart of the proposed 20-questions-based communication system.

2.3.3. Simulation

Using an offline version of the website, we tested the algorithm by changing the possible answers and simulating a BCI with errors on the classification of the “yes” and “no” answers.

Regarding the possible answers, we considered three different cases, as follows:

1. “yes”, “no”, and “unsure” answers, with the questions answered as “unsure” excluded from the total number of questions (same as the online system);
2. “yes”, “no”, and “unsure” answers, with the questions answered as “unsure” included in the total number of questions; and
3. “yes” and “no” answers only.

As the expected answer is a direct expression of the target-question weight, we considered a “yes” answer when the weight was positive, “no” when negative, and “unsure” when the weight was zero. In the third case, considering the “yes” and “no” answers only, if the target-question weight was zero, we chose “yes” or “no” randomly.

In order to emulate the non-optimal BCI classification, according to the simulated accuracy, each answer had a certain probability of being wrong (if “unsure”, the answer was not changed). The algorithm performance has been tested, varying the classification accuracy between 50%

(i.e., random classification) and 100% (i.e., perfect classification). As for the online and the offline analyses, we considered a statement as correctly estimated if, after 20 questions, it was among the three most probable target statements.

3. Algorithm

3.1. Definitions

The two main agents of the ANN are the target statements (i.e., the possible final sentences) and the questions (i.e., the descriptors of the sentences). Both of the target statements and sentences are stored in a database, therefore, the only possible sentences and questions are the ones present in the communication system.

As explained in Section 2.2, the core of the ANN is the weight matrix that puts in relation the target statements and questions. The weight depends on the answer that each statement is required from each question (i.e., if the expected answer is “yes”, the weight will be positive, if “no”, it will be negative).

A value is assigned to each statement. This value indicates the probability of each statement to be the final target; the higher the value assigned to one statement, the higher the probability of that statement to be the thought one. The value is updated after each question, based on the statement–question weight and on the received answer.

The elements of the ANN are shown in Figure 2, and are summarized below:

- N targets (T_i with $i = 1:N$) (i.e., sentences thought by the patient);
- Each target is described by M descriptors (D_j with $j = 1:M$) (i.e., “yes”/“no” questions);
- Strength of T – D connection is expressed by a weight (W_{T_i,D_j} with $i = 1:N, j = 1:M$); and
- Each target T_i is ranked using a current value (V_{T_i} with $i = 1:N$).

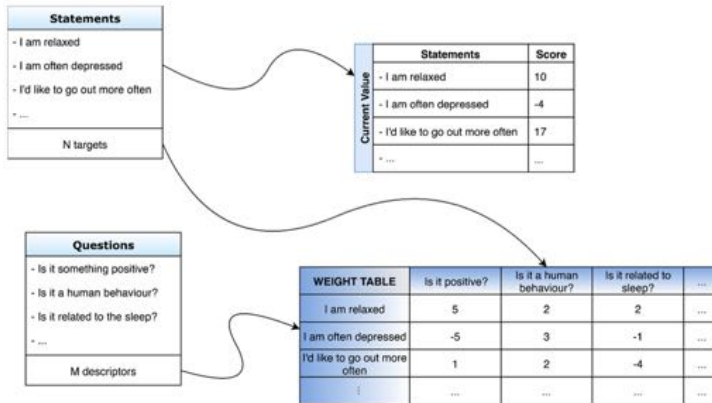


Figure 2. Structure of the artificial neural network. In particular, the structure of the databases of statements and questions, of the table of current values, and of the weight table are shown.

3.2. Current Value Adjustment

During each run, all of the target statements start with the same probability of being the final sentence, therefore, all of the current values V_T are initialized to 0. This probability (i.e., the current value) changes after each presented question, based on the answer of the user. In particular, if D_j is the n -th question presented to the user, for each target statement T_i , the current value V_{T_i} is updated using the formula, as follows:

$$V_{T_i}(n) = V_{T_i}(n-1) + W_{T_i, D_j} \text{ if answer is "yes"}$$

$$V_{T_i}(n) = V_{T_i}(n-1) - W_{T_i, D_j} \text{ if answer is "no"}$$

where n is the number of the question, and W_{T_i, D_j} is the weight between question D_j and statement T_i . It is positive if the expected answer is "yes" and negative if the expected answer is "no". Therefore, the formula increases the current value if the given answer is the expected one, and decreases it otherwise.

In order to decrease the impact of the wrong answers, the adjustment of the current value has been increased for those statements that receive many answers coherent with the expected ones. After each question, every statement where the expected answer matches with the received one is marked as a 'priority target'. This priority is lost whenever the statement receives an answer that does not match with the expected answer. The priority targets receive an adjustment for their current value, equal to double the weight. This leads to the following modified formula for updating the current value:

$$V_{T_i}(n) = V_{T_i}(n-1) + W_{T_i, D_j} (\times 2 \text{ if } T_i \text{ has priority}) \text{ if answer is "yes"}$$

$$V_{T_i}(n) = V_{T_i}(n-1) - W_{T_i, D_j} (\times 2 \text{ if } T_i \text{ has priority}) \text{ if answer is "no"}$$

where the variables are the same as described above.

3.3. Choice of the Question

One of the crucial points of the algorithm is the choice of the question. The best question is the one whose answer will give more information about the most probable targets, or, in other words, the one whose answer splits the most probable targets in two similar sets. Therefore, the best question is the one that maximizes the entropy

$$H(D_j) = \sum_{x \in X} -p(x) \log_2 p(x)$$

where X is the two classes of statements with positive and negative weights, with respect to the question D_j ; and $p(x)$ is the proportion of the most probable statements that belong to the class x .

In the implementation, all of the targets with a positive current value were considered as the most probable targets. It is possible to choose the most probable targets in a different way, using a more or less strict definition (e.g., the targets with a current value greater than a certain threshold), and this will obviously change the choice of the questions accordingly.

3.4. Estimate the Target

The goal of the ANN is to estimate the target statement that the patient is thinking. After 15 questions, the ANN will check if there is only one target statement with a positive value; if this happens, it will estimate that statement. If this condition never occurs, after 20 questions, the ANN will estimate the target statement with the highest current value.

The lower threshold of 15 questions is based on the minimum number of questions needed for an optimal solution of the Rényi–Ulam game; considering a search space of 91 statements and a signal classification accuracy of 75%, the minimum number of questions for a deterministic optimal solution is 23 (Table 2.3 from Cicalese, 2013, p. 28). We decided to check whether there was only one

statement with a positive value after two thirds of the minimum number of questions for an optimal solution. This condition is meant to speed up the communication process, avoiding asking unnecessary questions when one statement is likely the correct target.

3.5. Learning Step

The last step of the algorithm is teaching the neural network. After each correct estimation, the system will update the weight matrix. For each question that was asked during the run, it will update the weight that associates that question to the correctly estimated statement, based on the answer that the user gave; if the given answer is “yes”, it will increase the weight value, otherwise it will decrease it. In order to avoid excessive values, the weights are upper and lower bounded.

4. Results

In the next paragraphs the online and offline results of the proposed algorithm will be presented. The results are based on the web-based version and on the simulations described in Sections 2.3.2 and 2.3.3, respectively.

4.1. Online Results

The results of the games played online are reported in Table 1. Half of the time the game was played with a statement that was not in the system; considering that only the games that played with statements already in the system, the percentage of correct estimations is 65.95%, against 34.04% of games where the ANN was not able to correctly estimate the thought sentence. Focusing on the sentences correctly estimated, 67.74% of the time the sentence was estimated on the first attempt.

Table 1. Results of the game played online on the website. The table lists the total number of times of the game play. The game was played for a total of 92 times, out of which it was played for 45 times on new statements (not in the database) and 47 times on old statements (in the database). For the statements already in the database, the table also lists the number of times that they were estimated incorrectly and correctly. For the correctly estimated statements the table lists the number of times the statements were the first, second, or third guess.

New Statements	Old Statements		
45	47		
	Incorrect	Correct	
	16	31	
		1st Estimation	2nd Estimation
		21	5
			3rd Estimation
			5

4.2. Offline Results

The offline results, reported in Figure 3, were obtained by simulating the performance of the ANN in the cases mentioned in Section 2.3.3. For each of the three cases, the simulation was performed by varying the signal classification accuracy between random (i.e., 50%) and perfect (i.e., 100%). Figure 3a–c represents the percentage of statements correctly estimated by the ANN after 1000 simulations, with respect to the simulated BCI classification accuracy of “yes” and “no”. In each figure, blue, green, and yellow represent the percentage of statements correctly estimated as the most, second most, and third most probable statement, respectively.

In order to evaluate the time performance of the proposed communication system, we compared the typing speed of the ANN to those of the classic P300-based matrix speller [25]. The fNIRS-based BCI developed for CLIS patients is able to present one question every 20 s [15]. Therefore, a spelling interface that uses this BCI has an information transfer rate (ITR) of 3 bits/min, while the matrix speller

reaches 12 bits/min, which means a typing speed of approximately one character every 26 s. The target statements in the database of the ANN (Table A1) have an average length of 23.625 characters. Hence, as in the simulations, the statements were estimated in 20 questions, the fNIRS-BCI for the CLIS patients using the 20-questions-based spelling interface will have an average typing speed of one character every 17 s.

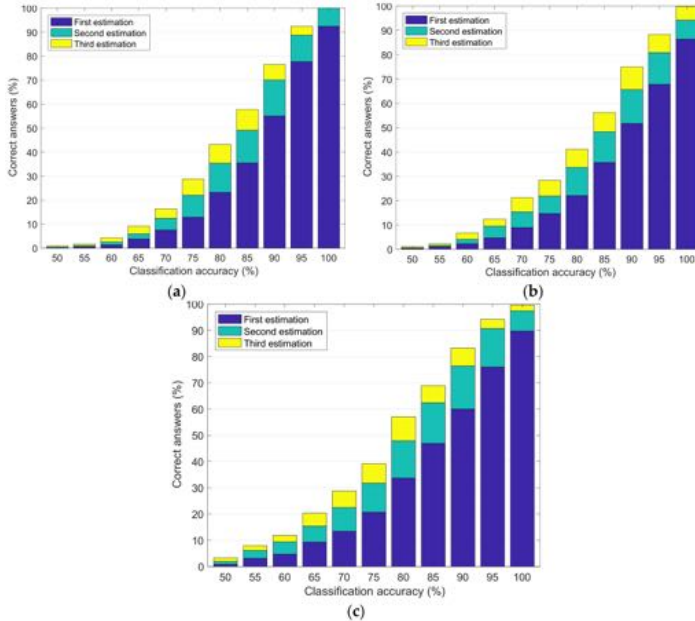


Figure 3. Results of the offline simulation in the three different cases. Blue, green, and yellow represent the percentage of statements correctly estimated as most, second most, and third most probable statement, respectively. (a) Simulated results using “yes”, “no”, and “unsure” answers, with the questions answered as “unsure” excluded from the total number of questions; (b) simulated results using “yes”, “no”, and “unsure” answers, with the questions answered as “unsure” included in the total number of questions; and (c) simulated results using “yes” and “no” answers only.

5. Discussion and Conclusions

The results in the offline analyses show that the performances are very similar in the first two analyzed cases, discarding and including “unsure” answers. Surprisingly, when giving random answers instead of “unsure”, the results improve. We believe that this is due to the randomization of the target statements and does not represent a real improvement in the results.

Figure 3a–c shows that considering a classification accuracy of 100%, the ANN is always able to correctly estimate the target statement. This result means that, using a BCI that perfectly classifies “yes” and “no” answers, a patient could communicate entire words, or even sentences, by answering

only 20 questions. The result is very promising, considering that, under the condition of a perfect signal classification, in order to select one character, a usual 6×6 grid-based speller needs at least 12 inputs [26].

However, we also notice that if the accuracy drops down to 80%, the correct rate decreases to 57%. Nevertheless, we have to consider that we did not put any constraint on the possible target statements, so in the same database, there were very different sentences like, “This movie is beautiful” and “I would like to go more out from the bed”. This generality of the sentences put the program in a bad case scenario. Although, it is important to notice that these results are still significant, as, considering a random classification (accuracy of 50%), the correct rate is close to 0%.

Both in the online games and in the simulations, the system always asked 20 questions, therefore, after 15 questions, there were always at least two statements with positive value. Hence, the ANN always estimated the final target statement with a certain degree of uncertainty, probably because the number of played games was not enough for an optimal training of the weight table. In order to decrease the uncertainty, a possibility is to increase the number of questions from 20 to the optimal solution number, which depends on the cardinality of the search space and on the signal classification accuracy, as shown in Table 2.3, from Cicalese, 2013, p. 28. Nonetheless, we decided to keep the upper limit of 20 questions in order to build a communication system that could be used in a reasonable time, even using a fNIRS-based BCI (20 s for each question).

The comparison between the 20-questions-based system and the P300 matrix speller shows that, despite a lower ITR, the average typing speed of the proposed spelling interface is higher. Even if this result cannot be taken as a real typing speed comparison because the ANN can estimate only entire sentences, it shows that the proposed system has time performance comparable to the usual spellers and could allow communication in a reasonable time, even in presence of a slow signal like the fNIRS (3 bits/min).

Correlating the online and the offline results, we can say that the users gave the expected answers up to 85% of the time. Obviously, in that case, there were no errors in the signal classification, but we could not expect a perfect result because the questions could have been very general, and with a not unique answer (e.g., considering the sentence “I sleep a lot”, the question “Is it positive?” could be answered “yes” or “no” depending on the positive or negative connotation that a person gives to sleeping a lot).

The results show that the 20-questions-based system can be a valid interface for any BCI that uses a slow signal and/or has a classification with a low accuracy rate. Even in presence of fast signal (e.g., EEG), the proposed system can improve the typing speed performance, allowing the formulation of entire sentences using only 20 binary inputs. The main drawback, already highlighted in the previous sections, is that the only sentences that the ANN can estimate are the ones stored in the database, therefore, a patient will not be free to formulate his own sentences. This limitation, an intrinsic characteristic of a 20-questions-system, can be overcome by building an exhaustive database personalized for each patient. Before initiating any BCI session, the patients will be provided an option to choose between the proposed 20-questions-based system and a character-selection speller that gives more freedom at the expense of the typing speed and the error handling.

In the future, we will test the system by narrowing the possible sentences to a more restricted topic and personalizing the weight table for only one person, in order to adapt the weights to his or her individual biography and personality. Moreover, the system will be improved to work with multi-class BCIs, in order to have more possible answers and, therefore, better estimations. Finally, the interface will be tested with a BCI to study the reaction of the patients to this different approach of communication.

The results are promising and show that a communication system based on this algorithm could replace the usual speller-based approach. The main limitation of the 20-questions-based interface is that it does not allow the patient to create new sentences or new questions. Nevertheless, it could allow patients in CLIS to express their own thoughts and desires, instead of only answering to “yes”/“no”

questions chosen by someone else. For this reason, the communication system based on the proposed algorithm could be applied to estimate the inner mental and thought process of patients in CLIS.

Author Contributions: Conceptualization, A.T. and U.C.; Methodology, A.T., N.B. and U.C.; Software, A.T.; Validation, A.T., N.B. and U.C.; Formal Analysis, A.T.; Investigation, A.T., N.B. and U.C.; Resources, N.B. and U.C.; Data Curation, A.T. and U.C.; Writing-Original Draft Preparation, A.T.; Writing-Review & Editing, N.B. and U.C.; Visualization, A.T., N.B. and U.C.; Supervision, N.B. and U.C.; Project Administration, N.B. and U.C.; Funding Acquisition, N.B. and U.C.

Funding: Deutsche Forschungsgemeinschaft (DFG, BI 195/77-1), BMBF (German Ministry of Education and Research) 16SV7701 CoMiCon, Baden-Württemberg Stiftung, LUMINOUS-H2020- FETOPEN-2014- 2015-RIA (686764), and Wyss Center for Bio and Neuroengineering, Geneva.

Conflicts of Interest: The authors declare no conflict of interest.

Appendix

Reported here is the complete list of the statements and questions used both in the online and offline results.

Table A1. List of statements and questions used for the online 20-questions-system and offline simulations.

Statements		Questions	
"I am pleased with life"	"I want to travel"	"Would you like to be killed?"	"Is it related to a particular time of day?"
"I am living with pleasure"	"I love my brothers"	"Are you suffering?"	"Is it related to a means of transport?"
"I feel good right now"	"I want to sleep"	"Are you happy with your life?"	"Is it pleasant?"
"I feel bad right now"	"I am thirsty"	"Should I bring you something?"	"Is it just something about fantasy?"
"Most of the time I feel good"	"How beautiful is this movie!"	"Is it something about everyday life?"	"Is it intriguing?"
"Most of the time I feel bad"	"I want to know what the weather will be tomorrow"	"Is it about someone you know?"	"Is it funny?"
"I sleep mostly good"	"I want a beer"	"Is it a daily human need?"	"Is it fun?"
"I sleep mostly bad"	"I love my child"	"It involves a difficult test?"	"Is it exciting?"
"I sleep a lot"	"I would like to go on holiday in Sardinia"	"It has to do with the sea?"	"Is it an entertainment activity?"
"I sleep less"	"I would like to win scientific recognition"	"Is it a desire?"	"Is it an activity that can be associated with routine?"
"I also sleep during the day"	"I want an orange juice"	"Is this something that needs to be cooked?"	"Is it about your hygiene?"
"I sleep only in the night"	"I want to play the guitar"	"Is this something about your career?"	"Is it about the weather?"
"I can concentrate myself on questions"	"I want to have a shower"	"Is there anyone able to do the imagined action?"	"Is it about the future?"
"I cannot concentrate myself on questions"	"I am happy"	"Is the desire for enjoyment?"	"Is it about the bed?"
"I would like to go more out from the bed"	"The music"	"Is it something you do before you sleep?"	"Is it about sex?"
"I like to stay in bed"	"I want to read the newspaper"	"Is it something that you want to do often?"	"Is it about meeting your dreams?"
"I feel very relaxed"	"I had a nice dream"	"Is it something that you do in your house?"	"Is it about human needs?"
"I feel very stressed"	"Some people are really idiots"	"Is it something that you can do without?"	"Is it about food?"
"I am stressed"	"I am stupid"	"Is it something related to a specific season?"	"Is it about an animal?"

Table A1. Cont.

Statements		Questions	
"I am relaxed"	"I want to drink a coffee"	"Is it the result of hard work?"	"Is it a wish?"
"I would like to have more visitors"	"I want to play football"	"Is it something you want to do now?"	"Is it a pastime?"
"I would like to have less visitors"	"I wish the best for my loved ones"	"Is it something you eat?"	"Is it a human behavior?"
"I wish more rest"	"I want to go to the gym"	"Is it something to do indoor?"	"Is it a feeling?"
"I am glad when someone visits me"	"My cats are beautiful"	"Is it something to do in the open air?"	"Does it open your mind?"
"My life is good"	"I want to go boating"	"Is it something to do alone?"	"Does it need many attempts and failures?"
"My life is bad"	"I want to eat chocolate"	"Is it something to do accompanied?"	"Does it involve taking revenge?"
"I imagine I am walking"	"I would like to go out more often"	"Is it something that makes you happy?"	"Does it imply a shift?"
"I imagine I am running"	"I am rarely depressed"	"Is it something related to your city?"	"Does it have two eyes?"
"I imagine often I am flying"	"I am often depressed"	"Is it something regarding your loved ones?"	"Does it have to do with music?"
"I imagine often I am eating"	"I laugh often inside myself"	"Is it something positive?"	"Does it have something to do with drinking?"
"I dream a lot"	"I laugh rarely inside myself"	"Is it something physical?"	"Does it have something to do with a candy?"
"I dream less"	"I am hungry"	"Is it something negative?"	"Does it have anything to do with you?"
"I often think soon I will get better"	"I want a cat"	"Is it something emotional?"	"Does it concern your feelings?"
"Rarely I think I will get better soon"	"I want to have sex"	"Is it something abstract?"	"Does it concern nature?"
"I would like it if ... will be more often by me"	"I like to ride a bike"	"Is it something about your family?"	"Does it concern an anatomical part of a person?"
"I am glad that ... is by me"	"I am sleepy"	"Is it something about the sense of hearing?"	"Do you think about it often?"
		"Is it something about the drinks?"	"Do you need company?"
		"Is it something about being free?"	"Do you need an instrument?"
		"Is it something about a primary need?"	"Do you need a ball?"
		"Is it related with the body (care, etc.)?"	"Do you have a need?"
		"Is it related to the present"	"Do you do it for being in the company?"
		"Is it related to the night?"	"Do you do it either alone or in company?"
		"Is it related to the day?"	"Do you do because you need it?"
		"Is it related to sleep?"	"Can you do it alone?"
		"Is it related to imagination?"	"Are you sleepy?"
		"Is it related to a sport?"	"A tool is needed?"

References





- Chaudhary, U.; Birbaumer, N.; Curado, M.R. Brain-Machine Interface (BMI) in paralysis. *Ann. Phys. Rehabil. Med.* **2015**, *58*, 9–13. [CrossRef] [PubMed]
- Chaudhary, U.; Birbaumer, N.; Ramos-Murguialday, A. Brain-computer interfaces in the completely locked-in state and chronic stroke. *Prog. Brain Res.* **2016**, *228*, 131–161. [PubMed]
- Chaudhary, U.; Birbaumer, N.; Ramos-Murguialday, A. Brain-computer interfaces for communication and rehabilitation. *Nat. Rev. Neurol.* **2016**, *12*, 513–525. [CrossRef] [PubMed]
- Kübler, A.; Furdea, A.; Halder, S.; Hammer, E.M.; Nijboer, F.; Kotchoubey, B. A brain-computer interface controlled auditory event-related potential (p300) spelling system for locked-in patients. *Ann. N. Y. Acad. Sci.* **2009**, *1157*, 90–100. [CrossRef] [PubMed]
- Volosyak, I. SSVEP-based Bremen-BCI interface—Boosting information transfer rates. *J. Neural Eng.* **2011**, *8*, 036020. [CrossRef] [PubMed]
- Jiao, Y.; Zhang, Y.; Wang, Y.; Wang, B.; Jin, J.; Wang, X. A novel multilayer correlation maximization model for improving CCA-based frequency recognition in SSVEP brain—Computer interface. *Int. J. Neural Syst.* **2018**, *28*, 1750039. [CrossRef] [PubMed]
- Neumann, N.; Hinterberger, T.; Kaiser, J.; Leins, U.; Birbaumer, N.; Kübler, A. Automatic processing of self-regulation of slow cortical potentials: Evidence from brain-computer communication in paralysed patients. *Clin. Neurophysiol.* **2004**, *115*, 628–635. [CrossRef] [PubMed]
- Kübler, A.; Nijboer, F.; Mellinger, J.; Vaughan, T.M.; Pawelzik, H.; Schalk, G.; McFarland, D.J.; Birbaumer, N.; Wolpaw, J.R. Patients with ALS can use sensorimotor rhythms to operate a brain-computer interface. *Neurology* **2005**, *64*, 1775–1777. [CrossRef] [PubMed]
- Yang, Y.; Chevallier, S.; Wiert, J.; Bloch, I. Subject-specific time-frequency selection for multi-class motor imagery-based BCIs using few Laplacian EEG channels. *Biomed. Signal Process. Control* **2017**, *38*, 302–311. [CrossRef]
- Zhang, Y.; Zhou, G.; Jin, J.; Zhao, Q.; Wang, X.; Cichocki, A. Sparse Bayesian Classification of EEG for Brain-Computer Interface. *IEEE Trans. Neural Netw. Learn. Syst.* **2015**, *27*, 2256–2267. [CrossRef] [PubMed]
- Jiao, Y.; Zhang, Y.; Chen, X.; Yin, E.; Jin, J.; Wang, X.Y.; Cichocki, A. Sparse Group Representation Model for Motor Imagery EEG Classification. *IEEE J. Biomed. Heal. Inform.* **2018**. [CrossRef]
- Zhang, Y.; Wang, Y.; Zhou, G.; Jin, J.; Wang, B.; Wang, X.; Cichocki, A. Multi-kernel extreme learning machine for EEG classification in brain-computer interfaces. *Expert Syst. Appl.* **2018**, *96*, 302–310. [CrossRef]
- Kübler, A.; Birbaumer, N. Brain-computer interfaces and communication in paralysis: Extinction of goal directed thinking in completely paralysed patients? *Clin. Neurophysiol.* **2008**, *119*, 2658–2666. [CrossRef] [PubMed]
- Gallegos-Ayala, G.; Furdea, A.; Takano, K.; Ruf, C.A.; Flor, H.; Birbaumer, N. Brain communication in a completely locked-in patient using bedside near-infrared spectroscopy. *Neurology* **2014**, *82*, 1930–1932. [CrossRef] [PubMed]
- Chaudhary, U.; Xia, B.; Silvoni, S.; Cohen, L.G.; Birbaumer, N. Brain-Computer Interface–Based Communication in the Completely Locked-In State. *PLoS Biol.* **2017**, *15*. [CrossRef] [PubMed]
- Pelc, A. Searching games with errors—Fifty years of coping with liars. *Theor. Comput. Sci.* **2002**, *270*, 71–109. [CrossRef]
- 20q.net. Available online: www.webcitation.org/70btN1OFO (accessed on 2 July 2018).
- Rényi, A. On a problem of information theory. *MTA Mat. Kut. Int. Kozl.* **1961**, *6B*, 505–516.
- Ulam, S.M. *Adventures of a Mathematician*; University of California Press: Berkeley, CA, USA, 1991; p. 384. ISBN 9780520071544.
- Jedynak, B.; Frazier, P.I.; Sznitman, R. Twenty questions with noise: Bayes optimal policies for entropy loss. *J. Appl. Probab.* **2012**, *49*, 114–136. [CrossRef]
- Kazemzadeh, A.; Lee, S.; Georgiou, P.G.; Narayanan, S.S. Emotion twenty questions: Toward a crowd-sourced theory of emotions. In Proceedings of the International Conference on Affective Computing and Intelligent Interaction, Memphis, TN, USA, 9–12 October 2011; Volume 6975 LNCS, pp. 1–10. [CrossRef]
- Tsiligkaridis, T.; Sadler, B.M.; Hero, A.O. Collaborative 20 Questions for Target Localization. *IEEE Trans. Inf. Theory* **2014**, *60*, 2233–2252. [CrossRef]

23. Cicalese, F. *Fault-Tolerant Search Algorithms*; Monographs in Theoretical Computer Science; An EATCS Series; Springer: Berlin/Heidelberg, Germany, 2013; ISBN 9783642173264.
24. Burgener, R. Artificial Neural Network Guessing Method and Game. U.S. Patent 2010/0311130 A1, 12 October 2006.
25. Farwell, L.A.; Donchin, E. Talking off the top of your head: Toward a mental prosthesis utilizing event-related brain potentials. *Electroencephalogr. Clin. Neurophysiol.* **1988**, *70*, 510–523. [[CrossRef](#)]
26. Rezeika, A.; Benda, M.; Stawicki, P.; Gemblar, F.; Saboor, A.; Volosyak, I. Brain–Computer Interface Spellers: A Review. *Brain Sci.* **2018**, *8*, 57. [[CrossRef](#)] [[PubMed](#)]



© 2018 by the authors. Licensee MDPI, Basel, Switzerland. This article is an open access article distributed under the terms and conditions of the Creative Commons Attribution (CC BY) license (<http://creativecommons.org/licenses/by/4.0/>).

Spelling interface using intracortical signals in a completely locked-in patient enabled via auditory neurofeedback training

Ujwal Chaudhary^{1,8}[✉], Ioannis Vlachos^{2,8}, Jonas B. Zimmermann^{1,2,8}[✉], Arnau Espinosa^{1,2},
Alessandro Tonin^{2,3}, Andres Jaramillo-Gonzalez^{1,3}[✉], Majid Khalili-Ardali^{1,3}[✉], Helge Topka⁴, Jens Lehberg⁵,
Gerhard M. Friehs⁶, Alain Woodtli², John P. Donoghue⁷ & Niels Birbaumer^{3,8}[✉]

Patients with amyotrophic lateral sclerosis (ALS) can lose all muscle-based routes of communication as motor neuron degeneration progresses, and ultimately, they may be left without any means of communication. While others have evaluated communication in people with remaining muscle control, to the best of our knowledge, it is not known whether neural-based communication remains possible in a completely locked-in state. Here, we implanted two 64 microelectrode arrays in the supplementary and primary motor cortex of a patient in a completely locked-in state with ALS. The patient modulated neural firing rates based on auditory feedback and he used this strategy to select letters one at a time to form words and phrases to communicate his needs and experiences. This case study provides evidence that brain-based volitional communication is possible even in a completely locked-in state.

¹ALS Voice gGmbH, Mössingen, Germany. ²Wyss Center for Bio and Neuroengineering, Geneva, Switzerland. ³Institute of Medical Psychology and Behavioral Neurobiology, University of Tübingen, Tübingen, Germany. ⁴Department of Neurology, Clinical Neurophysiology, Cognitive Neurology and Stroke Unit, München Klinik Bogenhausen, Munich, Germany. ⁵Department of Neurosurgery, München Klinik Bogenhausen, Munich, Germany. ⁶Neurosurgery Department, European University, Nicosia, Cyprus. ⁷Carney Brain Institute, Brown University, Providence, RI, USA. ⁸These authors contributed equally: Ujwal Chaudhary, Ioannis Vlachos, Jonas B. Zimmermann. ✉email: chaudharyujwal@gmail.com; jonas.zimmermann@wysscenter.ch; niels.birbaumer@uni-tuebingen.de

Amyotrophic lateral sclerosis (ALS) is a devastating neurodegenerative disorder that leads to the progressive loss of voluntary muscular function of the body¹. As the disorder typically progresses, the affected individual loses the ability to breathe due to diaphragm paralysis. Upon accepting artificial ventilation and with oro-facial muscle paralysis, the individual in most cases can no longer speak and becomes dependent on assistive and augmentative communication (AAC) devices^{2,3}, and may progress into the locked-in state (LIS) with intact eye-movement or gaze control^{4,5}. Several invasive^{6–10} and non-invasive^{11–16} brain-computer interfaces (BCIs) have provided communication to individuals in LIS^{17–20} using control of remaining eye-movement or (facial) muscles or neural signals. Once the affected individual loses this control to communicate reliably or cannot open their eyes voluntarily anymore, no existing assistive technology has provided voluntary communication in this completely locked-in state (CLIS)^{17–20}. Non-invasive^{11–16} and invasive^{6–10} BCIs developed for communication have demonstrated successful cursor control and sentence formation by individuals up to the stage of LIS. However, none of these studies has demonstrated communication at the level of voluntary sentence formation in CLIS individuals, who lack stable and reliable eye-movement/muscle control or have closed eyes, leaving the possibility open that once all movement - and hence all possibility for communication - is lost, neural mechanisms to produce communication will concurrently fail. Several hypotheses have been formulated, based on the past BCI failures, to explain the inability of ALS-patients in CLIS to select letters to form words and sentences ranging from extinction of intentions²¹ related to protracted loss of sensory input and motor output, cognitive dysfunction, particularly when it occurs in association with fronto-temporal degeneration. A successful demonstration of any BCI enabling an individual without reliable eye-movement control and with eyes closed (CLIS) to form a complete sentence would upend these hypotheses, opening the door to communication and the investigation of psychological processes in the completely paralyzed ALS patients and probably also other disease or injury states leading to CLIS.

Here, we established that an individual was in the CLIS state and demonstrated that sentence-level communication is possible using a BCI without relying upon the patient's vision. This individual lacked reliable voluntary eye-movement control and, consequently, was unable to use an eye-tracker for communication. The patient was also ultimately unable to use a non-invasive eye-movement-based computerized communication system²². To restore communication in CLIS, this participant was implanted with intracortical microelectrode arrays in two motor cortex areas. The legally responsible family members provided informed written consent to the implantation, according to procedures established by regulatory authorities. The patient, who is in home care, then employed an auditory-guided neurofeedback-based strategy to modulate neural firing rates to select letters and to form words and sentences using custom software. Before implantation, this person was unable to express his needs and wishes through non-invasive methods, including eye-tracking, visual categorization of eye-movements, or an eye movement-based BCI-system. The patient started using the intracortical BCI system for voluntary verbal communication three months after implantation. With ALS progression, the patient lost the ability to open his eyes voluntarily as well as visual acuity, but he is still employing the auditory-guided neurofeedback-based strategy with his eyes closed to select letters and form words and sentences. Therefore, a CLIS patient who was unable to express his wishes and desires is employing the BCI system to express himself independent of vision.

Results

One day after the implantation, attempts were initiated to establish communication. The patient was asked to use his previously effective communication strategy employing eye movements to respond to questions with known “yes” and “no” answers, which did not result in a classifiable neural signal, no difference in spike rate and multi-unit-activity (MUA). Passive movements of the patient's right fingers, thumb, and wrist evoked consistent neural firing rate modulations on several electrodes on both arrays. However, when we instructed the patient to attempt or imagine hand, tongue, or foot movements, we could not detect consistent responses. Subsequently, the communication strategy was changed on the 86th day after implantation, and neurofeedback-based paradigms (described in the Online Methods section) were employed, as shown in Fig. 1. In this setting, the patient was provided auditory feedback of neural activity by mapping a spike rate metric (SRM) for one or more channels to the frequency of an auditory feedback tone, as displayed in Fig. 1 (described in the “Neurofeedback communication” section of Online Methods, see sample Supplementary Video V1). The patient was able to modulate the sound tone on his first attempt on day 86 and subsequently was able to successfully modulate the neural firing rate and match the frequency of the feedback to the target for the first time on day 98. Employing the neurofeedback strategy, the patient was able to modulate the neural firing rate and was able to use this method to select letters and to free spell from day 106 onwards. The Results reported here include data from days 106–462 after implantation. Three of the authors (UC, NB and AT) frequently traveled to the patient's home to perform communication sessions about every two weeks for 3 or 4 consecutive days until February 2020. Because of the COVID pandemic from March 2020 to June 2020, all the sessions were performed via secured remote access to the patient's laptop. During these sessions, the patient's wife performed locally all required hardware connections, and the experimenters, either UC or AT, controlled the software remotely. During the experimental period reported here, the authors UC, AT, and NB performed experimental sessions on 135 days. The patient was hospitalised due to unrelated adverse events between days 120 and 145, 163 and 172, and 212 and 223 after implantation, during which time no sessions were performed.

Each session day, we started with a 10-minutes baseline recording, where the patient was instructed to rest. During this time period the experimenter ran a software program to determine the firing rate of different individual channels and select their parameters for the first neurofeedback session-block. Two different types of neurofeedback sessions were performed consecutively on each day, “feedback without reward” and “feedback with reward” with the goal (1) to select channels suitable for voluntary control by the patient and (2) to train the patient to control the selected channels' spiking activity voluntarily. The first paradigm (“feedback without reward”) provided successive target tones, and the patient was asked to match the frequency of the feedback tone to the target tone. The second paradigm (“feedback with reward”) was the same. However, upon reaching and holding (during a configurable number of interactions, each interaction lasting 250 ms) the feedback tone within a predefined range around the target frequency, an additional reward sound was delivered for 250 ms, indicating successful performance to the patient. Holding the feedback tone at the high (low) end of the range for a minimum of 250 ms was then interpreted as a successful “yes” (“no”) response. After the first “feedback without reward” session, individual channels' firing rate distributions were automatically calculated. The experimenter selected channels with differential modulation for the high and low target tones and

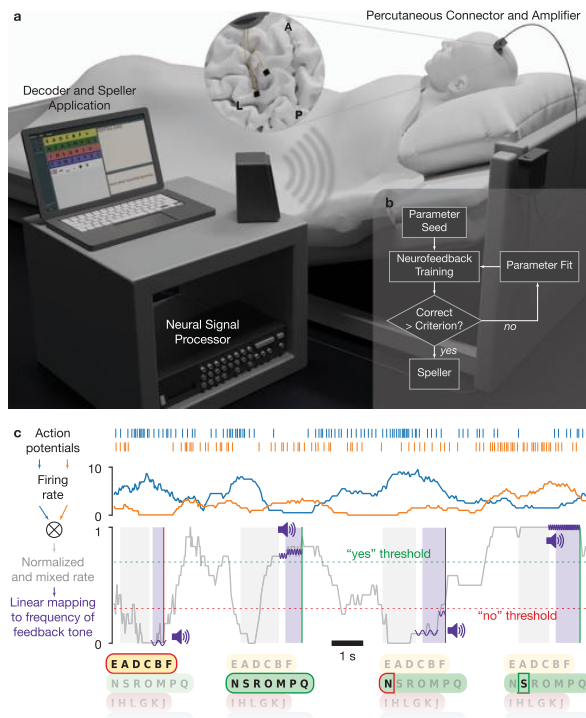


Fig. 1 Setup and neurofeedback paradigm. **a** Experimental setup. Two microelectrode arrays were placed in the precentral gyrus and superior frontal gyrus (insert, L: left central sulcus, A-P: midline from anterior to posterior). An amplifying and digitizing headstage recorded signals through a percutaneous pedestal connector. Neural signals were pre-processed on a Neural Signal Processor and further processed and decoded on a laptop computer. **b** Daily sessions began with Neurofeedback training. If the performance criterion was reached, the patient proceeded to speller use. If the criterion was not reached, parameters were re-estimated on neurofeedback data, and further training was performed. **c** Schematic representation of auditory neurofeedback and speller. Action potentials were detected and used to estimate neural firing rates. One or several channels were selected, their firing rates normalized and mixed (two channels shown here for illustration; see Online Methods). Options such as letter groups and letters were presented by a synthesized voice, followed by a response period during which the patient was asked to modulate the normalized and mixed firing rate up for a positive response and down for a negative response. The normalized rate was linearly mapped to the frequency of short tones that were played during the response period to give feedback to the patient. The patient had to hold the firing rate above (below) a certain threshold for typically 500 ms to evoke a “Yes” (“No”) response. Control over the neural firing rates was trained in neurofeedback blocks, in which the patient was instructed to match the frequency of target tones.

updated the parameters for subsequent sessions. Employing this iterative procedure on each day, we performed several neurofeedback blocks within a particular day to remind the patient of the correct strategy to control the firing rate, each typically consisting of 10 high-frequency target tones and 10 low-frequency target tones presented in pseudo-random order and also to tune and validate the classifier. Typically, if the patient could match the frequency of the feedback to the target in 80% of the trials, we proceeded with the speller.

Neurofeedback sessions. Figure 2a shows individual neurofeedback trials, including an error trial, of one representative block. Over the reported period, there were 1176 feedback sessions as shown in Supplementary Fig. S1. In the 281 neurofeedback blocks preceding the speller blocks, 4936 of 5700 trials (86.6%) were correct (Fig. 2b), i.e., for target tone up (higher frequency) the decision was up (a “yes” answer), and for target down (low frequency) the decision was down (a “no” answer). The difference in error rates between ‘up’ and ‘down’ trials, i.e., the fraction of trials

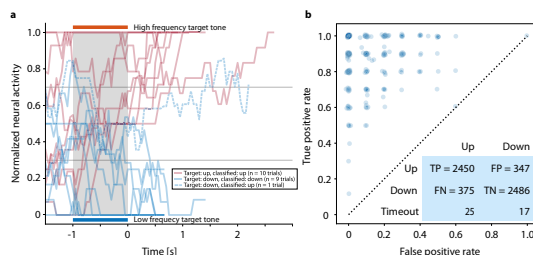


Fig. 2 Neurofeedback task and classification. **a** Representative example for normalized and mixed firing rate during ten high (red) and ten low (blue) target tone frequency feedback trials of day 247. The patient was asked to match the target tone by modulating the normalized and weighted firing rate, and he succeeded in all but one trial of this example. Trials were completed as soon as the firing rate was held above or below the upper or lower threshold, respectively. As defined in the Materials and Methods section, these feedback blocks were performed every day of recording for training, parameter selection, and validation of the selected parameters. The grey-shaded region from -1 to 0 s depicts the time period during which the high or low target tones were presented to the patient. The horizontal line at 0.3 and 0.7 shows the lower and upper threshold, respectively. Source data are provided as a Source Data file. **b** True positive rate vs. false positive rate of the trials in auditory neurofeedback blocks directly preceding speller blocks on days 123–462. Each circle represents one neurofeedback block; circles are jittered for better visibility. The blue insert at the bottom right corner shows the contingency table of all neurofeedback trials directly preceding speller blocks on days 123–462. In the blue insert—TP stands for true positive, i.e., up trials classified as up; FP stands for false positive, i.e., up trials classified as down; FN—stands for false negative, i.e., down trials classified as up; TN—stands for true negative, i.e., down trials classified as down; Timeout denotes the trials that were unclassified. Source data are provided as a Source Data file.

in which the modulated tone did not match the target tone, (13.2% and 12.2%, respectively), was significant (Pearson's χ^2 test: $p < 0.01$). The patient maintained a high level of accuracy in the neurofeedback condition throughout the reported period: on 52.6% of the days, the accuracy was at least 90% during at least one of the feedback trials blocks, i.e., the patient was able to match the frequency of the feedback to the target 18 out of 20 times. We observed considerable within-day variability of neural firing rates and hence performance of the neurofeedback classifier, necessitating manual recalibration throughout the day (see Supplementary Fig. S1). In the last feedback sessions before speller sessions, the median accuracy was 90.0%, the minimum was 50.0% (chance level). In 17.1% of the sessions, accuracy was below 80.0%.

Speller sessions. We continued with the speller paradigm when the patient's performance in a neurofeedback block exceeded an acceptance threshold (usually 80%). To verify that good performance in the neurofeedback task translated to volitional speller control (based on correct word spelling), we asked the patient to copy words before allowing free spelling. On the first three days of speller use, the patient correctly spelled his own, his son's, and his wife's names. After an unrelated stay at the hospital, we again attempted the speller using the same strategy on day 148.

Afterward, we relied on a good performance in the neurofeedback task, i.e., the patient's ability to match the frequency of the feedback to the target in 80% of trials, to advance to free spelling. The selection of two letters from a speller block on day 108 is shown in Fig. 3. Supplementary Video V2 presents a representative speller block.

Over the reported period, out of 135 days, speller sessions were attempted on 107 days, while on the remaining 28 days use of the speller was not attempted because the neurofeedback performance criterion was not reached. The patient produced intelligible output, as rated independently by three observers, on 44 of 107 days when the speller was used (Fig. 4). On average, 121 min were spent spelling and the average length of these

communications was 131 characters per day. The patient's intelligible messages comprised 5747 characters produced over 5338 min, corresponding to an average rate of 1.08 characters per minute. This rate varied across blocks (min/median/max: 0.2/1.1/5.1 characters per minute). Over the reported period, there was no apparent trend in spelling speed. There were 312 pairs of speller blocks and preceding neurofeedback blocks. The speller output was rated 0 for unintelligible by raters, 1 for partially intelligible, 2 for intelligible. The Spearman correlation between Neurofeedback task accuracy and subsequent speller intelligibility was 0.282 ($p = 4.002 \times 10^{-7}$). The Spearman correlation between Neurofeedback accuracy and number of letters spelled was 0.151 ($p = 7.671 \times 10^{-3}$). The information transfer rate (ITR) during intelligible speller sessions was 5.2 bits/minute on average (min/median/max: 0.3/4.9/21.4 bits/minute).

On the second day of free spelling, i.e., on the 107th day after implantation, the patient spelled phrases, spelled in three-time episodes, thanking NB and his team ('erst mal moechte ich mich niels und seine birbaumer bedanken' – 'first I would like to thank Niels and his birbaumer'). Many of the patient's communications concerned his care (e.g. 'kopf? immerlzq gerad' – 'head always straight', day 161; 'kein shirt aber socken' – 'no shirts but socks [for the night]', day 244; 'mama kopfmassage' – 'Mom head massage', day 247; 'erstmal kopfteil viel viel hoch ab jetzt imm' – 'first of all head position very high from now', day 251; 'an alle muessen mir viel oeffter gel augengel' – 'everybody must use gel on my eye more often', day 254; 'alle sollen meine haende direkten auf bauch' – 'everybody should put my hand direct on my stomach', day 344; 'zum glotze und wenn besuchen da ist das kopfteil immer gaanz rauf' – 'when visitors are here, head position always very high' on day 461). The patient also participated in social interactions and asked for entertainment ('come tonight [to continue with the speller]', day 203, 247, 251, 294, 295, 'wili ch tool ballbum mal laut hoeren' – 'I would like to listen to the album by Tool [a band] loud', day 245, 'und jetzst ein beer' – 'and now a beer', day 247 (fluids have to be inserted through the gastro-tube), 251, 253, 461). He even gave suggestions to improve his speller performance by spelling 'turn on word

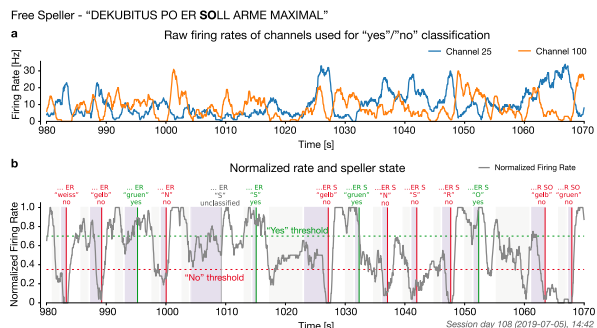


Fig. 3 Example of letter selection during a free spelling block. **a** Firing rate of the channels 25 and 100 used for "yes"/"no" classification on day 108. **b** Normalized firing rate and the speller state during the same 90 s period of a speller block. "Yes"/"no"/timeout decisions are marked by vertical lines and the option selected in green and not selected in red. This example is part of the phrase "dekubitus po er soll arme maximal", referring to bedside and instructing the aide to change arm position. Source data are provided as a Source Data file.

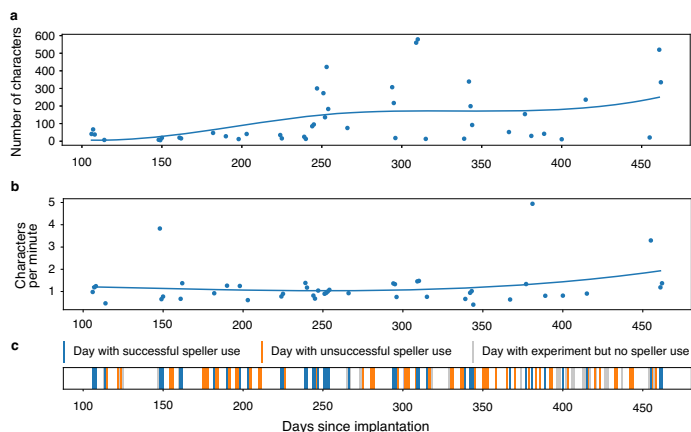


Fig. 4 Overview of BCI use. **a** Number of characters spelled by the patient during speller sessions whose output was rated 'intelligible' (rating described in text), aggregated by day. **b** Characters selected per minute in 'intelligible' speller sessions, aggregated by day. **c** Speller use during the period presented. Sessions span 135 days. Green bars represent days on which speller was used and yielded intelligible output (44 days). Yellow bars represent days on which speller use was attempted, but no intelligible output was produced (63 days). On 28 days, speller use was not attempted (red). Source data are provided as a Source Data file.

recognition' on day 183, 'is it easy back once confirmation' on Day 253, 'tell alessandro i need to save edit and delete whole phrases and all of that into the list where (patient's son name) on day 295, 'why cant you leave the system on. ifind that good' on day 461, in English as the patient knew that the experimenter UC and AT are not native German speakers and mostly spoke in English with the patient. On day 247 he gave his feedback on speller as, 'jungs es funktioniert gerade so muehelos', - 'boys, it

works so effortlessly'. The patient expressed his desire to have different kind of food in his tube as, 'mixer fuer suppen mit fleisch' - 'instructed his wife to buy a mixer for soup with meat' on day 247; 'gulashsuppe und dann erbsensuppe' - 'Gulash soup and sweet pea soup' on day 253; 'wegen essen da wird ich erst mal des curry mit kartoffeln haben und dann bologna und dann gefuellte und dann kartoffeln suppe' - 'for food I want to have curry with potato then Bolognese and potato soup on day 462. He

interacted with his 4 years old son and wife, '(son's name) ich liebe meinen coolen (son's name) - 'I love my cool son' on day 251; '(son's name) willst du mit mir bald disneys robin hood anschauen' - 'Do you want to watch Disney's Robin Hood with me' on day 253; 'alles von den dino ryders und brax autobahnund alle aufziehautos' - 'everything from dino riders and brax and cars' on day 309; '(son's name) moechtest du mit mir disneys die hexe und der zauberer anschauen auf amazon' - 'would you like to watch Disney's witch and wizard with me on amazon' on day 461; 'mein grosster wunsch ist eine neue bett und das ich morgen mitkommen darf zum grillen' - 'My biggest wish is a new bed and that tomorrow I come with you for barbecue' on day 462.

Discussion

We demonstrate that a paralyzed patient, according to the presently available physiological and clinical criteria in the completely locked-in state (CLIS), could volitionally select letters to form words and phrases to express his desires and experiences using a neurally-based auditory neurofeedback system independent of his vision. The patient used this intracortical BCI based on voluntarily modulated neural spiking from the motor cortex to spell semantically correct and personally useful phrases. Properties of the multielectrode array impedance and recordings across sessions are shown in the Supplementary Fig. S2. In all blocks, measurable spike rate differentiation between "yes" and "no" during the neurofeedback trials and "select" and "no select during speller blocks appeared in only a few channels in the SMA (supplementary motor area) out of all active channels, as shown in Supplementary Fig. S3a. After the establishment of successful communication after day 86, similar channels from the Supplementary Motor Cortex array were used for communication sessions with the patient, as shown in Supplementary Fig. S3b. Mainly electrode 21 and neighbouring electrodes were used, which demonstrated differential control of the feedback tones during the neurofeedback sessions before spelling. Because the neurofeedback procedure was the prerequisite for successful communication after 86 days of attempted, but unsuccessful decoding, a multichannel decoding algorithm was not implemented following our clinical judgment based on learning principles²³ that such a substantial change in the procedure might impede or extinguish the successful control of the patient and spelling. In addition, after this failure, we attempted a neural feedback approach, based on learning principles, capitalizing on the observation that neural firing rates could be used to achieve levels suitable to make yes/no choices. For the speller sessions, only one to four channels were used for control, as shown in Supplementary Fig. S3. There was insufficient time to explore other decoding approaches, and we wanted to establish that communication was feasible at all in CLIS. We cannot explain why the other electrodes did not provide modulation suitable for multichannel decoding. Perhaps with further sessions and other strategies, not possible in this experiment, we might have identified faster, or more accurate approaches. Speller use duration was highly variable, ranging from a few minutes to hours. As shown in Fig. 4, the patient generated a different number of characters on different days. He spelled only under 100 characters on some days, while on other days, he produced more than 400 characters. Despite the huge variation in the number of characters spelled, the number of characters spelled per minute was mostly around 1 character per minute, and ITR averaged 5 bits/minute. Communication rates are lower than in other studies using intracortical arrays⁷⁻⁹, but comparable to EEG P300 spellers for ALS patients^{24,25} and much faster than an SSVEP EEG BCI for advanced ALS patients¹². These apparent poor performances are primarily due to the completely auditory nature of these systems,

which are intrinsically slower than a system based on visual feedback. Lastly it was noteworthy that free voluntary spelling mainly concerned requests related to body position, health status, food, personal care and social activities suggesting that even with this slow speller the patient could relay his needs and desires to caretakers and family.

Our study showed communication in a patient with CLIS. It is worth mentioning that no universally accepted clinical definition exists to distinguish LIS from CLIS; the current standard criteria to differentiate LIS from CLIS is the presence or absence of means of communication. During the transition from LIS to CLIS, patients are initially left with limited, and finally, no means of communication. The time course of this transition process is patient and disease specific. In theory, other voluntary muscles than eye-movements could have been used for Electromyography (EMG)-based communication attempts. Particularly face muscles outside the extraocular muscles may remain under voluntary control in some cases even after the loss of eye-muscle control. To the best of the authors' knowledge, no study has extensively investigated the remaining muscle activity of CLIS patients, but in previous studies^{22,26} the authors showed that during the transition from LIS to CLIS some remaining muscles of the eyes continue to function and can be used for successful communication.

In the case of the patient described here, extensive electro-oculogram (EOG) recordings were performed to demonstrate that no other measurable neuromuscular output existed- a way to confirm CLIS. The patient employed an EOG-based BCI for communication successfully for the last time in February 2019 when the amplitude of EOG signal decreased below 20 μ V. Nevertheless, extensive post-hoc EOG analysis showed a significant difference in the maximum, mean, and variance feature of the eye movement corresponding to "yes" and "no" even after the patient's inability to employ the EOG-based system. This failure to communicate despite the presence of a significant difference in some of the features may be due to the limitations of the EOG-based BCI system. However, as differences of eye movement amplitudes were only detectable over tens of trials and not reliably from session to session, EOG was not a practical signal for communication. In this study, caretakers and family members denied the existence of any possible reliable communication from February 2019 onwards, when this study occurred. Thus, we conclude based on our reported measurements that the patient described was in a CLIS a few weeks before and also after implantation. This statement does not exclude the possibility that even more sensitive measurements of somatic-motor control could reveal some form of volitional control, which would render the diagnostic statement of CLIS at least for this case inaccurate. Nevertheless, by the measures we describe here no muscle-based signals useful for communication were evident, leading us to conclude that this patient could be classified as in the chronic complete locked in state but was able to communicate using an implanted BCI system usefully.

The present BCI communication demonstrates that an individual unable to move for protracted periods is capable of meaningful communication. Still, the current neurofeedback based BCI system has several limitations, as several software and hardware modifications would need to be implemented before the system could be used independently by the family or caretakers without technical oversight. The BCI-software is presently being modified to improve communication quality and rate and the self-reliance of the family.

In this study, communication rates were much lower compared to other studies using intracortical arrays, which include communication with a point-and-click screen keyboard⁷⁻⁹, and decoding of imagined handwriting in a spinal cord injured patient²⁷. People with ALS and not apparently completely locked-

in have been able to use multi neuron-based decoders for more rapid communication than seen here. The differences might be both technical—a failure of the electrode—or biological, i.e., related to the disease state. While the multielectrode array (MEA) used here typically shows some variable level of degradation in the quality and number of recordings over time, such arrays reportedly provide useful signals for years^{28,29}.

Our MEA retained impedances in the useful range across the entire experimental period of this study (Fig. S2) and neurons were recorded on many channels suggesting that the loss of recordable neural waveforms cannot explain performance differences. The most striking difference in the present data was the inability to record neurons that modulated with the participant's volitional intent. This could be the result of the disease processes on the neurons themselves or the protracted loss of sensory-motor input itself. The observation that control was intermittent may reflect changes in neural connectivity or the ability to be activated. Lack of any somatic sensory feedback, especially that from muscles, might impede voluntary modulation of neural activity. Participants with ALS enrolled in previous trials apparently had at least some residual voluntary control of muscles, whereas this participant had lost all control by the time of implantation. Additionally, advanced ALS may have led to cognitive or affective changes such as shortened attention span or modified motivational systems that may have made it difficult to achieve reliable modulation of large numbers of neurons (dozens to hundreds) achieved in other ALS participants with similar BCI systems implanted. Altered cortical evoked response amplitudes and latencies³⁰ seen in this individual may be a reflection of these abnormal states. CLIS patients with ALS show highly variable and often pathological neurophysiological signatures,³¹ such as heterogeneous sleep-waking cycles³² that may also affect the ability to engage neurons. Lastly, auditory cues may engage motor processes that will activate neurons in frontal areas outside of the motor cortex³³, which may have contributed to the changes with the auditory task used here.

To conclude, this case study has demonstrated that a patient without any stable and reliable means of eye-movement control or identifiable communication route employed a neurofeedback strategy to modulate the firing rates of neurons in a paradigm allowing him to select letters to form words and sentences to express his desires and experiences. It will be valuable to extend this study to other people with advanced ALS to address the aforementioned issues systematically.

Methods

The medical procedure was approved by the Bundesinstitut für Arzneimittel und Medizinprodukte ("BfArM"), the German Federal Institute for Drugs and Medical Devices. The study was declared as a single Case Study and has received a special authorization ("Sonderzulassung") by BfArM, according to §11 of the German Medical Device Law ("Medizin-Produkte-Gesetz") on December 20, 2018, with Case Nr. 5640-S-036/18. The Ethical Committee of the Medical Faculty of the Technische Universität München Rechts der Isar provided support to the study on 19 Jan 2019, along with the explicit permission to publish on 17 February 2020. Before the patient transitioned into CLIS, he gave informed consent to the surgical procedure using his eye movements for confirmation. The patient was visited at home by authors HT and JL, and thorough discussions were held with the legally responsible family members (wife and sister) in order to establish convincing evidence of the patient's informed consent and firm wish to undergo the procedure. The legally responsible family members then provided informed written permission to the implantation and the use of photographs, videos, and portions of his protected health information to be published for scientific and educational purposes. In addition, a family judge at the Ebersberg county court gave the permission to proceed with the implantation after reviewing the documented consent and a visit to the patient. The patient received no compensation for the participation.

Patient. The patient, born in 1985, was diagnosed with progressive muscle atrophy, a clinical variant of non-bulbar ALS, selectively affecting spinal motor neurons in August 2015. He lost verbal communication and the capability to walk by the end of 2015. He has been fed through a percutaneous endoscopic gastrostomy tube and

artificially ventilated since July 2016 and is in home care. He started using the MyTobii eye-tracking-based assistive and augmentative communication (AAC) device in August 2016. From August 2017 onwards, he could not use the eye-tracker for communication because of his inability to fixate his gaze. Subsequently, the family developed their own paper-based spelling system to communicate with the patient by observing the individual's eye movements. According to their scheme, any visible eye movement was identified as a "yes" response, lack of eye movement as "no". The patient anticipated complete loss of eye control and asked for an alternative communication system, which motivated the family to contact authors NB and UC for alternative approaches. Initial assessment sessions were performed in February 2018. During this interval, the detection of eye movements by relatives became increasingly difficult, and errors made communication attempts impossible up to the point when communication attempts were abandoned. The patient and family were informed that a BCI-system based on electrooculogram (EOG) and/or electroencephalogram (EEG) might allow "yes" - "no" communication for a limited period.

The patient began to use the non-invasive eye movement-based BCI-system described in Tonin et al.²¹. The Patient was instructed to move the eyes ("eye-movement") to say "yes" and not to move the eyes ("no eye-movement") to say "no". Features of the EOG signal corresponding to "eye-movement" and "no eye-movement" or "yes" and "no" were extracted to train a binary support vector machine (SVM) to identify "yes" and "no" response. This "yes" and "no" response was then used by the patient to audiotically select letters to form words and hence sentences. The patient and family were also informed that non-invasive BCI-systems might stop functioning satisfactorily, and in particular, selection of letters might not be possible if he became completely locked-in (where no eye movements could be recorded reliably). In that case, implementation of an intracortical BCI-system using neural spike-based recordings might allow for voluntary communication. As the patient's ability to communicate via non-invasive BCI systems deteriorated, in June 2018, preparations for the implantation of an intracortical BCI system were initiated. To this end, HT and JL and GF were approached in order to prepare the surgical procedure and ensure clinical care in a hospital close to the patient's home. The patient was able to use the non-invasive BCI system employing eye-movement to select letters, words, and sentences until February 2019, as described in Tonin et al.^{21,34}. By the time of implantation, the EOG/EEG based BCI system failed, as signals could not be used reliably for any form of communication in this investigation setting. The EOG/EEG recordings and their analysis are described in Supplementary Note 1 and Supplementary Fig. S4. Additionally, the patient reported low visual acuity caused by the drying of the cornea.

Surgical procedure. A head MRI scan was performed to aid surgical planning for electrode array placement. The MRI scan did not reveal any significant structural abnormalities, in particular no brain atrophy or signs of neural degeneration. A neuronavigation system (Brainlab, Munich, Germany) was used to plan and perform the surgery. In March 2019, two microelectrode arrays (8×8 electrodes each, 1.5 mm length, 0.4 mm electrode pitch; Blackrock Microsystems LLC) were implanted in the dominant left motor cortex under general anaesthesia. After a left central and precentral trepanation, the implantation sites were identified by neuronavigation and anatomical landmarks of the brain surface. A pneumatic inserter was used³⁵ to insert the electrode arrays through the arachnoid mater, where there were no major blood vessels. The pedestal connected to the microelectrode arrays connected via a bundle of fine wires (Blackrock Microsystems LLC), was attached to the calvaria using bone screws and was exited through the skin. The first array was inserted into the hand area region of the primary motor cortex³⁶, and the second array was placed 2 cm anteromedially from the first array into the region of the supplementary motor area (SMA) as anatomically identified. No implant-related medical adverse events were observed. After three days of post-operative recovery, the patient was discharged to his home.

Neural signal processing. A digitizing headstage and a Neural Signal Processor (Cereplex E and NSP, Blackrock Microsystems LLC) were used to record and process neural signals. Raw signals sampled at 30kS/s per channel were bandpass filtered with a window of 250–7500 Hz. Single and multi-unit action potentials were extracted from each channel by identifying threshold crossings (4.5 times root-mean-square of each channel's values). Depending on the activity and noise level, thresholds were manually adjusted for those channels used in the BCI sessions after visual inspection of the data to exclude noise but capture all of the visible spikes above the threshold. Neural data were further processed on a separate computer using a modified version of the CerLink library (<https://github.com/dashesy/Cerelink>) and additional custom software. For communication, we used spike rates from one or more channels. A spike rate metric (SRM) was calculated for each channel by counting threshold crossings in 50 ms bins. The SRM was calculated as the mean of these bins over the past one second.

Custom software written in Python and C++ was used to perform and control all BCI sessions. The software managed the complete data flow of the raw signals provided by the NSP, allowing manual configuration of recording parameters, selection of individual channels for neurofeedback and storing of neural data, and meta-information (timing information of trigger events, etc.) required for offline analysis.

The software enabled the experimenter to configure different experimental protocols, to select an experimental paradigm for each session, and to trigger the start and end of a session. The software-controlled the presentation of auditory stimuli to the patient, including the presentation of feedback from his neural activity. It also provided live feedback to the experimenter regarding ongoing progress, e.g. the currently spelled phrase. Also, the software provided live visualization of neural activity, including the original firing rate activity of selected channels and normalized firing rate activity used for neurofeedback. To secure smooth real-time processing and to avoid potential performance bottlenecks, the software supported multiprocessing. That is, all critical processes, including data acquisition, data storage, neurofeedback, classification, and visualization, were executed in separated cores.

Neurofeedback communication. The patient was provided auditory feedback of neural activity levels by mapping the SRM for one or more channels to the frequency of an auditory feedback tone, as shown in Fig. 1. Single channel spike rates were normalized according to the spike rate distribution of each channel. Selected channels' normalized SRMs were then summed and linearly mapped to the range of 120–480 Hz, determining the frequency of the feedback tone produced by an audio speaker. Feedback tones were updated every 250 ms. The firing rate r_i of each selected channel was constrained to the range $[a_i, b_i]$, normalized to the interval $[0, 1]$, and optionally inverted, and the resulting rates were averaged:

$$r(t) = \frac{1}{n} \sum_i \frac{1 - c_i}{2} + c_i \frac{\max(\min(r_i(t), b_i), a_i)}{b_i - a_i} \quad (1)$$

where $r(t)$ is the overall normalized firing rate, and the c_i are 1 or -1 . The normalized rate was then linearly mapped to a frequency between 120 and 480 Hz for auditory feedback. Feedback tones were pure sine waves lasting 250 ms each. Initially, channels were selected randomly for feedback. Then the parameters a_i, b_i, c_i as well as the channels used for control were chosen and iteratively optimized each day in the neurofeedback training paradigms.

The first paradigm ("feedback without reward") provided successive target tones at 120 or 480 Hz, and the patient was asked to match the frequency of the feedback to the target (typically 20 pseudorandom trials per block). In the "feedback with reward" paradigm, was essentially the same, however, upon reaching and holding (during a configurable number of interactions, each interaction lasting 250 ms) the feedback tone within a predefined range around the target frequency, an additional reward sound was delivered for 250 ms indicating successful performance to the patient. Holding the feedback tone at the high (low) end of the range for 250 ms was then interpreted by the patient upon instruction as a Yes (No) response (see Supplementary Video V1 as a typical example). The "feedback with reward" paradigm served to train and validate the responses.

We also validated the Yes/No responses in a question paradigm, in which the answers were assumed to be known to the patient. Furthermore, we used an "exploration" paradigm to test if the patient's attempted or imagined movements could lead to modulation of firing rates.

Finally, in an auditory speller paradigm, the patient could select letters and words using the previously trained Yes/No approach. The auditory speller paradigm is depicted in Fig. 1c. The speller system described here avoids long adaptation and learning phases because it is identical to the one used previously when he was still in control of eye movements. The original arrangement of the letters in their respective groups was chosen according to their respective frequency in the patient's native German language.

The speller's output was rated for intelligibility by three of the authors (UC, IV, and JZ). Three categories were used: unintelligible, ambiguous, and intelligible. Ambiguous speller output includes grammatically correct words that could not be interpreted in the context as well as strings of letters that could give rise to uncertain interpretations. Intelligible phrases may contain words with spelling mistakes or incomplete words, but the family or experimenter identified and agreed upon their meaning.

To evaluate the performance of the speller, the information transfer rate³⁶ (ITR) B during speller sessions that were rated as intelligible was calculated as:

$$B = \log_2 N + P \log_2 P + (1 - P) \log_2 \frac{1 - P}{N - 1} \quad (2)$$

where N is the number of possible speller selections (30 including space, delete, question mark and end program), and P is the probability that a correct letter was selected. Multiplication with selected symbols and division by session duration yields bits per minute.

Data handling. Software and procedures were designed to provide redundancy and automation to ensure that crucial information is always saved with each recording:

1. The BCI software was implemented with extensive automated logging for each session:
 - a. neural data (spike rates) used for BCI control
 - b. event timestamps from the neurofeedback training/validation and speller paradigms

- c. configuration used to run the particular session, including channel selection, normalization parameters, thresholds for yes/no detection, task timings, arrangement of letters in speller, etc.
- d. source code of the KIAP BCI software used on that day. The BCI software was kept under version control using git. The hash of the current commit was saved along with any changes compared to that commit.

2. Specific instructions were given to the personnel performing the experimental sessions to acquire raw neural data collected in parallel to the BCI data, which included loading a configuration file, starting data recording before a BCI session, and stopping the recording at the end. Two experimenters were on-site, when possible, to divide system operation and patient interaction tasks.
3. Information about each recording session was entered into a session log in a shared Excel file (which has a history of edits). Information logging included for each session:
 - a. kind of experiment
 - b. file names of raw data and KIAP BCI data
 - c. any additional EEG recordings if performed
 - d. names of video files if performed
 - e. experimenters present
 - f. observations/abnormalities if performed
 - g. data recording abnormalities, etc.
4. During the experiments, known issues were fixed, for example, a change in log file format was implemented (as noted in the accompanying dataset), which allowed to more easily interpret the data. The post hoc analysis, i.e., parsing log files and data compilation was checked manually for several sessions. Co-authors reviewed the results and the process.
5. Data handling procedures were implemented to ensure that data integrity was maintained from recording to safe storage.

Dataset reported in this article. The dataset here spans days 106 to 462 after implantation. For the analysis of neurofeedback trials in Fig. 2 and the corresponding main text, only blocks after day 123 were used because of a change in paradigm (before day 123, incorrect trials and time-outs were not differentiated). For Supplementary Fig. 1, all neurofeedback blocks were used, as time-out trials were counted as 'incorrect' as well. All speller sessions performed between days 106 and 462 were included in the analysis. The BCI data of one neurofeedback and one speller session were lost during data transfer and the loss was only discovered after the original data had been deleted. These sessions were therefore excluded from the analysis.

Reporting summary. Further information on research design is available in the Nature Research Reporting Summary linked to this article.

Data availability

The data upon which the findings in this paper are based (neural firing rates, event log files for data presented in Figs. 2, 3, 4, S1, S3, electrode impedances and spike event files for data presented in Fig. S2) are available at <https://doi.org/10.12751/g-node.jdwmqd37>. The EOG data which Fig. S4 is based on is available at <https://doi.org/10.12751/g-node.ng4df38>. Source data are provided with this paper. The raw neural recordings is available upon request to J.B.Z., yet owing to the potential sensitivity of the data, an agreement between the researcher's institution and the WvS Center is required to facilitate the sharing of these datasets. Source data are provided with this paper.

Code availability

The code used to run the BCI system is available at <https://doi.org/10.12751/g-node.ihc6qn39>.

Received: 23 June 2020; Accepted: 11 February 2022;

Published online: 22 March 2022

References

1. Chou, S. M. & Norris, F. H. Issues & opinions: amyotrophic lateral sclerosis: lower motor neuron disease spreading to upper motor neurons. *Muscle Nerve* **16**, 864–869 (1993).
2. Beukelman, D. R., Fager, S., Ball, L. & Dietz, A. AAC for adults with acquired neurological conditions: a review. *Augment. Alternative Commun.* **23**, 230–242 (2007).
3. Beukelman, D., Fager, S. & Nordness, A. Communication support for people with ALS. *Neural. Res. Int.* **2011**, 714693 (2011).

4. Birbaumer, N. Breaking the silence: brain-computer interfaces (BCI) for communication and motor control. *Psychophysiology* **43**, 517–532 (2006).
5. Bauer, G., Gerstenbrand, F. & Rimpl, E. Varieties of the locked-in syndrome. *J. Neurol.* **221**, 77–91 (1979).
6. Vansteensel, M. J. et al. Fully implanted brain-computer interface in a locked-in patient with ALS. *N. Engl. J. Med.* **375**, 2060–2066 (2016).
7. Jarosiewicz, B. et al. Virtual typing by people with tetraplegia using a self-calibrating intracortical brain-computer interface. *Sci. Transl. Med.* **7**, 313ra179 (2015).
8. Pandarinarath, C. et al. High performance communication by people with paralysis using an intracortical brain-computer interface. *Elife* **6**, e18554 (2017).
9. Milekovic, T. et al. Stable long-term BCI-enabled communication in ALS and locked-in syndrome using LFP signals. *J. Neurophysiol.* **120**, 343–360 (2018).
10. Kennedy, P. R. & Bakay, R. A. Restoration of neural output from a paralyzed patient by a direct brain connection. *Neuroreport* **9**, 1707–1711 (1998).
11. Birbaumer, N. et al. A spelling device for the paralysed. *Nature* **398**, 297–298 (1999).
12. Okahara, Y. et al. Long-term use of a neural prosthesis in progressive paralysis. *Sci. Rep.* **8**, 1–8 (2018).
13. Kübler, A. et al. Patients with ALS can use sensorimotor rhythms to operate a brain-computer interface. *Neurology* **64**, 1775–1777 (2005).
14. Sellers, E. W. & Donchin, E. A P300-based brain-computer interface: initial tests by ALS patients. *Clin. Neurophysiol.* **117**, 538–548 (2006).
15. Sellers, E. W., Vaughan, T. M. & Wolpaw, J. R. A brain-computer interface for long-term independent home use. *Amyotroph. lateral Scler.* **11**, 449–455 (2010).
16. Wolpaw, J. R. et al. Independent home use of a brain-computer interface by people with amyotrophic lateral sclerosis. *Neurology* **91**, e258–e267 (2018).
17. Chaudhary, U., Birbaumer, N. & Curado, M. R. Brain-machine interface (BMI) in paralysis. *Ann. Phys. Rehabil. Med.* **58**, 9–13 (2015).
18. Chaudhary, U., Birbaumer, N. & Ramos-Murguialday, A. Brain-computer interfaces in the completely locked-in state and chronic stroke. *Prog. Brain Res.* **228**, 131–161 (2016).
19. Chaudhary, U., Birbaumer, N. & Ramos-Murguialday, A. Brain-computer interfaces for communication and rehabilitation. *Nat. Rev. Neurol.* **12**, 513–525 (2016).
20. Chaudhary, U., Mračacz-Kersting, N. & Birbaumer, N. Neuropsychological and neurophysiological aspects of brain-computer-interface (BCI)-control in paralysis. *J. Physiol.* **599**, 2351–2359 (2021).
21. Kübler, A. & Birbaumer, N. Brain-computer interfaces and communication in paralysis: Extinction of goal directed thinking in completely paralysed patients? *Clin. Neurophysiol.* **119**, 2658–2666 (2008).
22. Tonin, A. et al. Auditory electrocolumgram-based communication system for ALS patients in transition from locked-in to complete locked-in state. *Sci. Rep.* **10**, 9452 (2020).
23. Birbaumer, N., Ruiz, S. & Sitaram, R. Learned regulation of brain metabolism. *Trends Cogn. Sci.* **17**, 295–302 (2013).
24. Nijboer, F. et al. A P300-based brain-computer interface for people with amyotrophic lateral sclerosis. *Clin. Neurophysiol.* **119**, 1909–1916 (2008).
25. McCane, L. et al. P300-based brain-computer interface (BCI) event-related potentials (ERPs): people with amyotrophic lateral sclerosis (ALS) vs. age-matched controls. *Clin. Neurophysiol.* **126**, 2124–2131 (2015).
26. Murguialday, A. R. et al. Transition from the locked in to the completely locked-in state: a physiological analysis. *Clin. Neurophysiol.* **122**, 925–933 (2011).
27. Willett, F. R. et al. High-performance brain-to-text communication via handwriting. *Nature* **593**, 249–254 (2021).
28. Hochberg, L. R. et al. Neuronal ensemble control of prosthetic devices by a human with tetraplegia. *Nature* **442**, 164–171 (2006).
29. Vargas-Irwin, C. E. et al. Watch, imagine, attempt: motor cortex single-unit activity reveals context-dependent movement encoding in humans with tetraplegia. *Front. Hum. Neurosci.* **12**, 450 (2018).
30. Chaudhary, U. et al. Brain computer interfaces for assisted communication in paralysis and quality of life. *Int. J. Neural Syst.* **31**, 2130003 (2021).
31. Khalili-Ardali, M. et al. Neuropsychological aspects of the completely locked-in syndrome in patients with advanced amyotrophic lateral sclerosis. *Clin. Neurophysiol.* **132**, 1064–1076 (2021).
32. Malekshahi, A. et al. Sleep in the completely locked-in state (CLIS) in amyotrophic lateral sclerosis. *Sleep* **42**, zsz185 (2019).
33. Hosman, T. et al. Auditory cues reveal intended movement information in middle frontal gyrus neuronal ensemble activity of a person with tetraplegia. *Sci. Rep.* **11**, 1–17 (2021).
34. Jaramillo-Gonzalez, A. et al. A dataset of EEG and EOG from an auditory EOG-based communication system for patients in locked-in state. *Sci. Data* **8**, 1–10 (2021).
35. Wu, W. et al. Bayesian population decoding of motor cortical activity using a Kalman filter. *Neural Comput.* **18**, 80–118 (2006).
36. McFarland, D. J., Sarnacki, W. A. & Wolpaw, J. R. Brain-computer interface (BCI) operation: optimizing information transfer rates. *Biol. Psychol.* **63**, 237–251 (2003).
37. Chaudhary, U. et al. Spelling interface using intracortical signals in a completely locked-in patient enabled via auditory neurofeedback training. *G-Node* <https://doi.org/10.12751/g-node.jdwmjd> (2021).
38. Tonin, A. et al. Auditory electrocolumgram-based communication system for ALS patient (pt11). *G-Node* <https://doi.org/10.12751/g-node.ngdfdr> (2021).
39. Vlachos, I. et al. KIAP BCI: a BCI framework for intracortical signals. *G-Node* <https://doi.org/10.12751/g-node.thc6qn> (2021).

Acknowledgements

This research was supported by the Wyss Center for Bio and Neuroengineering, Geneva, Deutsche Forschungsgemeinschaft (DFG BI 195/77-1) - N.B. and U.C.; German Ministry of Education and Research (BMBF) 16SV7701, CoMiCon - N.B. and U.C.; LUMINOUS-H2020-FETOPEN-2014-2015-RIA (686764) - N.B. and U.C.; Bogenhausen Staedische Klinik, Munich. The authors thank Andrew Jackson and Nick Ramsey for their comments on an earlier version of the manuscript. Aleksander Sobolevsky contributed the 3D model for Fig. 1. We thank the patient and his family.

Author contributions

U.C.—Initiation; Conceptualization; Ethics Approval; Performed 95% of the sessions with the patient before and after implantation; Figures; Neurofeedback paradigm; Manuscript writing. I.V.—Software development, integration and testing; Data analysis; Neurofeedback paradigm implementation; Performed 5% of the sessions after the implantation. J.B.Z.—Neurofeedback paradigm implementation; Data analysis; Figures; Manuscript writing. A.E.—Software testing; EEG/EOG analysis; Figures. A.T.—Speller software development; Performed 30% of sessions before implantation and 20% of the sessions after implantation; EEG/EOG analysis; Figures. A.J.—G.—EEG/EOG analysis; Figures. M.K.A.—Graphical user interface. H.R.T.—Ethics Approval; Medical patient care; Clinical and diagnostic neurological procedures. J.L.—Ethics approval; Neurosurgery; Clinical care. G.M.F.—Neurosurgical training. A.W.—Ethics approval; BfARM approval; Neurosurgical training. J.P.D.—Initiation; Conceptualization, writing, review, editing. N.B.—Initiation; Conceptualization; Coordination; Clinical-psychological procedures and care; Neurofeedback paradigm; performed 30% of the sessions with UC; Ethics approval; BfARM approval; Manuscript writing.

Competing interests

The authors declare no competing interests.

Additional information

Supplementary information The online version contains supplementary material available at <https://doi.org/10.1038/s41467-022-28859-8>.

Correspondence and requests for materials should be addressed to Ujwal Chaudhary, Jonas B. Zimmermann or Niels Birbaumer.

Peer review information *Nature Communications* thanks the anonymous reviewer(s) for their contribution to the peer review of this work. Peer reviewer reports are available.

Reprints and permission information is available at <http://www.nature.com/reprints>

Publisher's note Springer Nature remains neutral with regard to jurisdictional claims in published maps and institutional affiliations.



Open Access This article is licensed under a Creative Commons Attribution 4.0 International License, which permits use, sharing, adaptation, distribution and reproduction in any medium or format, as long as you give appropriate credit to the original author(s) and the source, provide a link to the Creative Commons license, and indicate if changes were made. The images or other third party material in this article are included in the article's Creative Commons license, unless indicated otherwise in a credit line to the material. If material is not included in the article's Creative Commons license and your intended use is not permitted by statutory regulation or exceeds the permitted use, you will need to obtain permission directly from the copyright holder. To view a copy of this license, visit <http://creativecommons.org/licenses/by/4.0/>.

© The Author(s) 2022

ORIGINAL ARTICLE

Binary Semantic Classification Using Cortical Activation with Pavlovian-Conditioned Vestibular Responses in Healthy and Locked-In Individuals

Natsue Yoshimura^{1,2,3,4}, Kaito Umetsu¹, Alessandro Tonin^{5,6}, Yasuhisa Maruyama¹, Kyosuke Harada¹, Aygul Rana⁶, Gowrishankar Ganesh^{7,8}, Ujwal Chaudhary^{6,9}, Yasuharu Koike¹ and Niels Birbaumer^{6,9}

¹Institute of Innovative Research, Tokyo Institute of Technology, Yokohama 226-8503, Japan, ²ATR Brain Information Communication Research Laboratory Group, Kyoto 619-0288, Japan, ³Integrative Brain Imaging Center, National Center of Neurology and Psychiatry, Tokyo 187-8551, Japan, ⁴PRESTO, JST, Saitama 332-0012, Japan, ⁵Wyss-Center for Bio and NeuroEngineering, Geneva CH-1202, Switzerland, ⁶Institute of Medical Psychology and Behavioral Neurobiology, University of Tübingen, 72076 Tübingen, Germany, ⁷Laboratoire d'Informatique, de Robotique et de Microélectronique de Montpellier, U. Montpellier, CNRS, 34095 Montpellier, France, ⁸CNRS-AIST Joint Robotics Laboratory, Tsukuba 305-8560 Japan and ⁹ALS Voice gGmbH, 72116 Mössingen, Germany

Address correspondence to Natsue Yoshimura, Institute of Innovative Research, Tokyo Institute of Technology 4259-R2-16, Nagatsuta-cho, Midori-ku, Yokohama 226-8503, Japan. Email: yoshimura.n.ac@m.titech.ac.jp

Abstract

To develop a more reliable brain–computer interface (BCI) for patients in the completely locked-in state (CLIS), here we propose a Pavlovian conditioning paradigm using galvanic vestibular stimulation (GVS), which can induce a strong sensation of equilibrium distortion in individuals. We hypothesized that associating two different sensations caused by two-directional GVS with the thoughts of “yes” and “no” by individuals would enable us to emphasize the differences in brain activity associated with the thoughts of yes and no and hence help us better distinguish the two from electroencephalography (EEG). We tested this hypothesis with 11 healthy and 1 CLIS participant. Our results showed that, first, conditioning of GVS with the thoughts of yes and no is possible. And second, the classification of whether an individual is thinking “yes” or “no” is significantly improved after the conditioning, even in the absence of subsequent GVS stimulations. We observed average classification accuracy of 73.0% over 11 healthy individuals and 85.3% with the CLIS patient. These results suggest the establishment of GVS-based Pavlovian conditioning and its usability as a noninvasive BCI.

Key words: brain–computer interface, completely locked-in state, electroencephalography, galvanic vestibular stimulation, Pavlovian conditioning

Received: 18 April 2021; Revised: 1 July 2021; Accepted: 4 July 2021

© The Author(s) 2021. Published by Oxford University Press.

This is an Open Access article distributed under the terms of the Creative Commons Attribution License (<http://creativecommons.org/licenses/by/4.0/>), which permits unrestricted reuse, distribution, and reproduction in any medium, provided the original work is properly cited.

Introduction

Amyotrophic lateral sclerosis (ALS) is a neuromuscular disease that leads to loss of all motor control, including movements of eyes, face, limbs, and external sphincter in the late stage of the disease (Kiernan et al. 2011). The state, after loss of all motor control, is called the completely locked-in state (CLIS), and patients in this state lose all communication channels with their surroundings (Murguialday et al. 2011). In order to improve their quality of life by providing communication, many studies have attempted to develop brain-computer interfaces (BCIs) using electroencephalography (EEG) and functional near-infrared spectroscopy (fNIRS). A semantic “Yes/No BCI,” where the BCI directly decodes whether an individual is thinking “yes” or “no” to a particular question, has been of great interest (Kübler and Birbaumer 2008; Murguialday et al. 2011; De Massari et al. 2013; Gallegos-Ayala et al. 2014; Chaudhary et al. 2017; Okahara et al. 2018; Han et al. 2019; Khalili Ardali et al. 2019). A Yes/No BCI can enable natural communication between the CLIS patients and their family and caretakers, without requiring the patients to perform any other cognitive tasks unrelated to the question posed to them, such as number calculation or motor imagery, in order for the BCI to decode and understand their answers. However, the neural representations of “yes” and “no” are arguably quite different depending on questions and individual experiences and memory background. Therefore, it may be helpful to introduce a procedure that emphasizes the difference between the thought of yes/no in neural activation and in addition enhances the signal-to-noise ratio of electrocortical activity.

In order to evoke additional brain activity allowing to better distinguish the neural response to the thought of yes/no, classical conditioning, also known as Pavlovian conditioning, seems to be a promising method. As shown in the famous example (Pavlov 1927), if a dog repeatedly listens to the sound of a bell preceding feeding, the mere sound of the bell will cause the animal to salivate in anticipation of the food (Fig. 1a). The salivation occurs unconsciously and cannot be controlled voluntarily. Here, the important point is to associate two previously unrelated events (the conditioned stimulus (CS), in this example the sound of the bell, and the unconditioned stimulus (US), in this example the sight of food), with the unconditioned response (UR, i.e., salivation), which before conditioning is a reflexive response induced by food (the US).

For establishing Pavlovian conditioning, we introduced galvanic vestibular stimulation (GVS) as a US because equilibrium distortion sensations (EDS) such as visual rotation and tilt of the body caused by GVS are reflexive responses and expected to serve as a UR. GVS is a variation of transcranial direct current stimulation (tDCS) and excites the vestibular system that controls our body balance (Fitzpatrick and Day 2004; Utz et al. 2010). Being noninvasive, nonpainful, and safe, GVS has drawn attention not only for scientific purposes but also for applications in clinical and engineering disciplines (Maeda et al. 2005; Pan et al. 2008; Sra et al. 2017; Długacznyk et al. 2019; Liu et al. 2019). Existing literature of fMRI analysis during GVS and the anatomical connections between the vestibular nuclei revealed involvement of sensorimotor-related areas (Mountcastle 1957; Lobel et al. 1998) and parietal areas to the vestibular functions (Stephan et al. 2005; Lopez et al. 2012; Reichenbach et al. 2016).

In this study, we established associations between thoughts of (i.e., covert) yes/no answers to questions and two EDSs with a Pavlovian conditioning paradigm. Using a differential conditioning paradigm as shown in Figure 1a (Razran 1971), two types of EDSs with different directions were constructed by altering

the polarity of the current from two electrodes (one anode and one cathode) attached to the mastoids behind the ears (Utz et al. 2010), and the two EDSs were associated with thoughts of yes and no, respectively. In this paradigm, the thought of yes/no is expected to function as the neutral stimulus (NS, i.e., sound of the bell) that will become a conditioned stimulus (CS) after establishing the conditioning successfully. If the conditioning succeeds, brain activity evoked by the EDSs will become the conditioned response (CR) as does salivation. Although attempts to associate yes/no with auditory and tactile stimulation in conditioning paradigms have been made in other studies (Furdea et al. 2012; De Massari et al. 2013; Ruf et al. 2013), GVS has not been used in this paradigm. Given the reflexive nature of the EDS compared with auditory and tactile perception, EDS is expected to be easier to associate it with thought of yes/no compared with other stimulations usually with additional auditory (such as two sounds with different frequencies) or visual cues or different types of imagery. In the context of this BCI, it is the stimulus question including its semantic content asked to the patient requiring a yes or no answer together with the GVS, which constitutes the conditioned stimulus. As in the original Pavlovian experimental situation, we assume—following Pavlov—that the pairing of the neutral CS with a biologically significant stimulus (sight of food) will make an associative contingency more stable and resistant to extinction than the semantic content and the sounds of the question alone. In our case, the biologically significant stimulus consists of the two types of GVS that cause EDS, which is impossible to escape and of obvious biological significance in order to keep the body balance. This is particularly important in the case of a CLIS patient when questions may lose their power to elicit a response through an extinction process because yes or no answers are not possible anymore due to the complete paralysis and have no biologically relevant effects (i.e., no answer responses from the social environment) and thus will lose the contingency through extinction. On the subjective level, this may be experienced as disattention and loss of interest to answer any question with a yes or no response.

To anticipate our results, we found that EDS could be clearly associated with the thoughts of “yes” and “no,” which we could verify using functional magnetic resonance imaging (fMRI) where we observed clear activation in sensorimotor-related and parietal areas induced by the thought of yes/no (after association). Following the conditioning, we performed a classification analysis for the thought of “yes” versus “no” using EEG cortical current source (EEG-CCS) signals. The methodology showed appreciable performance not only with healthy participants but also with a CLIS patient.

Materials and Methods

Participants

Eleven healthy human participants (H1 to H11) from 23 to 55 years old ($M = 34.5$, $SD = 12.7$, 10 males and 1 female) and an ALS patient in the CLIS (P1) (male, 39 years old) participated in this study. Six participants (H1 to H6) participated in the fMRI experiment to examine brain activation difference between the pre- and postconditioning sessions. These participants then participated in an EEG experiment to examine the decoding accuracy after the conditioning. Next, we invited five naive participants (H7 to H11) to the EEG experiment to examine the conditioning effect by comparing the yes versus no classification accuracies between the pre- and postconditioning sessions.

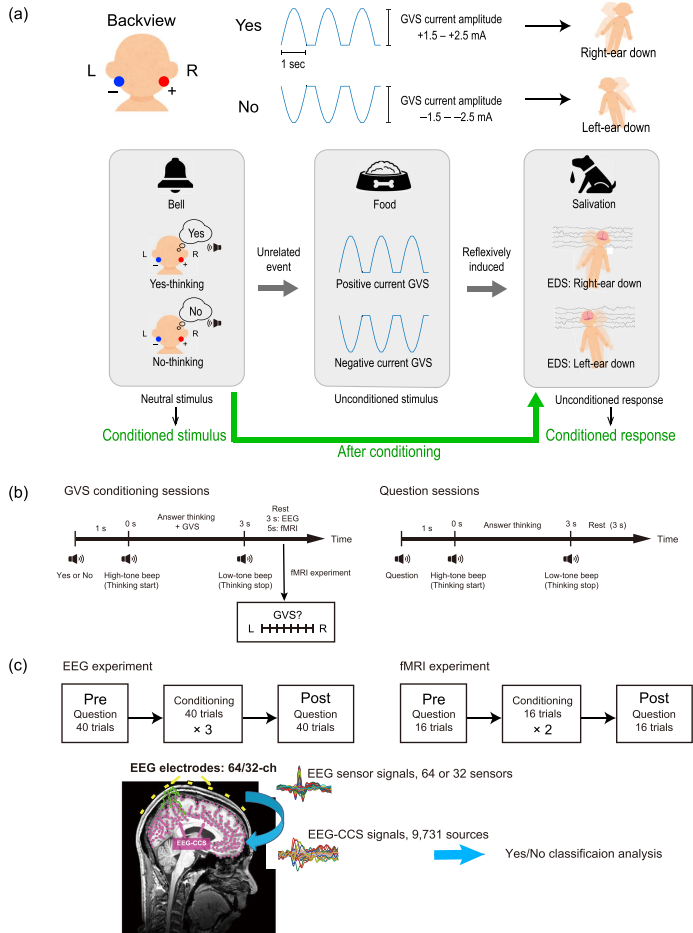


Figure 1. Experimental concept and paradigm. (a) Upper panel: Two GVS electrodes were placed behind the ears, an anode (red) electrode behind the right ear, and a cathode (blue) behind the left ear. Three positive half cycles of 0.5 Hz sine waves were provided for thought of “yes,” which resulted in right-ear-down tilt sensation. In the case of thought of “no,” 3 negative half cycles of 0.5 Hz sine waves were given to induce left-ear-down tilt sensation. Lower panel: Conceptual diagram of the thought of yes/no, GVS, and brain activity caused by EDS aligned with examples of Pavlovian conditioning. (b) One-trial time flow of GVS conditioning and question sessions. In both sessions, participants started thinking the answer after a high-tone beep and stopped thinking when they heard a low-tone beep. In fMRI experiments, they rated the EDS direction on a visual analog scale after the answering period of the conditioning sessions. (c) Session structures for EEG and fMRI experiments. Both EEG and fMRI data were used to investigate additional activated brain areas caused by the EDS after the conditioning (i.e., postconditioning sessions). We estimated EEG-CCS from EEG sensor signals, and the EEG-CCS signals were used for the yes/no classification analysis.

This is an exploratory study that aimed at formulating a basis for a clear hypothesis on the GVS conditioning effect for future studies with CLIS patients. In terms of applying this method to BCI, we intended to evaluate its effectiveness with a large effect size. In the past BCI studies, we found that even those with large effect sizes of decoding accuracies were in the range of 0.8 to 10 (Ruf et al. 2013; Fukuma et al. 2018; Irimia et al. 2018). Therefore, we calculated the effect size using our data from the six participants (H1-H6) and obtained a value of $d = 2.26$ (Mean accuracy \pm S.D. = 61.59 ± 5.31 ; Mean chance \pm S.D. = 51.43 ± 3.51). Then, a power analysis of the t-test was conducted using Gpower 3.1 (Faul et al. 2007) with power set at 0.8, effect size at 2, and alpha at 0.05, resulting in a sufficient sample size of five participants. Therefore, we recorded EEG from GVS-naïve five participants (H7-H11) to examine the significance of the conditioning effect between the pre- and postconditioning sessions. The effect size calculated from the results was $d = 1.64$. Since this value is higher than Cohen's recommendation for a large effect size (i.e., 0.8) (Cohen 1988), we assumed that a significant effect would allow a clear hypothesis for the future investigation with CLIS patients. An effect size of $d = 2.46$ was obtained using the comparison to chance level from all 11 participants.

The patient was diagnosed with bulbar ALS in 2009. He lost speech and capability to move by 2010. He has been artificially ventilated since April 2010 and is in home care. No communication with eye movements, other muscles, or assistive communication devices was possible since 2012. The study protocol for the healthy participant was approved by the ethics committee of the Tokyo Institute of Technology, Japan (Approval No. 2019017), and the protocol for the patient was approved by the Institutional Review Board of the Medical Faculty of the University of Tübingen, Germany, and the experiments were carried out in accordance with the Declaration of Helsinki. Written informed consent was obtained from each of the healthy participants before the experiment and, in the case of the patient, from the patient's legal representative.

GVS Procedure

The positive and negative half cycle of 0.5 Hz sine waves were created by MATLAB R2014a (The MathWorks, Inc.) and sent to the DC Stimulator Plus (neuroConn, neuroCare Group GmbH) via a digital-analog converter (NI USB-6225, National Instruments Corporation) to provide the electrical current to the two electrodes placed behind the ears. As shown in Figure 1a, 3 repetitions of the positive or negative half cycle wave were provided in one trial (i.e., during thoughts of "yes" or "no"), which resulted in 3-s stimulation per trial. The positive waves were provided during thoughts of yes, and the negative waves were used for the thought of no. The anode (positive) electrode was placed behind the right ear, and the cathode (negative) electrode was placed behind the left ear. Therefore, the direction of the EDS was different depending on the content of the thought; the EDS occurs toward the anode, which means persons felt a right-ear-down EDS during the thought of "yes" and a left-ear-down EDS during the thought of "no." The absolute maximum value of the sine waves was in a range of 1.0–3.0 mA as determined by each participant's scaling before the experiment so that she or he could recognize the direction difference of the EDS. For the CLIS patient, his sister (legal representative) decided the amplitude as 2.0 mA based on her own experience of the GVS.

Experimental Paradigms of Classical Conditioning and Question Sessions

The experiment was conducted in the following order: a preconditioning question session, conditioning sessions, and a postconditioning question session (Fig. 1c). GVS was provided to the participants only in the conditioning sessions (Fig. 1b). Both the fMRI and EEG experiments were conducted with the participants lying in supine position with their eyes closed so as to replicate the CLIS patient's posture. All the participants were instructed about the task sequence described below before the experiment.

In the conditioning sessions, GVS was applied to the participants when they thought "yes" and "no." Specifically, in one trial, they first heard the spoken word "yes" or "no" and started thinking that word after they heard a high-tone beep sound. Positive GVS, for "yes" (right-ear-down distortion), and negative GVS, for "no" (left-ear-down distortion), were given to the participants 1 s after the high-tone beep. The participants were instructed to stop thinking after 3 s when hearing a low-tone beep. In the case of the fMRI experiments, we asked the participants to report their perceived direction of EDS in each trial (Fig. 1b, left panel). The number of trial repetitions in one session varied between the EEG and fMRI experiments (See sections fMRI Experiment and EEG Experiment). We confirmed the effect of the conditioning by checking after each conditioning session whether the participants could easily or spontaneously associate the two types of EDS with the thoughts of "yes" and "no" answers. Precisely, after the training session, we confirmed that the participants could remember the difference of EDS between the thoughts of yes and no.

In the question sessions, the participants thought "yes" or "no" as an answer for an auditorily presented question in the absence of GVS. The question was randomly selected from 23 pairs of yes and no questions shown in Supplementary Table 1. All the questions were simple, and the answers were known to the participants and experimenters. The questions used for the CLIS patient in the EEG experiment were personal and chosen by his family, and the patient knew the answers to the questions according to family's information. The experiment with the patient was performed at the patient's home. The same beep sounds as in the conditioning sessions were used to provide starting and stopping cues.

The high- and low-tone beep sounds were created by extracting a portion of the "burn_failed.wav," a standard tone in the windows OS at sampling rates of 25 000 Hz and 8000 Hz, respectively. The "Yes" and "No" words and questions for the patient were recorded by the patient's legal representative, whereas the words for the healthy participants were synthesized using the Text-to-Speech function in the Macintosh OS.

fMRI Experiment

Six of the eleven healthy participants (H1–H6) participated in the fMRI experiment. The fMRI experiment consisted of two conditioning sessions and two question sessions including one preconditioning session and one postconditioning session (Fig. 1c). The auditory stimuli were presented to the participants via MRI-compatible earphones (KMR-512(S), KOBATEL Corporation) in an MRI scanner. In a conditioning session, 8 yes and 8 no auditory stimuli (i.e., 16 trials in total) were provided in random order. After the thought period, a visual analog scale asking the direction of the EDS was displayed (see Fig. 1b), and the participants answered it using an MRI-compatible trackball mouse

(HHSC-TRK-2, Current Designs Inc.). In a question session, 8 yes and 8 no questions were randomly selected from the list in Supplementary Table 1 and presented. The participants thought "yes" or "no" after the high-tone beep. The experimental software used for the conditioning and question sessions, such as presenting the auditory stimuli and sending the sine waves for GVS, were all written in MATLAB R2018b, using the Psychophysics Toolbox extensions (Brainard 1997; Pelli 1997; Kleiner et al. 2007).

A 3 T Magnetom Prisma MRI scanner equipped with a 32-channel array coil (Siemens) was used for the functional and anatomical MRI acquisition. During the experiment, the participants lay on the scanner bed in a supine position with eyes closed to replicate the posture of the CLIS patient. In the conditioning sessions, they opened their eyes when they heard the low-tone beep sound to indicate the direction of the GVS. The visual analog scale was displayed on a 32-inch BOLDscreen (Cambridge Research Systems) and presented to the participants through a mirror that was mounted over their faces. Functional data were acquired with a T2*-weighted gradient-echo, echo-planar imaging sequence using the following parameters: repetition time (TR) = 2.5 s; echo time (TE) = 30 ms; flip angle (FA) = 80°; field of view (FOV) = 212 × 212 mm; matrix size = 64 × 64; 40 slices; slice thickness = 3.2 mm. In the conditioning sessions, we did not fix the time for the participants to report the direction of GVS using the trackball mouse after the thoughts of yes and no. In the question sessions, the time period required for presenting questions was different from one question to another. A brain fMRI volume refers to one complete 3D image of the brain. The time taken to record one volume is TR (i.e., repetition time). Due to difference in the response time by our participants (which was not fixed) and due to differences in the length of questions presented to the participants, the length of the fMRI sessions and hence the number of brain volumes varied across sessions and participants. A 3D anatomical image was acquired using an MPRAGE T1-weighted sequence (TR = 1900 ms; TE = 2.52 ms; FA = 9°; FOV = 256 × 256 mm; matrix size = 256 × 256; 192 slices; slice thickness = 1.2 mm).

fMRI Data Analysis

fMRI data analysis was performed using SPM12 (Wellcome Department of Cognitive Neurology; <http://www.fil.ion.ucl.ac.uk/spm>) running on MATLAB R2016b for individual participant analysis. Statistical analyses were performed using a general linear model (GLM) after the standard preprocessing (i.e., spatial realignment to the mean EPI image, slice timing corrections, coregistration of a bias-corrected T1-weighted anatomical image to the realigned images, normalization to the Montreal Neurological Institute (MNI) standard brain, and smoothing with a full-width spatial Gaussian kernel of 8 mm at half maximum). The yes/no thought periods were modeled using boxcar functions and convolved with the hemodynamic response function. After the model parameters estimation, statistical parametric maps for each participant were created using four conditions: Yes > No (in preconditioning), No > Yes (in preconditioning), Yes > No (in postconditioning), and No > Yes (in postconditioning) with $P < 0.001$ (uncorrected for multiple comparisons). One-sample *t*-tests were conducted for the group analysis using the four contrasts from the six participants by setting the regions of interest (ROIs). Based on the existing literature on GVS and galvanic vestibular system (Mountcastle 1957; Lobel et al. 1998; Stephan et al. 2005; Lopez et al. 2012; Reichenbach et al. 2016), we fixed the ROI to sensorimotor-related areas [postcentral gyrus, precentral gyrus,

and supplemental motor areas (SMA)] and parietal areas (angular gyrus, precuneus, parietal operculum, supramarginal gyrus, and superior parietal lobule) using maximum probability tissue labels derived from the Neuromorphometric atlas (provided by Neuromorphometrics, Inc. <http://Neuromorphometrics.com>) as implemented in SPM12.

EEG Experiment

The EEG experiment consisted of three consecutive conditioning sessions with 40 trials, followed by one question session (post-conditioning session) with 40 questions (Fig. 1c). For the participants H7–H11, preconditioning session with 40 questions was performed before the conditioning sessions. The auditory stimuli were presented using stereo speakers. In one conditioning session, 20 yes and 20 no auditory stimuli were presented in random order. In a question session, 20 yes and 20 no questions were randomly selected from the list in Supplementary Table 1 and presented. As in the fMRI experiment, the participants thought "yes" or "no" after the high-tone beep and were instructed to stop the thought when they heard the low-tone beep. The experimental program was written using MATLAB R2014b.

For the healthy participants, EEG signals were recorded from 64-channel active electrodes placed according to the extended international 10–20 system layout using the ActiveTwo system and the ActiView software (BIOSEMI) with a sampling rate of 512 Hz. The 64-channel locations are Fp1, AF7, AF3, F1, F3, F5, F7, FT7, FC5, FC3, FC1, C1, C3, C5, T7, TP7, CP5, CP3, CP1, P1, P3, P5, P7, P9, PO7, PO3, O1, Oz, Iz, POz, Pz, CPz, Fpz, Fp2, AF8, AF4, Afz, Fz, F2, F4, F6, F8, FT8, FC6, FC4, FC2, FCz, Cz, C2, C4, C6, T8, TP8, CP6, CP4, CP2, P2, P4, P6, P8, P10, PO8, PO4, and O2. During the experiment, they lay on a bed in a supine position in an electrically shielded soundproof room (AMC-3515, O'HARA & Co., Ltd) with eyes closed so as to replicate the CLIS patient's posture.

For the patient, EEG signals were recorded from 32-channel active electrodes using a BrainAmp DC amplifier and actiCAP snap (Brain Products GmbH) with a sampling rate of 500 Hz. The 32-channel locations are Fp1, Fz, F3, F7, FT9, FC5, FC1, C3, T7, TP9, CP5, CP1, Pz, P3, P7, O1, Oz, O2, P4, P8, TP10, CP6, CP2, Cz, C4, T8, FT10, FC6, FC2, F4, F8, and Fp2. The patient also lay on a bed at his home in a supine position, which he usually stays in. His eyes were closed (only manual opening is possible in CLIS). We did not perform preconditioning session by considering the burden of the patient.

EEG Data Preprocessing

EEG raw data were loaded into MATLAB using the EEGLAB toolbox (<https://scn.ucsd.edu/wiki/EEGLAB>) (Delorme and Makeig 2004). The loaded data were band-pass filtered between 0.5 Hz and 40 Hz, and epoched in reference to the onset of GVS that started 1 s after the high-tone beep sound that indicated the start of the imagery. Each epoch had a duration of 6 s, 2 s of preonset and 4 s of postonset. The epoched 3-dimensional matrix (i.e., channel × timepoints × trials) were saved with other information that was required for the following EEG-CCS estimation.

EEG-CCS Estimation

We examined whether the thoughts of yes and no could be discriminated using the EEG-CCS signals. EEG-CCS was estimated using the distributed source localization methods called Variational Bayesian Multimodal Encephalography method (VBMEG) toolbox (ATR Neural Information Analysis Laboratories; <http://vbmeg.atr.jp/?lang=en>) (Sato et al. 2004). The coordinate

positions of 9731 vertices are defined on the cortical surface of the MNI standard brain (Fig. 1c, pink dots in the left-bottom panel), and time series of the vertices (i.e., EEG-CCS) were estimated from the 64-channel EEG sensor signals (32-channels for the CLIS patient) using a hierarchical Bayesian framework (Sato et al. 2004). A T1-weighted MRI anatomical image is often used to create an individual brain model for each person. In this study, however, considering the difficulty of obtaining MRI images from patients in the CLIS, we used an MNI standard brain model and a lead-field matrix that is provided by the toolbox also for the healthy participants, instead of using their individual MRI images. The brain model includes XYZ coordinates of 9731 vertices, and the lead-field matrix is a forward filter to calculate EEG signals from the defined EEG-CCS signals based on sulci and gyri geometry and difference of electrical conductivities between scalp, skull, and cerebrospinal fluid (CSF). A Bayesian framework was used to estimate an inverse filter that calculates EEG-CCS signals from EEG sensor signals. We used default parameters defined by VBMEG throughout the EEG-CCS estimation. The inverse filter was estimated using all the trial data including both answers with the Bayesian activation prior as “uniform,” and EEG-CCSs were calculated by applying the preprocessed EEG data to the inverse filter. The EEG-CCSs were estimated for the whole cortex.

Yes/No Classification Using EEG-CCS

We performed a binary classification analysis between the thoughts of yes and no using the estimated EEG-CCS and Sparse Logistic Regression (SLR) toolbox version 1.2.1 alpha (Yamashita et al. 2008) (ATR Computational Neuroscience Laboratories; https://bicr.ctr.jp/~oyamashi/SLR_WEB.html). Since locations of current source vertices are assigned to the cortical areas according to the automated anatomical labeling atlas (AAL) (Tzourio-Mazoyer et al. 2002) in the toolbox, we can select EEG-CCS signals to be used for the classification analysis based on anatomically defined areas. In order to examine the conditioning effect on the classification accuracy, it is desirable to use signals from all areas of six sensorimotor-related areas (i.e., left and right precentral, postcentral, and SMA) and twelve parietal areas (left and right superior parietal gyrus, inferior parietal gyrus, supramarginal gyrus, angular gyrus, precuneus, and paracentral lobule). However, the total number of vertices in the areas are 2648 that will not provide high accuracy due to overfitting. On the other hand, there are countless combinations of areas to select some of the 18 areas, and the aim of this study is not developing an algorithm but proposing the concept of the GVS conditioning to enhance binary semantic classification performance. Therefore, at first, we examined the conditioning effect using the average time series of each of the 18 anatomical areas. Next, to see the possibility to achieve higher accuracies, we performed a classification analysis using unaveraged signals, by selecting anatomical areas on a trial-and-error basis, with sensorimotor-related areas as the priority. For participants except H2, H3, H5, and H7, in cases where the classification accuracy was less than 60% when using areas from the six areas only, other areas were additionally selected on a trial-and-error basis by referring to activation areas observed by individual fMRI analysis results of participants H1–H6. The mean classification accuracy was calculated using 20-times 20-fold cross-validations for each pre- and postconditioning session (i.e., using 40 trials data consisting of 20-yes and 20-no). Statistical analyses were performed using a two-sample t-test. Chance levels were calculated in a data-driven manner by randomizing

the dataset labels of the postconditioning session in order to test for significance more rigorously.

Results

Association between the EDSs and Thought of Yes/No

Reports from all participants who performed the fMRI experiment (H1–H6) revealed that they recognized the GVS directions in all trials without any inconsistency in the conditioning sessions. All of the participants (H1–H11) reported that they felt their own EDSs even in the absence of GVS in the question sessions. The type of EDS varied from participant to participant, with some reporting that their body was being pushed from one side or pulled, their vision was rotating, or they felt as if the center of their body was rotating.

Activations in the Sensorimotor-Related and Parietal Areas during Thoughts of Yes and No after the GVS Conditioning

Figure 2a shows the results of the fMRI group analysis depicting the difference in brain activity during the thought of yes and no in participants H1–H6. Although the laterality differences in activity varied depending on the participants, the group analysis revealed significant difference mainly in the angular gyrus, precuneus, and postcentral gyrus with a higher activation during “no” with respect to “yes” ($T=19.63$, 15.73 , and 15.31 for the areas, respectively, degrees of freedom = 5 and $P < 0.001$ for all, uncorrected, Table 1). The difference was observed not in the preconditioning session but in the postconditioning session only, and no significant higher activation difference was observed during “yes” with respect to “no” ($T=1.48$, degrees of freedom = 5, $P=0.095$, uncorrected, for the highest activation in the precentral gyrus right). Table 1 shows detailed information of the significant activity differences in the selected areas.

Next, we examined the brain areas of strong activity in the EEG-CCS during the postconditioning session as well. High activation tended to be observed in the postcentral gyrus as shown in Figure 2b, although the exact location and the intensity of the activity varied among participants.

GVS Conditioning Improves on the Yes/No Classification Using EEG-CCS Signals

The classification accuracy using the average signals of the 18 anatomical areas in sensorimotor-related and parietal areas was significantly higher in the postconditioning session (mean \pm S.D. = 63.87 ± 7.96) than in the preconditioning session (mean \pm S.D. = 53.09 ± 4.86) ($T=3.19$, $P=0.03$, effect size $d=1.64$, five participants). The results from the 11 participants also showed that the mean accuracy significantly exceeded the mean chance level (postconditioning session: mean \pm S.D. = 62.63 ± 6.39 ; chance level: mean \pm S.D. = 50.37 ± 3.00 ; $T=5.91$, $P=1.49e-04$, effect size $d=2.46$).

Next, we investigated the possibility of obtaining higher accuracies by using unaveraged signals in anatomical areas selected on a trial-and-error basis. Figures 3a, b show the comparisons between individual mean accuracies of the postconditioning session and the chance level and the individual mean accuracies of the preconditioning session, respectively. As shown in Figure 3a, our methodology showed the mean accuracies significantly higher than chance level with all the participants (H1–H11) and the CLIS patient (P1). The mean accuracy (\pm standard deviation) across the participants and the patient was $74.0 \pm 8.7\%$. In addition, as shown in Figure 3b, we also confirmed that the mean

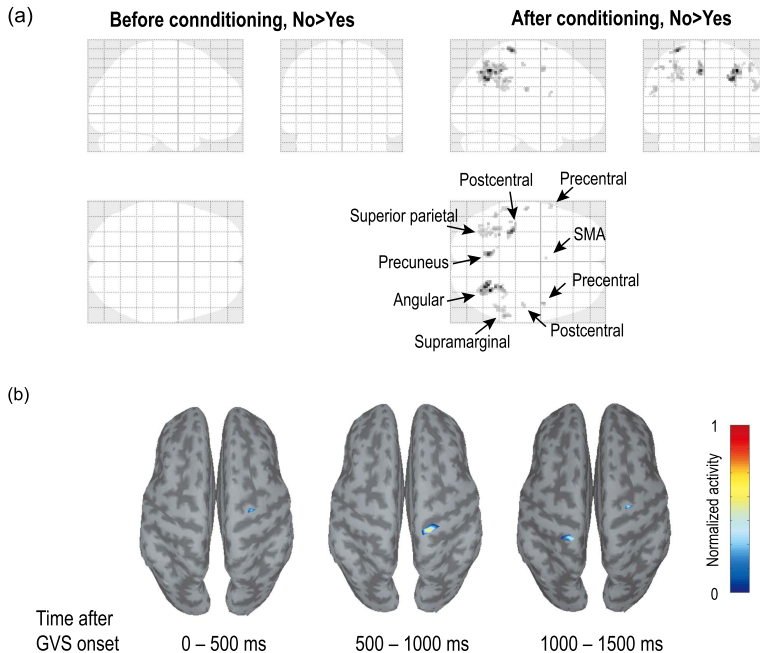


Figure 2. Differential brain-activity areas during the pre- and postconditioning sessions. (a) Results of an fMRI group analysis displaying areas of higher activity during “no” with respect to “yes” before and after conditioning. Each map represents the difference between the thoughts of yes and no, and the ROIs were set to sensorimotor-related (the postcentral, the precentral gyri, and the SMA on the left and right hemispheres) and parietal (the angular gyrus, precuneus, parietal operculum, supramarginal gyrus, and superior parietal lobule on the left and right hemispheres) areas. The activation areas projected on standard transparent brains are presented in coronal, axial, and sagittal views. The areas are statistically significant without multiple comparison corrections, uncorrected $P < 0.001$. (b) Brain topographical maps showing averaged EEG-CCS activation during the thought of “no” in the postconditioning session in participant H3. The dark gray and the light gray areas represent sulci and gyri, respectively. The high activation area was located in the postcentral gyrus around 500–1000 ms after the “expected” GVS onset when GVS was supposed to be applied.

accuracies of the postconditioning session were significantly higher than those of the preconditioning for all participants (H7–H11). Table 2 summarizes brain areas used for the yes/no classification analysis by each participant. The postcentral gyrus contributed to the significant accuracy in all participants, four of the participants (H2, H3, H5, and H7) showed significant accuracies using areas in sensorimotor-related areas only, and the other participants required other areas such as parietal areas: the right angular gyrus, the left calcarine, the bilateral medial superior frontal gyrus (mSFG), the bilateral cuneus, the right inferior parietal gyrus (IPG), the left precuneus, the left inferior temporal gyrus, and the right superior parietal gyrus (SPG). Our methodology also showed high significant classification accuracy (85.3±5.4%) for the CLIS patient using sensorimotor-related areas as well as the healthy participants.

To visualize the activation difference between the thoughts of yes and no in EEG-CCS, the temporal patterns from representative participant H2 and patient P1 are shown in Figure 4. We

found that the healthy participants tended to show activation difference between the thoughts of yes and no in sensorimotor-related areas mainly within 1 s after the expected GVS onset (note that GVS was not actually presented). On the other hand, the CLIS patient showed high activity in the postcentral gyrus in the EEG-CCS topographical map as well as the healthy participants, but the temporal peak differences between yes and no especially in the precentral and postcentral gyri were observed later in time than in the healthy participants (i.e., around 2 s after the GVS onset).

Discussion

Based on the hypothesis that GVS, which evokes reflexive EDS, is suitable for Pavlovian conditioning, the present study tested whether EDS can be conditioned to thoughts of “yes” and “no.” In addition, we also investigated whether sensorimotor-related

Table 1. Brain areas showing increased differential activation between thoughts of yes and no during the postconditioning session from the fMRI analysis

Name of area	MNI coordinates	T-values
Angular gyrus right	[34, -58, 46]	19.63
Precuneus left	[-6, -60, 46]	15.73
Postcentral gyrus left	[-32, -34, 68]	15.31
Supramarginal gyrus right	[62, -42, 34]	9.53
Superior parietal lobule left	[-34, -52, 50]	9.14
Precentral gyrus right	[48, 2, 48]	8.70
Postcentral gyrus left	[-56, -18, 24]	8.63
Angular gyrus left	[-50, -52, 50]	8.17
Superior parietal lobule left	[-30, -56, 38]	7.82
Supramarginal gyrus left	[-56, -40, 48]	7.69
Postcentral gyrus right	[50, -22, 54]	7.43
Precentral gyrus left	[-60, 10, 22]	7.34
Angular gyrus left	[-28, -68, 36]	7.15
Supramarginal gyrus left	[-42, -36, 38]	6.99
Angular gyrus left	[-38, -68, 40]	6.85
Supramarginal gyrus left	[-58, -44, 28]	6.79
SMA left	[-2, 4, 70]	6.74
Precentral gyrus left	[-58, 8, 18]	6.57
Precentral gyrus left	[-62, 8, 20]	6.56

The statistical analysis was performed by restricting the ROI to the left and right postcentral and precentral gyri, and the SMA, angular gyrus, precuneus, parietal operculum, supramarginal gyrus, and superior parietal lobule, respectively, with no multiple comparison correction (uncorrected $P < 0.001$). XYZ coordinates of the centroid of the activated areas were defined according to Montreal Neurological Institute (MNI) coordinate system.

and parietal areas were activated by the EDS contingent with the thoughts of yes and no using fMRI and examined whether EEG-CCS in those areas improved the accuracy of predicting “yes” and “no” covert (i.e., cognitive) responses. All healthy participants reported that the EDS was induced by the thoughts of yes and no after conditioning, and not only fMRI but also EEG-CCS analyses confirmed that the difference in brain activity between “yes” and “no” was especially found in the postcentral gyrus. Furthermore, prediction of cognitive “yes” and “no” responses using EEG-CCS signals after conditioning achieved significant classification accuracies not only with all the healthy participants but also with the CLIS patient ($73.0 \pm 8.3\%$ for healthy, $85.3 \pm 5.4\%$ for the CLIS patient).

Activation Areas Induced by the EDS in the Postconditioning

Consistent with the classical conditioning literature (Razran 1971), we verified that after conditioning, EDS occurred as expected even in the absence of GVS and was associated with the thoughts of yes and no. GVS evokes EDS as UR to keep the body balance in equilibrium against gravity and constitutes an ideal biologically relevant US without producing negative emotional side effects of painful or unpleasant USs (Utz et al. 2011).

As shown in Figure 2, comparing the results between the pre- and postconditioning sessions using the fMRI group analysis, it was confirmed that the brain activity indicating the difference between “yes” and “no” was increased in the sensorimotor-related and parietal areas, especially in the angular gyrus, precuneus, and postcentral gyrus. This finding is not only consistent with previous fMRI (Lobel et al. 1998; Stephan et al. 2005), TMS (Reichenbach et al. 2016), and GVS (Lopez et al. 2012; Ganesh et al. 2018) research, but also with an anatomical study in cats showing that the vestibular nuclei project to the primary somatosensory cortex via the thalamus (Mountcastle 1957). Therefore, the present results, in which vestibular-related activity was observed even while the GVS was not given, may indicate successful conditioning.

In addition, it is noteworthy that the relevant area was recognized by the EEG-CCS topographical maps as well as the fMRI analysis, which may support the validity of the significant classification accuracies in this study. In the EEG-CCS classification analysis, not only the postcentral gyrus but also the precentral gyrus and SMA showed high differentiation in some participants. Since the precentral gyrus and SMA are included in the representative areas related to motor control, conditioned reflexes evoked by EDS may include neural activity related to motor control as well as sensory perception.

Contribution of Other Areas to the Yes/No Classification

Conditioning induced differential activity in areas other than sensorimotor-related areas used in the EEG-CCS classification analysis in some participants. The areas were the right angular gyrus, the left calcarine, the bilateral mSFG, the bilateral cuneus, the right IPG, the left precuneus, the left ITG, and the right SPG. Among these areas, the angular gyrus, IPG, precuneus, and SPG are included in parietal areas, which have been reported to be activated by GVS in several studies (Stephan et al. 2005; Lopez et al. 2012; Reichenbach et al. 2016; Ganesh et al. 2018).

Regarding the involvement of the other areas (i.e., calcarine, mSFG, cuneus, and ITG), the calcarine cortex (used by H4), the bilateral cuneus (used by H6 and H11), and the ITG (used by P1) have been reported to be involved in visual processing. The calcarine cortex is located in the primary visual cortex, and an EEG study has indicated its involvement in visuospatial attention (Di Russo et al. 2003). The cuneus is also located in the primary visual cortex and receives visual information from the primary visual area V1 (Vanni et al. 2001), and the ITG is reported to be involved in visual processing via the inferior occipital gyrus (Kastner and Ungerleider 2000). The mSFG used by H6 and H9 is involved in motor control since it includes SMA and presupplementary motor area. These findings suggest that all areas used for the classification along with the sensorimotor-related areas in all participants are involved in sensorimotor integration and visual

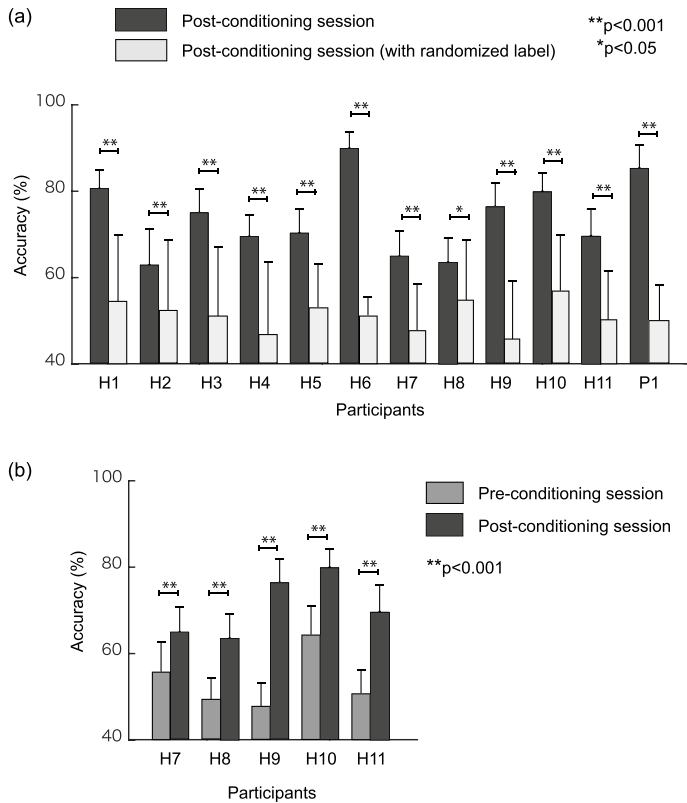


Figure 3. Yes/No classification accuracies using EEG-CCS for healthy participants and a CLIS patient. (a) Comparisons between the postconditioning session and chance level. Dark gray and light gray bars represent classification accuracies using question session data after the conditioning (i.e., postconditioning session), and postconditioning session with randomized label (i.e., chance level), respectively. (b) Comparisons between the pre- and postconditioning sessions. Dark gray and gray bars represent classification accuracies using question session data in the postconditioning session, and a question session data in the preconditioning session, respectively, for the last 5 participants. The first six participants did not perform a preconditioning session. For both figures, the mean accuracies were calculated from 20-time 20-fold cross-validation analysis, and statistical significance was evaluated using two-sample t-test. Error bars represent standard deviations.

processing, contributing to the classification of the different EDS between the thoughts of yes and no.

Efficacy of the GVS for Differential Conditioning

The significant accuracies in the yes/no classification revealed the effectiveness of the GVS for differential conditioning both for the healthy and the CLIS participants.

A similar conditioning approach has been used in yes/no BCI studies with healthy participants, a CLIS patient, and two LIS

(locked-in-state with intact eye movements) (Furdea et al. 2012; De Massari et al. 2013; Ruf et al. 2013). In one of these studies with CLIS and LIS patients, only thought of “yes” as a CS and a tactile sensation of electrical stimulation over the left thumb as a US were used (De Massari et al. 2013), but mean accuracies were around chance level though in some sessions yes/no classification accuracies of 70% were reached. The remaining studies tried a differential paradigm with healthy participants using pink and white noises as USs to condition thoughts of yes

Table 2. Brain areas used in the yes/no classification for the participants and the patient

ID	Areas used for the classification analysis
H1	Postcentral right, SMA left, Angular right
H2	Postcentral right, Precentral right, SMA right
H3	Postcentral right and left, Precentral right and left, SMA right and left
H4	Postcentral left, Precentral left, SMA left, Calcarine left, mSFG right
H5	Postcentral left, Precentral left, SMA right
H6	Postcentral right, SMA left, Cuneus right, mSFG left and right
H7	Postcentral left, Precentral left, SMA left
H8	Postcentral left, Precentral left, IPG right
H9	Postcentral left, SMA right, mSFG left and right
H10	Postcentral right, SMA left, IPG right, Precuneus left
H11	Postcentral right, SMA right, ITG left, Cuneus left
P1	Postcentral right, Precentral right, SPG right, ITG left

All of them showed EEG-CCS signals from the postcentral gyrus. SMA, supplementary motor area; IPG, inferior parietal gyrus; mSFG, medial superior frontal gyrus; ITG, inferior temporal gyrus; SPG, superior parietal gyrus.

and no as CSs, and at most around 70% accuracies were observed. Considering that mean accuracy across the 11 participants and the CLIS patient in our study was $74.0 \pm 8.7\%$ (\pm standard deviation) and the accuracies may be further improved by expanding and optimizing the areas used for classification, the current results suggest efficacy of GVS for differential conditioning to create an association between the thoughts of yes and no and the EDS. The USs used in the previous studies (i.e., tactile sensation by electrical stimulation and auditory stimuli) may not activate a stable and/or intensive and biologically relevant response compared with galvanic vestibular responses. In GVS, the participants felt not only the sensation on the skin caused by the electrical stimulation but also the EDS that adds to the unconditioned response complex. This might have been the key to the success of the current study as hypothesized.

Differences between Healthy Participants and a CLIS Patient

Our methodology also showed high yes/no classification accuracy of 85.3% in the CLIS patient using mainly the sensorimotor-related areas as shown in the healthy participants. Under the plausible assumption that the galvanic vestibular function remains unchanged by the disease, we expected the GVS conditioning to be also effective for the patient.

The brain areas that provided the high accuracy included the postcentral gyrus right and the precentral gyrus right that are known to be crucial sensorimotor areas. Although we did not ask the patient if he felt the EDS because of the communication deficit, the brain activity patterns in these areas shown by EEG-CCS (Fig. 4) and the high accuracy suggested intact galvanic vestibular function in the patient. In addition, we observed a notable difference between healthy participants and the CLIS patient, which may be important for future BCI developments for CLIS: While healthy participants differentiated between the two requested responses for the thoughts of yes and no within 1 s after the expected GVS onset, the patient showed a delayed response (around 2 s after the onset). This might suggest delayed neural response in the CLIS patient, which may be correlated with the dominance of slow EEG frequencies in CLIS patients

(Hohmann et al. 2018; Malekshahi et al. 2019; Maruyama et al. 2021). Also, the patient involved in this study shows a dominant slow EEG of 2–4 Hz during waking hours, compared with the dominant 10 Hz frequency in healthy people, which may indicate lower arousal and/or slower cognitive processing.

Toward Clinical Application: Critical Comments

We need to address the following issues to develop a practical application based on this methodology. At first, identification of brain areas used for the classification should be optimized. In this study, we aimed to clarify the efficacy of the GVS conditioning. Therefore, we used brain areas primarily from sensorimotor-related areas and did not optimize the accuracies using other areas. Despite significant accuracies, there may be better area combinations for each participant. To develop a practical application, as a next step, we are going to develop an algorithm to select optimal brain areas for each participant using EEG-CCS.

In the process of the algorithm development, the second issue, reproducibility, also needs to be considered for online classification. The significantly high accuracies revealed the physiological stability of topographically specific brain responses across participants and between fMRI and EEG-CCS, and they also suggest the possibility of the classical conditioning paradigm as a robust and reproducible basis for BCI development (Birbaumer 2006). Since we calculated yes/no classifiers using data selected from a session from the same day as the data used for test, we need to investigate further the effectiveness of classification in those areas using data from other days. Reproducibility is the most challenging problem of BCIs based on machine learning. Recent developments of machine learning techniques have provided powerful means to extract detailed information hidden in the brain data, especially for noninvasively recorded brain activity that consists of a complex combination of physiological processes. However, when it comes to applications of online BCIs, such detailed information extracted from experimental data rarely shows reproducibility, and it is difficult to obtain high classification accuracies with a classifier calculated with data from another day.

Among the BCIs that try to extract covert thoughts from neural activity, a paradigm based on event-related desynchronization (ERD) occurring with motor imagery has shown reliable results (Pfurtscheller et al. 1996; Pfurtscheller and Neuper 2001). The “thinking” paradigm used here constitutes a comparable approach. Considering that neural activity relative to ERD can also be observed in fMRI (Halder et al. 2011), the key to develop a reliable BCI will be the use of a paradigm that shows robust differential activation in most noninvasive brain measures such as EEG, fMRI, and NIRS. Since our results suggest the physiological stability of the CRs in terms of topographical brain responses between fMRI and EEG-CCS, the challenge will be to prove the efficacy of classifiers calculated from different days.

The third issue is optimization of the conditioning learning process. The most effective procedures to secure stable associations between CS-CR need to be varied systematically. It is usually assumed that the association between CS and US will become stronger as the number of conditioning trials increases. However, a few participants reported decreasing EDS (i.e., perception) as the number of conditioning trials increased, indicating habituation. That might be due to the low electrical currents used, and on the other hand, the brain activation still might occur even if participants do not perceive the EDS consciously.

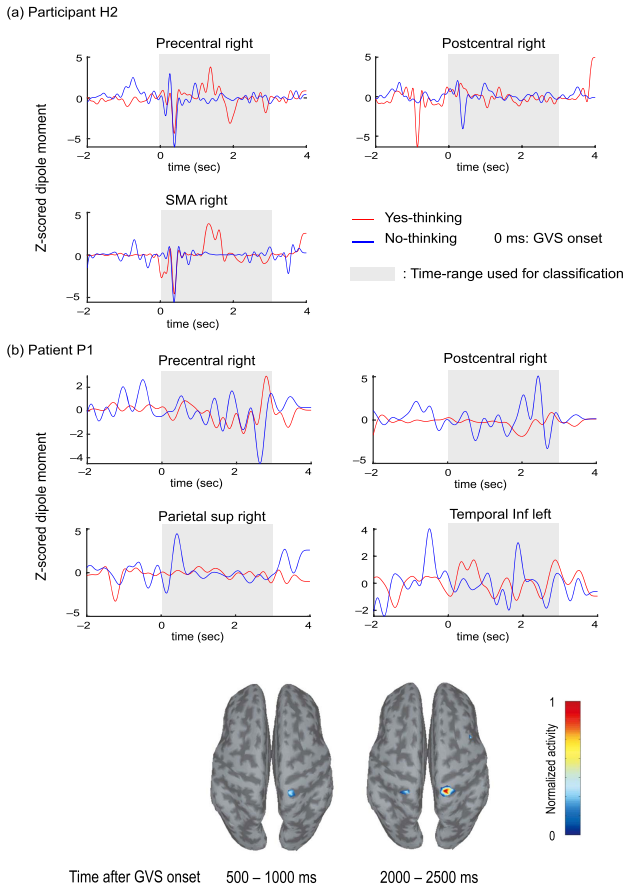


Figure 4. EEG-CCS activation pattern comparison between thoughts of yes and no. Mean time-series activation patterns of representative participant H2 (a) and patient P1 (b) were plotted. Red and blue lines represent the thoughts of yes and no, respectively. The gray-shaded time range was used for the classification. All time-series signals were band-pass filtered for the range of 5–15 Hz. The brain topographical maps at the bottom panel show averaged EEG-CCS activation during the question session of patient P1. The dark gray areas represent sulci and the light gray areas represent gyri. The highest activation area located in the postcentral gyrus around 2000–2500 ms after the GVS onset when GVS was supposed to be applied.

In any case, we may need to optimize and individualize the timing, frequencies, and strength of GVS to keep the conditioning effect. Even though activation areas differ between participants,

observing the regional transitions of activation before, during, and after conditioning could provide insights into the process of learning.

Supplementary Material

Supplementary material can be found at Cerebral Cortex Communications online.

Funding

Japan-Germany Research Cooperative Program between JSPS and DAAD [grant number JPJSBP 120193510]; Tokyo Tech World Research Hub Initiative from Tokyo Institute of Technology; JST PRESTO (Precursory Research for the Embryonic Science and Technology) [grant number JPMJPR17A]; Deutsche Forschungsgemeinschaft (DFG, Kosellek) [grant number BI 195/77-1]; BMBF (German Ministry of Education and Research) [grant number 16SV7701 CoMiCon; LUMINOUS-H2020-FETOPEN-2014-2015-RIA [grant number (686764)]; Eva and Horst Köhler-Stiftung; DAAD (German Academic Exchange Service: Japanese-German Exchange program).

Notes

We deeply thank the CLIS patient, his family, and the healthy participants. Conflict of Interest: N.Y., G.G., and Y.K. have a pending patent regarding the method demonstrated in this study (Japanese Patent application number: 2020-108549).

References

Birbaumer N. 2006. Breaking the silence: brain-computer interfaces (BCI) for communication and motor control. *Psychophysiology*. 43:517–532.

Brainard DH. 1997. The psychophysics toolbox. *Spat Vis*. 10:433–436.

Chaudhary U, Xia B, Silvoni S, Cohen LG, Birbaumer N. 2017. Brain-computer interface-based communication in the completely locked-in state. *PLoS Biol*. 15:1–25.

Cohen J. 1988. *Statistical power for the social sciences*. Hillsdale (NJ): Lawrence Erlbaum and Associates.

De Massari D, Ruf CA, Furdea A, Matuz T, Van Der Heiden L, Halder S, Silvoni S, Birbaumer N. 2013. Brain communication in the locked-in state. *Brain*. 136:1989–2000.

Delorme A, Makeig S. 2004. EEGLAB: an open source toolbox for analysis of single-trial EEG dynamics including independent component analysis. *J Neurosci Methods*. 134:9–21.

Di Russo F, Martinez A, Hillyard SA. 2003. Source analysis of event-related cortical activity during visuo-spatial attention. *Cereb Cortex*. 13:486–499.

Đlugaičzyk J, Gensberger KD, Straka H. 2019. Galvanic vestibular stimulation: from basic concepts to clinical applications. *J Neurophysiol*. 121:2237–2255.

Faul F, Erdfelder E, Lang A-G, Buchner A. 2007. G*Power 3: A flexible statistical power analysis program for the social, behavioral, and biomedical sciences. *Behav Res Methods*. 39:175–191.

Fitzpatrick RC, Day BL. 2004. Probing the human vestibular system with galvanic stimulation. *J Appl Physiol*. 96:2301–2316.

Fukuma R, Yanagisawa T, Yokoi H, Hirata M, Yoshimine T, Saitoh Y, Kamitani Y, Kishima H. 2018. Training in use of brain-machine interface-controlled robotic hand improves accuracy decoding two types of hand movements. *Front Neurosci*. 12:478.

Furdea A, Ruf CA, Halder S, De Massari D, Bogdan M, Rosenstiel W, Matuz T, Birbaumer N. 2012. A new (semantic) reflexive brain-computer interface: in search for a suitable classifier. *J Neurosci Methods*. 203:233–240.

Gallegos-Ayala G, Furdea A, Takano K, Ruf CA, Flor H, Birbaumer N. 2014. Brain communication in a completely locked-in patient using bedside near-infrared spectroscopy. *Neurology*. 82:1930–1932.

Ganesh G, Nakamura K, Saetia S, Tobar AM, Yoshida E, Ando H, Yoshimura N, Koike Y. 2018. Utilizing sensory prediction errors for movement intention decoding: a new methodology. *Sci Adv*. 4:1–8.

Halder S, Agorastos D, Veit R, Hammer EM, Lee S, Varkuti B, Bogdan M, Rosenstiel W, Birbaumer N, Kübler A. 2011. Neural mechanisms of brain-computer interface control. *Neuroimage*. 55:1779–1790.

Han CH, Kim YW, Kim DY, Kim SH, Nenadic Z, Im CH. 2019. Electroencephalography-based endogenous brain-computer interface for online communication with a completely locked-in patient. *J Neuroeng Rehabil*. 16:1–13.

Hohmann MR, Fomina T, Jayaram V, Emde T, Just J, Synofzik M, Schölkopf B, Schöls L, Grosse-Wentrup M. 2018. Case series: slowing alpha rhythm in late-stage ALS patients. *Clin Neurophysiol*. 129:406–408.

Irimia DC, Ortner R, Poboronius MS, Ignat BE, Guger C. 2018. High classification accuracy of a motor imagery based brain-computer interface for stroke rehabilitation training. *Front Robot AI*. 5:130.

Kastner S, Ungerleider LG. 2000. Mechanisms of visual attention in the human cortex. *Annu Rev Neurosci*. 23:315–341.

Khalili Ardali M, Rana A, Purmohammad M, Birbaumer N, Chaudhary U. 2019. Semantic and BCI-performance in completely paralyzed patients: possibility of language attrition in completely locked in syndrome. *Brain Lang*. 194:93–97.

Kiernan MC, Vucic S, Cheah BC, Turner MR, Eisen A, Hardiman O, Burrell JR, Zoing MC. 2011. Amyotrophic lateral sclerosis. *Lancet*. 377:942–955.

Kleiner M, Brainard DH, Pelli DG, Broussard C, Wolf T, Niehorster D. 2007. What's new in psychtoolbox-3? *Perception*. 36:1–16.

Kübler A, Birbaumer N. 2008. *Brain-computer interfaces and communication in paralysis: extinction of goal directed thinking in completely paralysed patients?* *Clin Neurophysiol* 119:2658–2666.

Liu SH, Yu NH, Chan L, Peng YH, Sun WZ, Chen MY. 2019. PhantomLegs: reducing virtual reality sickness using head-worn haptic devices. In: 26th IEEE conference on virtual reality and 3D user interfaces, VR 2019 - Proceedings. New York: IEEE.

Lobel E, Kleine JF, Le Bihan D, Leroy-Willig A, Berthoz A. 1998. Functional MRI of galvanic vestibular stimulation. *J Neurophysiol*. 80:2699–2709.

Lopez C, Blanke O, Mast FW. 2012. The human vestibular cortex revealed by coordinate-based activation likelihood estimation meta-analysis. *Neuroscience*. 212:159–179.

Maeda T, Ando H, Amemiya T, Nagaya N, Sugimoto M, Inami M. 2005. Shaking the world: galvanic vestibular stimulation as a novel sensation interface. In: *ACM SIGGRAPH 2005 Emerging Technologies, SIGGRAPH 2005*.

Malekshahi A, Chaudhary U, Jaramillo-Gonzalez A, Luna AL, Rana A, Tonin A, Birbaumer N, Gais S. 2019. Sleep in the completely locked-in state (CLIS) in amyotrophic lateral sclerosis. *Sleep*. 42:1–8.

Maruyama Y, Yoshimura N, Rana A, Malekshahi A, Tonin A, Jaramillo-Gonzalez A, Birbaumer N, Chaudhary U. 2021. Electroencephalography of completely locked-in state patients with amyotrophic lateral sclerosis. *Neurosci Res*. 162: 45–51.

Mountcastle VB. 1957. Modality and topographic properties of single neurons of cat's somatic sensory cortex. *J Neurophysiol*. 20:408–434.




- Murguialday AR, Hill J, Bensch M, Martens S, Halder S, Nijboer F, Schoelkopf B, Birbaumer N, Gharabaghi A. 2011. Transition from the locked in to the completely locked-in state: a physiological analysis. *Clin Neurophysiol.* 122:925–933.
- Okahara Y, Takano K, Nagao M, Kondo K, Iwade Y, Birbaumer N, Kansaku K. 2018. Long-term use of a neural prosthesis in progressive paralysis. *Sci Rep.* 8:16787.
- Pan W, Soma R, Kwak S, Yamamoto Y. 2008. Improvement of motor functions by noisy vestibular stimulation in central neurodegenerative disorders. *J Neurol.* 255:1657–1661.
- Pavlov IP. 1927. *Conditioned reflexes*. Oxford, UK: Oxford University Press.
- Pelli DG. 1997. The VideoToolbox software for visual psychophysics: transforming numbers into movies. *Spat Vis.* 10:437–442.
- Pfurtscheller G, Neuper C. 2001. Motor imagery and direct brain-computer communication. *Proc IEEE.* 89:1123–1134.
- Pfurtscheller G, Stancák A, Neuper C. 1996. Event-related synchronization (ERS) in the alpha band - an electrophysiological correlate of cortical idling: a review. *Int J Psychophysiol.* 24: 39–46.
- Razran G. 1971. *Mind in evolution*. Boston, USA: Houghton Mifflin.
- Reichenbach A, Bresciani JP, Bühlhoff HH, Thielscher A. 2016. Reaching with the sixth sense: vestibular contributions to voluntary motor control in the human right parietal cortex. *Neuroimage.* 124:869–875.
- Ruf CA, De Massari D, Furdea A, Matuz T, Fioravanti C, Van Der Heiden L, Halder S, Birbaumer N. 2013. Semantic classical conditioning and brain-computer interface control: encoding of affirmative and negative thinking. *Front Neurosci.* 7: 1–13.
- Sato MA, Yoshioka T, Kajihara S, Toyama K, Goda N, Doya K, Kawato M. 2004. Hierarchical Bayesian estimation for MEG inverse problem. *Neuroimage.* 23:806–826.
- Sra M, Xu X, Maes P. 2017. *GalVR: a novel collaboration interface using GVS*. In: Proceedings of the ACM Symposium on Virtual Reality Software and Technology, VRST.
- Stephan T, Deuschländer A, Nolte A, Schneider E, Wiesmann M, Brandt T, Dieterich M. 2005. Functional MRI of galvanic vestibular stimulation with alternating currents at different frequencies. *Neuroimage.* 26:721–732.
- Tzourio-Mazoyer N, Landeau B, Papathanassiou D, Crivello F, Etard O, Delcroix N, Mazoyer B, Joliot M. 2002. Automated anatomical labeling of activations in SPM using a macroscopic anatomical parcellation of the MNI MRI single-subject brain. *Neuroimage.* 15:273–289.
- Utz KS, Dimova V, Oppenländer K, Kerkhoff G. 2010. Electrified minds: transcranial direct current stimulation (tDCS) and Galvanic Vestibular Stimulation (GVS) as methods of non-invasive brain stimulation in neuropsychology—a review of current data and future implications. *Neuropsychologia.* 48: 2789–2810.
- Utz KS, Korluss K, Schmidt L, Rosenthal A, Oppenländer K, Keller I, Kerkhoff G. 2011. Minor adverse effects of galvanic vestibular stimulation in persons with stroke and healthy individuals. *Brain Inj.* 25:1058–1069.
- Vanni S, Tanskanen T, Seppä M, Utela K, Hari R. 2001. Coinciding early activation of the human primary visual cortex and anteromedial cuneus. *Proc Nat Acad Sci USA.* 98:2776–2780.
- Yamashita O, Sato MA, Yoshioka T, Tong F, Kamitani Y. 2008. Sparse estimation automatically selects voxels relevant for the decoding of fMRI activity patterns. *Neuroimage.* 42:1414–1429.



OPEN

DATA DESCRIPTOR

A dataset of EEG and EOG from an auditory EOG-based communication system for patients in locked-in state

Andres Jaramillo-Gonzalez¹ , Shizhe Wu¹, Alessandro Tonin², Aygul Rana¹, Majid Khalili Ardali¹ , Niels Birbaumer^{1,3} & Ujwal Chaudhary^{1,2,3} 

The dataset presented here contains recordings of electroencephalogram (EEG) and electrooculogram (EOG) from four advanced locked-in state (LIS) patients suffering from ALS (amyotrophic lateral sclerosis). These patients could no longer use commercial eye-trackers, but they could still move their eyes and used the remnant oculomotor activity to select letters to form words and sentences using a novel auditory communication system. Data were recorded from four patients during a variable range of visits (from 2 to 10), each visit comprised of 3.22 ± 1.21 days and consisted of 5.57 ± 2.61 sessions recorded per day. The patients performed a succession of different sessions, namely, Training, Feedback, Copy spelling, and Free spelling. The dataset provides an insight into the progression of ALS and presents a valuable opportunity to design and improve assistive and alternative communication technologies and brain-computer interfaces. It might also help redefine the course of progression in ALS, thereby improving clinical judgement and treatment.

Background & Summary

Amyotrophic lateral sclerosis (ALS) is a neurodegenerative disorder that, in its final stages, paralyzes affected individuals impairing their ability to communicate^{1–4}. Those patients with intact consciousness, voluntary eye movement control, who can blink their eyes or twitch their muscles are said to be in a locked-in state (LIS)^{5,6}. Patients in LIS rely on eye-tracking based assistive and augmentative communication (AAC) technologies to communicate^{5,6}. In the case of patients who survive attached to life-support systems, the progression of the disease ultimately destroys oculomotor control, leading to the loss of gaze-fixation and impeding the use of eye-tracking based communication technologies^{7–11}. Nevertheless, even in the late stages of this condition, some remaining controllable muscles of the eyes continue to function for an unspecified length of time, which can be used to provide a means of communication to these patients^{11,12}.

An auditory electrooculogram (EOG) based communication system¹² was developed to provide a means of communication to ALS patients without gaze-fixation and who were unable to use the commercial AAC eye-tracking devices, but who had remnant oculomotor control to form words, phrases, and sentences using the system described in Tonin & Jaramillo-Gonzalez *et al.*¹². Four ALS patients with progressively decreasing EOG signal amplitude in the range of $\pm 200 \mu\text{V}$ to $\pm 40 \mu\text{V}$ were able to select letters to construct words to form sentences and hence communicate freely using an auditory speller system. The auditory speller system is based on a binary system in which a patient is asked to respond to auditory questions by moving the eyes to say “yes” and not moving the eyes to say “no”. The system must use the auditory modality because, in these patients, vision is often impaired due to drying and necrosis of the cornea and the partly or fully paralyzed eye-muscles. The study design and paradigm are described in detail in the Methods section.

This data descriptor outlines the EEG and EOG recordings from four different patients recorded during their use of the auditory communication system, having first trained progressively, and then ultimately controlling the

¹Institute of Medical Psychology and Behavioral Neurobiology, University of Tübingen, Tübingen, Germany. ²Wyss Center for Bio and Neuroengineering, Geneva, Switzerland. ³Ospedale San Camillo, IRCCS, Venice, Italy. [✉]e-mail: chaudharyujwal@gmail.com

system to communicate. Electromyography (EMG) recordings are available for some sessions, according to the clinical conditions.

There have been other studies with similar goals, but only one has an available online dataset¹³, with different features. To our knowledge, in the available open-access specialized repositories^{14–16}, there are no datasets with similar properties to the one described here. It must be emphasized that the data described here are both the EOG and EEG signals recorded with a dedicated set of electrodes for each type of signal simultaneously. These EEG and EOG data are recorded from patients with ALS in the most advanced stage, whose disease progression is not well defined and is, to a certain extent, unknown. The data highlight a phase in ALS where communication becomes difficult and gradually impossible with existing commercial AAC. It includes recordings of over the course of a year during which one of the users became unable to use the system because of disease progression. As a consequence, we believe that the study of this dataset might help towards improving the clinical definition of ALS in its very advanced state, the testing of hypotheses on the brain's electrophysiological changes during this progression and evaluating the impact of advanced ALS on the cognitive state of the patients. Nevertheless, even though the data is quite specific, further investigation of the data can support novel clinical and therapeutic practices. It could help develop augmentative and alternative assistive communication technologies and brain-computer interfaces that can be generalized to other types of disorders and patients with pervasive communication deficits and motor impairments due to CNS damage, such as stroke or high spinal cord injury. Lastly, although the system can be considered successful in enabling communication, other analytical methods can still improve the system's speed and efficiency, for example, offline testing of other feature extraction methods or testing and comparing the performance with different machine-learning methods to classify the patients' response.

Methods

The Internal Review Board of the Medical Faculty of the University of Tübingen approved the experiment reported in this study. The study was performed according to guidelines established by the Medical Faculty of the University of Tübingen. The patient, or the patient's legal representative, gave informed consent with permission to publish the data. The clinical trial registration number is: ClinicalTrials.gov - Identifier: NCT02980380. The methods described here are complementary to an in-depth description of the results derived from this dataset that have been presented in related work¹².

Participating patients. Four ALS patients with amyotrophic lateral sclerosis with a functional rating scale revised (ALSF_{RS-R})¹⁷ score of 0 in the locked-in state (LIS) were visited on subsequent months starting from Feb 2018 to May 2019. Team members travelled to the patient's home to perform the communication sessions, depending on the health status and convenience of the patient. The medical history of patients is described in our related work¹². Every visit (V), lasted for a few days (D), during which the patient performed different session (S), as detailed in the Online-only Tables 1–4, with the precise dates of all the visits and details of the sessions.

Auditory communication system. *Prerequisites for performing the study.* In agreement with the patients' caretakers and considering the patients' health and wellness and optimization of resources, it was established that the visits should be performed every two months approximately, with each visit no longer than four days. However, on some occasions the condition of the patients led to shorter visits, from three days to a single day. (see Online-only Tables 1–4). For each visit, guided by the same criteria of health and wellness of the patient, two team members transported all equipment and set up all systems in the patient's home or accommodation.

Before the beginning of the study, at least 100 questions with known "yes" or "no" answers were formulated and recorded by a family member or caretaker in their own voice, in close proximity to the patient. Each question with a "yes" answer is paired with a similar question with "no" answer (e.g., "Paris is the capital of France" and "Berlin is the capital of France"). Each question is saved as an audio file with an explicit identifier, a question with a "yes" answer is saved with a 001_NUMBER identifier, and a question with "no" answer is saved with a 002_NUMBER identifier. The value of the label NUMBER is the same for a semantically paired sentence. The same procedure was repeated with biographical-related questions with at least 100 for every patient. Sentences are then stored on a laptop and accessed and played by the communication system during the sessions.

Study and paradigm. The study consisted of patients performing four different types of sessions, namely, Training, Feedback, Copy speller, and Free speller session, to train and enable the patient to employ an oculomotor strategy to control the spelling system successfully. During the visit, the patient performed different sessions, as depicted in Fig. 1. The patients developed a strategy to respond during successive trials to an auditory question (the questions previously recorded) by moving the eyes to say "yes" and by not moving the eyes to say "no". To control the activities during the trials, specific paradigms were designed for the different sessions, as depicted in Fig. 2.

The different sessions performed by the patients are described below.

a. Training session

The study on a single day always started with Training sessions during which the patients were instructed to listen to a sequence of 20 personal questions consisting of 10 sentences with a "yes" answer and 10 with "no" answer, presented in pseudo-random order. After the system presents an auditory question, patients are asked to move their eyes to respond "yes" and not to move the eyes to respond "no" during a response time window. The duration of the response segment depended on the patient's performance, i.e., if the patient could move his/her eye with ease, the duration was kept shorter and vice versa. Therefore, this window has a range from 3 to 10 seconds. For each Training session, the set of triggers indicating the sequence of events were recorded on the raw file, using the labels shown in Fig. 2a. Alongside, the system creates a questions sequence text file (Block_X_senlist.txt) that includes the list of identifiers of the presented audio/

Sessions performed by the patient

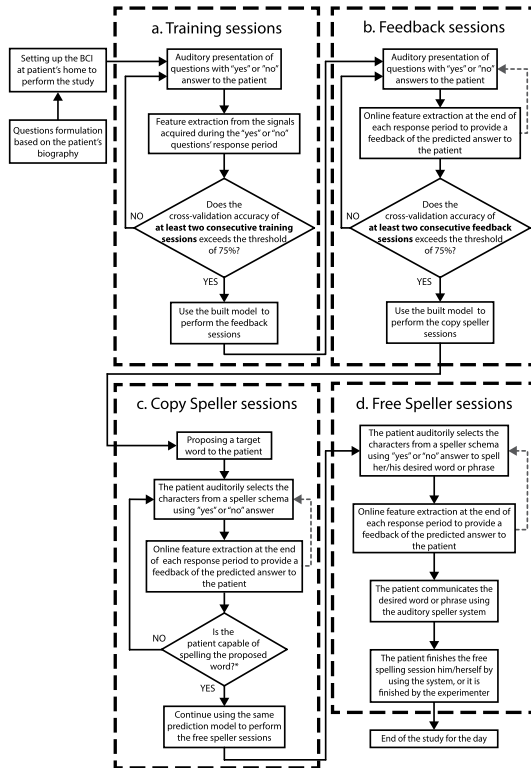


Fig. 1 The procedure performed during a single day. The figure depicts the sequence of the types of sessions performed by patients and the criteria to progress from one type of session to the next. The patients first performed the Training sessions during which the patient learned to move his/her eyes to generate the signal to control the auditory communication system. At the end of the Training session, a classification model was built, and when the accuracy of the built model was greater than 75% the patients performed the feedback session. During the feedback sessions the patients were provided the feedback of their response, i.e., whether their answer was classified as “yes” or “no”. When the feedback accuracy exceeded 75% the patients first performed a copy speller session and then a free speller during which they could spell whatever they desired.

question files during the session (e.g., 001_13012a.wav), including also the label of the corresponding type of answer (“0” for sentences with “no” as an answer, and “1” for sentences with “yes” as an answer). The .txt lists are included inside the raw data folder structure, as described in the section Data Records. After at least two consecutive Training sessions with a classification accuracy result greater than 75%, the patient progresses to the Feedback sessions (see Fig. 1).

b. Feedback session

As in the Training session, the patients were presented with a sequence of a familiar question, but, at the end of the response segment, they were provided with auditory feedback as to whether their answer was

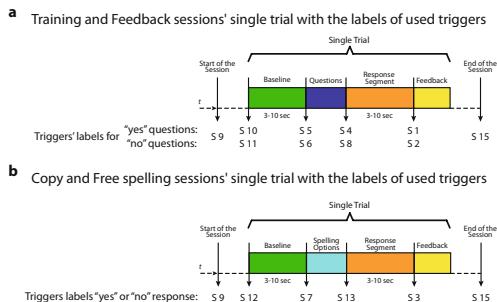


Fig. 2 Different types of trials in the study. **(a)** Paradigm describing the sequence of events and sequence of the triggers' labels used in a single trial for the Training and Feedback sessions. In these types of sessions, 20 questions with "yes" and "no" answers, known by the patient, are presented in a pseudo-random order. **(b)** Paradigm describing the sequence of events and sequence of the triggers' labels used during a single trial for the Copy and Free spelling sessions. In these sessions, instead of questions, the patient is presented with options that allow him/her to navigate through his/her predetermined spelling scheme (e.g., sectors, letters). For both spelling sessions, the limit in the number of trials depends only on the patient's attempts to spell the given target (i.e., Copy speller sessions) or her/his desired sentence (i.e., Open speller sessions). For any type of session recorded, the recording's start and end are indicated by an "S 9" and an "S 15" trigger.

recognized as "yes" or "no" by the system. For each Feedback session, the triggers indicating the events' sequence were recorded on the raw file, using the labels shown in Fig. 2a. The system creates a sentence list (Block_X_senlist.txt) in the same way it was created for the Training sessions. In the case of Feedback sessions, in addition to the sequence of the questions text file, the system creates a result file (Date_result_fl_X.txt) listing the predicted results, i.e., "1" if the answer was recognized as "no", "0" if the answer was recognized as "yes", and "2" if the answer was unable to be classified by the system. The system gives the patient auditory feedback with the sentence: "Your answer was classified as yes/no". Both.txt lists are also included inside the raw data folder structure, as described in the section Data Records. After at least two consecutive Feedback sessions with a classification accuracy result greater than 75%, the patient progresses to the Copy spelling sessions (see Fig. 1).

The sequence of events and triggers (with their labels) for a single trial of the Training and Feedback sessions is depicted in Fig. 2a. Each of these trials consists of the segment of baseline (i.e., no sound presented), stimulus, during which the question is presented auditorily to the patients, followed by the segment of response time, in which the patient moves or does not move the eye according to his/her answer, and lastly the segment of feedback. For a Training session trail, the feedback is "thank you" to mark the end of the response while for a Feedback session trail, the feedback is "yes" or "no" depending on the answer classified by the system.

c. Copy spelling session

During the Copy spelling sessions, the patients were asked to spell a specific word described in our previous work¹². For each Copy spelling session, the set of triggers indicating the sequence of events was recorded on the raw file, as shown in Fig. 2b. For the Spelling sessions, there are no questions sequence text files, but there are results files (Date_result_fl_X.txt) with the label of the predicted answer, listing the predicted results as "1" if the answer was recognized as "no", "0" if the answer was recognized as "yes", and "2" if the system was unable to classify the answer. The.txt lists are also included in the raw data folder structure described in the section Data Records.

d. Free spelling session

After completing the Copy spelling session, the patients were asked to spell whatever he/she desired. For each Free spelling session, the set of triggers indicating the sequence of events were recorded on the raw file, as shown in Fig. 2b. As in the Copy spelling case, each Free spelling session created a result file (Date_result_fl_X.txt) using the same label code. The.txt lists are also included in the raw data folder structure described in the section Data Records.

The trials for the Copy and Free spelling sessions do not consist of the pre-recorded personal questions, but instead, of "yes"/"no" questions asking the patient whether to select or not, a particular letter, group of letters, or command, from his/her particular speller scheme¹². Copy and Free spelling sessions differ in terms of the instruction given to the patient. During the Copy spelling sessions, the patient was asked to spell a specific word, while during the Free spelling sessions, the patient was asked to spell whatever he/she desired. Consequently, instead

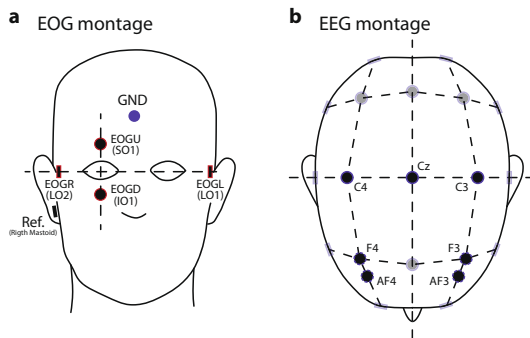


Fig. 3 EOG and EEG setup. **(a)** Montage for the minimum number of EOG channels for each recorded session, using the locations LO1 (left cantus) and LO2 (right cantus) for horizontal eye movement, and SO1 (above superior orbit) and IO1 (below inferior orbit) for vertical eye movement. We used the labels EOGL, EOGR, EOGU, and EOGD, respectively, for the *online* study. **(b)** Montage for the minimum number of EEG electrodes for each recorded session, emphasizing the central motor (C4, Cz, C3) and prefrontal areas. In this latter case, the location of used electrodes might vary between F3 and F4, or AF4 and AF3. Nevertheless, the total number of electrodes might vary between days of the visits due to the patient's wellness conditions. The exact number of electrodes and labels used can be verified in the Online-only Tables S1–S4.

of being a fixed number, the number of trials in these sessions depends on the number of attempts performed by the patient to spell the given target (for the Copy speller sessions) or his/her desired sentence (for the Free speller sessions).

The sequence of events and triggers (with their labels) for a single trial for the Copy and Free spelling sessions is depicted in Fig. 2b. The trials consist of the segment of baseline (i.e., no sound presented), stimulus, where instead of questions the patient is presented with auditory options that allow him/her to navigate through his/her predetermined spelling scheme¹² (e.g., sectors, characters, letters), followed by the response time segment in which the patient move or not move the eye according to his/her answer. Lastly, the feedback segment, during which depending on the answer classified by the system, “yes” or “no” auditory feedback is given to the patient.

Regardless of the session type, the recording time's start and end are labeled by “S 9” and “S 15” triggers. During each trial, the sequence of events is presented to the patient and simultaneously, in a synchronized manner, a system of digital triggers is created by a Matlab script interacting with the V-Amp amplifier, to indicate the onset of each event in the time series. Both Fig. 2a,b show the sequence of triggers (their labels) as used in each trial. Information on the onset and labels of each event is also provided (see section Data Records).

We have to add that during the setting up of the system or the sessions' execution, patients' care and wellness were a high priority; therefore, under any request or signal of unease, sessions or even the day's study were stopped.

System for data acquisition. The communication system is composed of the different elements described below.

- Laptop: The present setup uses a laptop with 8 GB RAM, Windows 7 operating system, and 3.3 GHz processor.
- EEG amplifier and recorder: For each session, EEG and EOG channels were recorded according to the 10-20 EEG electrode positioning system, with a 16 channel EEG amplifier (V-Amp DC, Brain Products, Germany) with Ag/AgCl active electrodes.
- EOG channels: at least four electrodes were recorded (positions SO1 and IO1 for vertical eye movement, and LO1 and LO2 for horizontal eye movement).
- EEG channels: at least seven channels located in central and prefrontal areas were recorded (exact locations per day in the Online-only Tables 1–4).
- EMG channels: on a limited number of sessions electrodes located on the chin of the patient or any other face muscle with assumed remaining function.

All the channels were referenced to an electrode on the right mastoid and grounded to electrode FPz on the forehead. For the montage, electrode impedances were kept below 10 k Ω . The sampling frequency was 500 Hz. The standard montage for the minimum number of available EOG and EEG electrodes is specified in Fig. 3. The precise number and location of electrodes available for each session are detailed in the Online-only Tables 1–4, including recording EMG electrodes.

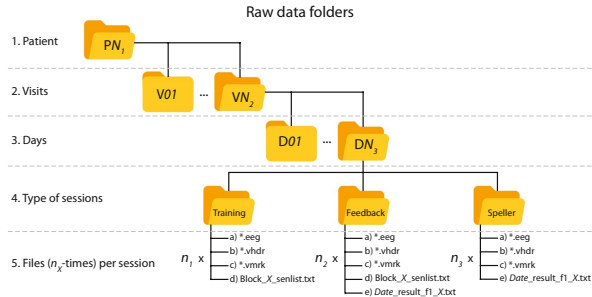


Fig. 4 Raw data folder structure. Structure of nested folders containing the raw recordings of the study. According to the patient identifier, the upper level is the folder, which can be $PN_1 = 11, 13, 15$ or 16 . In the next level, VN_2 indicates the total number of visits available for that patient, and inside it, DN_3 indicates the number of days that the visit lasted. Each day's folder stores subfolders for the Training, Feedback, and spelling (that stores recordings from both the Copy and Free speller sessions). Each of these folders contains a set of files that are the outcome of a recorded session (detailed in the section Data Records), times the number that particular type of session (i.e., n_1 , n_2 , and n_3) was respectively performed during the day.

- Serial cable: This cable is used to connect the Laptop and the EEG amplifier to send the triggers with the custom Matlab code to mark the EEG-EOG recording with the different segments' starting point.
- Loudspeakers: Loudspeakers connected to the laptop performs the function of delivering the audio stimuli to patients during the Training/Feedback/Copy spelling/Free spelling sessions, as described below.

Data Records

Raw data folders. The data stream was recorded directly from the EEG amplifier and stored with the proprietary BrainVision Recorder format¹⁹ during the sessions. According to the dongle key available during the visit, the data were stored in two possible formats, necessary to access and use BrainVision Recorder, 42% of data were recorded in *.ahdr and the rest 58% in *.vhdr format. For consistency here, we present the data in *.vhdr after converting the other 42% *.ahdr format data also to *.vhdr format. Thus, as an output of this recording scheme, three output files per recording had the same name but different extension:

- Header file (*.vhdr), containing recording parameters and further meta-information, as the scaling factor necessary to convert the recorded raw amplitude to millivolts.
- Marker file (*.vmrk) describes the events and their onset during the data recording, in this case, the sequence of triggers.
- Raw EEG data file (*.eeg) is a binary file containing the EEG and EOG data and additional recorded signals.

Nevertheless, to assist with handling the unmodified raw data, we have used the BrainVision Analyzer²⁰ software to export all the recordings to the more accessible.vhdr format, but without altering anyhow the content of the data itself.

For storing the raw data, a database was created using a nested structure of five levels (see Fig. 4), from the top:

1. Patient folder, where PN_1 can be either P11, P13, P15, or P16.
2. Visits folder, where VN_2 indicates the total number of visits available for each particular patient.
3. Day folder, where DN_3 indicates the number of days that the particular visit lasted.
4. Type of sessions, where data has been separated according to the type of sessions. Training, Feedback, and Spelling sessions (consisting of both Copy and Free spelling sessions).

At the 5th level, according to the type of session, there might be up to five types of files stored, times the number of that particular session recorded on the day, i.e., n_1 , n_2 , and n_3 (see Fig. 4). Namely, the hosted files can be:

- *.vhdr, the exported version of the *.ahdr file.
- *.vmrk, the exported version of the *.amrk file.
- *.eeg, that is a binary file with the recorded data.
- Block sentence list (Block_X_senlist.txt), where X is the counter of the number of ongoing sessions. This type of *.txt file was only created for Training and Feedback sessions.
- Result list (Date_result_f1_X.txt), with the Date in which the recording was made, and X is the counter of the ongoing sessions. This type of *.txt file was only created for Feedback and both Speller sessions.

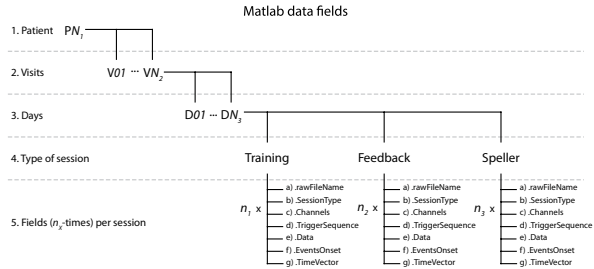


Fig. 5 Matlab data fields structure. Nested structure elements containing the values and features of recordings from the study. According to the patient identifier, the upper level is the main structure, which can be $PN_1 = 11, 13, 15$ or 16 . In the next level, VN_2 indicates the total number of visits available for that patient, and inside it, DN_3 indicates the number of days that the visit lasted. Inside each day, there are structures for the Training and Feedback sessions and the spelling sessions (containing recordings from both the Copy and Free speller sessions). Each of these contains a set of structures that result from exporting the *.vhdr raw files for each recorded session, times the number of that particular session type (i.e., n_1 , n_2 , and n_3) was performed during the day. Read the Data Records section for details on the data exporting.

Matlab data fields. Additionally, another format has been chosen to present and share the data obtained from exporting the original raw files (details in the section Usage Notes). In this rectangular form, a Matlab variable is stored (*.mat), corresponding to the patient's name, i.e., P11. In the variable, nested structures were created using a somehow similar architecture for the raw files, as detailed in Fig. 5. The levels, from upper to lower, are:

1. Patient structure, where PN_1 can be either P11, P13, P15, or P16.
2. Visits structure, where VN_2 indicates the total number of visits available for each particular patient.
3. Day structure, where DN_3 indicates the number of days that the particular visit lasted.
4. Type of sessions structure, where data has been separated according to the type of sessions. Training, Feedback, and Spelling sessions (containing both copy and free spelling sessions).

At the 5th level, according to the type of session, there are seven fields stored, times the number of that particular session recorded on the day, i.e., n_1 , n_2 , and n_3 (see Fig. 6). The hosted fields are:

- (a) .rawFileName: character type variable with the name of the original raw file that was exported
- (b) .SessionType: character type variable with the label of the type of session that the data belongs to
- (c) .Channels: cell array with $I \times K$ dimensions, with K being the total number of EEG, EOG and EMG channels recorded, where each cell element is the label of a channel.
- (d) .TriggerSequence: cell array with $I \times M$ dimensions, including the M th events of all the trials recorded and the session as a sequence of triggers, with the labels indicated in Fig. 2, e.g., S 9, S 10, S 5, S 4, S 1, S 11, ..., S 15
- (e) .Data: a $K \times R$ dimensional matrix of numerical values, being K the number of channels recorded, and R the number of data points in the time domain of the recording, each element being the amplitude values of the recording. It is highly relevant to consider that the default amplitude of the recording needs to be multiplied for a scaling factor of 0.0488281 (± 410 mV range in 24 bits) to convert to μV^{21} . The scaling factor can be verified inside every *.vhdr file produced for every recording
- (f) .EventsOnset: a $I \times R$ dimensional vector of numerical values, being R the number of data points in the time domain of the recording, and to each time point we have assigned the numerical value of the trigger labels (see Fig. 2) occurring at that time point, e.g., 9, 10, 5, 4, 1, 11, ..., 15, and a value of zero otherwise. This vector aims to help quickly locate each event's onset and nature in the time domain
- (g) .TimeVector: a $I \times R$ dimensional vector of numerical values, being R the number of data points in the time domain of the recording, where an element of R indicates the time value in seconds of the recording.

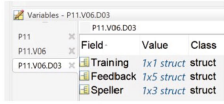
As an example of the previous variable description, Fig. 6 illustrates the data structure using P11's data from visit V01 and day D03.

All the datasets described in this section can be freely downloaded from the open access repository²².

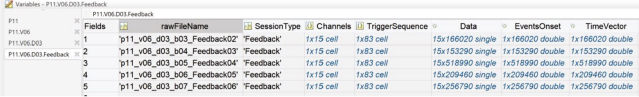
Technical Validation

The raw data referred to in this descriptor was recorded using a Brain Products V-Amp amplifier, without any type of hardware or software filter besides the physical instrumental restriction of the amplifier (wideband filter in the range of 0 Hz (DC) – 320 Hz or 4 kHz for the high-speed mode)²¹.

a



b



Fields	rawFileName	SessionType	Channels	TriggerSequence	Data	EventsOnset	TimeVector
1	p11_v06_d03_b03_Feedback02	Feedback	1x15 cell	1x83 cell	15x166020 single	1x166020 double	1x166020 double
2	p11_v06_d03_b04_Feedback03	Feedback	1x15 cell	1x83 cell	15x153290 single	1x153290 double	1x153290 double
3	p11_v06_d03_b05_Feedback04	Feedback	1x15 cell	1x83 cell	15x150900 single	1x150900 double	1x150900 double
4	p11_v06_d03_b06_Feedback05	Feedback	1x15 cell	1x83 cell	15x209460 single	1x209460 double	1x209460 double
5	p11_v06_d03_b07_Feedback06	Feedback	1x15 cell	1x83 cell	15x256790 single	1x256790 double	1x256790 double

Fig. 6 Example of a Matlab structure of the data using P11's data. The figure illustrates the data structure using P11's data from visit V06 and day D03. **(a)** Indicates the selection of patient variables and the data fields corresponding to a particular visit and day and inside it, the type and number of sessions performed on the given day. **(b)** Depicts the presence of different fields upon selecting a session type, in this case, the number of Feedback sessions performed by P11, upon selection of Field named Feedback, and their different elements, as shown in the figure. Read the Data Records section for the detailed description.

The raw data recorded with BrainVision Recorder software (v2.1.0) in *.ahdr, *.amrk, *.eeg formats were exported using BrainVision Analyzer software³⁰ (v2.2.0) to obtain the formats¹⁹ *.vhdr, *.vmrk and *.eeg.

The data given as a Matlab format variable (*.mat) has been exported from the raw files taking advantage of the EEGLAB²³ toolbox (<https://scn.ucsd.edu/eeGLab/index.php>, v2019.0) and the "bva-io" plugin (https://scn.ucsd.edu/eeGLab/plugin_uploader/plugin_list_all.php, v1.5.13), to save in the described variable structure desired features of the original raw file, as detailed in the Data Records section. No special parameter was used for exporting these data, and therefore we consider both raw and exported to the same values. Nevertheless, the amplitude of the recorded data (either.eeg or exported files using the "bva-io" plugin) is defined by the ADC bit resolution of the device, that is a ± 410 mV range in 24 bits, and therefore, the amplitude value needs to be multiplied by the scaling factor of 0.0488281²¹ to be converted to μ V (microvolts) units. The resolution of each recording can be found per channel inside each *.vhdr given file.

The Matlab script used to export the raw files to Matlab variables (see Code Availability section) includes a deactivated code line that can be used to convert to μ V the amplitude.

EOG electrodes were located and placed according to the standard 10-20 system with EEG neoprene caps (Neuroelectrics, Barcelona, Spain), inserted in the cap using plastic holders. Once the whole set of electrodes was in place, they were filled with SuperVisc electrolyte gel (Easycap, Germany, GmbH). Impedance was measured on the whole set using an ImpBox (Brain Products, Germany, GmbH), to achieve a target impedance of 10 k Ω . Researchers in charge of the study ensured that the recorded activity had the proper impedance and a clean signal for all the channels. Recordings are not affected by muscular or blinking artifacts, besides eye movements related to the patients' intentions.

Usage Notes

Performance of the communication system. The communication system can present a question every nine seconds with an information transfer rate of 6.7 bits/min. The system's optimal speed can be improved depending on the speller scheme's design for each individual patient and the corpus of sentences stored for word prediction. Descriptive statistics on each patient's performance can be found in the related publication¹⁴.

A minimal criterion for communicating using the system is the presence of eye-movements recordable with state of the art EOG recording devices in the microvolt range. For one of the patients, the progression of the disease over the course of a year eventually prevented him from controlling his oculomotor activity. He was however capable of producing undifferentiated EOG activity with low amplitude in the range of ± 30 μ V which reached that minimal criterion. The other patients never arrived at such a total loss of control when the data described here was recorded. Therefore, the duration of the transition period to CLIS, and whether voluntary communication with non-invasive physiological recording technologies, as described here, will be possible in CLIS, is still a matter of future research.

Date and time of the recordings. The original timestamp of the beginning of a recorded session can be found both inside the *.vhdr and the *.vmrk files, as the occurrence of the first marker in the recording. It can also be found as the timestamp of the sentence lists (Block_X_senlist.txt), or indicating the end of a session in the results text files (Date_result_fl_X.txt).

Name of the raw files. During the study, files recorded with BrainVision Recorder software (v2.1.0) (i.e., *.vhdr, *.vmrk and *.eeg) were labeled by the experimenters, and therefore, human error or discrepancies might have been committed during the labeling process. To clarify any possible confusion, the Online-only Tables 1–4 include a set of columns that show the correspondence between the name of the raw file, the session's sequence, and any *.txt files attached to it.

Patient	Visits	Days	Sessions		
			Training	Feedback	Speller
P11	9	27	68 (including 2 lost files)	56	26
P13	4	14	28	22	21
P15	2	7	7	16 (including 1 lost files)	18
P16	2	9	27	22	8

Table 1. The number of sessions in the dataset. Detail of the number of visits and total days of the study, and the total number of different types of sessions recorded for each patient. Indicated in parenthesis are the numbers of lost recordings. Copy speller and free speller sessions are considered in the same column. A more detailed description of the days, dates, and sessions can be verified in the Online-only Tables 1–4.

The text lists (Block_X_senlist.txt and Date_result_fl_X.txt) were created automatically by a Matlab script running during each session.

From the given recordings, either raw or Matlab fields, it can be noticed from the labels that some files or sessions are lacking. This is because during the visits, sessions belonging to another paradigm for a different and unrelated study were also recorded, and they have been deliberately removed from the actual data descriptor to focus on the auditory communication recordings. Removed files are indicated in the Online-only Tables 1–4. Additionally, a number of files were lost or corrupted; the precise number and sessions are indicated in Table 1 and Online-only Tables 1–4.

EEG locations and inconsistency. Working with patients who have critical health conditions means being completely dependent on their current (minute by minute) state. These limitations were considered in the design of the study. The number of EEG electrodes was limited by restrictions of accessibility of some scalp regions. Since the patients lie on their backs most of the time, it is impossible to access occipital areas.

Nevertheless, the most relevant restriction is the time constraint, that is, to place a minimal number of EEG electrodes in appropriate locations, in the minimum possible time, so to maximize the time available to work with the patient before tiredness or another need (for example, sucking of saliva) prevents them from participating in the study. Consequently, the montages of electrodes might be affected by inconsistency in EEG electrode locations, even for the same patient, and different visits, since it is always dependent on changing circumstances of health and time.

Therefore, the criterion we follow aims to reach with the minimal number of electrodes the greatest coverage of the prefrontal and mesial surfaces of the brain (besides the EOG electrodes), under the assumption that the cognitive activity implicated in the processing of these questions might elicit changes in the electrical activity of the aforementioned cortical regions.

Regardless of that, we managed to keep a constant number of seven EEG electrodes and four EOG electrodes for most of the patients, for most of the visits, as can be verified in the Online-only Tables 1–4.

Audio files. The audio files (recorded questions) used in this research contains personal information of the patients and their relatives and consequently, to make these audio files fully open and public will compromise their identities. These data²⁴ have been uploaded with restricted access, therefore any researcher or laboratory interested in accessing the data to perform the analysis will have to sign an identity protection agreement document provided as a “Data Use Agreement” Supplementary material with this manuscript.

Code availability

The given Matlab data variables were obtained by exporting the raw files (i.e., *.vhdr, *.vmrk, and *.eeg) using the EEGLAB²⁴ toolbox (v2019.1.0) and exporting the data using the “bva-io” plugin (v1.5.1.3). We wrote a short Matlab script (ExportingCode_vhdr2mat.m) to export and save the desired features of the recordings, as thoroughly detailed in the section Data Records. The code is included in the same repository as the rest of the data, and it is accompanied by a brief document (ExportingCode_vhdr2mat.docx) explaining details of the code.

Received: 24 April 2020; Accepted: 30 November 2020;

Published online: 11 January 2021

References

- Birbaumer, N. & Chaudhary, U. Learning from brain control: clinical application of brain–computer interfaces. *Neuroforum*. **21**(4), 87–96 (2015).
- Birbaumer, N. Breaking the silence: Brain–computer interfaces (BCI) for communication and motor control. *Psychophysiology*. **43**, 517–532 (2006).
- Chaudhary, U., Birbaumer, N. & Ramos-Murguialday, A. Brain–computer interfaces for communication and rehabilitation. *Nat. Rev. Neurol.* **12**, 513–525 (2016).
- Brownlee, A. & Bruening, L. M. Methods of communication at end of life for the person with amyotrophic lateral sclerosis. *Top. Lang. Disord.* **32**(2), 168–185 (2012).
- Bauer, G., Gerstenbrand, F. & Rimpl, E. Varieties of the locked-in syndrome. *J. Neurol.* **221**, 77–91 (1979).
- Kübler, A. & Birbaumer, N. Brain–computer interfaces and communication in paralysis: Extinction of goal directed thinking in completely paralyzed patients? *Clin. Neurophysiol.* **119**, 2658–2666 (2008).
- Calvo A. *et al.* In *International Conference on Computers for Handicapped Persons 2008*, vol 5105 (eds. Miesenberger K., Klaus J., Zagler W., Karshmer A.) pp 70–77 (Springer, Berlin, Heidelberg, 2008).
- Beukelman, D., Fager, S. & Nordness, A. Communication Support for People with ALS. *Neur. Res. Int* **04**, 714693 (2011).

9. Chaudhary, U., Birbaumer, N. & Ramos-Murguialday, A. Brain-computer interfaces in the completely locked-in state and chronic stroke. *Prog. Brain Res* **228**, 131–61 (2016).
10. Chaudhary, U., Birbaumer, N. & Curado, M. R. Brain-machine interface (BMI) in paralysis. *Annals of Physical and Rehabilitation Medicine* **58**(1), 9–13 (2015).
11. Chaudhary, U., Mrachacz-Kersting, N. & Birbaumer, N. Neuropsychological and neurophysiological aspects of brain-computer-interface (BCI)-control in paralysis. *J. Physiol.* **00**, 0, 1–9 (2020).
12. Tonin, A. & Jaramillo-Gonzalez, A. *et al.* Auditory Electrooculogram-based Communication System for ALS Patients in Transition from Locked-in to Complete Locked-in State. *Sci. Rep.* **10**, 1 (2020).
13. Gorges, M. *et al.* Eye movement deficits are consistent with a staging model of pTDP-43 pathology in Amyotrophic Lateral Sclerosis. *PLoS One* **10**(11), e0142546 (2015).
14. *BNCI Horizon 2020* <http://bnci-horizon-2020.eu/database> (2020).
15. *PhysioNet: The research resource for complex physiological signals* <https://physionet.org/about/database/> (2020).
16. *BrainSignals: Publicly available brain signals EEG MEG ECoG data* <http://www.brainsignals.de/> (2020).
17. Cedarbaum, J. M. *et al.* The ALSFRS-R: a revised ALS functional rating scale that incorporates assessments of respiratory function. *J. Neurol. Sci.* **169**, 1–2 (1999).
18. Brain Products GmbH. *BrainVision Recorder User Manual* <https://www.brainproducts.com/downloads.php?kid=2> (2019).
19. Brain Products GmbH. *Description of the BrainVision Core Data Format 1.0* https://www.brainproducts.com/files/public/products/more/BrainVisionCoreDataFormat_1_0.pdf (2019).
20. Brain Products GmbH. *BrainVision Analyzer 2.0 User Manual* <https://www.brainproducts.com/downloads.php?kid=9> (2019).
21. Brain Products GmbH. *V-Amp & ImpBox Operating Instructions, 7th Version* https://www.brainproducts.com/files/secure/Manuals/V-Amp_OI.pdf (2016).
22. Jaramillo-Gonzalez, A. *et al.* A Dataset of EEG and EOG recordings from an Auditory EOG-based Communication System for Patients in Locked-In State. *Zenodo* <https://doi.org/10.5281/zenodo.4002038> (2020).
23. Delorme, A. & Makeig, S. EEGLAB: an open source toolbox for analysis of single-trial EEG dynamics including independent component analysis. *J. Neurosci. Methods*. **134**(1), 9–21 (2004).
24. Jaramillo-Gonzalez, A. *et al.* Audio files for A Dataset of EEG and EOG recordings from an Auditory EOG-based Communication System for Patients in Locked-In State. *Zenodo* <https://doi.org/10.5281/zenodo.4286416> (2020).

Acknowledgements

Deutsche Forschungsgemeinschaft (DFG) DFG BI 195/77-1, BMBF (German Ministry of Education and Research) 16SV7701 CoMiCon, and LUMINOUS-H2020-FETOPEN-2014-2015-RIA (686764).

Author contributions

Andres Jaramillo-Gonzalez – Performed 35% of the Auditory communication system (ACS) sessions and data collection; Data curation; Manuscript writing. Shihze Wu – Data curation and validation. Alessandro Tonin – Performed 35% of the ACS sessions and data collection. Aygul Rana – Performed 35% of the ACS sessions and data collection. Majid Khalili Ardali – Discussion in Laboratory. Niels Birbaumer – Study design and conceptualization; Manuscript correction. Ujjwal Chaudhary – Study design and conceptualization; Performed 65% of the ACS sessions and data collection; Supervision; Manuscript writing.

Competing interests

The authors declare no competing interests.

Additional information

Supplementary information is available for this paper at <https://doi.org/10.1038/s41597-020-00789-4>.

Correspondence and requests for materials should be addressed to U.C.

Reprints and permissions information is available at www.nature.com/reprints.

Publisher's note Springer Nature remains neutral with regard to jurisdictional claims in published maps and institutional affiliations.



Open Access This article is licensed under a Creative Commons Attribution 4.0 International License, which permits use, sharing, adaptation, distribution and reproduction in any medium or format, as long as you give appropriate credit to the original author(s) and the source, provide a link to the Creative Commons license, and indicate if changes were made. The images or other third party material in this article are included in the article's Creative Commons license, unless indicated otherwise in a credit line to the material. If material is not included in the article's Creative Commons license and your intended use is not permitted by statutory regulation or exceeds the permitted use, you will need to obtain permission directly from the copyright holder. To view a copy of this license, visit <http://creativecommons.org/licenses/by/4.0/>.

The Creative Commons Public Domain Dedication waiver <http://creativecommons.org/publicdomain/zero/1.0/> applies to the metadata files associated with this article.

© The Author(s) 2021



Neurophysiological aspects of the completely locked-in syndrome in patients with advanced amyotrophic lateral sclerosis



Majid Khalili-Ardali^a, Shizhe Wu^a, Alessandro Tonin^{a,b}, Niels Birbaumer^{a,*}, Ujwal Chaudhary^a

^a Institute of Medical Psychology and Behavioral Neurobiology, University of Tübingen, Germany

^b Wyss Center for Bio and Neuroengineering, Geneva, Switzerland

ARTICLE INFO

Article history:

Accepted 18 January 2021

Available online 3 February 2021

Keywords:

Amyotrophic lateral sclerosis
Completely locked-in syndrome
Resting-state
Somatosensory evoked potential
Auditory evoked potential

HIGHLIGHTS

- Resting-EEG shows slow frequencies after complete paralysis in the advanced stage of amyotrophic lateral sclerosis (ALS).
- Neurophysiological metrics of ALS patients in completely locked-in syndrome (CLIS) are altered with highly variable patterns between patients.
- Heterogeneity of the results between patients precludes the use of single criteria to assess psychophysiological state in CLIS.

ABSTRACT

Objective: Amyotrophic lateral sclerosis (ALS) patients in completely locked-in syndrome (CLIS) are incapable of expressing themselves, and their state of consciousness and awareness is difficult to evaluate. Due to the complete paralysis included paralysis of eye muscles, any assessment of the perceptual and psychophysiological state can only be implemented in passive experimental paradigms with neurophysiological recordings.

Methods: Four patients in CLIS were investigated in several experiments including resting state, visual stimulation (eyes open vs eyes closed), auditory stimulation (modified local-global paradigm), somatosensory stimulation (electrical stimulation of the median nerve), and during sleep.

Results: All patients showed altered neurophysiological metrics, but a unique and common pattern could not be found between patients. However, slowing of the electroencephalography (EEG) and attenuation or absence of alpha wave activity was common in all patients. In two of the four patients, a slow dominant frequency emerged at 4 Hz with synchronized EEG at all channels. In the other two patients slowing of EEG appears less synchronized. EEGs between eyes open and eyes closed were significantly different in all patients. The dominant slow frequency during the day changes during slow-wave sleep (supposedly sleep stage 3) to even slower frequencies below 2 Hz. Somatosensory evoked potentials (SEPs) were absent or significantly altered in comparison to healthy subjects, similarly for auditory evoked potentials (AEPs).

Conclusions: The heterogeneity of the results underscores the fact that no single neurophysiological index is available to assess psychophysiological states in unresponsive ALS patients in CLIS. This caveat may also be valid for the assessment of cognitive processes; a functioning BCI can be the solution.

Significance: Most of the studies of the neurophysiology of ALS patients focused on the early stage of the disease, and there are very few studies on the late stage when patients are completely paralyzed with no means of communication (i.e., CLIS). This study provides quantitative metrics of different neurophysiological aspects of these patients.

© 2021 International Federation of Clinical Neurophysiology. Published by Elsevier B.V. All rights reserved.

1. Introduction

Completely locked-in syndrome (CLIS) was defined as total immobility with intact cognitive processing (Bauer et al., 1979)

* Corresponding author.

E-mail address: niels.birbaumer@uni-tuebingen.de (N. Birbaumer).

in which the patient is fully conscious but unable to express herself/himself (Hayashi and Kato, 1989; Smith and Delargy, 2005). By this definition, any disease such as quadriplegia and anarthria or neurodegenerative motor neuron disease (MND) like amyotrophic lateral sclerosis (ALS) that is accompanied by total immobility is categorized as CLIS as long as conscious awareness is assumed to be intact (Patterson and Grabois, 1986). It has recently been proposed to use a lack of communication as the main criteria for CLIS (Chaudhary et al., 2020a), which we also use in this manuscript. However, with this definition, the patients' conscious and cognitive state remains undefined, and differentiation to other non-responsive states such as unresponsive wakefulness state (UWS) is not possible. Existence of different approaches in the assessment of consciousness precludes a clinical definition of CLIS in unresponsive patients. Hence a clinical assessment of CLIS is not established yet, and attempts to differentiate unresponsive disorders of consciousness from CLIS with neurophysiological measures and neuroimaging were mostly unsuccessful (Kotchoubey et al., 2003; Kübler et al., 2001).

All patients reported in this study suffer from ALS and are in CLIS. CLIS is not reserved for ALS only: subcortical stroke, traumatic or infectious, or toxic brain damage may also lead to locked-in syndrome (LIS) and/or CLIS. LIS can be differentiated clearly from CLIS through intact voluntary eye movements in all these etiologies (Smith and Delargy, 2005). ALS is a progressive MND that causes loss of motor neurons and eventually completely paralyzes the patient and leads to CLIS (Thorns et al., 2010). Progression of the disease is not necessarily correlated with a cognitive deficit (Schnakers et al., 2008), although cognitive dysfunction is reported in some cases (Huynh et al., 2020; Stanton et al., 2007). It has been proposed that somatosensory and auditory perception, as well as cognitive processing are preserved and not affected even after the transition to CLIS (Kübler and Birbaumer, 2008). These shreds of evidence are the main reasons why it is hypothesized that in the final stage of the disease when the patient is completely paralyzed and unable to express herself/himself, s/he is still cognitively intact with preserved consciousness. Of course, this is only a deductive argument, and valid and reliable experimental clinical observations are required to validate this claim. However, experimental findings have sometimes challenged the idea of intact sensory processing of patients in CLIS. A case study on a patient in CLIS with intracranial recordings reported selective somatosensory dysfunction in joint-mechanoreceptor pathways and raised doubts about the intactness of proprioception in CLIS (Murguialday et al., 2011). Also, vision is said to be impaired or absent in most patients in LIS and CLIS with ALS due to drying and necrosis of the cornea (Tonin et al., 2020). A theoretical analysis of cognition in CLIS based on a motor theory of thinking (Ferster and Skinner, 2005; Washburn, 1916) has speculated "extinction of goal-directed thinking" due to the lack of contingent reinforcement after the transition to CLIS (Kübler and Birbaumer, 2008). The only hope for ALS-CLIS patients to communicate is through brain-computer interface (BCI) (Birbaumer, 2006; Chaudhary et al., 2016, 2015) and so far, no case of non-invasive BCI is reported with the ability of free spelling communication (De Massari et al., 2013). However, an invasive approach resulted in free spelling communication with a patient in CLIS and demonstrated preserved cognitive functionality several months after transitioning to CLIS (Chaudhary et al., 2020b). The failure of BCI in most ALS-CLIS patients after transitioning to CLIS together with the progressive nature of the disease provokes the question of whether basic sensory processing as well as cognitive functionalities are preserved in patients after transitioning to CLIS.

Two of the main approaches to assess the brain functionalities in unresponsive patients are to investigate first the spontaneous brain activity during wakeful resting and sleep, and second the

brain reactivity to various external stimuli (Schnakers and Majerus, 2012). Depending on the design of the experiment and the performed analysis, it is commonly accepted that some of the neurophysiological metrics are correlated with cognitive functions (Squires et al., 1975; Sutton et al., 1965; Ulanovsky et al., 2003). While spontaneous brain activity can uncover basic brain function, event-related potentials (ERPs) may serve as correlates of higher cognitive functionalities such as selective attention, memory updating, semantic comprehension (Duncan et al., 2009). Early ERPs (until 200 ms latency) are correlated with automatic, unconscious processing of the stimuli, while later components are usually signs of conscious processing of an event. The early and late ERP components are not mutually exclusive responses; rather they follow each other in a proper experimental paradigm, but there are occasions when they vary independently, particularly in neuro-pathological cases (Kotchoubey et al., 2005). Bekinschtein et al. (2009) proposed an experimental paradigm known as Local-Global (LG) processing, in which the distinction between unconscious and conscious processing in the auditory evoked potentials (AEPs) is easier to distinguish (Bekinschtein et al., 2009) and several versions of it have been modified and validated on healthy people and patients with disorders of consciousness (DoC) (Rohaut and Naccache, 2017). The main idea behind this paradigm is that, in a set of consecutive sensory stimuli with Local and Global pattern changes, two different types of ERP can be detected. The Local pattern refers to the order of consecutive stimuli within a trial, and the Global pattern refers to the order of trials within an experimental block. Detecting any violation in the order of stimuli within a trial (i.e., local pattern) only requires pre-attentive mechanisms and elicits the early evoked response (before 200 ms), called local effect (LE), while detecting a violation in the order of presented trials within an experimental block (i.e., global pattern) requires controlled attention and memory updating and is reflected in the later evoked potentials components (after 200 ms), called global effect (GE). In this study, a modified version of LG was used to assess auditory perception and cognitive capacities of patients in CLIS and compared to healthy subjects. In addition, somatosensory evoked potentials (SEPs) were investigated to assess sensory processing in ALS-CLIS. SEPs are used to assess the functional status of the somatosensory pathways and to identify the sensory portion of the sensorimotor cortex (Tolakis, 2005) and are expected to remain intact in CLIS due to ALS. However, studies on ALS patients before the transition to CLIS suggested a pathological slowing of the conduction along central sensory pathways (Constantinovic, 1993; Cusi et al., 1984; Murguialday et al., 2011). Particularly, abnormal SEPs are reported in LIS and patients in CLIS with no specific pattern of SEP abnormality (Bassetti et al., 1994; Güttling et al., 1996). Furthermore, alpha suppression in electroencephalography (EEG) recordings is known as a neural signature of an attentional arousal mechanism (Danko, 2006; Toscani et al., 2010) which can even be detected in complete darkness with no visual input (Boytsova and Danko, 2010).

Although there already exist several reports on neurophysiological measurements in unresponsive patients, all previously published reports include only a few patients with ALS in their heterogeneous samples and mainly consists of patients with brain damage and other origins than motor neuron disease such as ALS (Laureys et al., 2005; Patterson and Grabois, 1986; Schnakers et al., 2008). Previous studies focusing on CLIS patients with ALS usually report single cases (Gallegos-Ayala et al., 2014; Kotchoubey et al., 2003; Murguialday et al., 2011; Silvoni et al., 2013). The literature still suffers from coherent studies on the topic with different measurements for comparing of the same patients at different time points with appropriate controls. Particularly in ALS, in which the patients' condition is constantly changing over time, different neurophysiological indexes of different studies cannot

be compared, because they report different metrics from different patients investigated and measured at different stages of their disease. The few number of surviving patients and the fact that they are usually kept at home-care dictates the problem of large enough homogenous samples. Thus, we decided to perform a systematic observational study of neurophysiological aspects of patients in CLIS focusing only on ALS patients.

In this manuscript, we report neurophysiological measures in four ALS patients in the advanced stages of the disease, with no means of communication, i.e., in CLIS. We selected neurophysiological indices which are known to correlate with cognitive and/or perceptual processing. However, we are aware that existence or non-existence of a particular measure in CLIS, as realized in this study, do not allow generalization to cognition in these CLIS patients or CLIS patients in general. However, they may serve as generating new hypotheses and guide the clinician in the selection of appropriate assessment instruments. We investigated the spontaneous brain activity during rest and sleep, as well as brain reactivity to various external stimuli including AEPs, SEPs, and EEGs after eye-opening. We also investigated the resting-state EEG of patients in CLIS and identified the sources of the dominant slow oscillations previously reported in the literature (Maruyama et al., 2020). While spontaneous brain activity and variation of EEG features during sleep and sensory responses to external stimuli uncover the brain's capacity at perceptual levels, AEPs in the Local-Global paradigm are shown to be correlated with higher cognitive functionalities (Duncan et al., 2009). This study tries to uncover basic brain functions in a very rare group of ALS patients long after transitioning to CLIS. Due to the small sample size, which is due to the nature of the disease, group analyses between patients and healthy controls are not performed. However, analysis pipelines are validated in the healthy control group and reported along with patients. We intended to provide an individual neurophysiological picture with the same metrics for each patient and compare it qualitatively with healthy people to emphasize particularly on the obvious pathophysiological changes.

2. Materials and methods

A four days visit occurred with all four patients in CLIS. On the first day, the SEP stimulation experiment was performed. On the second day, AEPs with a modified local-global paradigm (Bekinschtein et al., 2011) was realized. On both days, resting-state EEG was recorded while eyes were open and closed. On the remaining two days, simultaneous EEG and fNIRS recordings were performed in a BCI experiment. The BCI experiments resulted in a negative outcome: none of the four patients achieved reliable yes-no communication on this occasion. The BCI protocol is described in Tonin et al. (2020). However, P1 had previously achieved significant yes-no communication with a NIRS-BCI (Gallegos-Ayala et al., 2014). Two nights of sleep recording were performed in three patients. The fourth patient (P1) had to decline because of health problems. This article reports all the neurophysiological assessments recorded during this visit, including the resting state analysis, the EEG changes during sleep, and the brain response to SEPs and AEPs on a dataset that has never been reported before.

All the EEG was recordings reported here were performed using BrainAmp device (Brain Products Inc. GmbH, Munich, Germany). The recording sites were based on the 10–10 international systems for electrode placement, using actiCAP from the same company, and by manually adding extra electrodes. In these patients, occipital electrodes cannot be used because patients rest for 24 hours a day on their back in a supine position with the back of their head on a pillow: attaching electrodes on the occipital region thus causes pain and discomfort, as we know from reports of patients

and healthy persons lying on their back with electrodes attached at that position, therefore, the recording electrodes included the following channels: Fp1, Fp2, F7, F3, Fz, F4, F8, Fc5, FC3, FC1, FC2, FC4, FC6, T7, C3, Cz, C4, T8, CP5, CP1, CP2, CP2, CP6. Moreover, mastoids were recorded to be later used as a reference programmatically. Bilateral Erb's points 2–3 cm above the clavicle were recorded for the SEP analysis. Recordings were performed with a 500 Hz sampling rate referenced to Fcz and grounded to Fpz. In addition, two electrodes were used above and below one of the eyes to record eye movements. Ten healthy subjects underwent the same experiments with the same recording montage, with a 3000 Hz sampling rate resampled to the same frequency as the patient group for the analysis. For the sleep recordings, eight passive electrodes were placed over Cz, C3, C4, Fz, F3, F4, AF3, and AF4, referenced to the forehead and grounded to a mastoid. Also, four electrodes were used for electrooculography (EOG) recordings. Two electrodes were placed on either side of the eyes close to the lateral canthus, and two electrodes were placed above and below one of the eyes, depending on the physical accessibility.

All the analyses reported in this paper are performed using Matlab (Mathworks, 2018). The data was analyzed using Fieldtrip toolbox (Oostenveld et al., 2011), and EEGlab (Delorme and Makeig, 2004) for some plots.

2.1. Ethical approval

The Internal Review Board of the Medical Faculty of the University of Tübingen approved the experiment reported in this study. The study was performed per the guideline established by the Medical Faculty of the University of Tübingen. The patient or the patients' legal representative gave informed consent with permission to publish the data. The clinical trial registration number is: ClinicalTrials.gov - Identifier: NCT02980380.

2.2. Participants

Three patients except patient 17 were investigated in a sleep study (Malekshahi et al., 2019) and also served as subjects in different studies previously investigating power spectral EEG-densities (Maruyama et al., 2020; Secco et al., 2020). The here used patient numbers (P1, P4, P9, P17) match the same patients' numbering in all studies of our laboratory. In addition, 10 healthy subjects (2 females) with mean age of 28.8 years (SD 4.5) underwent the same procedure as the patients for comparison. Again, we note that no statistical group comparison is possible because of the apparent age and biographical differences and the small sample size of these two groups. The healthy group served to validate the correctness of the metrics used and as a contrast for the severe pathophysiology of the patients.

Patient 1 (P1), female, 75 years old, and CLIS, was diagnosed with sporadic bulbar ALS in May 2007, was diagnosed as locked-in in 2009, and as completely locked-in May 2010, based on the diagnosis of experienced neurologists. She has been artificially ventilated since September 2007, fed through a percutaneous endoscopic gastrostomy tube since October 2007, and was in homecare. No communication with eye movements, other muscles, or assistive communication devices was possible. She passed away in 2019.

Patient 4 (P4), female, 29 years old, and CLIS, was diagnosed with juvenile ALS in December 2012. She was completely paralyzed within half a year after diagnosis and has been artificially ventilated since March 2013, fed through a percutaneous endoscopic gastrostomy tube since April 2013, and is in homecare. She was able to communicate with the eye-tracking device from early 2013 to August 2014 and was unable to use the eye-tracking device after the loss of eye control in August 2014. After

August 2014, family members were able to communicate with her by training her to move her eyes to the right to answer “yes” and to the left to answer “no” questions until December 2014. In January 2015, eye control was completely lost, and she tried to answer “yes” by twitching the right corner of her mouth, and that too varied considerably, and parents lost reliable communication contact.

Patient 9 (P9), male, 25 years old, and CLIS, was diagnosed with juvenile ALS with FUS mutation heterozygote on Exon 14: c.1504delG, gene mutation diagnosed in 2013. He has been artificially ventilated since August 2014 and is in homecare. He started communication using Tobii eye-tracking device (Tobii Dynavox, Danderyd, Sweden) in January 2015. He was able to communicate until December 2015, after which the family members attempted to communicate by training him to move his facial muscles to answer “yes” but the response was unreliable. No communication with eye movements, other muscles, or assistive communication devices was possible since 2016.

Patient 17 (P17), male, 63 years old, and CLIS, was diagnosed with ALS of the second motor neuron in spring 2009. He was not able to breathe after one year, is artificially ventilated, and fed through a percutaneous endoscopic gastrostomy tube since spring 2010. He was able to communicate with the Tobii eye tracking device (Tobii Dynavox, Danderyd, Sweden) until 2014. After that the family was trying to communicate based on his eye-movements. Family members were able to communicate with him by training him to move his eyes to the right to answer “yes” and to the left to answer “no” to the questions. For the last 2–3 years, it is almost not possible to recognize any voluntary response. He had constant involuntary eye movements even when his eyes were closed. Movements were similar to horizontal optokinetic nystagmus with a large range of motion. He passed away in 2019.

2.3. Resting-state EEG

The data acquired from each patient was filtered using a notch filter at 50 Hz, and bandpass filtered between 0.5 Hz and 45 Hz. Noisy channels were interpolated, and the signal was re-referenced to both earlobes. Independent component analysis (ICA) was performed and the components were extracted from EEG, and noise components were removed manually by visual inspection. This signal is referred to as “cleaned data” in this text. For each patient, the 64 seconds of cleaned data in the eyes closed condition are plotted, and the time domain EEG abnormalities are highlighted. ICA was used to remove artifacts and plotted around the EEG trace to illustrate the spatial distribution of the source of the EEG activity. The power spectral density (PSD) for four representative EEG channels are plotted to compare eyes open and closed.

2.4. Source localization

Dynamic Imaging of Coherent Sources (DICS), as an optimal Beamforming technique for solving the inverse problem (Fuchs, 2007; Gross et al., 2001; Jonmohamadi et al., 2014), was used to localize the frequency of interest (FOI) for each subject. Partial Canonical Coherence (PCC) which essentially implements DICS and provides more flexibility in data handling (REF: FieldTrip, 2011) was used to calculate neural activity index using the frequency transformation of the signal. For the forward model, the standard head volume conduction model proposed by Oostenveld et al. was used (Oostenveld et al., 2003). To validate the analysis pipeline of the source localization method and the used hyperparameters, source of alpha activity in healthy controls was determined and compared with the literature. Then the same analysis pipeline was used to localize the source of the dominant slow oscil-

lations in patients. For healthy subjects, the individual alpha peak frequency of eyes closed resting, and for patients, the dominant slow frequency of eyes closed resting was selected as the FOI.

2.5. Eyes open vs. eyes closed

In the recordings of this study, the occipital region was not covered due to the patients’ physical condition (see above). Therefore, the commonly used PSD comparison method might not be an option to capture the difference between eyes open (EO) vs eyes closed (EC). The commonly detected alpha blockade after eye-opening in healthy people is also present at parietal sites and sometimes even further anterior. Thus lack of occipital electrodes should not invalidate the comparison of eyes opening and closing on the EEG traces. To overcome this issue, in addition to the PSD comparison, another metric called Second-order plots (SOP) was used. SOP is based on the comparison of the variability of the signals in different conditions. SOP of the time-domain EEG data is proposed to be more sensitive to the EEG changes than PSD comparison in healthy subjects (Thuraisingham et al., 2007).

All subjects were recorded 3 minutes in EO, followed by 3 minutes EC. In patients for EO recordings, the eyelids were taped open by the experimenter (MKH) and using eye drops, the corneas were kept wet, and for EC condition, the eyelids were closed passively and covered with dark covers. In some recording of patients, the time of EO was reduced by caretakers and varied between 2 and 3 min.

2.5.1. PSD comparison

The power spectrums were calculated on the cleaned EEG for both conditions using a Welch’s overlapping window of 5 seconds and 30% overlap, using multitaper frequency transformation and the boxcar taper. For each single frequency bin, a student t-test was performed to compare EC and EO with 0.01 significant level, corrected for multiple comparisons using the Bonferroni method. Each channel is marked as different if it contained at least 10 consecutive frequency bins (equivalent to 2 Hz) with a significant difference between the two conditions below 25 Hz.

2.5.2. Second-order plots

For a cleaned EEG of each condition, the time domain EEG is shifted one data point and subtracted from the original signal, and denoted as X. Similarly, the signal is shifted two data points and is subtracted from X and denoted as Y. Plotting X over Y represents the variability of the original signal in three consecutive data points (embedding dimension equals to three). Measure for central tendency was defined as the minimum radius for a circle that holds at least 90% of all the data points in it and denoted as r. Finally, r is calculated for every time window in the cleaned data, epoched to five seconds with a 30% overlap. The variability of the r in EO and EC is compared using student t-test with 0.01 significant level, corrected for multiple comparisons; for details see Thuraisingham et al. (2007).

2.6. Sleep

Patients in CLIS need constant medical care also during the night, and patients are repositioned by caretakers during the night to avoid decubitus. Thus displacement or detachment of recording electrodes is very common in sleep recordings. Therefore, two nights of sleep were recorded, and by visual inspection of the raw data, one of the recordings with fewer artifacts, preferably the second night, is analyzed and reported here. Selected recordings are then separated between EEG and EOG signals for visualization. EEG signal is filtered between 0.5 Hz and 30 Hz and the EOG signal is filtered between 5 Hz and 75 Hz. Noisy channels in EEG

were interpolated. Noisy channels in EOG data were rejected. The filtered data is segmented to 30 seconds data with no overlap, and power spectral density is computed. For each frequency in the 30-second window, the median of absolute power in all channels is calculated then normalized and plotted over the night. In contrast to the previous study of our laboratory in which Malekshahi et al. (2019) focused on the identification of sleep stages in CLIS, in this study, we did sleep recordings again in order to identify and differentiate the sources of the dominant slow-wave activity during waking day hours from the slow activity during sleep.

2.7. Somatosensory evoked potentials

Monophasic electrical square pulse with 200 μ s pulse width -3 Hz rate was applied with the intensity of stimulation range proposed by the American Clinical Neurophysiology Society (ACNS) at 30 mA (American Clinical Neurophysiology Society, 2009). For P4, P9, and P17 for whom caretakers believed communication with the patient seemed possible from time to time by movements of a facial muscle or eyes at a very slow rate, the stimulation intensity was determined with caretakers but still in range proposed by ACNS. However, during this visit no reliable communication was achieved with these patients. The stimulation was performed on two blocks with 250 repetitions. Between the median nerve stimulation, the tibial nerve of the contralateral site was stimulated with the same protocol. Since the recording of spinal cord evoked potentials (SCEPs) was not possible, the tibial stimulation is not reported here. For the stimulation, bar electrodes with 8 mm diameter and 3 cm distance by Technomed (Technomed, The Netherlands) were placed over the wrists, cathode proximal, and connected to a D188 digital switch connected to DS7A constant current Stimulator (Digitimer Ltd., Welwyn Garden City, UK). Ten healthy subjects underwent the same procedure for comparison.

Data were resampled to 3000 Hz and the electrical noise of the stimulation was removed by replacing the data points between the beginning of stimulation (zero lag) to 7 ms after the stimulation by a flat line (Waterstraat et al., 2015) and then filtered between 3 and 1000 Hz. Epochs from -15 ms to $+150$ ms were extracted and averaged over all 500 trials. Representative channel was manually selected from ERP images among the CP5/6, CP3/2, C1/2, or C3/C4 channels and referenced to F1/F3. For plotting N9, Erb's point ipsilateral to the stimulation was referenced to the contralateral Erb's point. Topoplots for the P50 is plotted as the most significant lateralized response to the stimulation.

2.8. Auditory evoked potentials

Auditory stimuli consisted of two pure tones with 500 Hz and 1000 Hz frequency with 50 ms duration, 5 ms rise up, and 5 ms rise down. Five sets of auditory stimuli were presented with 100 ms inter stimulus interval (ISI) and referred to as a stimulation epoch in this text. A trial was defined as a repetition of 5 epochs with 650 ms ISI (Fig. 1). Brain response to the changes in the order of auditory stimuli within an epoch was defined as a local effect (LE) and the brain response to the change in the order of trials within a block was defined as a global effect (GE). As depicted in Fig. 1, two different global patterns in two experimental blocks were used. Each block consisted of 120 trials with the first 20 as training trials for the participant to learn the rule of global regularity within that block. In each block, the order of presenting trials was randomized with an 80% probability of the trials that were not violating the global pattern (i.e., globally similar) and 20% for the ones that were violating the global regularity (i.e., globally deviant). The difference between the two blocks was in the pattern of stimuli in one epoch (i.e., local pattern). In the first experimental

block, in the first four epochs, all the auditory stimuli are the same (i.e., locally similar), while in the second experimental block, the last auditory stimulus is different from the first four (i.e., locally deviant). In summary, as depicted in Fig. 1, four different conditions resulted in two blocks, Globally Similar Locally Similar (GSLs), Globally Similar Locally Deviant (GSLD), Globally Deviant Locally Similar (GDLS), and Globally Deviant Locally Deviant (GDLD). GSLs and GDLD are used as a control condition for GDLS and GSLD, respectively. For details, see Bekinschtein et al. (2009).

The significant difference between the first four epochs in the first and second block, which is only due to the violation of local pattern, was calculated as LE. The significant difference between the two conditions in the second block and their control condition in the first block, which had the same local pattern while their global pattern was changing, was calculated as the GE. The p-Value obtained from the t-test comparison for LE and GE is scaled in 10 gradual levels and plotted for comparison, in which 0 indicates no significant difference and 9 indicates a significant difference at 0.01 level corrected for multiple comparisons. For the healthy subjects' plot, LE and GE are averaged across all subjects.

For the ERPs, the signal was resampled to 500 Hz and filtered between 1 Hz and 20 Hz, noisy channels were interpolated, trials averaged across conditions, and the baseline was removed. ICA ran on epoched trials and noise components were removed, by visual inspection, outliers were rejected, using the FieldTrip visual inspection toolbox.

3. Results

A figure with the same structure is provided that summarizes all the experimental findings for each patient. Fig. 2 for P1, Fig. 3 for P4, Fig. 4 for P9, and Fig. 5 for P17. Descriptive and analytic findings of the most important findings for each experimental paradigm in each patient are reported separately below.

3.1. Resting-State

All patients had an EEG amplitude range of ± 50 μ V. The alpha peak was completely missing in P1 and P9, but a minimal peak at around 8 Hz can be detected in P4 and P17. In P4 and P9 a slow oscillation at around 4 Hz with a huge power is emerged and can be detected both in time domain and frequency domain plots (Fig. 3a&b and Fig. 4a&b). Although the patient does not show any visible and detectable eye movements for communication purposes with caretakers, there exists eye activity in the list of ICA components of all patients, except for P9, speculating the presence of attenuated remaining eye activity after the patient is considered to be CLIS. PSD pattern did not significantly change between eyes open and eyes closed conditions in none of the patients (Figs. 2-5b), which is described in detail in section 2.5. Eyes Open vs. Eyes Closed.

In P4 and P9 abnormal EEG patterns can be detected that synchronizes EEG in all channels at the same time and lasts for almost two seconds (Fig. 3a and Fig. 4a). This pattern repeats periodically every five to eight seconds and has a similar morphology to the burst suppression and triphasic waves that can be found in coma patients and anesthetic subjects (Emilia Cosenza Andraus et al., 2011; Niedermeier, 2009). This synchronization signal at -4 Hz dominates the background activity at all channels at the same time with progressive increase and decrease of the amplitude (Figs. 3-4a&b) and activities above 4 Hz that are superimposed with the dominant slow frequency are not appearing in EEG plots. Thus the EEG of these two patients shows more unpredictability than the EEG of P1 and P17.



Fig. 1. Design of experiment for modified local-global paradigm used for auditory stimulation in patients and healthy. Two blocks (B1 and B2), each consisting of five epochs (EP1 to EP5), with local and global regularity patterns generate four conditions including Globally Similar Locally Similar (GSLS), Globally Deviant Locally Deviant (GDL), Globally Similar Locally Deviant (GDS), and Globally Deviant Locally Similar (GDL).

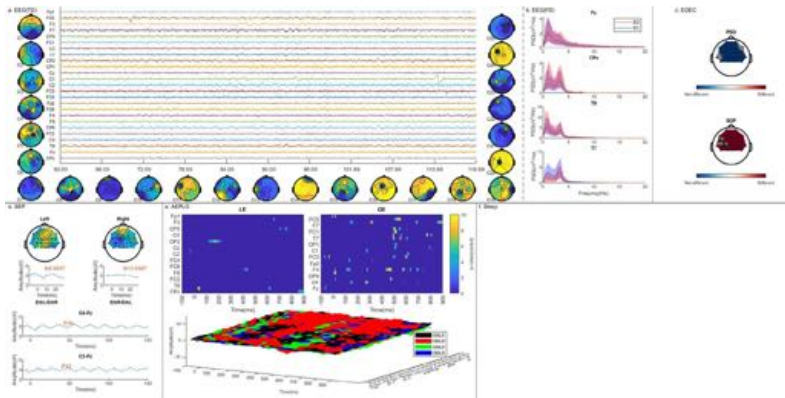


Fig. 2. Neurophysiological map of P1 a) 60 seconds of resting-state electroencephalography (EEG) while eyes closed with the amplitude range of $\pm 31 \mu\text{V}$; C7&C9 components from independent component analysis (ICA) might indicate remaining eye activity b) Power spectral density (PSD) of four representative central and parietal EEG channels in eyes closed (EC, red) vs. eyes open (EO, blue) c) Significant differences between EO vs. EC using PSD comparison (top) and second-order plot (SOP, down), d) Somatosensory evoked potentials (SEPs) for the stimulation of the right and left median nerves; topo plots of most significant evoked response at 50 (PSD); N9 responses recorded from Erb's points; cortical SEPs of right (top) and left (bottom) median nerves. e) The significance level of local (Top-Left) and global (Top-Right) effects in auditory evoked potentials (AEPs) of local-global paradigm and their corresponding event-related potentials (ERPs) in four conditions: Globally Similar Locally Similar (GSLS, black), Globally Deviant Locally Deviant (GDL, red), Globally Similar Locally Deviant (GSLD, green), and Globally Deviant Locally Similar (GDL, blue). f) Sleep recordings not available for this patient.

3.2. Source localization

As demonstrated in Fig. 6a, in every healthy subject, the alpha activity source is reconstructed over the posterior cortices, even though there was no electrode covering the occipital region. This result validates the mathematically hired method as a proper tool for localizing the source of a particular frequency of interest in EEG activity with the recording montage used in this study. Source localization results for patients (Fig. 7) demonstrate that in all patients, deeper structures of the brain are the origin of the slow dominant frequency. However, the exact location varied among patients, and no common pattern could be found among patients.

3.3. Sleep

For P1 due to the family's request only one night was recorded, which contained a continuous recording noise that could not be removed. In the other three patients, the domi-

nant slow frequency in the EEG loses power periodically during the episodes at night concurrent with an increase of the power in the EOG channels. It should be noted that no voluntary EOG activity can be visually or instrumentally detected for communication during the day. In P4, these episodes repeated 3 times during the night with the duration was almost an hour (Fig. 3f). In P9, these episodes had a lower duration of approximately 15 minutes but were more frequent (Fig. 4f). In P17, the power of attenuated alpha activity at 8 Hz reduced during episodes at night, and the dominant 2 Hz frequency of the day is replaced by the dominant 1 Hz activity during the two episodes of supposedly slow-wave sleep; During these episodes at night, the EOG activity increases in P4 and P17, for P9 that EOG is not recorded. P4 receives a benzodiazepine (Lorazepam, low dose 0.5mg) for anxiety problems, which does not seem to affect on the sequence of slow-wave episodes during the night as it is not differing from the other patients.

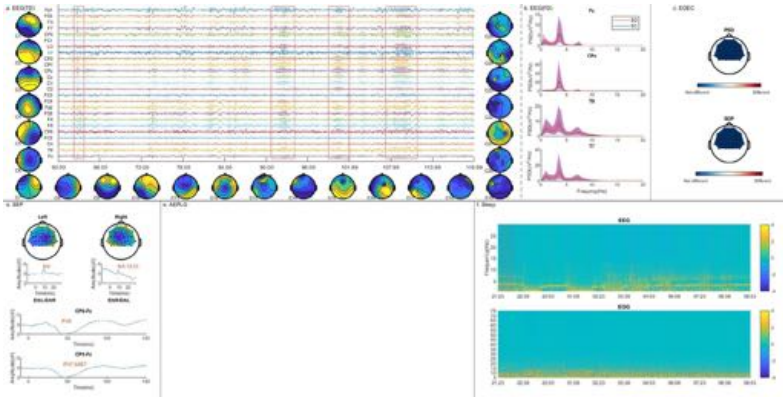


Fig. 3. Neurophysiological map of P4 a) 60 seconds of resting-state electroencephalography (EEG) while eyes closed with the amplitude range of $\pm 36 \mu\text{V}$; C7 component from independent component analysis (ICA) might indicate remaining eye activity b) Power spectral density (PSD) of four representative central and parietal EEG channels in eyes closed (EC, red) vs. Eyes Open (EO, blue) c) Significant differences between EO vs. EC using PSD comparison (top) and second-order plot (SOP, down). d) Somatosensory evoked potentials (SEPs) for the stimulation of the right and left median nerves; top plots of most significant evoked response at 50 (P50); N9 responses recorded from Erb's points; cortical SEPs of right (top) and left (bottom) median nerves. e) Auditory evoked potentials data not available for this patient. f) Periodic decrease in the power dominant frequency in the sleep EEG (top) and increase of electrooculogram (EOG) activity (bottom) during a night. Vertical lines represent environmental noises such as truing lights on or off, medication, or auditory noises.

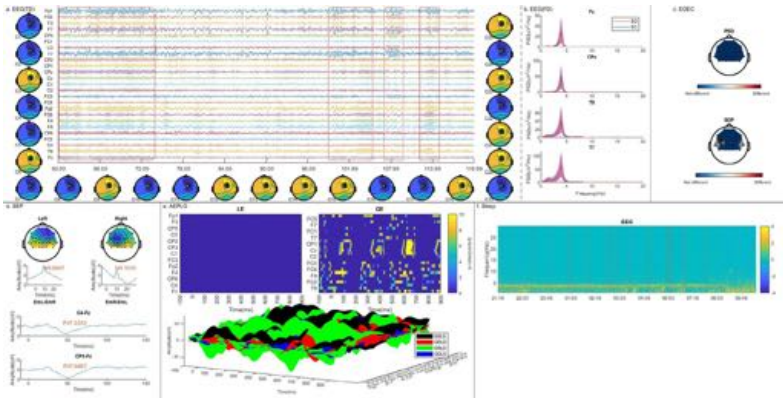


Fig. 4. Neurophysiological map of P9 a) 60 seconds of resting-state electroencephalography (EEG) while eyes closed with the amplitude range of $\pm 30 \mu\text{V}$; b) Power spectral density (PSD) of four representative central and parietal EEG channels in eyes closed (EC, red) vs eyes open (EO, blue) c) Significant differences between EO vs EC using PSD comparison (top) and second-order plot (SOP, down). d) Somatosensory evoked potentials (SEPs) for the stimulation of the right and left median nerves; top plots of most significant evoked response at 50 (P50); N9 responses recorded from Erb's points; cortical SEPs of right (top) and left (bottom) median nerves. e) The significance level of local (Top-Left) and global (Top-Right) effects in auditory evoked potentials (AEPs) of local-global paradigm and their corresponding event-related potentials (ERPs) in four conditions: Globally Similar Locally Similar (GSLs, black), Globally Deviant Locally Deviant (GDLD, red), Globally Similar Locally Deviant (GSLD, green), and Globally Deviant Locally Similar (GDLS, blue). f) Periodic decrease in the power of dominant frequency in the sleep EEG during a night. Vertical lines represent environmental noises such as truing lights on or off, medication, or auditory noises.

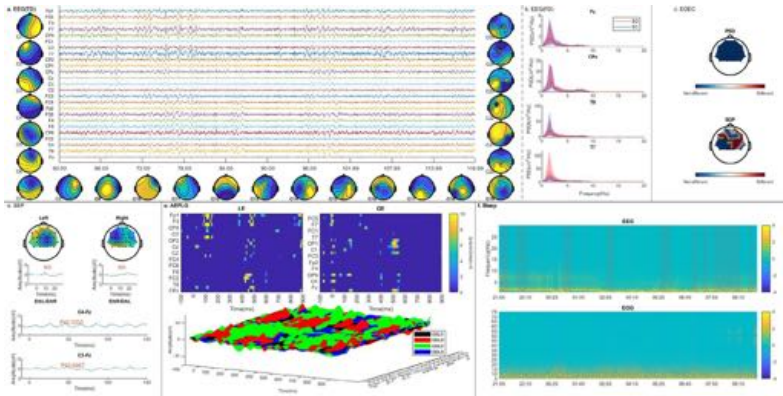


Fig. 5. Neurophysiological map of P17 a) 60 seconds of resting-state electroencephalography (EEG) while eyes closed with the amplitude range of $\pm 45 \mu\text{V}$; C2, C4, & C17 components from independent component analysis (ICA) might indicate remaining eye activity b) Power spectral density (PSD) of four representative central and parietal EEG channels in eyes closed (EC, red) vs. eyes open (EO, blue) c) Significant differences between EO vs. EC using PSD comparison (top) and second-order plot (SOP, down). d) Somatosensory evoked potentials (SEPs) for the stimulation of the right and left median nerves; top plots of most significant evoked response at 50 (P50); N9 responses recorded from Erb's points; cortical SEPs of right (top) and left (bottom) median nerves. e) The significance level of local (Top-Left) and global (Top-Right) effects in auditory evoked potentials (AEPs) of local-global paradigm and their corresponding event-related potentials (ERPs) in four conditions: Globally Similar Locally Similar (GSLs, black), Globally Deviant Locally Deviant (GDLD, red), Globally Similar Locally Deviant (GSLD, green), and Globally Deviant Locally Similar (GDLS, blue). f) Periodic decrease in the power dominant frequency in the sleep EEG (top) and increase of electrooculogram (EOG) activity (bottom) during a night. Vertical lines represent environmental noises such as truing lights on or off, medication, or auditory noises.

3.4. Eyes open vs. eyes closed

Using bootstrapping, a 95% confidence interval for the number of channels that showed a significant difference between EO and EC, in the healthy subjects, was calculated between 20.4% and 45.6% using PSD comparison, and between 39.6% and 66.4% using the SOP method (Fig. 6c). In all healthy subjects, a significant difference in the PSD comparison was detected between EO and EC, except for one healthy subject. In this subject, although a clear alpha peak was present in the PSD, no significant difference was detected in the PSD comparison in none of the channels, while in the same subject using the SOP method, a significant difference between the two conditions was detected in some channels. This subject had no history of visual, neurological, or psychiatric disorders and was excluded from the PSD method's bootstrapping iterations. None of the patients showed any EEG changes while opening the eyes using the PSD comparison method, while the SOP method captured significant differences at least in four channels in all patients (Figs. 2-5b&d).

3.5. Somatosensory evoked potentials

In all healthy subjects, the N9 component on Erb's indicated intact peripheral somatosensory pathway. The early and lateralized component before 50 ms were detected in all subjects. Although the SEP patterns were different among subjects and inter-individual variability was high. Nevertheless, the non-cephalic N9, and cortical P50, and the propagation of the stimulation response in the brain were found in all healthy subjects.

In P1 and P17, the N9 is missing on the Erb's point (Fig. 2c and Fig. 5c). This might indicate the absence of the sensory neural pathways or a considerable increase in the sensory threshold for

stimulation intensity. However, the possibility of experimental failure, as it is inherent in any experiment, cannot be excluded. Replication of the experiment (as with all other paradigms used here) with higher stimulation intensity can rule out an increased threshold hypothesis. In P4 and P9 intactness of afferent fibers could be detected with the N9 response on Erb's points, the N20 was missing bilaterally and P50 was the most significant earliest brain response (Figs. 3-4c), which propagated over the sensory cortex bilaterally with a uniform spatial distribution.

3.6. Auditory evoked potentials

As presented in Fig. 6b results from healthy subjects indicate that LE can be detected in earlier latencies (before 150 ms) in comparison to GE, which appears at latencies after almost 200 ms. However, the inter-individual variability was high due to the small number of subjects in the healthy group.

In P1, no LE was detected, while very late GE appeared after 500 ms in only some frontal channels. A closer look at the ERP pattern in Fig. 2d indicates that in the deviant condition in block 1 (i.e., GDLD) a clear P3 peak can be found. However, this peak is not statistically significantly different from the baseline due to the large variance of the baseline activity. In P9, also no LE could be detected but there seems to be a strong GE. A closer look at the ERP raw signal in Fig. 4d clarifies that the highly synchronous sinusoidal background EEG is the main reason behind this statistical difference, while no physiologically relevant response can be detected, which means that a phase shift in the raw EEG signal is causing a significant difference between any two conditions independently from experimental conditions. In P17, both LE and GE are present, however, the responses are delayed to 500 ms after the stimulation

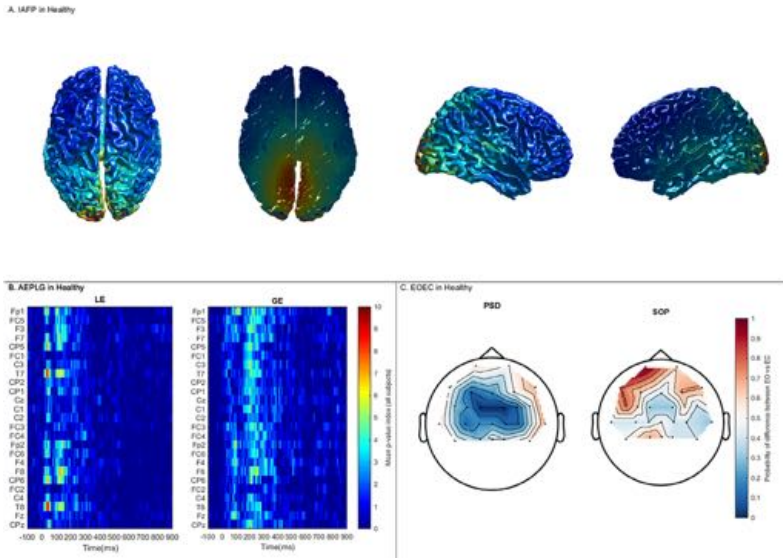


Fig. 6. Resting and Auditory evoked response in Healthy controls. A) Source of individual alpha peak frequency (IAPF) sum of all subjects. B) The local (Top-Left) and global (Top-Right) effect in auditory evoked potentials (AEP/PLG) due to the auditory stimulation averaged of all subjects. C) Eyes open vs eyes closed (EEOC) comparison illustrates the number of healthy subjects showing a significant difference between eyes open and eyes closed conditions, using two different metrics: Power spectral density (PSD) comparison (left) and second-order plots (SOP, right).

onset. For P4, the experiment was terminated due to technical issues no report is available.

4. Discussion

Each experiment's results are discussed individually below, and a summary discussion of all the findings is provided at the end. This study reports for the first time a small sample of a particular rare subcategory of patients with ALS after transitioning to CLIS. Even though in P1 no sleep data are available and in P4 AEPs are missing, some consistencies between the four patients emerge as discussed below. One way to overcome the problem of small sample size of CLIS studies is that laboratories and clinicians with access to such patients perform standardized neurophysiological experimental paradigms and report it and release the dataset for other researchers; Only with the accumulation of these small sample size reports a large dataset can be acquired. This report is one step in that direction.

4.1. Resting-state EEG

Given that ALS patients before the transition to CLIS show normal or close to normal spontaneous EEG (Hohmann et al., 2018), the large difference found here in every patient after the transition to CLIS is considerable. This is not the first time that the slowing of EEG activity is reported in patients in CLIS (Hohmann et al., 2018; Malekshahi et al., 2019; Maruyama et al., 2020). Although EEG

changes seem to be different from patient to patient, the slowing of the signal is common in all of them. The slowing of the EEG and lack of alpha peak is not limited to patients in CLIS and is also found in aging (Scally et al., 2018), Alzheimer (Cantero et al., 2009), attention-deficit hyperactivity disorders (Lansbergen et al., 2011). However, a large increase in the power in a particular frequency band below 5 Hz and synchronization of the signal in all channels is unique in patients in CLIS and to some extent similar to coma patients (Hofmeijer et al., 2014; Niedermeyer, 2009), particularly for P4 and P9. Due to the neurodegenerative nature of ALS, loss of motor neurons in the central nervous system, loss of mass and volume, and atrophy of the brain are frequently reported (Kassubek et al., 2005; Mezzapesa et al., 2007; Mioshi et al., 2013), which alone can effectively change the EEG pattern in the latest stage of the disease in CLIS. Unfortunately, due to patients' physical condition, there is no structural MRI available of a CLIS to validate this speculation. Overall, it seems that there are two distinct EEG patterns in CLIS. In the first group EEG characteristics are attenuation or loss of power in the alpha band, decrease in the EEG amplitude, more complex and not predictable EEG, and weak alpha-like activity at around 8 Hz, such as P1 and P17. The second group is the lack of alpha waves and emergence of a very slow and high power at around 4 Hz, which dominates the whole spectrum and is phase synchronized in all the channels, such as P4 and P9. Of course, a small sample of four patients is not enough to generalize to all patients in CLIS but most of the patients reported by the authors can be classified in one of the two mentioned categories

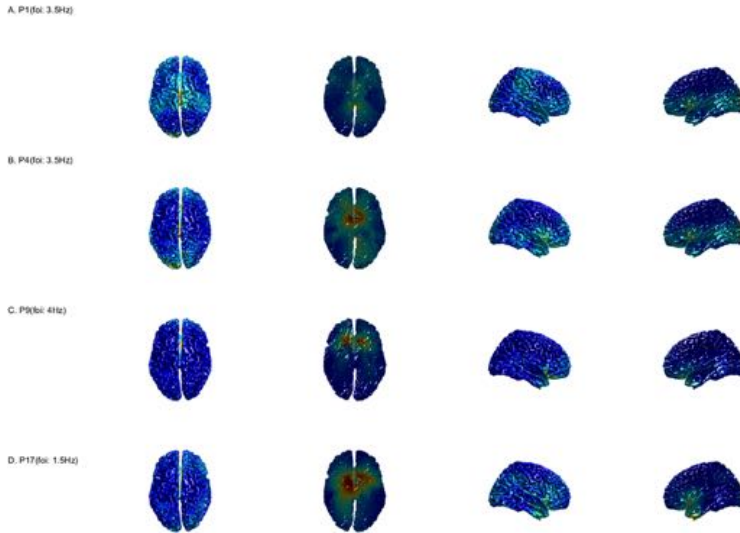


Fig. 7. Source of slow activity in patients.

(Hohmann et al., 2018; Malekshahi et al., 2019; Maruyama et al., 2020; Ramos-Murguialday et al., 2013, 2011).

4.2. Source localization

Different criticism could be raised against source localization techniques, especially when the source of the activity is located in the deeper structure of the brain, and when only a few electrodes are used. The algorithm is forced to locate the source of activity in such a way that the input data can be reproduced, and the easiest way (in terms of computational costs) would be to assume the source of the common activity in the center of the head model. However, anatomically is also more plausible to find the source of common slow activity that synchronizes all EEG recording channels at the same time with no phase lag in a deeper structure of the brain with symmetric cortical accessibility. Particularly in P4 and P9 that all EEG channels are episodically synchronized in one particular low frequency without any phase shift between channels, it is highly probable that the source of activity is subcortical, probably, thalamic. In ALS patients, after total loss of upper or lower motor neurons, brain networks with presynaptic and postsynaptic connections to the motor assemblies in the diencephalon such as the subthalamic network that together with striatum are controlling skeletal muscle movements might also be disrupted. This is in line with different observations reporting atrophy and shape changes of the cerebral and corticospinal tract in ALS patients before transitioning to the CLIS (Kumar et al., 2016; Mioishi et al., 2013; Rajagopalan et al., 2013). It has been reported that the functional connectivity of the sensorimotor cortex (SMC) to the cingulate cortex is increased in ALS patients prior to the transition to CLIS (Agosta et al., 2011). Additionally, default mode

network connectivity is reported to be increased in ALS patients before the transition to CLIS (Chenji et al., 2016). Loss of inhibitory motor neurons in ALS patients (Lloyd et al., 2000) is proposed as the main reason for the increase in brain connectivity and baseline activity (Chenji et al., 2016; Douaud et al., 2011) and are expected to be even stronger after the transition to CLIS and might be the reason behind the emergence of high power and slow activity in EEG of patients in CLIS.

4.3. Sleep

Authors have recently reported that patients in CLIS have similar to normal sleep behavior and circadian rhythms, including 3 patients reported here (Malekshahi et al., 2019). Continuous several days recordings of a single patient in CLIS have shown that the sleep cycles are distributed during the day and are not only limited to the night (Ramos-Murguialday et al., 2013). In this report, we investigated the fluctuation of the dominant slow frequency in the EEG data during the nighttime recordings and demonstrated that in all patients, except for P1 where sleep was not recorded, the dominant frequency of the day is slower at night, down to 1 Hz in some patients. We also demonstrated cyclic changes in the EEG band power during the night that might be correlated with different slow-wave sleep stages. However, due to the patient's significant changes in the EEG pattern, the classification of different sleep stages with criteria from healthy subjects is not possible in any of the patients. Overall, in all patients, the power of slow dominant frequency in the EEG during the day is lost in those cyclic episodes of ultraslow waves during the night. This may suggest that the slow dominant background EEG that is common in all patients in CLIS should not necessarily be interpreted

pathological and the ultraslow activity during the night might indicate the typical slow-wave sleep episodes (Sleep stage 3). For the sleep analysis see Malekshahi et al. (2019).

4.4. Eyes open vs. eyes closed

The increase of the confidence interval to detect EO vs. EC in healthy subjects while using the SOP method in comparison to the PSD comparison method supports the idea that SOP is more sensitive than PSD comparison in detecting brain reactivity while opening the eyes. Besides, lost or attenuated alpha peak in the patients and failure of the PSD comparison method to detect the EO condition indicates that the methodologies used healthy subjects' analysis might be insufficient in patients with significantly altered EEG. Although for P4 and P9, the number of channels that showed significant differences using the SOP method is smaller than in healthy subjects, the fact that there is some difference at all might indicate some level of visual processing in patients. Also, in these two patients only in one of the two days recordings, brain reactivity to the opening of the eyes could have been detected. With non-responsive patients like CLIS, it is a challenge to detect arousal changes during an experiment; here, we assume that the difference between the two days is due to the arousal level in the recording of these days. Studies have shown that episodes of sleep during the daytime are a common behavior in patients in CLIS and it is a possibility that the patient is not attentively aroused during an experiment.

4.5. Somatosensory evoked potentials

Diagnosis is not the primary function of SEPs, yet, loss of all cortical and subcortical SEP components is usually associated with brain death in anoxic coma (Crucru et al., 2008). On the other hand, ALS patients before the transition to CLIS show altered SEPs probably because of the compensatory activity of the sensory-motor cortex (Hamada et al., 2007). Considering that the pathology of sensory pathways in ALS patients is not well known yet, any diagnosis based only on SEPs in ALS-CLIS patients should be avoided.

The absence of the N9 response on the Erb's point in P1 and P17, which only requires proper functioning of the peripheral somatosensory neural pathway, may represent the dysfunction of sensory pathways in the latest stage of the disease. Although experimental failure cannot be ruled out, and no further hypotheses can be given before repetition in the same subjects and others. In P4 and P9, with the presence of N9 and bilaterally absence of cortical responses before 50 ms, the patients' condition might be more critical, since the absence of bilateral N20 in median nerve stimulation of anoxic coma has always been associated with severe brain damage (Crucru et al., 2008). But, as mentioned before, due to the alteration of the SEPs in ALS before the transition to CLIS, any diagnosis solely based on the SEPs should be avoided.

4.6. Auditory evoked potentials

Patients in CLIS, with altered background EEG, did not show similar ERP response to auditory stimuli compared to healthy people and each patient had a unique brain response. Although, lack of LE and delayed CE was common in all patients, except for P4 for which the AEPs were not recorded, which is in line with previous findings reporting delayed auditory ERP response in CLIS (Kotchoubey et al., 2003). Even with insufficient attentional early analysis of the stimulus characteristics like modality and intensity, a cognitive differentiation of differential characteristics (global or local without the presence of both) is possible late in the processing stream. Kotchoubey et al. (2005) reported similar paradoxical findings in severe brain-damaged patients, where a semantic mis-

match potential (N400) was present late in the processing stream (at around 600 ms) while all early components such as the mismatch negativity after 150–200 ms were completely absent (Kotchoubey et al., 2005). Whether this indicates conscious processing in the absence or only rudimentary early automatic differentiation of stimulus characteristics is more a basic theoretical question than an empirical question, but such a separation seems possible. A similar paradox was observed in autistic savant patients, where early (unconscious) processing ERP components are excessively large while late (conscious) components are completely absent (Birbaumer, 1999).

5. Conclusion

The slow and high power 4 Hz signal emerged in two patients out of the four cannot be compared with sleep-wave activity in these patients because the sleep slow-wave episodes were slower around 1.5 Hz. The two patients with slow and high amplitude EEG with high synchronization in all the recording channels were bilaterally missing the N20 to electrical stimulation of the median nerves (SEPs) and the first peak was found at 50 ms, and the SEPs were significantly different from the healthy. In the other two patients, no response could be detected, and electrical stimulation did not reach to the Erb's point, consequently, did not cause any cortical evoked response; reasons remained unclear. In the two patients with dominant slow frequency at 4 Hz, no AEPs could be found. While in the other two patients, pre-attentive evoked responses were absent, and attentive late evoked responses were retained but delayed to 500 ms. We proposed a pathology in the early automatic perceptual sensory systems with an intact but delayed higher cognitive processing system analogously to findings in autistic spectrum disorder (Birbaumer, 1999). "Extinction of goal-directed thinking" (Kübler and Birbaumer, 2008) and lack of contingent reinforcement and rewards in the absence of any type of communication from a behavioral point of view, might reduce cognitive capability after longer periods in CLIS. Due to the small number of patients in this report, results are vulnerable to bias and need to be validated with more patients. It is important to follow patients longitudinally before the transition to CLIS until months after that, to elucidate the relation between the progress of the disease and changes in brain responses. It is unclear yet if these changes are gradual or occur in a rapid stepwise fashion.

The extreme heterogeneity of the results of different brain measures in CLIS reflecting different neural and therefore different cognitive processes remind us of a similar dilemma in the diagnosis of conscious processes in the severe brain-damaged patients (Laureys and Boly, 2007; Majerus et al., 2005; Real et al., 2016); while one measure (i.e. SEP) denies any conscious or cognitive process the other measurement points to the existence of highly complex semantic thinking and reasoning in the same patient at the same time. This warns us not only of seemingly consistent theoretical explanations and theories in CLIS and DoC but also of any clinical diagnostic statements and assurances; we just do not know what is possible yet. From this work on patients in CLIS who were never investigated with such measurements all at the same occasion before we are forced to conclude that we have some neural indices indicating intact or only deviant cognitive processing while others suggest severe disorders of perception and reasoning.

Declaration of Competing Interest

None of the authors have potential conflicts of interest to be disclosed.

Acknowledgements

Supported by Deutsche Forschungsgemeinschaft (DFG, BI 195/77-1), BMBF (German Ministry of Education and Research) 16SV7701 CoMiCon, Deutsche Forschungsgemeinschaft (DFG, BI195, Koselleck), LUMINOUS-H2020- FETOPEN-2014- 2015-RIA (686764), and Wyss Center for Bio and Neuroengineering, Geneva. We thank the four anonymous reviewers whose comments/suggestions helped improve and clarify this manuscript.

Authors contribution

MKH designed the study, acquired the data, performed the analysis, and wrote the first draft of the paper. SW verified the analysis and interpretation of the result and acquired the data. AT helped in the implementation of the experimental paradigms. NB conceptualized the work, designed the experiments, and substantially revised the paper. UC funding acquisition, project initiation, revised the paper, and managed patients' interactions.

References

Agosta F, Valsasina P, Absinta M, Riva N, Sala S, Prelle A, et al. Sensorimotor functional connectivity changes in amyotrophic lateral sclerosis. *Cereb Cortex* 2011;21:2291–8. <https://doi.org/10.1093/cercor/bhr002>.

American Clinical Neurophysiology Society. Guideline 11B: Recommended standards for intraoperative monitoring of somatosensory evoked potentials; 2009. https://www.acns.org/pdf/guidelines/Guideline_11B.pdf.

Bassetti C, Mathis J, Hess CW. Multimodal electrophysiological studies including motor evoked potentials in patients with locked-in syndrome: Report of six patients. *J Neurol Neurosurg Psychiatry* 1994;57:1403–6. <https://doi.org/10.1136/jnnp.57.11.1403>.

Bauer G, Gerstenbrand F, Rimpl E. Varieties of the locked-in syndrome. *J Neurol* 1979;221:777–91. <https://doi.org/10.1007/BF00313105>.

Bekinschtein TA, Davis MH, Rood JM, Owen AM. Why clowns taste funny: The relationship between humor and semantic ambiguity. *J Neurosci* 2011;31:9665–71. <https://doi.org/10.1523/JNEUROSCI.5058-10.2011>.

Bekinschtein TA, Dehaene S, Rohaut B, Tadel F, Cohen L, Naccache L. Neural signature of the conscious processing of auditory regularities. *Proc Natl Acad Sci USA* 2009;106:1672–7. <https://doi.org/10.1073/pnas.0809667106>.

Birbaumer N. Breaking the silence: The silence: Brain-Computer Interfaces (BCI) for communication and motor control. *Psychophysiology* 2006;43:517–32. <https://doi.org/10.1111/j.1469-8986.2006.04456.x>.

Birbaumer N. Rain Man's revelations. *Nature* 1999;399:211–2. <https://doi.org/10.1038/20329>.

Boytsova YA, Danko SG. EEG differences between resting states with eyes open and closed in darkness. *Hum Physiol* 2010;36:367–9. <https://doi.org/10.1134/S0022197710030190>.

Cantero JL, Atienza M, Gomez-Herrero G, Cruz-Vadell A, Gil-Neigra E, Rodriguez-Romero R, et al. Functional integrity of thalamocortical circuits differentiates normal aging from mild cognitive impairment. *Hum Brain Mapp* 2009;30:3944–57. <https://doi.org/10.1002/hbm.20813>.

Chaudhary U, Birbaumer N, Curado MR. Brain-Machine Interface (BMI) in paralysis. *Ann Phys Rehabil Med* 2015;58:9–13. <https://doi.org/10.1016/j.aphr.2014.11.002>.

Chaudhary U, Birbaumer N, Ramos-Murguialday A. Brain-computer interfaces for communication and rehabilitation. *Nat Rev Neurol* 2016;12:513–25. <https://doi.org/10.1038/nrneurol.2016.113>.

Chaudhary U, Mrachek-Kersting N, Birbaumer N. Neurophysiological and neurophysiological aspects of brain-computer-interface (BCI)-control in paralysis. *J Physiol* 2020a;362:7875. <https://doi.org/10.1113/jphysiol.2020.06.011>.

Chaudhary U, Vlachos I, Zimmermann JB, Espinosa A, Tonin A, Jaramillo-Gonzalez A, et al. Verbal Communication using Intracortical Signals in a Completely Locked In-Patient. *medRxiv* 2020:2020.06.10.20122408. <https://doi.org/10.1101/2020.06.10.20122408>.

Chenji S, Jha S, Lee D, Brown M, Seres P, Mah D, et al. Investigating default mode and sensorimotor network connectivity in amyotrophic lateral sclerosis. *PLoS One* 2016;11:1–14. <https://doi.org/10.1371/journal.pone.0157443>.

Constantinovic A. Abnormal somatosensory evoked potentials in amyotrophic lateral sclerosis. *Rom J Neurol Psychiatry* 1993;31:273–8. <https://doi.org/10.1212/wnp.36.6.796>.

Cosi V, Poloni M, Mazzini L, Calicco R. Somatosensory evoked potentials in amyotrophic lateral sclerosis. *J Neurol Neurosurg Psychiatry* 1984;47:857–61. <https://doi.org/10.1136/jnnp.47.8.857>.

Cruecu C, Aminoff MJ, Curio C, Guevit JM, Kaligri R, Mauguier E, et al. Recommendations for the clinical use of somatosensory-evoked potentials. *Clin Neurophysiol* 2008;119:1705–19. <https://doi.org/10.1016/j.clinph.2008.03.016>.

Danko SG. The reflection of different aspects of brain activation in the electroencephalogram: Quantitative electroencephalography of the states of rest with the eyes open and closed. *Hum Physiol* 2006;32:377–88. <https://doi.org/10.1134/S0167141070604013>.

Delorme A, Makeig S. EEGLAB: An open source toolbox for analysis of single-trial EEG dynamics including independent component analysis. *J Neurosci Methods* 2004;134:9–21. <https://doi.org/10.1016/j.jneumeth.2003.10.069>.

Doua G, Filippini N, Knight S, Talbot K, Turner MR. Integration of structural and functional magnetic resonance imaging in amyotrophic lateral sclerosis. *Brain* 2011;134:3470–9. <https://doi.org/10.1093/brain/awt223>.

Duncan CC, Barry RJ, Connolly FJ, Fischer C, Michie P, Näätänen R, et al. Event-related potentials in clinical research: Guidelines for eliciting, recording, and quantifying mismatch negativity, P300, and N400. *Clin Neurophysiol* 2009;120:1883–908. <https://doi.org/10.1016/j.clinph.2009.07.045>.

Emilia Cosenza Andraus M, Fantezia Andraus C, Vieira Alves-Leon S. Periodic EEG patterns: importance of their recognition and clinical significance. *Padrões eletroencefalográficos periódicos: importância do seu reconhecimento e significado clínico* 2011:145–51.

Ferster CB, Skinner BF. Schedules of reinforcement. Appleton-Century-Crofts 2005. <https://doi.org/10.1037/10627000>.

Fuchs A. Beamforming and its applications to brain connectivity. *Understand Complex Syst* 2007;2007:357–78. https://doi.org/10.1002/978-3-540-31512-2_12.

Gallegos-Ayala C, Furdea A, Takano K, Ruf CA, Flor H, Birbaumer N. Brain communication in a completely locked-in patient using bedside near-infrared spectroscopy. *Neurology* 2014;82:1930–2. <https://doi.org/10.1212/WNL.0000000000000439>.

Gross J, Kujala J, Hämäläinen M, Timmermann L, Schnitzler A, Salmelin R. Dynamic imaging of coherent sources: Studying neural interactions in the human brain. *Proc Natl Acad Sci USA* 2001;98:694–9. <https://doi.org/10.1073/pnas.98.2.694>.

Gütting E, Iseemann S, Wichmann W. Electrophysiology in the locked-in-syndrome. *Neurology* 1996;46:1092–101. <https://doi.org/10.1212/WNL.46.4.1092>.

Hanada M, Hanajima R, Terao Y, Sato F, Okano T, Yuasa K, et al. Median nerve somatosensory evoked potentials and their high-frequency oscillations in amyotrophic lateral sclerosis. *Clin Neurophysiol* 2007;118:877–86. <https://doi.org/10.1016/j.clinph.2006.12.001>.

Hayashi H, Kato S. Total manifestations of amyotrophic lateral sclerosis. ALS in the totally locked-in state. *J Neurol Sci* 1989;93:19–35. [https://doi.org/10.1016/0022-5106\(89\)90158-5](https://doi.org/10.1016/0022-5106(89)90158-5).

Hofmeijer J, Tjepkema-Cloostermans MC, van Putten MJAM. Burst-suppression with identical bursts: A distinct EEG pattern with poor outcome in postanoxic coma. *Clin Neurophysiol* 2014;125:947–54. <https://doi.org/10.1016/j.clinph.2013.10.017>.

Hohmann MR, Fomina T, Jayaram V, Emde T, Just J, Synofzik M, et al. Case series: Slowing alpha rhythm in late-stage ALS patients. *Clin Neurophysiol* 2018;129:406–8. <https://doi.org/10.1016/j.clinph.2017.11.013>.

Huynh V, Ahmed R, Mahoney CJ, Nguyen C, Tu S, Caga J, et al. The impact of cognitive and behavioral impairment in amyotrophic lateral sclerosis. *Expert Rev Neurother* 2020;20:281–93. <https://doi.org/10.1080/14737175.2020.1727240>.

Jonhmadami Y, Poudel G, Innes C, Weiss D, Krueger R, Jones R. Comparison of beamformers for EEG source signal reconstruction. *Biomed Signal Process Control* 2014;14:175–88. <https://doi.org/10.1016/j.bspc.2014.07.012>.

Kassubeck J, Umrath A, Huppertz HJ, Lulé D, Ethofer T, Sperfeld AD, et al. Global brain atrophy and corticospinal tract alterations in ALS as investigated by voxel-based morphometry of 3-D MRI. *Amyotrophic Lateral Scler Other Mot Neuron Disord* 2005;6:213–20. <https://doi.org/10.1080/14660820510038538>.

Kotchoubey B, Lang S, Mezger G, Schmalhorn D, Schneck M, Semmler A, et al. Information processing in severe disorders of consciousness: Vegetative state and minimally conscious state. *Clin Neurophysiol* 2005;116:2441–53. <https://doi.org/10.1016/j.clinph.2005.03.028>.

Kotchoubey B, Lang S, Winter S, Birbaumer N. Cognitive processing in completely paralyzed patients with amyotrophic lateral sclerosis. *Eur J Neurol* 2003;10:551–8. <https://doi.org/10.1046/j.1468-1331.2003.00647.x>.

Kübler A, Birbaumer N. Brain-computer interfaces and communication in paralysis: Extinction of goal directed thinking in completely paralyzed patients? *Clin Neurophysiol* 2008;119:2658–66. <https://doi.org/10.1016/j.clinph.2008.06.019>.

Kübler A, Kotchoubey B, Kaiser J, Birbaumer N, Wolpaw JR. Brain-computer communication: Unlocking the locked in. *Psychol Bull* 2001;127:358–75. <https://doi.org/10.1037/0033-2909.127.3.358>.

Kumar S, Aga P, Gupta A, Kohli N. Juvenile amyotrophic lateral sclerosis: Classical wine glass sign on magnetic resonance imaging. *J Pediatr Neurosci* 2016;11:56–7. <https://doi.org/10.4103/1817-1745.181251>.

Lansbergen MM, Arns M, van Dongen-Boomsma Martine M, Spronk D, Buitelaar JK. The increase in theta/beta ratio on resting-state EEG in boys with attention-deficit/hyperactivity disorder is mediated by slow alpha peak frequency. *Prog Neuro-Psychopharmacol Biol Psychiatry* 2011;35:47–52. <https://doi.org/10.1016/j.pnpb.2010.08.004>.

Laureys S, Boly M. What is it like to be vegetative or minimally conscious? *Curr Opin Neurol* 2007;20:609–13. <https://doi.org/10.1097/WCO.0b013e318023146d>.

Laureys S, Pellas F, Van Eckhout P, Ghorbel S, Schnakers C, Perrin F, et al. The locked-in syndrome: What is it like to be conscious but paralyzed and voiceless? *Prog Brain Res* 2005;150:495–511. [https://doi.org/10.1016/S0079-6123\(05\)50034-7](https://doi.org/10.1016/S0079-6123(05)50034-7).

- Lloyd CM, Richardson MP, Brooks DJ, Al-Chalabi A, Leigh PN. Extramotor involvement in ALS: PET studies with the GABA(A) ligand [(11C)]flumazenil. *Brain* 2000;123(Pt 11):2289–96. <https://doi.org/10.1093/brain/123.11.2289>.
- Majeurs S, Gill-Thwaites H, Andrews K, Laureys S. Behavioral evaluation of consciousness in severe brain damage. *Prog Brain Res* 2005;150:397–413. [https://doi.org/10.1016/S0079-6123\(05\)00298-1](https://doi.org/10.1016/S0079-6123(05)00298-1).
- Maleskshahi A, Chaudhary U, Jaramillo-Gonzalez A, Lucas Luna A, Rana A, Tonin A, et al. Sleep in the completely locked-in state (CLIS) in amyotrophic lateral sclerosis. *Sleep* 2019;42. <https://doi.org/10.1093/sleep/zsz185>.
- Mariyama Y, Yoshimura N, Rana A, Maleskshahi A, Tonin A, Jaramillo-Gonzalez A, et al. Electroencephalography of completely locked-in state patients with amyotrophic lateral sclerosis. *Neurosci Res* 2020. <https://doi.org/10.1016/j.neures.2020.01.013>.
- De Massari D, Ruf CA, Furdea A, Matuz T, Van Der Heiden L, Halder S, et al. Brain communication in the locked-in state. *Brain* 2013;136:1989–2000. <https://doi.org/10.1093/brain/awt072>.
- Mathworks C. MATLAB® External Interfaces R 2018 a 2018.
- Mezazepes DM, Ceccarelli A, Diconzio F, Carella A, De Caro MF, Lopez M, et al. Whole-Brain and Regional Brain Atrophy in Amyotrophic Lateral Sclerosis. *AJNR Am J Neuroradiol* 2007;28(2):255–9.
- Mioshi E, Lillo P, Yew B, Hsieh S, Savage S, Hodges JR, et al. Cortical atrophy in ALS is critically associated with neuropsychiatric and cognitive changes. *Neurology* 2013;80:1117–23. <https://doi.org/10.1212/WNL.0b013e31828869da>.
- Murguialday AR, Hill J, Bensch M, Martens S, Halder S, Nijboer F, et al. Transition from the locked in to the completely locked-in state: A physiological analysis. *Clin Neurophysiol* 2011;122:925–33. <https://doi.org/10.1016/j.clinph.2010.08.019>.
- Niedermeyer E. The burst-suppression electroencephalogram. *Am J Electroencephalogr Technol* 2009;49:333–41. <https://doi.org/10.1080/1085508x.2009.11079736>.
- Oostenvelde R, Fries P, Maris E, Schoffelen JM. FieldTrip: Open source software for advanced analysis of MEG, EEG, and invasive electrophysiological data. *Comput Intel Neurosci* 2011;2011. <https://doi.org/10.1155/2011/1456869>.
- Oostenvelde R, Stegeman DE, Praamstra P, Van Oosterom A. Brain symmetry and topographic analysis of lateralized event-related potentials. *Clin Neurophysiol* 2003;114:1194–202. [https://doi.org/10.1016/s1388-2457\(03\)00059-2](https://doi.org/10.1016/s1388-2457(03)00059-2).
- Patterson JR, Grabois M. Locked-in syndrome: A review of 139 cases. *Stroke* 1986;17:758–64. <https://doi.org/10.1161/01.STR.17.4.758>.
- Rajagopalan V, Liu Z, Alexandre D, Zhang L, Wang XF, Piroo EP, et al. Brain White Matter Shape Changes in Amyotrophic Lateral Sclerosis (ALS): A Fractal Dimension Study. *PLoS One* 2013;8. <https://doi.org/10.1371/journal.pone.0073614>.
- Ramos-Murguialday A, Hill J, Bensch M, Martens S, Halder S, Nijboer F, et al. Transition from the locked in to the completely locked-in state: A physiological analysis. *Clin Neurophysiol* 2011;122:925–33. <https://doi.org/10.1016/j.clinph.2010.08.019>.
- Ramos-Murguialday A, Gharabaghi A, Nijboer F, Schölkopf B, Martens S. Fragmentation of slow Wave sleep after onset of complete locked-in state 2013;9:15–7.
- Real RGL, Vesper S, Erlbeck H, Risetti M, Vogel D, Müller F, et al. Information processing in patients in vegetative and minimally conscious states. *Clin Neurophysiol* 2016;127:1395–402. <https://doi.org/10.1016/j.clinph.2015.07.020>.
- REF: FieldTrip. Whole brain connectivity and network analysis - FieldTrip toolbox. Donders Inst Brain, Cogn Behav Radboud Univ Netherlands; 2011. <http://www.fieldtriptoolbox.org/tutorial/networkanalysis/> [accessed March 26, 2020].
- Rohaut B, Naccache L. Disentangling conscious from unconscious cognitive processing with event-related EEG potentials. *Rev Neurol (Paris)* 2017;173:521–8. <https://doi.org/10.1016/j.neuro.2017.08.001>.
- Scally B, Burke MR, Bunce D, Delvenne JF. Resting-state EEG power and connectivity are associated with alpha peak frequency slowing in healthy aging. *Neurobiol Aging* 2018;71:149–55. <https://doi.org/10.1016/j.neurobiolaging.2018.07.004>.
- Schnakers C, Majeurs S. Behavioral assessment and diagnosis of disorders of consciousness. *Coma Disord. Conscious., Springer-Verlag London Ltd*; 2012. p. 1–10. https://doi.org/10.1007/978-1-4471-2440-5_1.
- Schnakers C, Majeurs S, Goldman S, Boly M, Van Eckhout P, Gay S, et al. Cognitive function in the locked-in syndrome. *J Neurol* 2008;255:323–30. <https://doi.org/10.1007/s00415-008-0544-0>.
- Secco A, Tonin A, Rana A, Jaramillo-Gonzalez A, Khalili-Ardali M, Birbaumer N, et al. EEG power spectral density in locked-in and completely locked-in state patients: a longitudinal study. *Cogn Neurodyn* 2020. <https://doi.org/10.1007/s11571-020-09633-3>.
- Silvoni S, Cavinato M, Volpato C, Ruf CA, Birbaumer N, Piccione F. Amyotrophic lateral sclerosis progression and stability of brain-computer interface communication. *Amyotroph Lateral Scler Front Degener* 2013;14:390–6. <https://doi.org/10.3109/21678421.2013.770029>.
- Smith E, Delagy M. Locked-in syndrome. *Br Med J* 2005;330–36. <https://doi.org/10.1136/bmj.37249>.
- Squires NK, Squires KC, Hillyard SA. Two varieties of long-latency positive waves evoked by unpredictable auditory stimuli in man. *Electroencephalogr Clin Neurophysiol* 1975;38:387–401. [https://doi.org/10.1016/0013-4694\(75\)90263-1](https://doi.org/10.1016/0013-4694(75)90263-1).
- Stanton BR, Williams VC, Leigh PN, Williams SCR, Brain CR, Jarosz JM, et al. Altered cortical activation during a motor task in ALS: Evidence for involvement of central pathways. *J Neurol* 2007;254:1260–7. <https://doi.org/10.1007/s00415-006-0513-4>.
- Sutton S, Braren M, Zubin J, John ER. Evoked-potential correlates of stimulus uncertainty. *Science* (80-) 1965;150:1187–8. <https://doi.org/10.1126/science.150.3700.1187>.
- Thorns J, Wieringa BM, Mohammadi B, Hammer A, Dengler R, Münte TF. Movement initiation and inhibition are impaired in amyotrophic lateral sclerosis. *Exp Neurol* 2010;224:389–94. <https://doi.org/10.1016/j.expneurol.2010.04.014>.
- Thuraisingham RA, Tran Y, Boord P, Craig A. Analysis of eyes open, eye closed EEG signals using second-order difference plot. *Med Biol Eng Comput* 2007;45:1243–9. <https://doi.org/10.1007/s11517-007-0268-9>.
- Tolekis JR. Intraoperative monitoring using somatosensory evoked potentials. A position statement by the American Society of Neurophysiological Monitoring. *J Clin Monit Comput* 2005;19:241–58. <https://doi.org/10.1007/s10877-005-4397-0>.
- Tonin A, Jaramillo-Gonzalez A, Rana A, Khalili-Ardali M, Birbaumer N, Chaudhary U, et al. Auditory Electrooculogram-based Communication System for ALS Patients in Transition from Locked-in to Complete Locked-in State Manuscript:8452. *Sci Rep* 2020. <https://doi.org/10.1038/s41598-020-65333-1>.
- Toscani M, Marzi T, Righi S, Viggiano MP, Baldassi S. Alpha waves: A neural signature of visual suppression. *Exp Brain Res* 2010;207:213–9. <https://doi.org/10.1007/s00221-010-2444-7>.
- Ulanovsky N, Las L, Nelken I. Processing of low-probability sounds by cortical neurons. *Nat Neurosci* 2003;6:391–8. <https://doi.org/10.1038/nn1032>.
- Washburn MF. Movement and mental imagery: Outlines of a motor theory of the complex mental processes. Houghton Mifflin 1916.
- Waterstraat C, Fedele T, Burghoff M, Scheer HJ, Curio G. Recording human cortical population spikes non-invasively—An EEG tutorial. *J Neurosci Methods* 2015;250:74–84. <https://doi.org/10.1016/j.jneumeth.2014.08.013>.



Electroencephalography of completely locked-in state patients with amyotrophic lateral sclerosis

Yasuhisa Maruyama^{a,1}, Natsue Yoshimura^{a,b,c,d,e,*,1}, Aygul Rana^e, Azim Malekshahi^e, Alessandro Tonin^e, Andres Jaramillo-Gonzalez^e, Niels Birbaumer^f, Ujwal Chaudhary^{e,f}

^a Institute of Innovative Research, Tokyo Institute of Technology, Yokohama, Japan

^b Department of Advanced Neuroimaging, Integrative Brain Imaging Center, National Center of Neurology and Psychiatry, Tokyo, Japan

^c PRESTO, JST, Saitama, Japan

^d Neural Information Analysis Laboratories, ATR, Kyoto, Japan

^e Institute of Medical Psychology and Behavioral Neurobiology, University of Tübingen, Tübingen, Germany

^f Wyss-Center for Bio and NeuroEngineering, Geneva, Switzerland



ARTICLE INFO

Article history:

Received 7 December 2019

Received in revised form 25 January 2020

Accepted 28 January 2020

Available online 31 January 2020

Keywords:

Completely locked-in state
Amyotrophic lateral sclerosis
Electroencephalography
Resting state
Power spectral density

ABSTRACT

Patients in completely locked-in state (CLIS) due to amyotrophic lateral sclerosis (ALS) lose the control of each and every muscle of their body rendering them motionless and without any means of communication. Though some studies have attempted to develop brain-computer interface (BCI)-based communication methods with CLIS patients, little information is available of the neuroelectric brain activity of CLIS patients. However, because of the difficulties with and often loss of communication, the neuroelectric signature may provide some indications of the state of consciousness in these patients. We recorded electroencephalography (EEG) signals from 10 CLIS patients during resting state and compared their power spectral densities with those of healthy participants in fronto-central, central, and centro-parietal channels. The results showed significant power reduction in the high alpha, beta, and gamma bands in CLIS patients, indicating the dominance of slower EEG frequencies in their oscillatory activity. This is the first study showing group-level EEG change of CLIS patients, though the reason for the observed EEG change cannot be concluded without any reliable communication methods with this population.

© 2020 Elsevier B.V. and Japan Neuroscience Society. All rights reserved.

1. Introduction

Amyotrophic lateral sclerosis (ALS) is a progressive disease that affects patients' motor control. ALS patients suffer from progressing impaired motor control, and often their options for communication methods become limited. In the advanced stage of ALS called locked-in state (LIS), patients lose most voluntary body movements but still can communicate using their eye movements or any other muscular response. However, in the further advanced stage called completely locked-in state (CLIS), patients lose all muscular control including their eyes and thus all communication methods are lost, although cognitive function of CLIS patients is assumed to be functioning (Kotchoubey et al., 2003; Fuchino et al., 2008).

Some studies have attempted to establish brain-computer interface (BCI)-based communication methods with CLIS patients using brain signals such as electrocorticography (ECoG), electroencephalography (EEG), and functional Near-Infrared Spectroscopy (fNIRS) (Kübler and Birbaumer, 2008; Murguialday et al., 2011; Gallegos-Ayala et al., 2014; Okahara et al., 2018; Ardali et al., 2019; Han et al., 2019). Though some of such attempts partly succeeded in communication (Okahara et al., 2018; Han et al., 2019), it is still a quite challenging problem. Characterization of EEG in CLIS patients can assist in the development of EEG-BCI-based communication methods with CLIS patients because the knowledge of the EEG frequency characteristics is crucial in the correct selection and exclusion criteria of classification algorithms for BCIs (Nicolás-Alonso and Gomez-Gil, 2012).

Though EEG of non-late-stage ALS patients during resting state have been reported in some studies (Mai et al., 1998; Santhosh et al., 2005; Iyer et al., 2015; Jayaram et al., 2015; Fraschini et al., 2016, 2018; Nasseroleslami et al., 2019) and reviews (Kellmeyer et al., 2018; Proudfoot et al., 2019), little EEG information is available of late-stage ALS patients such as LIS and CLIS. Only one case

* Corresponding author at: Institute of Innovative Research, Tokyo Institute of Technology, R2-16, 4259, Nagatsuta-cho, Midori-ku, Yokohama, Kanagawa, 226-8503, Japan.

E-mail address: yoshimura.n.ac@m.titech.ac.jp (N. Yoshimura).

¹ These authors contributed equally to this work.

Table 1
Demographic data and EEG measurement conditions of the participants.

Participant ID	Gender	Age (years)	ALS duration (years)	Recording time (seconds)	EEG sensor positions
ALS-CLIS Patients					
P1	F	72	10	311	FC3, FC4, FC5, FC6, Cz ^a
P2	M	62	4	603	AF3, AF4, FC1 ^a , FC5 ^a , FC6 ^a , CP1 ^a , CP5 ^a , CP6 ^a
P3	F	79	7	584	FC3, FC4, FC5 ^a , FC6 ^a , Cz ^a
P4	F	26	4	487	FC1 ^a , FC2, FC5 ^a , FC6 ^a , CP1 ^a , CP2, CP5 ^a , CP6 ^a
P5	M	58	7	600	FC1 ^a , FC2, FC5 ^a , FC6 ^a , CP1 ^a , CP2, CP5 ^a , CP6 ^a
P6	M	37	8	623	FC5 ^a , FC6 ^a , C5, C6, Cz ^a , T9, T10
P7	F	56	7	753	FC3, FC4, FC5 ^a , FC6 ^a , Cz ^a
P8	F	33	6	630	FC1 ^a
P9	M	23	4	1032	F3, F4, C3, C4, Cz ^a
P10	M	25	5	641	FC5 ^a , FC6 ^a , C5, C6
Healthy Participants					
H1	M	26		684	
H2	F	29		1166	AF3, AF4, FC1 ^a , FC2, FC3, FC4,
H3	F	51		682	FC5 ^a , FC6 ^a , C5, C6, Cz ^a , CP1 ^a ,
H4 ^b	M	50	N.A. ^c	1268	CP2, CP5 ^a , CP6 ^a , Oz
H5	M	65		1258	
H6	M	49		1272	
H7	M	50		1214	

^a EEG sensors used in the analysis.

^b Data of H4 was excluded from the analysis due to recording failure and artefact contamination.

^c Not applicable.

study investigated power spectral densities (PSDs) of 2 ALS-CLIS patients (Hohmann et al., 2018). This study quantitatively reported shifts of the alpha peak frequencies in the CLIS patients toward the lower frequency ranges compared with healthy participants and ALS patients who showed ALSFRS-R (The Revised ALS Functional Rating Scale) (Cedarbaum et al., 1999) scores larger than 0. Other single case studies also reported dominance of low EEG frequencies in ALS-CLIS patients (Hayashi and Kato, 1989; Kotchoubey et al., 2003). However, group-level comparison between ALS-CLIS and healthy people has not been performed yet.

In this study, therefore, to describe the EEG characteristics of ALS-CLIS patients at group level, we investigated the resting-state PSDs of ALS-CLIS patients. The PSD analysis was performed for signals recorded from fronto-central, central, and centro-parietal sensors that could be placed over the scalp of the bedridden patients.

2. Materials and methods

The Institutional Review Boards of the Medical Faculty of the University of Tübingen and Tokyo Institute of Technology approved the study reported in this study. This study is in full compliance with the ethical practice of Medical Faculty of the University of Tübingen and follows the criteria of the Helsinki Accords. Written informed consent for this study was obtained from the patients' legal representatives and the healthy participants.

2.1. Participants

We recorded EEG signals from 10 ALS-CLIS patients and 7 healthy participants. The number of healthy participants was decided so that mean and variance of age were not significantly different in each comparison, considering the different numbers and positions of sensors between the patients due to clinical needs. Table 1 shows the demographic data and EEG measurement conditions. The mean age (standard deviation) was 47.1 (19.7) in patients and 45.7 (12.6) in healthy participants. All patients were in home care and bed-ridden, artificially ventilated and fed. CLIS was defined as inability to communicate with eye movements or any other voluntary muscle with use or non-use of eye trackers for more than 6 months. (After failure of eye-trackers caretakers tried to "read" "yes" - signals from eye or face muscles, in none of the patients any

reliable communication was possible. A detailed description of the patients can be found in Malekshahi et al., 2019). All of the patients showed regular circadian patterns of slow wave sleep and waking (Malekshahi et al., 2019).

2.2. EEG acquisition

In the EEG measurement, the CLIS patients and the healthy participants were instructed to relax, try not to think anything, and refrain from sleeping. Eyes of the CLIS patients were closed (they can only be opened actively by caretakers). Healthy participants were additionally instructed to keep their eyes closed and not to move throughout the measurement. EEG sensors were attached according to the 10–5 system, with one reference channel attached to their right mastoids. EEG signals were recorded using a V-Amp amplifier and passive electrodes (Brain Products GmbH, Gilching, Germany). In the measurement of the patients, electrooculogram (EOG), chin electromyogram (EMG), and Near-Infrared Spectroscopy (NIRS) sensors were also attached to faces and heads for other clinical and research purposes. Due to clinical needs, the numbers and positions of sensors were different between the patients, while they were identical across the healthy participants (Table 1). The EEG data were measured in the afternoon for all the CLIS patients and healthy participants to equalize their conditions in terms of the circadian rhythm. The EEG data from one of the healthy participants (H4) was excluded from the analysis due to recording failure of EEG sensors and artefact contamination.

2.3. EEG processing

EEG signals were processed using Matlab R2016b (The MathWorks, Inc., Natick, Massachusetts, U.S.A.) and EEGLAB 14.1.1 software (Delorme and Makeig, 2004). In the preprocessing, a high-pass finite impulse response (FIR) filter at 0.5 Hz and a low-pass FIR filter at 45 Hz were applied to the raw EEG signals, followed by down-sampling to 100 Hz to save computational cost. Subsequently, we extracted five 1-minute epochs (i.e., 5-minute data in total) containing minimal artefacts such as muscle activities and body movements by visual inspection.

Considering the difference of sensor positions in CLIS patients due to clinical limitation, we decided to use 7 sensors FC5, FC6, Cz, FC1, CP1, CP5, and CP6 (Table 1) for the PSD comparison analysis.

Specifically, FC5 and FC6 were used for 7 patients (patient ID: P2, P3, P4, P5, P6, P7, and P10), Cz was used for 5 patients (patient ID: P1, P3, P6, P7, and P9), FC1 was used for 4 patients (patient ID: P2, P4, P5, and P8), and CP1, CP5, and CP6 were used for 3 patients (patient ID: P2, P4, and P5). For these 7 sensors (FC5, FC6, Cz, FC1, CP1, CP5, and CP6), PSDs of these patients were compared with PSDs of all the 6 healthy participants (H1, H2, H3, H5, H6, and H7), respectively. For each sensor, PSD for each 1-minute epoch was calculated by Fast Fourier Transform (FFT) of 1-second time window with 0.25-second overlap, and each participant's PSD was obtained by averaging five 1-minute PSDs. Hann window was applied as the window function. We averaged 1185 PSDs (237 PSDs per 1-minute epoch \times 5 epochs) to get each participant's representative resting-state PSD. From the PSD, delta (1–3 Hz), theta (4–7 Hz), low alpha (8–10 Hz), high alpha (11–13 Hz), beta (14–30 Hz), and gamma (31–40 Hz) band power was calculated by averaging power in the corresponding frequencies.

2.4. Statistical analysis

Statistical tests were performed in free software R (R Core Team, 2018). Due to small sample sizes, we applied a two-tailed Wilcoxon rank sum test to test the power difference between the CLIS patients and the healthy participants for each frequency band and sensor. The obtained *p*-values were False Discovery Rate (FDR) corrected using the Benjamini-Hochberg method to compensate for the multiple comparison of 6 frequency bands and 7 sensors (Benjamini and Hochberg, 1995). Additionally, at sensors where significant difference of frequency band power was observed in the above comparison, correlation between frequency band power and ALS duration in the CLIS patients was tested based on Spearman's rank correlation coefficient for each frequency band. The obtained *p*-values were FDR corrected for the multiple comparisons (Benjamini and Hochberg, 1995).

3. Results

For each comparison the mean and the variance of age were not significantly different between the CLIS patients and the healthy participants (two-tailed *t*-test and *F*-test).

On Figs. 1A and B, we show filtered EEG time series of a representative CLIS patient (Fig. 1A) and a healthy participant (Fig. 1B) at sensor Cz. Figs. 1C and D show PSDs at Cz for the 5 CLIS patients who could use Cz for the recording (patient ID: P1, P3, P6, P7, and P9 as described above and in Table 1) and the 6 healthy participants, and their mean PSDs are compared in Fig. 1E. These figures show the dominance of slow oscillations in the CLIS patients. In the same manner, we also calculated PSDs of the other sensors (FC1, FC5, FC6, CP1, CP5, and CP6), and frequency band power of the CLIS patients and the healthy participants at all of the sensors are statistically compared and summarized in Fig. 2. Figs. 2A–F show power in the delta, theta, low alpha, high alpha, beta, and gamma bands, respectively. In the high alpha band (Fig. 2D), power between the two groups was significantly different at sensor FC5 ($p = 0.044$). In the beta and gamma bands (Figs. 2E and F), power between the two groups was significantly different at sensors FC1, FC5, FC6, and Cz ($p = 0.044, 0.016, 0.016, \text{ and } 0.030$ respectively in the beta band and $p = 0.044, 0.016, 0.024, \text{ and } 0.030$ respectively in the gamma band).

In the correlation analyses, we included only sensors FC1, FC5, FC6, and Cz because significant differences of frequency band power between the CLIS patients and the healthy participants were observed at these sensors. Relationships between frequency band power and ALS duration in the CLIS patients at these 4 sensors are depicted in Figs. 3A–F. Spearman's rank correlation coefficients at sensors FC1, FC5, FC6, and Cz were $-0.32,$

$0.17, -0.24, \text{ and } -0.82$ respectively in the delta band, $-0.32, -0.37, -0.71, \text{ and } -0.87$ respectively in the theta band, $-0.63, -0.51, -0.88, \text{ and } -0.46$ respectively in the low alpha band, $-0.95, -0.51, -0.88, \text{ and } -0.46$ respectively in the high alpha band, $-0.95, -0.75, -0.73, \text{ and } -0.46$ respectively in the beta band, and $-0.95, 0.15, -0.47, \text{ and } -0.41$ respectively in the gamma band. No correlation coefficients were statistically significant after FDR correction.

4. Discussion

We investigated resting-state EEG of ALS-CLIS patients to provide insight into their electric brain activities and possible state of consciousness. The CLIS patients showed significant power decrease in the high alpha band at sensor FC5 and in the beta and gamma bands at sensors FC1, FC5, FC6, and Cz. This group-level comparison using EEG data of CLIS patients and healthy participants demonstrated clear EEG power differences.

Different state of consciousness and arousal is the most discussed reason for the power decrease in the alpha and beta bands. Patients with Alzheimer's dementia show a decrease of the absolute power in the alpha and beta bands together with an increase in the delta and theta bands in comparison with healthy participants during eyes-closed resting state (Pucci et al., 1998). Some ALS patients may also show cognitive impairment in various domains such as executive function, language, and fluency (Phukan et al., 2007; Raaphorst et al., 2010; Goldstein and Abrahams, 2013; Beeldman et al., 2016). Mild cognitive deficits are more frequently observed in the advanced stage of ALS than in the early stage (Crockford et al., 2018). However, there is also a report with LIS patients suffering from ALS who showed no signs of cognitive decline during testing using an eye-tracking system (Linse et al., 2017). None of the studies cited here found a significant relationship between the reduction of band power and cognitive performance. At present, testing of cognitive capacities becomes increasingly difficult with progressing paralysis and finally impossible in LIS and CLIS. Thus, any conclusion about such a relationship remains highly speculative. However, a decreased state of central arousal during waking seems plausible associated with the complete immobility and consequent deprivation of environmental stimulation.

There are inconsistent reports about the relationship between the decrease of the gamma band power and cognitive impairment. Herrmann and Demiralp suggested relationship between the alteration of the gamma band activity and disturbed cognitive function (Herrmann and Demiralp, 2005), while van Deursen et al. reported that patients with Alzheimer's dementia showed power increase in the gamma band during eye-open resting state in comparison with healthy participants (van Deursen et al., 2008). In comparison with healthy people, we should not ignore the effect of absence of muscle activities in CLIS patients because high frequency bands such as the gamma band are easily contaminated by muscle activities (Pope et al., 2009). Though we instructed the healthy participants not to move during the EEG recordings, the decrease of the gamma band power in the CLIS patients in comparison with the healthy participants can be partly due to the loss of muscle activity. Accordingly, it is premature to associate the gamma band power reduction with cognitive impairment without reliable findings from a cognitive testing procedure.

Another reason for the power decrease in the alpha band could be reduced vigilance and outward attention, since the alpha peak frequency is suggested to be associated with the activities in brain regions modulating attention in healthy people (Jann et al., 2010). The "extinction of goal-directed thinking" hypothesis formulated by Kübler and Birbaumer predicts the reduction of arousability and vigilance in CLIS patients due to suppressed social-cognitive inter-

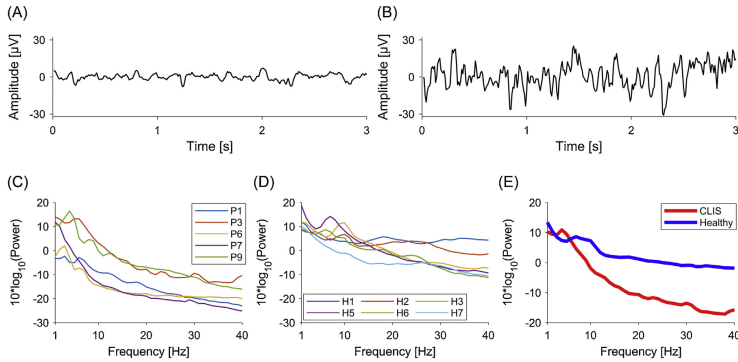


Fig. 1. EEG time series and power spectral densities of the CLIS patients and the healthy participants at sensor Cz. (A) EEG of a CLIS patient (P1). (B) EEG of a healthy participant (H3). (C) PSDs of the 5 CLIS patients (P1, P3, P6, P7, and P9). (D) PSDs of the 6 healthy participants (H1, H2, H3, H5, H6, and H7). (E) Mean PSDs of the 5 CLIS patients and the 6 healthy participants.

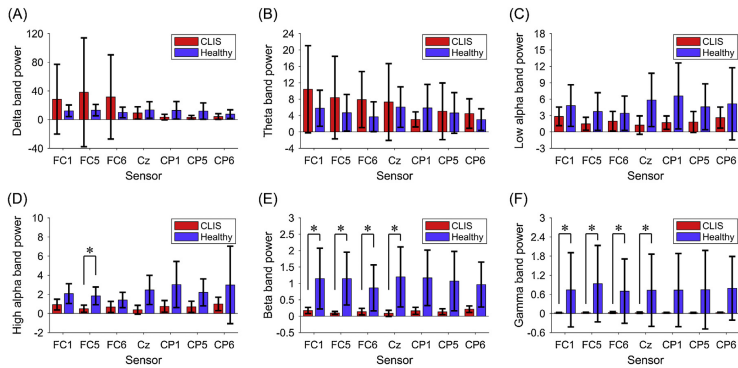


Fig. 2. Mean frequency band power at sensors FC1, FC5, FC6, Cz, CP1, CP5, and CP6. Error bars represent standard deviations. Significant power differences between the CLIS patients and the healthy participants in two-tailed Wilcoxon rank sum test with False Discovery Rate correction are marked: * $p < 0.05$. (A) Delta band (1–3 Hz). (B) Theta band (4–7 Hz). (C) Low alpha band (8–10 Hz). (D) High alpha band (11–13 Hz). (E) Beta band (14–30 Hz). (F) Gamma band (31–40 Hz).

action (Kübler and Birbaumer, 2008). However, it is also impossible to affirm a reduced vigilance and outward attention in CLIS patients without any existing behavioral evidence. To investigate the attentional and cognitive function in CLIS patients and their relationship with the EEG characteristics, functioning BCI systems allowing more flexible communication than simple yes/no responses are necessary (Ardali et al., 2019).

Both, the decrease of the alpha and gamma band power may be in part due to loss of motor control. Most EEG-based BCIs use power changes in the alpha band in accordance with preparation and start and stop of imagined or executed body movements. These phenomena are called event-related desynchronization (ERD) for movement and event-related synchronization (ERS) for stopping movements, and are commonly observed in EEG signals recorded from central area (Pfurtscheller and Aranibar, 1979). Although the exact neuro-physiological mechanisms of the phenomena have not

been clarified yet, CLIS patients may have less neural activation in the motor related areas, which may be related to the power decrease in the alpha band. Gamma band power is also reported to be involved in action execution in studies using ECoG (Pistohl et al., 2008; Nakanishi et al., 2013; Babiloni et al., 2016). On the other hand, some BCI studies reported that LIS and non-late-stage ALS patients succeeded in controlling a speller or a web browser using neuronal signals from intracortical electrodes placed in the hand area of dominant motor cortex (Vansteensel et al., 2016; Pandarinath et al., 2017; Nuyujukian et al., 2018). Considering the success of the BCI-use in these studies, the power decrease in the frequency bands may just indicate shifts of alpha frequency to lower frequencies such as theta or delta, which has been suggested in previous studies (Hohmann et al., 2018; Malekshahi et al., 2019). Our results may also indicate this tendency of a shift of alpha as shown in Fig. 1.

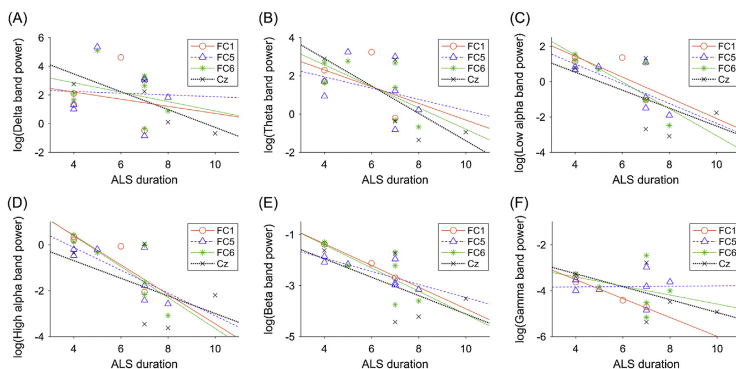


Fig. 3. Scatter plot of ALS duration and frequency band power at sensors FC1, FC5, FC6, and Cz. Red circles, blue triangles, green stars, and black crosses represent individual patients' data for FC1, FC5, FC6, and Cz, respectively. The corresponding lines represent linear approximation calculated by a least-squares method. (A) Delta band (1–3 Hz). Spearman's correlation coefficients (ρ s) were -0.32 , 0.17 , -0.24 , and -0.82 at sensors FC1, FC5, FC6, and Cz respectively. (B) Theta band (4–7 Hz). ρ s were -0.32 , -0.37 , -0.71 , and -0.87 at sensors FC1, FC5, FC6, and Cz respectively. (C) Low alpha band (8–10 Hz). ρ s were -0.63 , -0.51 , -0.88 , and -0.46 at sensors FC1, FC5, FC6, and Cz respectively. (D) High alpha band (11–13 Hz). ρ s were -0.95 , -0.51 , -0.88 , and -0.46 at sensors FC1, FC5, FC6, and Cz respectively. (E) Beta band (14–30 Hz). ρ s were -0.95 , -0.75 , -0.73 , and -0.46 at sensors FC1, FC5, FC6, and Cz respectively. (F) Gamma band (31–40 Hz). ρ s were -0.95 , 0.15 , -0.47 , and -0.41 at sensors FC1, FC5, FC6, and Cz respectively.

We calculated the correlation coefficients between the EEG power and the disease duration. Though we found no significant correlation in this study and it is difficult to reach a conclusion with such a limited number of patients, the frequency band power at most sensors tended to decrease as the ALS duration was long. In addition to the disease duration, other factors such as progression rate of the disease, age, and medication may be responsible for such hypothetical relationships with the demonstrated power reduction. An important factor affecting the difference between CLIS patients and healthy participants may result from artificial respiration over extensive time periods, a rule in CLIS patients. Hyperventilation as well as hypoventilation is strongly related with EEG-slowing (Hoshi et al., 1999). However, both, long-term hyperventilation and lack of oxygen lasting minutes or more, are causing reduced central and subjective arousal and are thus compatible with our conclusion of lowered arousal level in CLIS. If resting-state EEG of ALS patients progressing toward CLIS can be recorded longitudinally before and after artificial respiration, it will reveal the relationship between the EEG power and ALS progression and respiration-related changes. Furthermore, if ALS patients would use a BCI-based communication method already in the early stage of the disease, the BCI-use might play a role as a device to prevent the power decrease in the higher frequency bands due to continued cognitive demands and increased environmental stimulation. For stroke patients, an ERD-based BCI has been used as a rehabilitation to restore or reorganize their neural processing for their partially paralyzed body (Ramos-Murguialday et al., 2013). To investigate whether the use of BCI-based communication has the effect of preventing the power decreases and/or changing subjective arousal and activation in ALS patients, studies applying BCI for ALS patients from the early stage are needed. In addition, although the population of CLIS is small, a study with more CLIS patients in comparison with non-late-stage ALS patients is necessary to further quantify their EEG signatures.

In conclusion, this study showed altered oscillatory brain activities of CLIS patients compared with healthy participants. We found significant power decrease in the high alpha, beta, and gamma bands at fronto-central and/or central channels in the CLIS patients

suggesting reduced central arousal. We think the observed EEG change may indicate a shift of the alpha band toward lower frequencies. This overall slowing may indicate a different state of vigilance and attention and may not allow the application of comparable cognitive tasks as in healthy subjects for which most BCI paradigms were developed. Thus, BCIs that entail tasks that seem difficult for LIS and CLIS patients should be replaced. In addition, many BCIs that rely on the classification of ERD/ERS using the defined frequency band of 8–15 Hz will not function because in LIS and CLIS frequency bands below 8 Hz seem to be relevant. Changes of the target frequencies may be needed because the target brain activities may be represented in the slower frequency ranges in CLIS patients. Further investigation using longitudinal recordings and use of BCIs are required to clarify the effect of BCI-use as a rehabilitation method and if the power decrease correlates with loss of motor control, cognitive changes, reduced vigilance, and/or emergency treatment effects such as artificial respiration and feeding.

Author contributions

NY, NB, and UC conceptualized and designed the study. AR, AM, AT, AJ, and UC collected the data. YM performed analysis. NY supervised analysis. YM, NY, NB, and UC wrote the manuscript. All authors read and approved the final manuscript.

Declaration of Competing Interest

The authors declare no conflicts of interest.

Acknowledgements

We thank the CLIS patients, their families, caretakers, and the healthy participants for the participation. This work was supported in part by Tokyo Tech World Research Hub Initiative from Tokyo Institute of Technology, Japan Society for the Promotion of Science and DAAD under the Japan-Germany Research Cooperative Program [grant number JSPSJP 120193510], Japan Society for the

Promotion of Science, KAKENHI [grant number 17H05903], Japan Science and Technology Agency PRESTO (Precursory Research for Embryonic Science and Technology) [grant number JPMJPR17JA], Deutsche Forschungsgemeinschaft (DFG, Kosellek), DFG [grant number BI 195/77-1], BMBWF (German Ministry of Education and Research) [grant number 16SV7701] CoMiCon, LUMINOUS-H2020-FETOPEN-2014-2015-RIA [grant number (686764)], Wyss Center for Bio and Neuroengineering, Geneva, 9. DAAD (German Academic Exchange Service: Japanese-German Exchange program)

References

- Ardali, M.K., Rana, A., Purmohammad, M., Birbaumer, N., Chaudhary, U., 2019. Semantic and BCI-performance in completely paralyzed patients: possibility of language attrition in completely locked-in syndrome. *Brain Lang.* 194, 93–97. <http://dx.doi.org/10.1016/j.bandl.2019.05.004>.
- Babiloni, C., Del Percio, C., Vecchio, F., Sebastiani, F., Di Genaro, G., Quarato, P.P., Morace, R., Pavone, L., Soricelli, A., Noce, G., Esposito, V., Rossini, P.M., Gallese, V., Mirabella, G., 2016. Alpha, beta and gamma electroencephalographic rhythms in somatosensory motor, premotor and prefrontal cortical areas differ in movement execution and observation in humans. *Clin. Neurophysiol.* 127, 641–654. <http://dx.doi.org/10.1016/j.clinph.2015.04.068>.
- Beeldman, E., Raaphorst, J., Klein Twennaar, M., de Visser, M., Schmand, B.A., de Haan, R.J., 2016. The cognitive profile of ALS: a systematic review and meta-analysis update. *J. Neurol. Neurosurg. Psychiatry* 87, 611–619. <http://dx.doi.org/10.1136/jnnp-2015-510734>.
- Benjamini, Y., Hochberg, Y., 1995. Controlling the false discovery rate: a practical and powerful approach to multiple testing. *J. R. Stat. Soc. Ser. B* 57, 289–300.
- Cedarbaum, J.M., Stambler, N., Malta, E., Fuller, C., Hilt, D., Thurmond, B., Nakanishi, A., 1999. The ALSFRS-R: a revised ALS functional rating scale that incorporates assessments of respiratory function. *J. Neurol. Sci.* 169, 13–21. [http://dx.doi.org/10.1016/S0022-510X\(99\)00210-5](http://dx.doi.org/10.1016/S0022-510X(99)00210-5).
- Crockford, C., Newton, J., Lonergan, K., Chivera, T., Booth, T., Chandran, S., Colville, S., Heverin, M., Mays, L., Pal, S., Pender, N., Pinto-Grau, M., Radakovic, R., Shaw, C.E., Stephenson, L., Swinger, R., Vajda, A., Al-Chalabi, A., Hardiman, O., Abrahams, S., 2018. ALS-specific cognitive and behavioral changes associated with advancing disease stage in ALS. *Neurology* 91, e1370–e1380. <http://dx.doi.org/10.1212/WNL.00000000000006317>.
- Delorme, A., Makeig, S., 2004. EEGLAB: an open source toolbox for analysis of single-trial EEG dynamics including independent component analysis. *J. Neurosci. Methods* 134, 9–21. <http://dx.doi.org/10.1016/j.jneumeth.2003.10.093>.
- Fraschini, M., Demuru, M., Hillebrand, A., Cuccu, L., Porcu, S., Di Stefano, F., Puligheddu, M., Floris, G., Borghero, G., Marrosu, F., 2016. EEG functional network topology is associated with disability in patients with amyotrophic lateral sclerosis. *Sci. Rep.* 6, 38653. <http://dx.doi.org/10.1038/srep38653>.
- Fraschini, M., Lai, M., Demuru, M., Puligheddu, M., Floris, G., Borghero, G., Marrosu, F., 2018. Functional brain connectivity analysis in amyotrophic lateral sclerosis: an EEG source-space study. *Biomed. Phys. Eng. Express* 4, 037004. <http://dx.doi.org/10.1088/2057-1976/aa9c64>.
- Fuchino, Y., Nagao, M., Katura, T., Bando, M., Naito, M., Maki, A., Nakamura, K., Hayashi, H., Koizumi, H., Yoro, T., 2008. High cognitive function of an ALS patient in the totally locked-in state. *Neurosci. Lett.* 435, 85–89. <http://dx.doi.org/10.1016/j.neulet.2008.01.046>.
- Gallejos-Ayala, G., Furdea, A., Takano, K., Ruf, C.A., Flor, H., Birbaumer, N., 2014. Brain communication in a completely locked-in patient using bedside near-infrared spectroscopy. *Neurology* 82, 1930–1932. <http://dx.doi.org/10.1212/WNL.0000000000000449>.
- Goldstein, L.H., Abrahams, S., 2013. Changes in cognition and behavior in amyotrophic lateral sclerosis: nature of impairment and implications for assessment. *Lancet Neurol.* 12, 368–380. [http://dx.doi.org/10.1016/S1473-4422\(13\)70026-7](http://dx.doi.org/10.1016/S1473-4422(13)70026-7).
- Han, C.-H., Kim, Y.-W., Kim, D.Y., Kim, S.H., Nenadic, Z., Im, C.-H., 2019. Electroencephalography-based endogenous brain-computer interface for online communication with a completely locked-in patient. *J. Neuroeng. Rehabil.* 16, 18. <http://dx.doi.org/10.1186/s12984-019-0493-0>.
- Hayashi, H., Kato, S., 1989. Total manifestation of amyotrophic lateral sclerosis: ALS in the totally locked-in state. *J. Neurol. Sci.* 93, 19–35. [http://dx.doi.org/10.1016/0022-510X\(89\)90158-5](http://dx.doi.org/10.1016/0022-510X(89)90158-5).
- Herrmann, C.S., Demiralp, T., 2005. Human EEG gamma oscillations in neuropsychiatric disorders. *Clin. Neurophysiol.* 116, 2719–2733. <http://dx.doi.org/10.1016/j.clinph.2005.07.007>.
- Hohmann, M.R., Fomina, T., Jayaram, V., Emde, T., Just, J., Synofzik, M., Schölkopf, B., Schöls, L., Grosse-Wentrup, M., 2018. Case series: slowing alpha rhythm in late-stage ALS patients. *Clin. Neurophysiol.* 129, 406–408. <http://dx.doi.org/10.1016/j.clinph.2017.11.013>.
- Hoshi, Y., Okuhara, H., Nakane, S., Hayakawa, K., Kobayashi, N., Kajii, N., 1999. Re-evaluation of the hypoxia theory as the mechanism of hyperventilation-induced EEG slowing. *Pediatr. Neurol.* 21, 638–643. [http://dx.doi.org/10.1016/S0887-8994\(99\)00063-6](http://dx.doi.org/10.1016/S0887-8994(99)00063-6).
- Iyer, P.M., Egan, C., Pinto-Grau, M., Burke, T., Elamin, M., Nasserollesami, B., Pender, N., Lalor, E.C., Hardiman, O., 2015. Functional connectivity changes in resting-state EEG as potential biomarker for amyotrophic lateral sclerosis. *PLoS One* 10, e0128682. <http://dx.doi.org/10.1371/journal.pone.0128682>.
- Jann, K., Koenig, T., Dietts, T., Boesch, C., Federspiel, A., 2010. Association of individual resting state EEG alpha frequency and cerebral blood flow. *Neuroimage* 51, 365–372. <http://dx.doi.org/10.1016/j.neuroimage.2010.02.024>.
- Jayaram, V., Widmann, N., Förster, C., Fomina, T., Hohmann, M., von Hagen, J.M., Synofzik, M., Schölkopf, B., Schöls, L., Grosse-Wentrup, M., 2015. Brain-computer interfacing in amyotrophic lateral sclerosis: implications of a resting-state EEG analysis. 2015 37th Annual International Conference of the IEEE Engineering in Medicine and Biology Society (EMBC), 6979–6982. <http://dx.doi.org/10.1109/EMBC.2015.7319998>.
- Kellmeyer, P., Grosse-Wentrup, M., Schulze-Bonhage, A., Ziemann, U., Ball, T., 2018. Electrophysiological correlates of neurodegeneration in motor and non-motor brain regions in amyotrophic lateral sclerosis—implications for brain-computer interfacing. *J. Neural Eng.* 15, 041003. <http://dx.doi.org/10.1088/1741-2552/aa8f55>.
- Kotchoubey, B., Lang, S., Winter, S., Birbaumer, N., 2003. Cognitive processing in completely paralyzed patients with amyotrophic lateral sclerosis. *Eur. J. Neurol.* 10, 551–558. <http://dx.doi.org/10.1046/j.1468-1331.2003.00647.x>.
- Kübler, A., Birbaumer, N., 2008. Brain-computer interfaces and communication in paralysis: extinction of goal directed thinking in completely paralyzed patients. *Prog. Clin. Neurophysiol.* 119, 2658–2666. <http://dx.doi.org/10.1016/j.clinph.2008.06.019>.
- Linse, K., Rieger, W., Joos, M., Schmitz-Peiffer, H., Storch, A., Herrmann, A., 2017. Eye-tracking-based assessment suggests preserved well-being in locked-in patients. *Ann. Neurol.* 81, 310–315. <http://dx.doi.org/10.1002/ana.24871>.
- Mai, R., Facchetti, D., Micheli, A., Poloni, M., 1998. Quantitative electroencephalography in amyotrophic lateral sclerosis. *Electroencephalogr. Clin. Neurophysiol.* 106, 383–386. [http://dx.doi.org/10.1016/S0013-4694\(97\)00159-4](http://dx.doi.org/10.1016/S0013-4694(97)00159-4).
- Malekshahi, A., Chaudhary, U., Jaramillo-Gonzalez, A., Lucas Luna, A., Rana, A., Tonin, A., Birbaumer, N., Gais, S., 2019. Sleep in the completely locked-in state (CLIS) in amyotrophic lateral sclerosis. *Sleep* 42, zsz185. <http://dx.doi.org/10.1093/sleep/zsz185>.
- Murguialday, A.R., Hill, J., Bensch, M., Martens, S., Halder, S., Nijboer, F., Schoelkopf, B., Birbaumer, N., Charabagh, A., 2011. Transition from the locked in to the completely locked-in state: a physiological analysis. *Clin. Neurophysiol.* 122, 925–933. <http://dx.doi.org/10.1016/j.clinph.2010.08.019>.
- Nakanishi, Y., Yanagisawa, T., Shin, D., Fukuma, R., Chen, C., Kambara, H., Yoshimura, N., Hirata, M., Yoshimie, T., Koike, Y., 2013. Prediction of three-dimensional arm trajectories based on ECoG signals recorded from human sensorimotor cortex. *PLoS One* 8, e72085. <http://dx.doi.org/10.1371/journal.pone.0072085>.
- Nasserollesami, B., Dukic, S., Broderick, M., Mohr, K., Schuster, C., Gavin, B., McLaughlin, R., Heverin, M., Vajda, A., Iyer, P.M., Pender, N., Bede, P., Lalor, E.C., Hardiman, O., 2019. Characteristic increases in EEG connectivity correlate with changes of structural MRI in amyotrophic lateral sclerosis. *Cereb. Cortex* 29, 27–41. <http://dx.doi.org/10.1093/cercor/bhx301>.
- Nicolas-Alonso, L.F., Gomez-Gil, J., 2012. Brain computer interfaces, a review. *Sensors* 12, 1211–1279. <http://dx.doi.org/10.3390/s120201211>.
- Nuyujukian, P., Alberts Sarabathi, J., Saab, J., Pandarinath, C., Jarosiewicz, B., Blabe, C.H., Franco, B., Merhoff, S.T., Eskandar, E.N., Simeral, J.D., Hochberg, L.R., Shenoy, K.V., Henderson, J.M., 2018. Cortical control of a tablet computer by people with paralysis. *PLoS One* 13, e0204566. <http://dx.doi.org/10.1371/journal.pone.0204566>.
- Okahara, Y., Takano, K., Nagao, M., Kondo, K., Iwade, Y., Birbaumer, N., Kansaku, K., 2018. Long-term use of a neural prosthesis in progressive paralysis. *Sci. Rep.* 8, 16787. <http://dx.doi.org/10.1038/s41598-018-35211-y>.
- Pandarinath, C., Nuyujukian, P., Blabe, C.H., Sonice, B.L., Saab, J., Willett, F.R., Hochberg, L.R., Shenoy, K.V., Henderson, J.M., 2017. High performance communication by people with paralysis using an intracortical brain-computer interface. *Elife* 6, e18554. <http://dx.doi.org/10.7554/eLife.18554>.
- Plurtscheller, G., Aranibar, A., 1979. Evaluation of event-related desynchronization (ERD) preceding and following voluntary self-paced movement. *Electroencephalogr. Clin. Neurophysiol.* 46, 138–146. [http://dx.doi.org/10.1016/0013-4694\(79\)90063-4](http://dx.doi.org/10.1016/0013-4694(79)90063-4).
- Phukan, J., Pender, N.P., Hardiman, O., 2007. Cognitive impairment in amyotrophic lateral sclerosis. *Lancet Neurol.* 6, 994–1003. [http://dx.doi.org/10.1016/S1473-4422\(07\)70265-X](http://dx.doi.org/10.1016/S1473-4422(07)70265-X).
- Pistohl, T., Ball, T., Schulze-Bonhage, A., Aertsen, S., Mehring, C., 2008. Prediction of arm movement trajectories from ECoG-recordings in humans. *J. Neurosci. Methods* 167, 105–114. <http://dx.doi.org/10.1016/j.jneumeth.2007.10.001>.
- Pope, K.J., Fitzgibbon, S.P., Lewis, T.W., Whitham, E.M., Willoughby, J.O., 2009. Relation of gamma oscillations in scalp recordings to muscular activity. *Brain Topogr.* 22, 13–17. <http://dx.doi.org/10.1007/s10548-009-0081-x>.
- Proudfoot, M., Bede, P., Turner, M.R., 2019. Imaging cerebral activity in amyotrophic lateral sclerosis. *Front. Neurol.* 9, 1148. <http://dx.doi.org/10.3389/fneur.2018.01148>.
- Pucci, E., Cacchiò, G., Angeloni, R., Belardinelli, N., Nolfi, G., Signorino, M., Angeleri, F., 1998. EEG spectral analysis in Alzheimer's disease and different degenerative dementias. *Arch. Gerontol. Geriatr.* 26, 283–297. [http://dx.doi.org/10.1016/S0167-4943\(98\)00012-0](http://dx.doi.org/10.1016/S0167-4943(98)00012-0).
- R Core Team, 2018. R: A Language and Environment for Statistical Computing. R Foundation for Statistical Computing, Vienna, Austria. <https://www.R-project.org/>.
- Raaphorst, J., de Visser, M., Linszen, W.H.J.P., de Haan, R.J., Schmand, B., 2010. The cognitive profile of amyotrophic lateral sclerosis: a meta-analysis. *Amyotroph. Later. Scler.* 11, 27–37. <http://dx.doi.org/10.13109/17482960802645008>.

- Ramos-Murguialday, A., Broetz, D., Rea, M., Läer, L., Yilmaz, Ö., Brasil, F.L., Liberati, G., Curado, M.R., García-Cossío, E., Vyziotis, A., Cho, W., Agostini, M., Soares, E., Soekadar, S., Caria, A., Cohen, L.G., Birbaumer, N., 2013. Brain-machine interface in chronic stroke rehabilitation: a controlled study. *Ann. Neurol.* 74, 100–108, <http://dx.doi.org/10.1002/ana.23879>.
- Santhosh, J., Bhatia, M., Sahu, S., Anand, S., 2005. Decreased electroencephalogram alpha band [8–13 Hz] power in amyotrophic lateral sclerosis patients: a study of alpha activity in an awake relaxed state. *Neurol. India* 53, 99–101, <http://dx.doi.org/10.4103/0028-3886.15071>.
- van Deursen, J.A., Vuurman, E.F.P.M., Verhey, F.R.J., van Kranen-Mastenbroek, V.H.J.M., Riedel, W.J., 2008. Increased EEG gamma band activity in Alzheimer's disease and mild cognitive impairment. *J. Neural Transm.* 115, 1301–1311, <http://dx.doi.org/10.1007/s00702-008-0083-y>.
- Vansteensel, M.J., Pels, E.G.M., Bleichner, M.G., Branco, M.P., Denison, T., Freudenburg, Z.V., Gosselaar, P., Leinders, S., Ottens, T.H., Van Den Boom, M.A., Van Rijen, P.C., Aarnoutse, E.J., Ramsey, N.F., 2016. Fully implanted brain-computer interface in a locked-in patient with ALS. *N. Engl. J. Med.* 375, 2060–2066, <http://dx.doi.org/10.1056/NEJMoa1608085>.



EEG power spectral density in locked-in and completely locked-in state patients: a longitudinal study

Arianna Secco¹ · Alessandro Tonin² · Aygul Rana³ · Andres Jaramillo-Gonzalez³ · Majid Khalili-Ardali³ · Niels Birbaumer³ · Ujwal Chaudhary^{2,3}

Received: 1 March 2020 / Revised: 14 August 2020 / Accepted: 30 September 2020
© The Author(s) 2020

Abstract

Persons with their eye closed and without any means of communication is said to be in a completely locked-in state (CLIS) while when they could still open their eyes actively or passively and have some means of communication are said to be in locked-in state (LIS). Two patients in CLIS without any means of communication, and one patient in the transition from LIS to CLIS with means of communication, who have Amyotrophic Lateral Sclerosis were followed at a regular interval for more than 1 year. During each visit, resting-state EEG was recorded before the brain–computer interface (BCI) based communication sessions. The resting-state EEG of the patients was analyzed to elucidate the evolution of their EEG spectrum over time with the disease’s progression to provide future BCI-research with the relevant information to classify changes in EEG evolution. Comparison of power spectral density (PSD) of these patients revealed a significant difference in the PSD’s of patients in CLIS without any means of communication and the patient in the transition from LIS to CLIS with means of communication. The EEG of patients without any means of communication is devoid of alpha, beta, and higher frequencies than the patient in transition who still had means of communication. The results show that the change in the EEG frequency spectrum may serve as an indicator of the communication ability of such patients.

Keywords Resting-state electroencephalogram (EEG) · Completely locked-in state (CLIS) · LIS (locked-in state) · Power spectrum density (PSD) · Alpha frequency

Introduction

The cardinal feature of a patient in a locked-in state (LIS) is paralysis of most of the voluntary motor function of the body except the oculomotor function with preserved consciousness (Bauer et al. 1979; Chaudhary et al. 2020a). Because of the preserved oculomotor function and

consciousness (Schnakers et al. 2008), patients in LIS have several means of communication (Birbaumer et al. 1999; Wolpaw and McFarland 2004; Kübler et al. 2005; Sellers et al. 2010; Lesenfants et al. 2014; Wolpaw et al. 2018; Tonin et al. 2020). A patient can be in LIS because of the severe brain injury or pontine stroke (Sacco et al. 2008; Sarà et al. 2018; Pistoia et al. 2010; Conson et al. 2010), or progressive neurodegenerative motor neuron disorders (Birbaumer 2006; Birbaumer et al. 2012; Chaudhary et al. 2015, 2016a, b). Amyotrophic lateral sclerosis (ALS) is a severe of all progressive neurodegenerative disorder leading to complete paralysis with symptoms involving both upper and lower motor neurons (Rowland and Shneider 2001). Like any other LIS patient, an ALS patient in LIS are paralyzed with preserved voluntary eye movement control, eye blinks or twitching of other muscles, and intact consciousness. The LIS is not a final state for a patient who has ALS. As the disorder progresses, ALS leads to a state of complete paralysis, including eye movements, transferring patients to the completely locked-in state (CLIS)

Electronic supplementary material The online version of this article (<https://doi.org/10.1007/s11571-020-09639-w>) contains supplementary material, which is available to authorized users.

✉ Ujwal Chaudhary
chaudharyujwal@gmail.com

¹ Department of Information Engineering, Bioengineering, Università Degli Studi di Padova, Padua, Italy

² Wyss-Center for Bio- and Neuro-Engineering, Chemin de Mines 9, 1202 Geneva, Switzerland

³ Institute of Medical Psychology and Behavioral Neurobiology, University of Tübingen, Tübingen, Germany

(Bauer et al. 1979; Chaudhary et al. 2020a). The transition from LIS to CLIS is usually a gradual process that is patient specific. During this transition phase from LIS to CLIS, the patient starts losing their eye movement control and ultimately losing the ability to open their eyes is lost. In all, the patients in CLIS have their eyes closed all the time, even in the CLIS, patients are assumed to preserve their cognitive functions (Kübler and Birbaumer 2008).

Many studies have compared electrophysiological signatures from ALS patients and controls (Jayaram et al. 2015; Nasserroleslami et al. 2019; Dukic et al. 2019; Maruyama et al. 2020), reporting features distinguishing the two groups. The most reliable evidence found is a decrease in alpha relative power, with a shift of the peak in the alpha frequency band (generally present in healthy patients' EEG power spectrum) to lower frequencies (Mai et al. 1998; Hohmann et al. 2018). Several other studies with a different patient population such as depression (Goshvarpour and Goshvarpour 2019), Alzheimer's disease (Nobukawa et al. 2019), stress (Subhani et al. 2018), autism (Gabard-Durnam et al. 2019), epilepsy (Myers and Kozma 2018) and Parkinson's disease (Yi et al. 2017) have shown a difference in EEG spectral power, fractal change, power correlation and complexity of resting-state EEG as compared with the healthy participants (Buiza et al. 2018). However, how these features and biomarkers evolve during the ALS progression, reaching a state where they separate patients in different stages of the disease, is still unclear.

This study aims to perform a longitudinal analysis of EEG frequency in three ALS patients, analyzing how the power spectral densities of EEG resting-state recordings evolve in each patient. Two out of three patients considered here are in CLIS (P6 and P9), while the third patient was first in the transition from LIS to CLIS (P11) and, ultimately, in CLIS. The decrease in relative alpha band power is registered in LIS and CLIS patients with respect to controls (Babiloni et al. 2010) (Maruyama et al. 2020), but a direct comparison between these states is still missing. Investigating whether these conditions differ from the electrophysiological point of view can help understand the effects of the transition and possibly monitor the patients for BCI use. In addition, an earlier report on several CLIS patients (Maruyama et al. 2020) needs replication, finding a reduction of higher frequencies in CLIS in a one-session protocol. Whether such a change in spontaneous EEG frequency spectrums indicates functional changes in the central nervous system is now a question of further investigations.

Materials and methods

The Internal Review Board of the Medical Faculty of the University of Tübingen approved the experiment reported in this study. The study was performed per the guideline established by the Medical Faculty of the University of Tübingen and Helsinki declaration. The patient or the patients' legal representative gave informed consent. The clinical trial registration number is ClinicalTrials.gov Identifier: NCT02980380.

Patients

The patients chosen for this study were selected from the available database if the EEG resting-state recordings were in a sufficient number for a longitudinal comparison and covering a time range of at least 1 year. Table 1 lists the most relevant clinical information for each patient and the dates of the acquired EEG recordings.

EEG data acquisition

EEG resting-state recordings were acquired during visits to the patients for BCI experiments before the experimental sessions started. From now on, "visits" refers to a period of several subsequent days in which acquisitions were performed. Usually, a single visit lasted for 4 to 5 days, and two subsequent visits were at least 30 days apart from each other.

During the resting state recordings, patients were lying in their beds, being instructed to relax. EEG electrodes were attached according to the 10-5 system, with reference and ground channels placed respectively to their right mastoid and the forehead. EEG signals were recorded using a V-Amp amplifier and active electrodes (Brain Products, Germany). The numbers and positions of electrodes were different between patients and visits due to clinical and experimental needs, as outlined in Supplementary Table 1.

EEG preprocessing

EEG data were processed using Matlab R2018_b (The MathWorks, Inc., Natick, Massachusetts, U.S.A.) and EEGLAB 14.1.1 (Delorme and Makeig 2004). First, a windowed band-pass filter at 0.5 to 45 Hz was applied to the raw EEG data, followed by down-sampling to 128 Hz. Data were then cleaned from the ocular signal by removing the artifacts using the AAR plug-in (Gómez-Herrero et al. 2006) of EEGLAB. The AAR toolbox process EEG data by first decomposing the time series into spatial components using a Blind Source Separation (BSS) algorithm, then identifying the artifactual components and finally

Table 1 List of patients—the table lists for each patient the respective ID, the age and gender, the ALS type diagnosed, a short report of the progression of the disease, and the month and year of visits

Patient ID	Birthday/sex	ALS type	Medical history	Resting state data acquisition date
P6	40/M	Bulbar	2009: Diagnosis	May 2017
			Sept 2010: Percutaneous feeding and artificial ventilation	September 2017
			Dec 2010: Lost speech and walk	April 2018
			2012: Transition to CLIS	May 2018
P9	24/M	Juvenile	2013: Diagnosis	January 2019
			Aug 2014: Percutaneous feeding and artificial ventilation	June 2017
			2016: Transition to CLIS	November 2017
				March 2018
P11	35/M	Non-bulbar	Aug 2015: Diagnosis	June 2018
			Dec 2015: Lost of speech and walk	May 2018
			Jul 2016: Percutaneous feeding and artificial ventilation	August 2018
			March 2019: Transition to CLIS	September 2018
				November 2018
				December 2018
				January 2019
				February 2019
				March 2019
	August 2019			
	September 2019			

reconstructing the signals using the non-artifactual components. For this study, the decomposition in independent components was obtained through second-order blind identification (SOBI) algorithm (Belouchrani et al. 1997), and artifactual components were automatically identified based on the value of the fractal dimension of the waveform (Gómez-Herrero et al. 2006). In particular, each EEG recording (comprehensive of all the channels acquired) was processed on sliding windows of 180 s, with an overlap period equal to 60 s, and the components with smaller fractal dimensions were selected as artifactual as they correspond to the ones with less low-frequency components. After ocular artifacts rejection was applied singularly to each EEG resting-state record on the complete set of channels, the Cz channel was selected for further analysis.

PSD was obtained through Welch's overlapped segments averaging estimator, using windows of 5 s length with an overlap of 2 s on a segment of 180 s extracted from the middle of each recording (samples were taken equally before and after the central sample of the complete EEG recording). Then, each PSD was normalized by its median to reduce the effect of different offsets in the recordings. The representative resting-state PSD of each visit was obtained averaging Cz's PSDs from recordings belonging to the same visit.

The relative band-power was then computed from each PSD (for each visit-wise PSD of each patient) to compare relative power values in the three patients quantitatively. The frequency range was divided into delta (0–4 Hz), theta (4–8 Hz), alpha (8–12 Hz), low beta (12–20 Hz), high beta (20–30 Hz), and gamma (30–45 Hz) bands (Fig. 1).

Results

Statistical tests were applied using Matlab 2018b. Pearson's linear correlation coefficient was computed on subsequent values of relative band-power, obtained for each patient's set of visits, to investigate the correlation with the corresponding timeline. Then, the Mann–Whitney *U* test was applied to test the power difference between the three patients for each frequency band at the Cz sensor, considering for each of them the whole set of PSDs. The obtained *p* values were corrected through the False Discovery Rate (FDR) using the Benjamini–Hochberg method (Benjamini and Hochberg 1995) to compensate for the multiple comparisons of 6 frequency bands. The results are reported through the visualization of the PSD profile's evolution within the period of observation for each patient separately. The evolution of PSD of patients 6, 9, and 11 are shown in Figs. 2, 3, and 4, respectively. The results on the variance within visits relative band power and power



Fig. 1 Schematic workflow showing EEG's processing steps

Fig. 2 EEG power spectral density evolution in Patient 6. The PSDs corresponding to different visits is shown in different colors, as explained in the box in the top right corner of the figure. The x-axis represents the frequency in Hz. The y-axis represents the normalized amplitude of the power spectral densities on a logarithmic scale. In dashed lines are shown the frequency bands of interest. The frequency range analyzed is divided in the canonical frequency bands, represented in dashed lines in the figures: delta (1 to 4 Hz), theta (4 to 8 Hz), alpha (8 to 12 Hz), beta (12 to 30 Hz) and gamma (30 to 45 Hz)

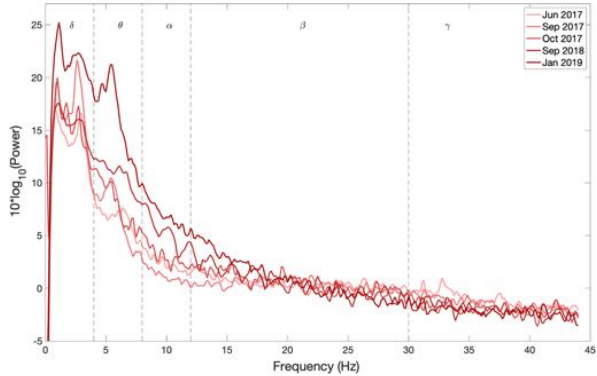
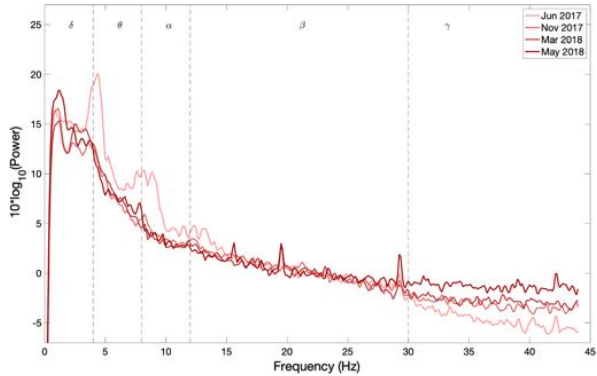


Fig. 3 EEG power spectral density evolution in Patient 9. The details of the figure are the same as explained in the legend of Fig. 2



spectral density of each patient is shown in Supplementary Text 1, where we show that the variance within a visit to be insignificant.

It can be observed from Figs. 2 and 3 that the frequency content of patients 6 and 9, who are in CLIS, are shifted

towards delta and theta frequency bands. During the observation period reported in this paper, no general evolution of trends could be seen in patients 6 and 9. While Patient 11 has activity in the alpha band, present in all the recordings within the observation period, as shown in

Fig. 4 EEG power spectral density evolution in Patient 11. The details of the figure are the same as explained in the legend of Fig. 2

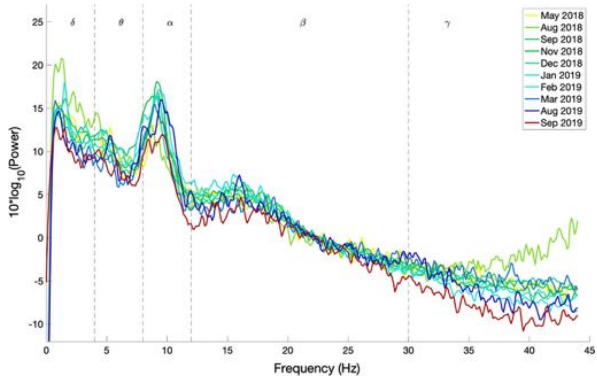


Fig. 4. Nevertheless, a decrease in the power of the EEG signal as the patient transitioned from LIS to CLIS and, ultimately, in CLIS could be observed. The frequency content of patients' 6 and 9 EEG is very different from the EEG of patient 11. This aspect is more evident in Fig. 5, where the average of the PSDs related to all the visits grouped for patients is presented. These results were confirmed by the results of the Mann-Whitney *U* test shown in Fig. 6, which revealed the significant difference in the relative band power between Patient 11 and the two CLIS patients (Patients 6 and 9) at delta, alpha, and low-beta frequency bands. On the other hand, no significant

difference was found over the values of relative power between patients 6 and 9.

Discussion and conclusion

A longitudinal resting-state analysis of patients in LIS and CLIS reveals a trend on the variation of EEG relative band power within the observation period. Patient 6, who is in CLIS since 2012 and was recorded for the first time in May 2017, shows a stable EEG frequency spectrum with dominant frequency in the delta and theta band. Patient 9, who is in CLIS since 2017 and was recorded for the first in June

Fig. 5 Comparison of average EEG power spectral densities in Patients 6, 9, and 11. The red, blue, and green traces correspond to the average PSDs at electrode Cz for patients 6, 9, and 11, respectively. The x-axis represents the frequency in Hz. The y-axis represents the normalized amplitude of the power spectral densities in the logarithmic scale. In dashed lines are shown the frequency bands of interest as described in the legend of Fig. 2

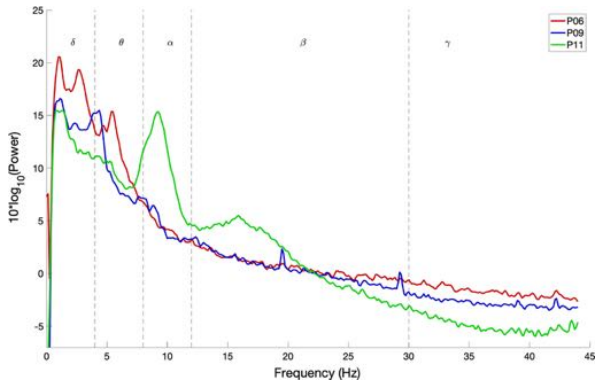
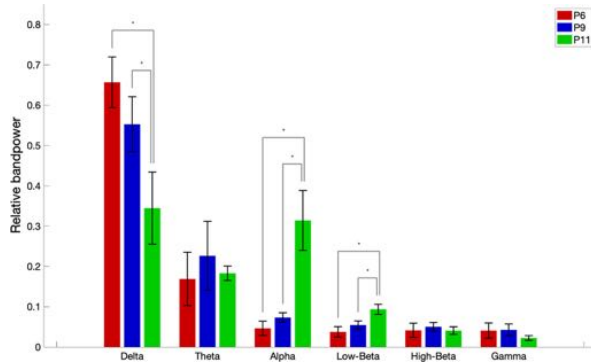


Fig. 6 Relative band power at electrode Cz. Error bars represent standard deviations. The figure depicts the significant power differences between patients 6, 9, and 11 in the two-tailed Wilcoxon rank-sum test with False Discovery Rate correction are marked: $^*p < 0.05$. The x-axis represents the different frequency bands in Hz, and the y-axis represents the relative band power



2017 also shows a trend similar to patient 6. When we started recording Patient 11 in May 2018, the patient had control over his eye-movements but was unable to communicate with the eye-tracker based communication system because of his inability to fixate his gaze. During every visit to each patient, brain-computer interface (BCI)-based communication was attempted after resting-state recording. With patients 6 and 9, functional near-infrared spectroscopy (fNIRS) based communication was attempted, except for the visit 1 of patient 6, we were not able to establish a reliable means of communication using fNIRS based BCI communication system (Chaudhary et al. 2017) with these two patients. The fNIRS based BCI communication system was employed for patient 6 and 9 because it was demonstrated earlier that EEG-based BCI system had failed so far to provide a means of communication to the patients in CLIS (Kübler and Birbaumer 2008) except for a short one-session period report (Okahara et al. 2018) while fNIRS based BCI communication system showed some promise (Gallegos-Ayala et al. 2014). Since the patient 11 still had eye-movement an electrooculogram (EOG) based BCI communication was developed and implemented to provide a means of communication to the patient. The EOG-based communication by patient 11 is described in Tonin et al. (2020). As described in Tonin et al. (2020), patient 11 was able to employ his eye movement ability to communicate his thoughts and desires until February 2019, albeit with increasing difficulties due to the progressive paralysis of his eye muscles associated with the progression of the amyotrophic lateral sclerosis. From February 2019, the patient 11 could not employ his eye-movement to drive the EOG-based communication system (please refer to (Tonin et al. 2020) for further details). Patient 11 could not

communicate reliably with his eyes from March 2019 onwards. He was implanted with microelectrodes in the motor region to provide him a means of communication (Please refer to Chaudhary et al. 2020b for details). The patient although in CLIS was able to form phrases and sentences to express his desires and wishes (Chaudhary et al. 2020b). His EEG spectrum remained constant throughout the observation period reported in this paper.

Patients 6 and 9, although of different ages and being in CLIS for different time periods, have the same EEG spectrum, which is significantly different from patient 11, who was first in LIS, then in the transition from LIS to CLIS and ultimately in CLIS during the period of observation reported in this paper. The main difference between patients 6 and 9 and patient 11 is that since we started following patients 6 and 9, they never had any means of communication. While we were able to provide a means of communication to patient 11 despite his degrading oculomotor function. It can be stated that from the patients reported in this longitudinal analysis, patients without any means of communication have different EEG spectrums than a patient who, despite being in CLIS, has a means of communication. It can also be hypothesized that if a patient has a means of communication despite being in CLIS the general shift in EEG spectrum to the lower bands might not occur, but to generalize these results to other patients in LIS and CLIS with and without means of communication, there is a need to perform such a longitudinal study on the large patient population. Also, a contrary causality is possible: with loss of normal EEG power spectrum and the underlying neurological functionality a loss of communication may be the consequence.

These results are partly supporting an earlier report from our lab of a remarkable reduction of higher frequencies in CLIS (Maruyama et al. 2020), all without any means of communication. It can also be hypothesized that the reason for the failure to establish communication with patients already in CLIS might be due to general shift of their EEG spectrum to the lower bands and absence of alpha and higher frequency bands since all the current EEG based BCI communication systems rely on the alpha and higher frequency bands (Jayaram et al. 2015; Lazarou et al. 2018). Nevertheless, it can also be argued that lack of alpha, in general, might also indicate reduced cognitive processing or compromised vigilance state of the patient (Klimesch 1999). However, in a recent study reported by Khalili-Ardali et al. (2019), patient in CLIS was shown to have the ability to process sentences with motor semantic content and self-related content better than control sentences indicating comprehension and some level of cognitive processing in CLIS in ALS patients. It can also be argued that the patients might be asleep during the period of data acquisition, but recently we showed in a larger sample of patients in CLIS (Malekshahi et al. 2019) that despite a general decrease in their EEG spectrum, patients in CLIS still have an intact sleep and wake cycle.

Thus, there is a need to perform long-term longitudinal studies with patients in LIS, the transition to LIS, and CLIS and parallel cognitive evaluation with BCI assistance to elucidate the evolution in their EEG signature, which afterward may then be used in the development of more efficient non-invasive BCI-systems.

Acknowledgements Deutsche Forschungsgemeinschaft (DFG) DFG BI 195/77-1, BMBF (German Ministry of Education and Research) 16SV7701 CoMiCon, and. LUMINOUS-H2020-FETOPEN-2014-2015-RIA (686764).

Author's contribution AS: data analysis; manuscript writing. AT: performed 40% of data collection; data analysis discussion. AR: performed 30% of the data collection. AJ-G: data analysis discussion. MK-A: data analysis discussion. NB: study design and conceptualization; manuscript correction. UC: study design and conceptualization; performed 70% of the data collection; data analysis supervision; manuscript writing.

Funding Open Access funding enabled and organized by Projekt DEAL.

Compliance with ethical standards

Conflict of interest The authors declare that they have no conflict of interest.

Open Access This article is licensed under a Creative Commons Attribution 4.0 International License, which permits use, sharing, adaptation, distribution and reproduction in any medium or format, as long as you give appropriate credit to the original author(s) and the source, provide a link to the Creative Commons licence, and indicate

if changes were made. The images or other third party material in this article are included in the article's Creative Commons licence, unless indicated otherwise in a credit line to the material. If material is not included in the article's Creative Commons licence and your intended use is not permitted by statutory regulation or exceeds the permitted use, you will need to obtain permission directly from the copyright holder. To view a copy of this licence, visit <http://creativecommons.org/licenses/by/4.0/>.

References


- Babiloni C, Pistoia F, Sarà M, Vecchio F, Buffo P, Conson M, Onorati P, Albertini G, Rossini PM (2010) Resting state eyes-closed cortical rhythms in patients with locked-in-syndrome: an EEG study. *Clin Neurophysiol* 121:1816–1824
- Bauer G, Gerstenbrand F, Rimpl E (1979) Varieties of the locked-in syndrome. *J Neurol* 221:77–91
- Belouchrani A, Abed-Meraim K, Cardoso JF, Moulines E (1997) A blind source separation technique using second-order statistics. *IEEE Trans Signal Process* 45(2):434–444
- Benjamini Y, Hochberg Y (1995) Controlling the false discovery rate: a practical and powerful approach to multiple testing. *J R Stat Soc Ser B (Methodol)* 57(1):289–300
- Birbaumer N (2006) Breaking the silence: brain–computer interfaces (BCI) for communication and motor control. *Psychophysiology* 43(6):517–532
- Birbaumer N, Ghanayim N, Hinterberger T, Iversen I, Kotchoubey B, Kübler A, Perelmutter J, Taub E, Flor H (1999) A spelling device for the paralysed. *Nature* 398(6725):297–298
- Birbaumer N, Piccione F, Silvoni S, Wildgruber M (2012) Ideomotor silence: the case of complete paralysis and brain–computer interfaces (BCI). *Psychol Res* 76(2):183–191
- Buiza E, Rodríguez-Martínez EI, Barriga-Paulino CI, Arjona A, Gomez CM (2018) Developmental trends of theta–beta inter-electrode power correlation during resting state in normal children. *Cogn Neurodyn* 12(3):255–269
- Chaudhary U, Birbaumer N, Curado MR (2015) Brain–machine interface (BMI) in paralysis. *Ann Phys Rehabil Med* 58(1):9–13
- Chaudhary U, Birbaumer N, Ramos-Murguialday A (2016a) Brain–computer interfaces for communication and rehabilitation. *Nat Rev Neurol* 12(9):513
- Chaudhary U, Birbaumer N, Ramos-Murguialday A (2016b) Brain–computer interfaces in the completely locked-in state and chronic stroke. In: *Progress in brain research*, vol. 228. Elsevier, Amsterdam, pp 131–161
- Chaudhary U, Xia B, Silvoni S, Cohen LG, Birbaumer N (2017) Brain–computer interface-based communication in the completely locked-in state. *PLoS Biol* 15(1):e1002593
- Chaudhary U, Mrachacz-Kersting N, Birbaumer N (2020a) Neuropsychological and neurophysiological aspects of brain–computer interface (BCI) control in paralysis. *J Physiol*. <https://doi.org/10.1113/JP278775>
- Chaudhary U, Vlachos I, Zimmermann JB, Espinosa A, Tonin A, Jaramillo-Gonzalez A, Khalili-Ardali M, Topka H, Lehmburg J, Friehs GM, Woodtli A (2020b) Verbal communication using intracortical signals in a completely locked-in-patient. *medRxiv*. <https://doi.org/10.1101/2020.06.10.20122408>
- Conson M, Pistoia F, Sarà M, Grossi D, Trojano L (2010) Recognition and mental manipulation of body parts dissociate in locked-in syndrome. *Brain Cogn* 73(3):189–193
- Delorme A, Makeig S (2004) EEGLAB: an open source toolbox for analysis of single-trial EEG dynamics including independent component analysis. *J Neurosci Methods* 134:9–21

- Dukic S, McMackin R, Buxo T, Fasano A, Chipika R, Pinto-Grau M, Costello E, Schuster C, Hammond M, Heverin M, Coffey A (2019) Patterned functional network disruption in amyotrophic lateral sclerosis. *Hum Brain Mapp* 40:4827–4842
- Gabard-Durnam LJ, Wilkinson C, Kapur K, Tager-Flusberg H, Levin AR, Nelson CA (2019) Longitudinal EEG power in the first postnatal year differentiates autism outcomes. *Nat Commun* 10(1):1–2
- Gallegos-Ayala G, Furdea A, Takano K, Ruf CA, Flor H, Birbaumer N (2014) Brain communication in a completely locked-in patient using bedside near-infrared spectroscopy. *Neurology* 82:930–1932
- Gómez-Herrero G, De Clercq W, Anwar H, Kara O, Egiazarian K, Van Huffel S, Van Paesschen W (2006) Automatic removal of ocular artifacts in the EEG without an EOG reference channel. In: Proceedings of the 7th nordic signal processing symposium-NORSIG 2006. IEEE, pp 130–133
- Goshvarpour A, Goshvarpour A (2019) EEG spectral powers and source localization in depressing, sad, and fun music videos focusing on gender differences. *Cogn Neurodyn* 13(2):161–173
- Hohmann MR, Fomina T, Jayaram V, Emde T, Just J, Synofzik M, Schölkopf B, Schöls L, Grosse-Wentrup M (2018) Case series: slowing alpha rhythm in late-stage ALS patients. *Clin Neurophysiol* 129:406–408
- Jayaram V, Widmann N, Förster C, Fomina T, Hohmann M, vom Hagen JM, Synofzik M, Schölkopf B, Schöls L, Grosse-Wentrup M (2015) Brain–computer interfacing in amyotrophic lateral sclerosis: implications of a resting-state EEG analysis. In: 2015 37th annual international conference of the IEEE engineering in medicine and biology society (EMBC). IEEE, pp 6979–6982
- Khalili-Ardali M, Rana A, Purnohammad M, Birbaumer N, Chaudhary U (2019) Semantic and BCI-performance in completely paralyzed patients: possibility of language attrition in completely locked in syndrome. *Brain Lang* 194:93–97
- Klimesch W (1999) EEG alpha and theta oscillations reflect cognitive and memory performance: a review and analysis. *Brain Res Rev* 29(2–3):169–195
- Kühler A, Birbaumer N (2008) Brain–computer interfaces and communication in paralysis: Extinction of goal directed thinking in completely paralysed patients? *Clin Neurophysiol* 119:2658–2666
- Kühler A, Nijboer F, Mellinger J, Vaughan TM, Pawelzik H, Schalk G, McFarland DJ, Birbaumer N, Wolpaw JR (2005) Patients with ALS can use sensorimotor rhythms to operate a brain-computer interface. *Neurology* 64(10):1775–1777
- Lazarou I, Nikolopoulos S, Petrantonis PC, Kompatsiaris I, Tsolaki M (2018) EEG-based brain–computer interfaces for communication and rehabilitation of people with motor impairment: a novel approach of the 21st century. *Front Hum Neurosci* 12:14
- Lesenfans D, Habbal D, Lugo Z, Lebeau M, Horki P, Amico E, Pokorny C, Gomez F, Soddu A, Müller-Putz G, Laureys S (2014) An independent SSVEP-based brain–computer interface in locked-in syndrome. *J Neural Eng* 11(3):035002
- Mai R, Fauchetti D, Micheli A, Poloni M (1998) Quantitative electroencephalography in amyotrophic lateral sclerosis. *Electroencephalogr Clin Neurophysiol* 106:383–386
- Malekshahi A, Chaudhary U, Jaramillo-Gonzalez A, Lucas Luna A, Rana A, Tonin A, Birbaumer N, Gais S (2019) Sleep in the completely locked-in state (CLIS) in amyotrophic lateral sclerosis. *Sleep* 42(12):zsz185
- Maruyama Y, Yoshimura N, Rana A, Malekshahi A, Tonin A, Jaramillo-Gonzalez A, Birbaumer N, Chaudhary U (2020) Electroencephalography of completely locked-in state patients with amyotrophic lateral sclerosis. *Neurosci Res*. <https://doi.org/10.1016/j.neures.2020.01.013>
- Myers MH, Kozma R (2018) Mesoscopic neuron population modeling of normal/epileptic brain dynamics. *Cogn Neurodyn* 12(2):211–223
- Nasserolleslami B, Dukic S, Broderick M, Mohr K, Schuster C, Gavin B, McLaughlin R, Heverin M, Vajda A, Iyer PM, Pender N (2019) Characteristic increases in EEG connectivity correlate with changes of structural MRI in amyotrophic lateral sclerosis. *Cereb Cortex* 29:27–41
- Nobukawa S, Yamanishi T, Nishimura H, Wada Y, Kikuchi M, Takahashi T (2019) Atypical temporal-scale-specific fractal changes in Alzheimer's disease EEG and their relevance to cognitive decline. *Cogn Neurodyn* 13(1):1–11
- Okahara Y, Takano K, Nagao M, Kondo K, Iwadate Y, Birbaumer N, Kansaku K (2018) Long-term use of a neural prosthesis in progressive paralysis. *Sci Rep* 8(1):1–8
- Pistoia F, Conson M, Trojano L, Grossi D, Ponari M, Colonnese C, Pistoia ML, Carducci F, Sara M (2010) Impaired conscious recognition of negative facial expressions in patients with locked-in syndrome. *J Neurosci* 30(23):7838–7844
- Rowland LP, Sheidter NA (2001) Amyotrophic lateral sclerosis. *N Engl J Med* 344:1688–1700
- Sacco S, Sarà M, Pistoia F, Conson M, Albertini G, Carolei A (2008) Management of pathologic laughter and crying in patients with locked-in syndrome: a report of 4 cases. *Arch Phys Med Rehabil* 89(4):775–778
- Sarà M, Cornia R, Conson M, Carolei A, Sacco S, Pistoia F (2018) Cortical brain changes in patients with locked-in syndrome experiencing hallucinations and delusions. *Front Neurol* 9:354
- Schnakers C, Perrin F, Schabus M, Majerus S, Ledoux D, Damas P, Boly M, Vanhaudenhuyse A, Bruno MA, Moonen D, Laureys S (2008) Voluntary brain processing in disorders of consciousness. *Neurology* 71(20):1614–1620
- Sellers EW, Vaughan TM, Wolpaw JR (2010) A brain-computer interface for long-term independent home use. *Amyotroph Lateral Scler* 11(5):449–455
- Subhani AR, Kamel N, Saad MN, Nandagopal N, Kang K, Malik AS (2018) Mitigation of stress: new treatment alternatives. *Cogn Neurodyn* 12(1):1–20
- Tonin A, Jaramillo-Gonzalez A, Rana A, Khalili-Ardali M, Birbaumer N, Chaudhary U (2020) Auditory electrooculogram-based communication system for ALS patients in transition from locked-into complete locked-in state. *Sci Rep* 10(1):1
- Wolpaw JR, McFarland DJ (2004) Control of a two-dimensional movement signal by a non-invasive brain-computer interface in humans. *Proc Natl Acad Sci* 101(51):17849–17854
- Wolpaw JR, Bedlack RS, Reda DJ, Ringer RJ, Banks PG, Vaughan TM, Heckman SM, McCane LM, Carmack CS, Winden S, McFarland DJ (2018) Independent home use of a brain-computer interface by people with amyotrophic lateral sclerosis. *Neurology* 91(3):e258–e267
- Yi GS, Wang J, Deng B, Wei XL (2017) Complexity of resting-state EEG activity in the patients with early-stage Parkinson's disease. *Cogn Neurodyn* 11(2):147–160

Publisher's Note Springer Nature remains neutral with regard to jurisdictional claims in published maps and institutional affiliations.

Article

Open Software/Hardware Platform for Human-Computer Interface Based on Electrooculography (EOG) Signal Classification

Jayro Martínez-Cerveró ¹, Majid Khalili Ardali ¹, Andres Jaramillo-Gonzalez ¹, Shizhe Wu ¹, Alessandro Tonin ², Niels Birbaumer ¹ and Ujwal Chaudhary ^{1,2,*} 

¹ Institute of Medical Psychology and Behavioural Neurobiology, University of Tübingen, Silcherstraße 5, 72076 Tübingen, Germany

² Wyss-Center for Bio- and Neuro-Engineering, Chemin des Mines 9, Ch 1202 Geneva, Switzerland

* Correspondence: chaudharyujwal@gmail.com

Received: 21 February 2020; Accepted: 23 April 2020; Published: 25 April 2020



Abstract: Electrooculography (EOG) signals have been widely used in Human-Computer Interfaces (HCI). The HCI systems proposed in the literature make use of self-designed or closed environments, which restrict the number of potential users and applications. Here, we present a system for classifying four directions of eye movements employing EOG signals. The system is based on open source ecosystems, the Raspberry Pi single-board computer, the OpenBCI biosignal acquisition device, and an open-source python library. The designed system provides a cheap, compact, and easy to carry system that can be replicated or modified. We used Maximum, Minimum, and Median trial values as features to create a Support Vector Machine (SVM) classifier. A mean of 90% accuracy was obtained from 7 out of 10 subjects for online classification of Up, Down, Left, and Right movements. This classification system can be used as an input for an HCI, i.e., for assisted communication in paralyzed people.

Keywords: electrooculography (EOG); Human-Computer Interface (HCI); Support Vector Machine (SVM)

1. Introduction

In the past few years, we have seen an exponential growth in the development of Human-Computer Interface (HCI) systems. These systems have been applied for a wide range of purposes like controlling a computer cursor [1], a virtual keyboard [2], a prosthesis [3], or a wheelchair [4–7]. They could also be used for patient rehabilitation and communication [8–11]. HCI systems can make use of different input signals such as voice [7], electromyography (EMG) [12], electroencephalography (EEG) [13], near-infrared spectroscopy (NIRS) [14–16] or electrooculography (EOG) [5].

In this paper, we describe an EOG classification system capable of accurately and consistently classifying Up, Down, Left, and Right eye movements. The system is small, easy to carry, with considerable autonomy, and economical. It was developed using open hardware and software, not only because of economic reasons, but also to ensure that the system could reach as many people as possible and could be improved and adapted in the future by anyone with the required skills.

The end goal of this work is to build a system that could be easily connected to a communication or movement assistance device like a wheelchair, any kind of speller application, or merely a computer mouse and a virtual keyboard.

To achieve these objectives, we have developed and integrated the code needed for:

- Acquiring the Electrooculography (EOG) signals.

- Processing these signals.
- Extracting the signal features.
- Classifying the features previously extracted.

EOG measures the dipole direction changes of the eyeball, with the positive pole in the front [17]. The technique of recording these potentials was introduced for diagnostic purposes in the 1930s by R. Jung [18]. The presence of electrically active nerves in the posterior part of the eyeball, where the retina is placed, and the front part, mainly the cornea, creates the difference in potential on which EOG is based [19]. This creates an electrical dipole between the cornea and the retina, and its movements generate the potential differences that we can record in an EOG.

There are several EOG HCI solutions present in the literature. One of the issues with current HCI systems is their size and lack of autonomy, the use of proprietary software, or being based on self-designed acquisition and processing devices. Regarding the acquisition system, the most common approach is to use a self-designed acquisition device [1,4,20–22]. In our view, this solution dramatically restricts the number of users who can adopt this system. Other proposed systems make use of commercial amplifiers [23,24], which in turn make use of proprietary software and require robust processing systems, mainly laptops. This also reduces the number of potential users of the system and its applications since it increases the cost of the system and reduces its flexibility, portability, and autonomy. As far as signal processing is concerned, most systems choose to use a laptop to carry out these calculations [1,20–22,24,25], but we can also find the use of self-designed boards [6,26]. Table 1 shows the characteristics of some solutions present in literature as a representation of the current state of the art. The goal of our work is to achieve results equivalent to the present state of the art using an open paradigm, demonstrating that it is possible to arrive at a solution using cheaper components that could be modified to build a tailored solution. As far as we know, this is the first time that an open system is presented in this scope.

Table 1. Comparison of results between different studies.

Study	Movements	Acquisition	Processing	Method	Accuracy
Qi et al. [27]	Up, Down, Left, Right	Commercial	-	Offline	70%
Guo et al. [28]	Up, Down, Blink	Commercial	Laptop	Online	84%
Kherlopian et al. [24]	Left, Right, Center	Commercial	Laptop	Online	80%
Wu et al. [20]	Up, Down, Left, Right, Up-Right, Up-Left, Down-Right, Down-Left	Self-designed	Laptop	Online	88.59%
Heo et al. [26]	Up, Down, Left, Right, Blink	Self-designed	Self-designed + Laptop	Online	91.25%
Heo et al. [26]	Double Blink	Self-designed	Self-designed + Laptop	Online	95.12%
Erkaymaz et al. [29]	Up, Down, Left, Right, Blink, Tic	Commercial	Laptop	Offline	93.82%
Merino et al. [27]	Up, Down, Left, Right	Commercial	Laptop	Online	94.11%
Huang et al. [21]	Blink	Self-designed	Laptop	Online	96.7%
Lv et al. [19]	Up, Down, Left, Right	Commercial	Laptop	Offline	99%
Yathunanathan et al. [6]	Up, Down, Left, Right	Self-designed	Self-designed	Online	99%

In our system, the signal is acquired using the OpenBCI Cyton Board (Raspberry Pi 3B+ official website), a low-cost open software/hardware biosensing device, resulting in an open hardware/software-based system that is portable, with considerable autonomy and flexibility.

Once we have the EOG signal, this is processed using a Raspberry Pi (OpenBCI Cyton official website), a single board computer that allows installing a Linux-based distribution, which is small, cheap, and gives us the option to use non-proprietary software.

Features are then extracted from the acquired signal and classified employing a machine learning algorithm. The feature extraction process aims to reduce the dimensionality of the input data without losing relevant information for classification [28] and maximizing the separation between elements of different classes by minimizing it between elements of the same class [27]. To achieve this, several models have been proposed on EOG feature extraction [29–32]. We employed Support Vector Machine (SVM) to classify the data [33,34], which creates a boundary to split the given data points into two different groups.

The result of this process, in the context of signal (EOG) mentioned in this article, is the classification of the subject's eye movement to be used as input commands for further systems. This process and the tools used for it are explained in detail in Section 2. The Section 3 shows the performance achieved by the system. Finally, in the Section 4, we discuss the designed system and compare our system with existing related work along with the limitations of our system and future work.

2. Materials and Methods

2.1. Hardware-Software Integration

In the present study, OpenBCI Cyton board was used for the signal acquisition. This board contains a PIC32MX250F128B microcontroller, a Texas Instruments ADS1299 analog/digital converter, a signal amplifier and an eight-channel neural interface. This device is distributed by OpenBCI (USA). Figure 1 depicts the layout of the system.



Figure 1. Block diagram with system connection.

This device gives us enough precision and sampling rate (250 Hz) for our needs, it has an open-source environment (including a Python library to work with the boards (OpenBCI Python repository)), it has an active and large community and it can be powered with a power bank, which is a light and mobile solution. Attached to the board, we have 4 wet electrodes connected to two channels on the board in a differential mode. Differential mode computes the voltage difference between the two electrodes connected to the channel and doesn't need a reference electrode. The two channels correspond to the horizontal and vertical components of the signal.

The acquisition board is connected to a Raspberry Pi, a single-board computer developed by the Raspberry Pi company based in the United Kingdom. Although its firmware is not open source, it allows installing a Linux-based distribution keeping the open paradigm in our system. In this case, we chose to install Raspbian, a Debian-based distribution. The hardware connection between the OpenBCI board and the Raspberry Pi is made using a wireless RFDuino USB dongle. On the software side, we used an open Python library released by OpenBCI. To run this library over the Raspberry Pi, the source code of the mentioned library has been partially modified. It has also been necessary to recompile some third-party libraries so that they could run on the Raspberry Pi. We decided to power both the OpenBCI board and the Raspberry Pi via a USB connection to a power bank (20,000 mAh) to maximize the system autonomy and mobility.

This hardware configuration offers us all the characteristics that we were looking for: it has enough computational power to carry our calculations, it's small and light, it allows us to use free and

open-source software, and is economical. It should be noted that although we have used the OpenBCI board as acquisition system there are some other solutions that fit our needs like the BITalino biosignal acquisition board. This board offers an EOG acquisition module and an open environment which includes a Python-based API for connection and signal acquisition over Raspberry Pi.

It should be mentioned that the data presented in this article have been processed using a conventional laptop instead of the Raspberry Pi, just for the convenience of the experimenters. During the development of the research, several tests were carried out that did not show any difference in the data or the results depending on the platform used.

We decided to use EOG over other eye movement detection techniques like Infrared Reflection Oculography (IROG) [35] or video-based systems [25], as the EOG technique does not require the placement of any device that could obstruct the subjects' visual field. Four electrodes were placed in contact with the skin close to the eyes to record both the horizontal and the vertical components of the eye movements [36,37].

2.2. Experimental Paradigm

Ten healthy subjects between 24 and 35 years old participated in the study and gave their informed consent for inclusion. The signal acquisition was performed in two stages: training and online prediction. For both stages, we asked the subjects to perform four different movements: Up, Down, Left, and Right. Each movement should start with the subject looking forward and then look at one of these four points already mentioned and look again at the center. For the training stage, we acquired two blocks of 20 trials, 5 trials per movement. In these blocks, five "beep" tones were presented to the subject at the beginning of each block in 3 s intervals to indicate the subject the interval that they had to perform the requested action. After these initial tones, the desired action was presented via audio, and a "beep" tone was presented as a cue to perform the action. The system recorded during the 3 s after this tone was presented, and the system presented again another action to be performed. For some of the subjects, these two training blocks were appended in a single data file. The schematic of the training paradigm (offline acquisition) is shown in Figure 2a.

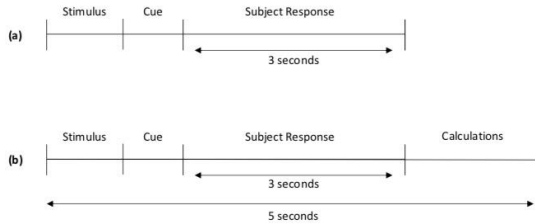


Figure 2. Acquisition paradigm. (a) Offline acquisition. (b) Online acquisition.

The online classification was performed with a block of 40 trials, 10 per movement, on Subject 1. After this experiment, we decided to reduce the number of trials per block to 20, 5 per movement, for the convenience of the subject. This online block had the same characteristics as the classification blocks except that the five initial tones were not presented, and the actions to be performed were separated by 5 s interval to have enough time for the prediction tasks. Furthermore, in these blocks, the system recorded only during the 3 s after the cue tone was presented. During this stage, we generate two auxiliary files: one with the acquired data and the other containing the action that the user should perform and the action predicted. We only considered predicted actions with a prediction probability higher than a certain threshold. For the first subject, we set this threshold as 0.7, but after that experiment, we changed the threshold to 0.5. In this case, the auxiliary file corresponding to

subject 1 contains the predictions made using 0.7 as a prediction probability threshold. Figure 2b depicts the schematic of the online prediction paradigm.

2.3. Signal Processing

A second-order 20 Hz lowpass Butterworth filter [37] was used to remove the artifacts arising from electrodes or head movements and illumination changes [19,27,38]. A 20 Hz lowpass filter was used because the artifacts, as mentioned earlier, appear in the high frequencies [17], and the EOG signal information is contained mainly in low frequencies [30]. The irregularities in the signal after the lowpass filter were removed using a smoothing filter [30]. For applying these filters, we used the SciPy library. This library is commonly used and has a big community supporting it.

The last step in pre-processing was to standardize the data. This is done to remove the baseline of EOG signals [27]. The standardization was done using the following formula:

$$X_t = \frac{x_t - \mu_i}{\sigma_i}, \quad (1)$$

where i is the sample that we are processing, t corresponds to a single datapoint inside a sample, X_t is the resulting datapoint, x_t is the data point value before standardization, μ_i is the mean value of the whole sample and σ_i is the standard deviation of the whole sample. An example of the processed signal can be seen in Figure 3, which shows a single Down trial extracted from a classification block of Subject 5.

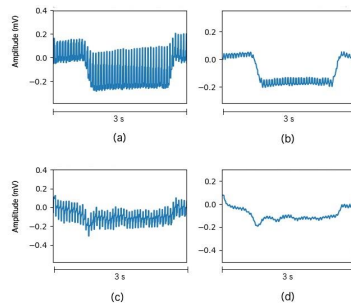


Figure 3. Down movement example taken from Subject 5. The x-axis depicts time (in seconds), and Y-axis represents the signal amplitude (in millivolts). (a) Unfiltered vertical component. (b) Filtered vertical component. (c) Unfiltered horizontal component. (d) Filtered horizontal component.

Figure 4 depicts the vertical and horizontal component for four different eye movement tasks performed by subject 5.

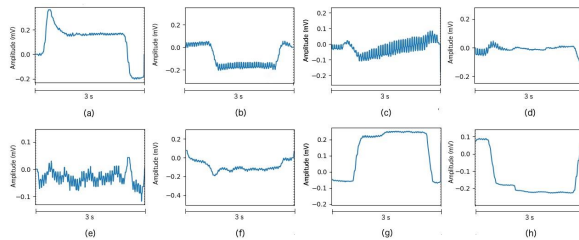


Figure 4. Processed signals examples taken from Subject 5. The *x*-axis depicts time (in seconds), and *Y*-axis represents the signal amplitude (in millivolts). (a) Vertical component for Up movement. (b) Vertical component for Down Movement. (c) Vertical component for Left movement. (d) Vertical component for the Right movement. (e) Horizontal component for Up movement. (f) Horizontal component for Down movement. (g) Horizontal component for Left movement. (h) Horizontal component for Right movement.

2.4. Feature Extraction

An essential step in our system's signal processing pipeline is feature extraction, which for each sample, calculates specific characteristics that will allow us to maximize the distance between elements in different classes and the similarity between those that belong to the same category. We use a model based on the calculation of 3 features for the horizontal and vertical components of our signal, i.e., 6 total features per sample. The features are the following:

- Min: The minimum amplitude value during the eye movement.
- Max: The maximum amplitude value during the eye movement.
- Median: The amplitude value during the eye movement that has 50% values above as below.

2.5. Classification

Once we have calculated the features of each sample, we create a model using that feature values and its class labels. Even though some biosignal-based HCI use other machine learning techniques, such as artificial neural networks [29,36] or other statistical techniques [19], most of the HCI present in the literature use the machine learning technique called Support Vector Machine. We have decided to use SVM because of its simplicity over other techniques, which results in a lower computational cost and excellent performance.

In this study, we have used the implementation of the SVM of Scikit-Learn, a free and open-source Machine Learning Python library. This library has a high reputation in Machine Learning, and it has been widely used. The selected parameters for creating the model are a Radial Basis Function (RBF) as kernel [39], which allows us to create a model using data points that are not linearly separable [40], and a One vs. One strategy [41], i.e., creating a classifier for each pair of movement classes. Finally, we have performed 5-fold cross-validation [42], splitting the training dataset into 5 mutually exclusive subsets and also creating 5 models, each one using one of these subsets to test the model and the other four to create it. Our model accuracy is calculated as the mean of these 5 models.

3. Results

The acquired signal is processed to remove those signal components that contain no information, resulting in a clearer signal. The data were acquired from 10 healthy subjects between 24 and 35 years old. The result of signal processing can be seen in Figures 3 and 4, which shows the single trials of a training block performed by Subject 5. As Figures 3 and 4 show, the result of this step is the one

expected. For Subject 8, we found flat or poor-quality signals in the vertical and horizontal component, so we decided to stop the acquisition and discard these data. Some trials extracted from this discarded block can be seen in Figure 5 which shows no clear steps or any other patterns for the four movements. This situation is probably due to an electrode movement, detachment, or misplacement that could not be solved during the experiment.

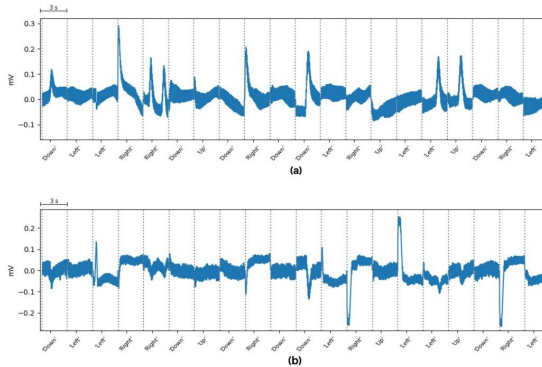


Figure 5. Example trials taken from Subject 8. The x-axis depicts time (each trial is 3 s), and Y-axis represents the signal amplitude (in millivolts). (a) Vertical component. (b) Horizontal component.

After artifact removal, feature extraction is performed to reduce the dimensionality in input, leading to characteristics that define the signal without information loss. As mentioned above, the features used were Maximum, Minimum, and Median. It should be noticed that Up and Down movements have relevant information only for the vertical channel of our signal as well as Left and Right movements have this relevant information in the horizontal component. Figures 6 and 7 present an example of this feature extraction process over two blocks of 20 trials, each corresponding to the training data of Subject 5, who ended up with 100% accuracy. Figures 8 and 9 present an example of the same feature extraction process over two blocks of 20 trials performed by Subject 6, who ended up with 78.7% accuracy. In these figures, we can appreciate that Subject 5, with 100% accuracy, shows a more evident difference in the data values than Subject 6, with 78.7% accuracy. Figures 8 and 9 show some overlapping in the data values, which explains the lower classification accuracy achieved.

The last step in our pipeline is to build a model and perform an online classification of the subject's eye movements. As we mentioned before, we build our model using 5-fold cross-validation. Table 2 shows the model accuracy, the accuracy-related on how good the model has been classifying the training data, as the mean of these five models for each subject. For the prediction accuracy—the accuracy related to the prediction of unseen data—we have asked the subject to perform 20 movements per block (five of each movement), as is explained in Section 2.2. We predicted those movements using the pre-built model and, finally, validated how accurate that prediction was.

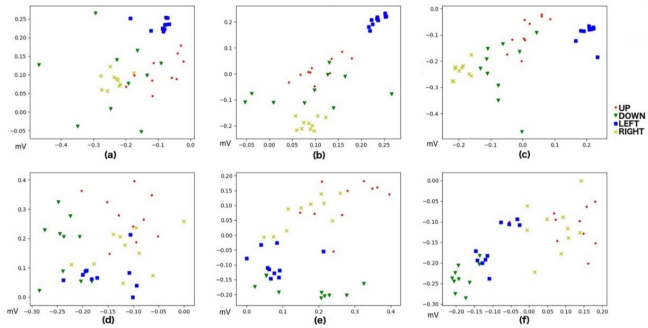


Figure 6. Values after Feature Extraction for Up, Down, Left, and Right movements performed by Subject 5 (100% model accuracy). Both X-axis and Y-axis depict signal values (in millivolts). (a) Horizontal Min vs. Max. (b) Horizontal Max vs. Median. (c) Horizontal Median vs. Min. (d) Vertical Min vs. Max. (e) Vertical Max vs. Median. (f) Median vs. Min.

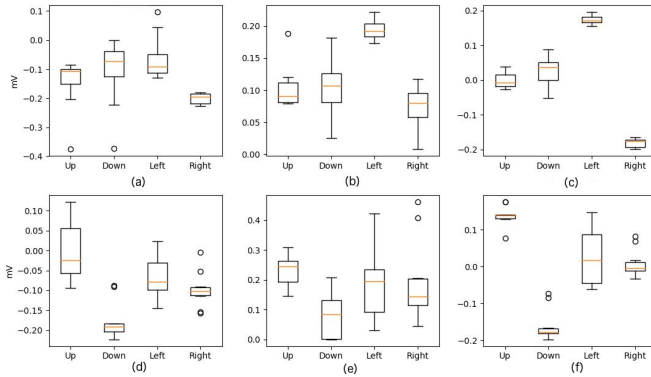


Figure 7. Values after Feature Extraction for Up, Down, Left, and Right Movements performed by Subject 5 (100% model accuracy). The x-axis depicts movement class, and Y-axis depicts signal amplitude (in millivolts). (a) Horizontal Min. (b) Horizontal Max. (c) Horizontal Median. (d) Vertical Min. (e) Vertical Max. (f) Vertical Median.

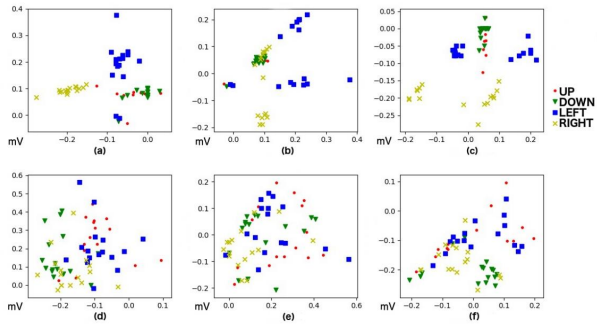


Figure 8. Values after Feature Extraction for Up, Down, Left, and Right movements performed by Subject 6 (78.7% model accuracy). Both X-axis and Y-axis depict signal values (in millivolts). (a) Horizontal Min vs. Max. (b) Horizontal Max vs. Median. (c) Horizontal Median vs. Min. (d) Vertical Min vs. Max. (e) Vertical Max vs. Median. (f) Median vs. Min.

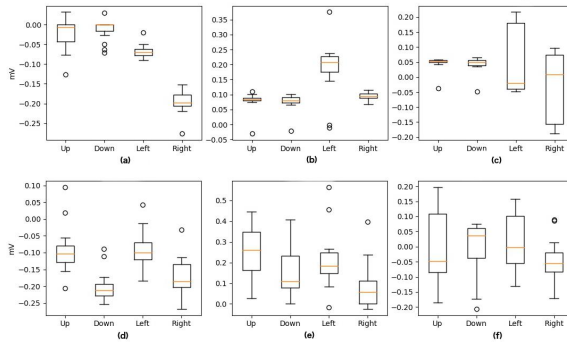


Figure 9. Values after Feature Extraction for Up, Down, Left, and Right Movements performed by Subject 6 (78.7% model accuracy). The x-axis depicts movement class, and Y-axis depicts signal amplitude (in millivolts). (a) Horizontal Min. (b) Horizontal Max. (c) Horizontal Median. (d) Vertical Min. (e) Vertical Max. (f) Vertical Median.

Table 2. Model and Prediction Accuracies.

Subject	Model Mean Accuracy	Online Accuracy
Subject 1	100%	90%
Subject 2	100%	95%
Subject 3	92.5%	85%
Subject 5	100%	100%
Subject 6	78.7%	85%
Subject 7	97.5%	95%
Subject 10	90.8%	80%
MEAN	94.21%	90%

As mentioned in Section 2.2., we only consider those predicted actions with a prediction probability higher than 0.5. For subject 1, the prediction probability threshold was set to 0.7 during the online acquisition, so the auxiliary file with the predictions corresponds to this threshold, and after experimenting, we re-analyzed the online data using a 0.5 threshold.

We acquired one single online block for subjects 1, 2, 5 and 7. For subject 3, we acquired three online blocks with 50%, 80%, and 85% accuracy. For subject 6, we acquired two online blocks with 80% and 85% accuracy. For subject 10, we acquired three online blocks with 55%, 70%, and 80% accuracy. It can be seen that for all subjects, the online accuracy increases with each block acquisition. The accuracy shown in Table 1 corresponds to those online blocks with the highest accuracy for each subject. For subject 4, the training and online data have poor quality (66.7% accuracy for the model and 20% accuracy for the online prediction). Subject 9 had a good model accuracy (95%) but poor-quality signals during online acquisition (50% and 20% accuracy). Post-experimental analysis of the data revealed noisy and flat signals, showing no clear pattern in the signal acquired from subjects 4 and 9, similar to the signal acquired from Subject 8 (Please see Figure 5 for the signal from patient 8). These distortions may have arisen due to the probable electrode movement, detachment, or misplacement. Thus, we decided to discard the data from Subjects 4, 8 and 9.

4. Discussion

It must be clear that in order to make a completely fair comparison between our system and the state-of-the-art systems, some extensive testing would be required. These tests should process the data acquired in this study with other processing pipelines, run our pipeline over the data acquired in other studies, and adapt our acquisition and processing modules to be connected to further systems found in the literature. The results obtained after this process would give us a full picture of the differences between our system and those already in place. Unfortunately, due to lack of time and materials, these tests could not be carried out.

Concentration loss and tiredness are two of the biggest challenges when it comes to EOG-based HCI. As reported in Barea et al. [43], the number of failures using this kind of system increases over time after a specific period of use. This has been seen during the development of this study, where long periods of system use have led to the appearance of irritation and watery eyes. This could be a problem for subjects who use the system for a long time. In the paper above mentioned [43], the researchers deal with this problem by retraining the system.

Another challenge related to our system is the presence of unintentional eye blinks. Eye blinks create artifacts in the EOG signal and, also, during the eye blinks, there is a slight eye movement [37]. The trials containing eye blinks can lead to a reduced model accuracy if it occurs in the training stage or to a trial misclassification if it is in the online acquisition stage. Pander et al. [44], and Merino et al. [30] have proposed methods to detect spontaneous blinks so these trials can be rejected. Yathunanathan et al. [6] proposed a system where eye blinks are automatically discarded.

Our system, like most of the available systems in the literature [19–21,29,30,38,43], uses a discrete approach, i.e., the user is not free to perform an action when desired, but the action must be performed at a specific time. This affects the agility of the system by increasing the time needed to perform an action. Barea et al. [38,43] and Arai et al. [25] have proposed systems with a continuous approach where the subject has no time restrictions to perform an action.

There are different ways to improve our system in future work. First, we could put in place a mechanism to detect and remove unintentional blinks. This would prevent us discarding training blocks, or could improve the training accuracy in the cases in which these unintentional blinks occur. In some cases, a continuous online classification means a considerable advantage. Therefore, it would be interesting to add the necessary strategies to perform this type of classification. Finally, by combining our system with further communication or movement assistance systems, we could check its performance in a complete HCI loop.

5. Conclusions

We have presented an EOG signal classification system that can achieve a 90% mean accuracy in online classifications. These results are equivalent to other state-of-the-art systems. Our system is built using only open components, showing that it is possible to avoid the usage of expensive and proprietary tools in this scope. As intended, the system is small, easy to carry, and has complete autonomy. This is achieved using OpenBCI and Raspberry Pi as hardware, connected to a power bank as a power source.

Because of the use of open hardware and software technologies, the system is also open, easy to replicate, and can be improved or modified by someone with the required skills to build a tailored solution. The use of open technologies also helps us to obtain a cheap platform.

Finally, the resulting system is easy to connect to subsequent communication or movement assistance systems.

Author Contributions: Conceptualization, J.M.-C., N.B., and U.C.; methodology, J.M.-C., M.K.A., A.J.-G. and U.C.; software, J.M.-C.; validation, A.J.-G.; formal analysis, J.M.-C.; data curation, J.M.-C. and S.W.; writing—Original draft preparation, J.M.-C., S.W., M.K.A. and U.C.; writing—Review and editing, J.M.-C., A.T., N.B., and U.C.; supervision—U.C. All authors have read and agreed to the published version of the manuscript.

Funding: This research was funded by Deutsche Forschungsgemeinschaft (DFG) DFG BI 195/77-1, BMBF (German Ministry of Education and Research) 16SV7701 CoMiCon, LUMINOUS-H2020-FETOPEN-2014-2015-RIA (686764), and Wyss Center for Bio and Neuroengineering, Geneva.

Conflicts of Interest: The authors declare no conflict of interest.

References

- Hossain, Z.; Shuvo, M.M.H.; Sarker, P. Hardware and Software Implementation of Real Time Electrooculogram (EOG) Acquisition System to Control Computer Cursor with Eyeball Movement. In Proceedings of the 4th International Conference on Advances in Electrical Engineering (ICAEE), Dhaka, Bangladesh, 28–30 September 2017; IEEE: Piscataway, NJ, USA, 2017; pp. 132–137. [\[CrossRef\]](#)
- Usakli, A.B.; Gurkan, S. Design of a Novel Efficient Human–Computer Interface: An Electrooculogram Based Virtual Keyboard. *IEEE Trans. Instrum. Meas.* **2010**, *59*, 2099–2108. [\[CrossRef\]](#)
- Argentim, L.M.; Castro, M.C.F.; Tomaz, P.A. Human Interface for a Neuroprosthesis Remotely Control. In Proceedings of the 11th International Joint Conference on Biomedical Engineering Systems and Technologies, Funchal, Madeira, Portugal, 19–21 January 2018; SCITEPRESS—Science and Technology Publications: Setubal, Portugal, 2018; pp. 247–253. [\[CrossRef\]](#)
- Rokonuzzaman, S.M.; Ferdous, S.M.; Tuhin, R.A.; Arman, S.I.; Manzar, T.; Hasan, M.N. Design of an Autonomous Mobile Wheelchair for Disabled Using Electrooculogram (EOG) Signals. In *Mechatronics*; Jablonski, R., Brezina, T., Eds.; Springer: Berlin/Heidelberg, Germany, 2011; pp. 41–53.
- Barea, R.; Boquete, L.; Bergasa, L.M.; López, E.; Mazo, M. Electro-Oculographic Guidance of a Wheelchair Using Eye Movements Codification. *Int. J. Robot. Res.* **2003**, *22*, 641–652. [\[CrossRef\]](#)
- Yathunathan, S.; Chandrasena, L.U.R.; Umakanthan, A.; Vasuki, V.; Munasinghe, S.R. Controlling a Wheelchair by Use of EOG Signal. In Proceedings of the 4th International Conference on Information and Automation for Sustainability, Colombo, Sri Lanka, 12–14 December 2008; IEEE: Piscataway, NJ, USA, 2008; pp. 283–288. [\[CrossRef\]](#)
- Mazo, M.; Rodríguez, F.J.; Lázaro, J.L.; Ureña, J.; García, J.C.; Santiso, E.; Revenga, P.A. Electronic Control of a Wheelchair Guided by Voice Commands. *Control. Eng. Pract.* **1995**, *3*, 665–674. [\[CrossRef\]](#)
- Chaudhary, U.; Mrachacz-Kersting, N.; Birbaumer, N. Neuropsychological and Neurophysiological Aspects of Brain-computer-interface (BCI)-control in Paralysis. *J. Physiol.* **2020**, JP278775. [\[CrossRef\]](#) [\[PubMed\]](#)
- Chaudhary, U.; Birbaumer, N.; Curado, M.R. Brain-Machine Interface (BMI) in Paralysis. *Ann. Phys. Rehabil. Med.* **2015**, *58*, 9–13. [\[CrossRef\]](#) [\[PubMed\]](#)
- Chaudhary, U.; Birbaumer, N.; Ramos-Murguialday, A. Brain–Computer Interfaces in the Completely Locked-in State and Chronic Stroke. In *Progress in Brain Research*; Elsevier: Amsterdam, The Netherlands, 2016; Volume 228, pp. 131–161. [\[CrossRef\]](#)

11. Chaudhary, U.; Birbaumer, N.; Ramos-Murguialday, A. Brain–Computer Interfaces for Communication and Rehabilitation. *Nat. Rev. Neurol.* **2016**, *12*, 513–525. [[CrossRef](#)]
12. Rosen, J.; Brand, M.; Fuchs, M.B.; Arcan, M. A Myosignal-Based Powered Exoskeleton System. *IEEE Trans. Syst. Man Cybern. Part. A Syst. Hum.* **2001**, *31*, 210–222. [[CrossRef](#)]
13. Ferreira, A.; Celeste, W.C.; Cheein, F.A.; Bastos-Filho, T.F.; Sarcinelli-Filho, M.; Carelli, R. Human-Machine Interfaces Based on EMG and EEG Applied to Robotic Systems. *J. NeuroEng. Rehabil.* **2008**, *5*, 10. [[CrossRef](#)]
14. Chaudhary, U.; Xia, B.; Silivoni, S.; Cohen, L.G.; Birbaumer, N. Brain–Computer Interface–Based Communication in the Completely Locked-In State. *PLOS Biol.* **2017**, *15*, e1002593. [[CrossRef](#)]
15. Khalili Ardali, M.; Rana, A.; Purmohammad, M.; Birbaumer, N.; Chaudhary, U. Semantic and BCI-Performance in Completely Paralyzed Patients: Possibility of Language Attrition in Completely Locked in Syndrome. *Brain Lang.* **2019**, *194*, 93–97. [[CrossRef](#)]
16. Gallegos-Ayala, G.; Furdea, A.; Takano, K.; Ruf, C.A.; Flor, H.; Birbaumer, N. Brain Communication in a Completely Locked-in Patient Using Bedside near-Infrared Spectroscopy. *Neurology* **2014**, *82*, 1930–1932. [[CrossRef](#)] [[PubMed](#)]
17. Bharadwaj, S.; Kumari, B.; Tech, M. Electrooculography: Analysis on Device Control by Signal Processing. *Int. J. Adv. Res. Comput. Sci.* **2017**, *8*, 787–790.
18. Heide, W.; Koenig, E.; Trillenber, P.; Kömpf, D.; Zee, D.S. Electrooculography: Technical Standards and Applications. *Electroencephalogr. Clin. Neurophysiol. Suppl.* **1999**, *52*, 223–240. [[PubMed](#)]
19. Lv, Z.; Wang, Y.; Zhang, C.; Gao, X.; Wu, X. An ICA-Based Spatial Filtering Approach to Saccadic EOG Signal Recognition. *Biomed. Signal. Process. Control.* **2018**, *43*, 9–17. [[CrossRef](#)]
20. Wu, S.L.; Liao, L.D.; Lu, S.W.; Jiang, W.L.; Chen, S.A.; Lin, C.T. Controlling a Human–Computer Interface System with a Novel Classification Method That Uses Electrooculography Signals. *IEEE Trans. Biomed. Eng.* **2013**, *60*, 2133–2141. [[CrossRef](#)]
21. Huang, Q.; He, S.; Wang, Q.; Gu, Z.; Peng, N.; Li, K.; Zhang, Y.; Shao, M.; Li, Y. An EOG-Based Human–Machine Interface for Wheelchair Control. *IEEE Trans. Biomed. Eng.* **2018**, *65*, 2023–2032. [[CrossRef](#)]
22. Larson, A.; Herrera, J.; George, K.; Matthews, A. Electrooculography Based Electronic Communication Device for Individuals with ALS. In Proceedings of the IEEE Sensors Applications Symposium (SAS), Glassboro, NJ, USA, 13–15 March 2017; IEEE: Piscataway, NJ, USA, 2017; pp. 1–5. [[CrossRef](#)]
23. Iñáñez, E.; Azorin, J.M.; Perez-Vidal, C. Using Eye Movement to Control a Computer: A Design for a Lightweight Electro-Oculogram Electrode Array and Computer Interface. *PLoS ONE* **2013**, *8*, e67099. [[CrossRef](#)]
24. Kherlopian, A.; Sajda, P.; Gerrein, J.; Yue, M.; Kim, K.; Kim, J.W.; Sukumaran, M. Electrooculogram Based System for Computer Control Using a Multiple Feature Classification Model. 4. In Proceedings of the 28th IEEE EMBS Annual International Conference, New York, NY, USA, 30 August–3 September 2006.
25. Arai, K.; Mardiyanto, R. A Prototype of Electric Wheelchair Controlled by Eye-Only for Paralyzed User. *J. Robot. Mechatron.* **2011**, *23*, 66–74. [[CrossRef](#)]
26. Heo, J.; Yoon, H.; Park, K. A Novel Wearable Forehead EOG Measurement System for Human Computer Interfaces. *Sensors* **2017**, *17*, 1485. [[CrossRef](#)]
27. Qi, L.J.; Alias, N. Comparison of ANN and SVM for Classification of Eye Movements in EOG Signals. *J. Phys. Conf. Ser.* **2018**, *971*, 012012. [[CrossRef](#)]
28. Guo, X.; Pei, W.; Wang, Y.; Chen, Y.; Zhang, H.; Wu, X.; Yang, X.; Chen, H.; Liu, Y.; Liu, R. A Human-Machine Interface Based on Single Channel EOG and Patchable Sensor. *Biomed. Signal. Process. Control.* **2016**, *30*, 98–105. [[CrossRef](#)]
29. Erkamaz, H.; Ozer, M.; Orak, İ.M. Detection of Directional Eye Movements Based on the Electrooculogram Signals through an Artificial Neural Network. *Chaos Solitons Fractals* **2015**, *77*, 225–229. [[CrossRef](#)]
30. Merino, M.; Rivera, O.; Gomez, I.; Molina, A.; Dorrnoro, E. A Method of EOG Signal Processing to Detect the Direction of Eye Movements. In Proceedings of the First International Conference on Sensor Device Technologies and Applications, Venice, Italy, 18–25 July 2010; IEEE: Piscataway, NJ, USA, 2010; pp. 100–105. [[CrossRef](#)]
31. Aungsakul, S.; Phinyomark, A.; Phukpattaranont, P.; Limsakul, C. Evaluating Feature Extraction Methods of Electrooculography (EOG) Signal for Human-Computer Interface. *Procedia Eng.* **2012**, *32*, 246–252. [[CrossRef](#)]
32. Phukpattaranont, P.; Aungsakul, S.; Phinyomark, A.; Limsakul, C. Efficient Feature for Classification of Eye Movements Using Electrooculography Signals. *Therm. Sci.* **2016**, *20*, 563–572. [[CrossRef](#)]

33. Boser, B.; Guyon, I.; Vapnik, V. A Training Algorithm for Optimal Margin Classifiers. In Proceedings of the Fifth Annual Workshop on Computational Learning Theory, Pittsburgh, PA, USA, 27–29 July 1992; Association for Computing Machinery: New York, NY, USA, 1992; pp. 144–152.
34. Vapnik, V.; Golowich, S.E.; Smola, A.J. Support Vector Method for Function Approximation, Regression Estimation and Signal Processing. In *Advances in Neural Information Processing Systems*; Mozer, M.C., Jordan, M.L., Petsche, T., Eds.; MIT Press: Cambridge, MA, USA, 1997.
35. Hess, C.W.; Muri, R.; Meienberg, O. Recording of Horizontal Saccadic Eye Movements: Methodological Comparison Between Electro-Oculography and Infrared Reflection Oculography. *Neuro Ophthalmol.* **1986**, *6*, 189–197. [[CrossRef](#)]
36. Barea, R.; Boquete, L.; Ortega, S.; López, E.; Rodríguez-Ascariz, J.M. EOG-Based Eye Movements Codification for Human Computer Interaction. *Expert Syst. Appl.* **2012**, *39*, 2677–2683. [[CrossRef](#)]
37. Chang, W.D. Electrooculograms for Human–Computer Interaction: A Review. *Sensors* **2019**, *19*, 2690. [[CrossRef](#)]
38. Barea, R.; Boquete, L.; Mazo, M.; Lopez, E. System for Assisted Mobility Using Eye Movements Based on Electrooculography. *IEEE Trans. Neural Syst. Rehabil. Eng.* **2002**, *10*, 209–218. [[CrossRef](#)]
39. Amari, S.; Wu, S. Improving Support Vector Machine Classifiers by Modifying Kernel Functions. *Neural Netw.* **1999**, *12*, 783–789. [[CrossRef](#)]
40. Ben-Hur, A.; Weston, J. A User’s Guide to Support Vector Machines. In *Data Mining Techniques for the Life Sciences*; Carugo, O., Eisenhaber, F., Eds.; Humana Press: Totowa, NJ, USA, 2010; Volume 609, pp. 223–239. [[CrossRef](#)]
41. Hsu, C.W.; Lin, C.J. A Comparison of Methods for Multiclass Support Vector Machines. *IEEE Trans. Neural Netw.* **2002**, *13*, 415–425. [[CrossRef](#)]
42. Kohavi, R. A Study of Cross-Validation and Bootstrap for Accuracy Estimation and Model Selection. *Int. Jt. Conf. Artif. Intell.* **1995**, *14*, 8.
43. Barea, R.; Boquete, L.; Rodríguez-Ascariz, J.M.; Ortega, S.; López, E. Sensory System for Implementing a Human-Computer Interface Based on Electrooculography. *Sensors* **2010**, *11*, 310–328. [[CrossRef](#)] [[PubMed](#)]
44. Pander, T.; Przybyła, T.; Czabanski, R. An Application of Detection Function for the Eye Blinking Detection. In Proceedings of the Conference on Human System Interactions, Krakow, Poland, 25–27 May 2008; IEEE: Piscataway, NJ, USA, 2008; pp. 287–291. [[CrossRef](#)]

Sample Availability: Corresponding code and data are available at <https://github.com/JayroMartinez/EOG-Classification>.



© 2020 by the authors. Licensee MDPI, Basel, Switzerland. This article is an open access article distributed under the terms and conditions of the Creative Commons Attribution (CC BY) license (<http://creativecommons.org/licenses/by/4.0/>).

ORIGINAL ARTICLE

Sleep in the completely locked-in state (CLIS) in amyotrophic lateral sclerosis

Azim Malekshahi^{1,†,‡}, Ujwal Chaudhary^{1,2,*†,‡,§}, Andres Jaramillo-Gonzalez¹, Alberto Lucas Luna^{1,‡}, Aaygul Rana^{1,‡}, Alessandro Tonin^{1,‡}, Niels Birbaumer^{1,2,*} and Steffen Gais¹

¹Institute of Medical Psychology and Behavioral Neurobiology, University of Tübingen, Tübingen, Germany and

²Wyss-Center for Bio- and Neuro-Engineering, Geneva, Switzerland

[†]These authors contributed equally.

[‡]Data collection.

[§]Principal investigator of the project.

*Corresponding author. Niels Birbaumer, Wyss-Center for Bio- and Neuro-Engineering, Chemin de Mines 9, CH 1202, Geneva. Email: niels.birbaumer@wysscenter.ch. Ujwal Chaudhary, Institute of Medical Psychology and Behavioral Neurobiology, Eberhard-Karls-University of Tübingen, Silberstraße 5, 72076 Tübingen, Germany. Email: chaudharyujwal@gmail.com.

Abstract

Persons in the completely locked-in state (CLIS) suffering from amyotrophic lateral sclerosis (ALS) are deprived of many zeitgebers of the circadian rhythm: While cognitively intact, they are completely paralyzed, eyes mostly closed, with artificial ventilation and artificial nutrition, and social communication extremely restricted or absent. Polysomnographic recordings in eight patients in CLIS, however, revealed the presence of regular episodes of deep sleep during night time in all patients. It was also possible to distinguish an alpha-like state and a wake-like state. Classification of rapid eye movement (REM) sleep is difficult because of absent eye movements and absent muscular activity. Four out of eight patients did not show any sleep spindles. Those who have spindles also show K-complexes and thus regular phases of sleep stage 2. Thus, despite some irregularities, we found a surprisingly healthy sleep pattern in these patients.

Statement of Significance

The presence of circadian variation in EEG activity points to a conserved sleep-wake cycle in amyotrophic lateral sclerosis (ALS) patients in completely locked-in state (CLIS). There are marked differences between these patients and healthy participants, e.g. a complete loss of sleep spindles in some patients and the presence of sinusoid, high-amplitude theta activity instead of alpha activity. Slow-wave generation, on the other hand, seems intact in all patients. Rapid eye movement (REM) sleep is present in at least some patients, but it cannot be ascertained in all patients. The existence of intact sleep in patients in CLIS is another important sign that their wakefulness is likewise intact. It also indicates that providing undisturbed sleep opportunity will be important for the patients' mental well-being.

Key words: movement disorders; neurological disorders; sleep/wake physiology; circadian rhythms; completely locked-in state; polysomnography

Submitted: 23 January, 2019; Revised: 7 June, 2019

© Sleep Research Society 2019. Published by Oxford University Press on behalf of the Sleep Research Society. All rights reserved. For permissions, please e-mail journals.permissions@oup.com.

Introduction

The sleep-wake cycle is a crucial component of neural and bodily development and restitution involved in a plethora of homeostatic processes [1]. Different exogenous zeitgebers, such as daylight, social stimulation, motor activity or food intake, synchronize the various central and peripheral endogenous oscillators [2-7]. In the locked-in condition and the completely locked-in state (CLIS) [8], most of these zeitgebers are absent or attenuated due to complete immobility and absence of muscular activity, artificial respiration, artificial feeding and artificial lighting [9-12]. Patients in CLIS suffering from advanced motor neuron diseases such as amyotrophic lateral sclerosis (ALS), who have an inability to open or close their eyes voluntarily, have their eyes closed most of the day and during the night to avoid drying of the immobile eyeball and cornea. In some cases, the complete closure of the eyelids remains impossible, leading to corneal lesions due to extensive drying with little or no differentiated vision left. Artificial feeding and breathing through a tracheostoma impose an extreme regularity on the internal organ systems, impeding the differentiation between day and nighttime. Social stimulation is certainly more frequent during the day but 24-hour care entails multiple activities also during the night (suction of saliva, excrements, eye care, position changes to avoid decubitus, change of tubes and feeding devices, etc.). The reduction of active social interaction and the complete lack of (verbal or signing) communication further minimize the differences between daytime and nighttime stimulation. Muscular paralysis also dramatically reduces the amount of afferent proprioceptive inputs towards the spinal cord and brain. Patients are bedridden and completely motionless over months and years, except during short periods of passive position changes. Although effects of constant conditions on homeostatic and circadian processes and on sleep have been investigated in constant routine studies and forced desynchrony protocols [13], in CLIS patients who constantly live in a controlled environment, the effects on their circadian rhythm are largely unknown [14]. Although, the scientific literature is rich on circadian rhythm and sleep-wake cycle in healthy populations [15-19] and patients with other neurological disorders [14, 20-25], there exists virtually no information about circadian rhythm and sleep-wake cycle in patients in the CLIS.

For brain-computer interface (BCI) communication with these patients, it is necessary to discriminate periods of sleep and wakefulness in the individual EEG. It has been argued that the main reason for decreased or random performance in BCI communication might be the lack of attention and the presence of micro sleep during the presentation of the questions [11]. In a study of one CLIS and two LIS patients over a whole year it has been shown that a reduced P300 amplitude during the BCI task predicted lower performance, again suggesting reduced wakefulness and attention as a major limiting factor for BCI applications in these severely compromised patients [26].

To our knowledge, the sleep pattern of only one patient from our lab shortly after the transition from the locked-in state to the CLIS has been reported [27]. An irregular sleep pattern with daytime episodes of slow-wave sleep disrupted slow-wave sleep during the night and irregular appearance of different sleep stages during day and night was reported in this patient. The overall slow-wave sleep duration was normal for the age of the patient. It is of clinical and theoretical importance to study sleep

in a larger sample of CLIS patients. The presence of distinguishable sleep and wake periods in these patients would constitute another piece of evidence for their cognitive functioning. Undisturbed sleep could also serve to prevent depression and maintain sufficiently high quality of life in these patients [28].

Hence, to elucidate their sleep-wake cycle, we recorded sleep in eight CLIS patients. We will outline criteria, which can be used to delineate the sleep stages, and describe and discuss the sleep cycles of the individual patients. Already at this point we need to mention the main limitations of this research, which are dictated by the clinical condition: the absence of eye movements and of changes in muscular tone due to the complete paralysis complicate scoring of rapid eye movement (REM) sleep. Mainly because of this limitation, it is impossible to label each 30-second epoch of the night with a sleep stage. We, therefore, refrain from presenting hypnograms and percentages of sleep stages, but only describe which sleep stages occur in a specific patient.

Materials and Methods

The Internal Review Board of the Medical Faculty of the University of Tübingen approved the experiment reported in this study and the patients' legal representatives gave written informed consent for the study with permission to publish the results. The study is in full compliance with the ethical practice of Medical Faculty of the University of Tübingen. The clinical trial registration number is ClinicalTrials.gov identifier: NCT02980380.

Patients

The details of patients 1, 3, and 4 are described in Ref. [11] as patients F, G, and W, respectively. The remaining patients are described below.

Patient 5 (male, 50 years old, CLIS) was diagnosed with bulbar sporadic ALS in May 2008, as locked-in in 2009, and as completely locked-in May 2010, based on the diagnosis of neurologists and on our recordings (see below and Ref. [11]). He has been artificially ventilated since September 2009, fed through a percutaneous endoscopic gastrostomy tube since October 2009, and is in home care. No communication with eye movements, other muscles, or assistive communication devices was possible since 2010.

Patient 6 (male, 38 years old, CLIS) was diagnosed with bulbar ALS in 2009. He lost speech and capability to move by 2010. He has been artificially ventilated since September 2010 and is in home care. No communication with eye movements, other muscles, or assistive communication devices was possible since 2012.

Patient 7 (female, 57 years old, CLIS) was diagnosed with Mills' syndrome of ALS with atypical progression at the beginning of 2010. She lost speech and capability to walk by 2011. She has been fed through a percutaneous endoscopic gastrostomy tube since June 2010, artificially ventilated since June 2010, and was in home care until she passed away in 2017. She started using assistive communication devices employing eye movement for communication in 2011. Eye-tracker-based communication failed at the beginning of 2015. The family and caretakers communicated with her since the middle of 2015 based on her thumb-movements, which after a year became unreliable.

Patient 9 (male, 23 years old, CLIS) was diagnosed with juvenile ALS with FUS mutation heterozygote on Exon 14: c.1504delG, gene mutation diagnosed in 2013. He has been artificially ventilated since August 2014 and is in home care. He started communication using MyTobii eye-tracking device in January 2015. He was able to communicate with MyTobii until December 2015 after which the family members attempted to communicate by training him to move his facial muscles near the nose to answer "yes" but the response was unreliable. No communication was possible since June 2016.

Patient 10 (male, 25 years old, locked-in state on the verge of CLIS) was diagnosed with familial juvenile ALS with ALS 6-FUS gene mutation in December 2012. He was completely paralyzed within a year after diagnosis, has been artificially ventilated since November 2013, and is in home care. He was able to communicate with eye-tracking from early 2014 to August 2016 but was unable to use the eye-tracking device after the loss of eye control in August 2016. No communication with eye movements, other muscles, or assistive communication devices was possible since 2016.

In none of these patients, voluntary eye movement responses to questions were recorded in any of the recording sessions. None of these patients showed any brain disease unrelated to ALS. CLIS onset was on average 38 months after initial diagnosis, which corresponds to expectations [29]. The proportion of juvenile-onset ALS was higher in our sample than in the general population of ALS patients [30].

Sleep recording

Sleep EEG was recorded consecutively for two nights from each patient, except patient 4 and 7 (one night only). The first recording was carried out in order to adapt the patients to the electrodes. The second night EEG, EMG, and EOG were recorded for later sleep scoring. As shown in Table 1, sleep EEG data was acquired for more than 12 hours for all the patients, except patient 4.

The sleep polysomnography was recorded with a multi-channel EEG amplifier (Brain Amp DC, Brain Products, Germany) from 11 Ag/AgCl passive electrodes mounted on a head cap. Six electrodes (F3, F4, C3, C4, O1, and O2) were used to acquire EEG signals, four electrodes were used to acquire the vertical and horizontal EOGs, and one electrode was used to acquire chin-EMG. EEG-channels were referenced to an electrode on the right mastoid and grounded to the electrode placed at the Fz location of the scalp. Electrode impedances were kept below 10 k Ω and the EEG signal was sampled at 500 Hz.

Table 1. Summary of findings for each patient

Patient	Start of recording	End of recording	W [active]	W [inactive]	α -like freq.	SWS	REM sleep	Sleep spindles
1	10:34 pm	11:14 am	+	+	4-6 Hz	+	(+)	-
3	10:00 pm	10:17 am	(+)	+	4-7 Hz	+	+	(few)
4	10:14 pm	07:33 am	+	+	2-4 Hz	+	(+)	+
5	08:32 pm	05:11 pm	+	+	3-6 Hz	+	+	-
6	08:38 pm	03:45 pm	+	+	2-4 Hz	+	(uncertain)	-
7	09:10 pm	08:50 am	(+)	+	1-3 Hz	+	(+)	+
9	02:04 pm	09:04 am	+	+	3-5 Hz	+	(+)	+
10	06:49 pm	09:53 am	(+)	+	2-4 Hz	+	(uncertain)	-

+: clear signs of sleep stage present; (+): some signs of sleep stage present; (uncertain): possible signs of sleep stage present; -: no sign of sleep stage present.

Preprocessing

The recorded EEG and EOG signals were low-pass filtered using a finite impulse response low-pass filter of 30 Hz. For the EMG, the signal was filtered with a 50 Hz notch filter.

Sleep scoring

The EEG of patients in CLIS is dissimilar in large extents to that of healthy participants. These patients show, e.g. regular high-amplitude oscillatory activity in the theta (4-8 Hz) frequency range for longer periods of time, which cannot be found in healthy participants. Moreover, they have no detectable eye movements during wakefulness and no muscle tone, due to their condition. Thus, the standard sleep-scoring criteria, particularly for REM sleep, have to be adapted to score the sleep stages from patients in CLIS. Still, initial visual inspection of the whole night EEG shows already obvious variations of EEG patterns over time. It can, therefore, be hypothesized that the states of arousal and consciousness also fluctuate throughout the night. Based on time of day and on interaction with the patient (movement artifacts), we had a starting point for a rough assumption of sleep and wakefulness: during the night, longer quiet periods without movement would have a higher probability of representing sleep than morning recordings and periods directly after movement (suction of saliva, repositioning of the patient). We then applied the criteria of Rechtschaffen and Kales [31] to the recordings to determine whether some features of sleep could be found. This scoring was performed visually on 30-s epochs. It resulted in the detection of a number of EEG patterns that generalized over patients, some of which resembled the classical sleep stages. Scoring was done by an experienced sleep scorer (S.G.) and discussed in detail among all authors. We describe the criteria that had to be adjusted as well as the criteria that could be applied directly in the results section.

Signal analysis

Power spectra were computed using Welch's method with a resolution of 0.5 Hz for each 30-second epoch for all EEG channels. Channels containing obvious artifacts were excluded from further analysis. Whole-night spectrograms were calculated based on the median of all artifact-free channels. The median was used to further suppress artifacts and unusually high or low power values. Spectrograms were normalized by subtracting the median and dividing by the value of the 75th quantile of each frequency, analogous to Z-standardization, in order to have comparable ranges. The scale of the spectrograms is, therefore,

dimensionless. Additionally, for all patients, the power spectra of a period of quiet wakefulness is presented to show peaks in EEG power.

As the heartbeat was clearly reflected in the EMG trace of two patients (Pat. 1 and Pat. 5), we used these recordings to calculate the continuous heart rate. The 50 Hz notch-filtered EMG channel was band-pass filtered between 5 and 70 Hz using an IIR filter. Individual heart beats were detected as spikes in the signal. Spikes that were too large or too small were removed as outliers. Then, heart rate was calculated from the distance between spikes. Finally, outliers in heart rate were removed and the whole time series filtered with a 30-point moving average filter.

Results

Three main observations could be made during visual sleep scoring: (1) All patients had cyclic changes in their brain activity throughout the recording in the sense that we found alternating periods with and without slow-wave activity. (2) The discrepancy to healthy sleep EEG differed between patients. (3) Some commonalities in EEG anomalies across patients could be found.

Because we observed that each patient has his or her own idiosyncrasies in the sleep-wake cycle, the result of each patient will be described first in this section. Subsequently, we will describe common patterns between participants and suggest heuristics for the scoring of sleep in CLIS patients. Exemplary epochs for individual sleep stages and whole-night power spectrograms can be found for each patient in the [Supplementary Material](#). Exemplary data for patient 9 is presented in [Figure 1](#).

Patient 9

This patient shows clear high amplitude slow waves during the night, starting at around 1:30 am ([Figure 1](#)). These waves are in shape and in their clustered occurrence indistinguishable from slow waves of healthy patients. In the spectrogram, they are visible as a strong <math><2\text{ Hz}</math> band. For longer periods of up to 45 minutes, the criteria for slow-wave sleep (SWS), sleep stages 3 (S3) or S4 are reached. For about 1 hour before the onset of S3, individual slow waves (K-complexes) and sleep spindles can be found (S2). In-between periods of S2, epochs dominated by bursts of regular, sinusoidal EEG activity of 3–5 Hz with medium to high amplitude can be found. These bursts have varying length, typically

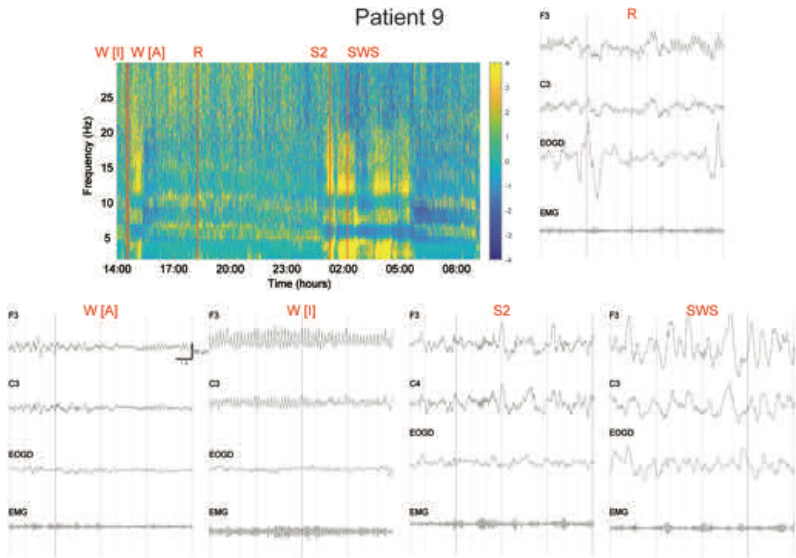


Figure 1. Normalized spectrogram (upper left) and segments of selected sleep epochs of patient 9. Yellow color in the spectrogram reflects higher than average activity in a frequency band; blue color signifies lower than average activity. Red lines on the spectrogram indicate epochs belonging to particular sleep stages. Twelve-second segments of these epochs are shown in the other panels. Here, vertical lines represent 1-s intervals. The EEG during active wakefulness (W[A]) is largely similar to that of healthy participants. EEG activity during inactive wakefulness (W[I]) is around 5 Hz, but resembles alpha activity rather than typical theta activity. Stage 2 sleep (S2) with spindles and K-complexes as well as slow-wave sleep (SWS) can be clearly discerned in this patient. Note the large eye movements during REM sleep (R), which the patient is unable to perform voluntarily during wakefulness. Recordings of the other patients are available in the [Supplementary Material](#), following the same arrangement.

between 5 and 20 seconds. Because of its regularity and the duration of bursts, this activity is strongly reminiscent of alpha activity (see Figure 1, section W[II]). It also occurs for longer periods of several hours in the afternoon and in the evening before the first signs of S2. Although having theta band frequency, these waves have no similarity to the typical, irregular, sawtooth-shaped theta activity of healthy participants. Except for its frequency, this activity, therefore, in all other aspects seems to be equivalent to alpha activity in healthy patients. We, therefore, use this alpha-like activity to score periods of inactive, relaxed wakefulness (W[II]). Starting around 6:00 am, after signs of S2 have diminished, longer periods of low amplitude, high-frequency activity appear. Frequencies are dominated by beta-band activity, with a varying degree of intermixed irregular theta activity. Because of its similarity to typical wake activity and because of its strongest occurrence in the morning after sleep, we score this activity pattern as active wakefulness (W[A]). In the morning, this high-frequency activity is occasionally interrupted by 5- to 20-second periods of regular theta activity as described above (W[II]). In the afternoon, the pattern inverts and long periods of W[II] are interrupted by epochs of W[A].

Unrelated to S2 or SWS sleep phases, there are some epochs that show eye movements that resemble those typical for REM sleep. These occur mainly in the afternoon in the middle of longer periods of W[II], and are accompanied by a brief discontinuation of the alpha-like regular theta activity and appearance of irregular theta and beta waves. Although the timing of these periods is not typical for REM sleep, we suggest that these signs are indicative of REM sleep-like processes and score the corresponding epochs as REM sleep (R).

Patient 1

This patient shows clear high amplitude slow waves (SWS) during the night, starting at around 2:00 am (Supplementary Figure S1). These waves are co-occurring with sinusoidal 4–7 Hz activity in some epochs. There are two more periods of SWS around 5:30 am and 7:30 am. There are no signs of sleep spindles throughout the night. The EEG in the evening before occurrence of SWS is dominated by the same regular, alpha-like 4–7 Hz (theta) activity (W[II]) as in patient 9, although with a lower amplitude. It is intermixed with high-frequency, low-amplitude activity (W[A]) to varying degrees. Interspersed throughout the recording are periods of dominant irregular theta activity during which REMs are manifest. Although the timing of these periods is not typical for REM sleep, we again suggest that these signs are indicative of REM sleep-like processes and score the corresponding epochs as R. Heart rate tententially increases or reaches maxima over periods during which we did not detect any SWS (e.g. 10:30 pm – 02:00 am and 08:30 am – 10:30 am). During periods of SWS (marked by strong < 1.5 Hz activity) heart rate tententially decreases.

Patient 3

The EEG of this patient is dominated by regular, high-amplitude, alpha-like 4–7 Hz (theta) activity (W[II]), particularly in the evening and in some parts of the night (Supplementary Figure S2). Starting at 2:00 am, slow waves occur, first together with the alpha-like activity then replacing it more and more. There are several periods of SWS, alternating with periods of W[II]. In

the morning, activity becomes more irregular (high-frequency beta and irregular theta activity), especially after intervals of (external) movement (W[A]); but still these periods contain amounts of alpha-like theta activity. After awakening and morning hygiene there is a 2-hour period of strong, continuous REM, accompanied mainly by irregular (sawtooth) theta activity and only little regular (sinusoidal) alpha-like theta activity. In this patient, the eye movement and EEG activity provide strong evidence for REM sleep. There is also evidence for a few sleep spindles in the morning after the period of morning hygiene and before REM sleep.

Patient 4

We find two >1-hour periods of extensive SWS, at 11:00 pm and at 2:00 am (Supplementary Figure S3). During SWS, strong sleep spindle activity (12–14 Hz) is present. Strong spindle activity is also found during a 1-hour period around 4:00 am, which also presents K-complexes (S2). In-between SWS periods, there are periods dominated by 5- to 20-second bursts of regular, sinusoidal 2–4 Hz activity, which resemble the 4–7 Hz activity described in the patients above. These also occur in the evening, intermixed with high-frequency, low-amplitude activity. Because it shows all properties of alpha activity except the frequency range, we score these periods as W[II]. In the evening before sleep, the EEG is dominated by irregular theta and low-amplitude beta activity W[A]. In the morning starting around 6:00 am, we see similar irregular theta and low-amplitude beta activity, but accompanied by (mainly small and a few larger) REMs. Although difficult to discriminate from W[A], the quieter EMG (no external disturbance), the REMs, and the absence of alpha-like activity lead us to score R.

Patient 5

This patient shows several periods of SWS between 10:00 pm and 5:00 am (Supplementary Figure S4). The slow waves are slower than usual and have a higher amplitude. In the evening before sleep and for 1 hour after the end of SWS in the morning, the EEG is dominated by 3–6 Hz alpha-like activity (W[II]). Starting at 6:00 am, the EEG becomes more mixed with irregular theta, beta, and only little alpha-like activity (W[A]). Throughout the day, periods of W[A] and W[II] alternate. In the afternoon at 05:00 pm, a period of clear REM sleep with strong REMs, irregular theta and low amplitude beta activity was found, which continued for >15 minutes until the end of the recording. No sleep spindles were found in this patient. Heart rate is minimal during the night period, during which strong <1.5 Hz activity is recorded (09:30 pm – 7:30 am). It increases in the morning during interaction with the patient.

Patient 6

In patient 6, there are two clear periods of SWS between 4:30 am and 7:00 am (Supplementary Figure S5). In between these two periods, we find several quiet epochs of low-amplitude, high-frequency activity that contain a certain degree of small eye movements. Because they do not resemble periods of wakefulness in this patient, we label these epochs tentatively as uncertain R. The rest of the day alternates between periods of

W[θ] (mainly in the evening) and W[A] (more abundant in the morning), showing more or less alpha-like 2–4 Hz activity, respectively. Again, no sleep spindles were found.

Patient 7

This patient shows about 1 hour of SWS with very slow, high-amplitude EEG around midnight (Supplementary Figure S6). Before this period, a few minutes of S2 sleep containing sleep spindles was found. This period is also represented with a yellow spot in the 12–15 Hz band in the spectrogram of this patient. The rest of the recording contains mainly mixed frequency activity in the 1–3 Hz, theta, and beta bands. The amount of low-frequency activity varies throughout the recording, probably reflecting W[θ] and W[A]. However, these variations are only gradual, so that a clear distinction between these two stages is difficult in this patient. Moreover, the 1–3 Hz low-frequency activity is less regular and sinusoidal than the alpha-like activity of the previous patients. Although it lies in the delta band and could be taken for slow-wave activity, it occurs also during periods where caretakers interact with the patients, and it much faster than the patients SWS activity, which can be clearly delineated in the patient's spectrogram. We, therefore, believe this activity corresponds to the alpha-like activity in the other patients. During an undisturbed period at the beginning of the night, we found irregular theta activity together with some REMs and an absence of 1–3 Hz activity. We score this as a brief period of R.

Patient 10

The spectrogram of this patient shows three periods of SWS between 3:00 am and 7:00 am (Supplementary Figure S7). During these periods, very slow (<1 Hz) activity can be seen in the sleep recording. These slow waves have the typical shape of sleep slow waves. In the evening before 3:00 am, the EEG is dominated by strong 2–4 Hz activity, which, as in patient 7, can be distinguished from SWS. Because of its regular sinusoidal shape, we score it as alpha-like activity and W[θ]. In the morning, alpha-like activity alternates with slightly faster regular and irregular theta activity, which we score as W[A]. During a period with only a minimum of 2–4 Hz activity, we see a few small eye movements that could represent REMs. We, therefore, score some epochs as uncertain R. Sleep spindles were not found.

The power spectra of channel C3 of all eight patients can be found in Supplementary Figure S8. The figure shows a single peak in the spectrum in most patients. This peak is not found in the alpha band, but in a lower range between 2 and 7 Hz depending on the patient. The individual alpha-like frequency band for each patient is shown in Table 1. Comparing all six recorded channels, we did not observe any obvious topography (e.g. anterior-posterior) of alpha-like activity across the scalp.

Discussion

Polysomnographic recordings in CLIS patients show that these patients have a circadian sleep-wake pattern. All patients show <1 Hz slow-wave activity during one or several periods during the night. In most patients, the dominant activity outside of SWS was a regular, sinusoidal 4–6 Hz or 2–4 Hz activity, which resembles alpha activity in its distribution and burst-like behavior.

This inactive wakefulness could be discriminated from active wakefulness in most patients, with active wakefulness showing irregular, higher frequency activity. Sleep spindles were absent in half of the patients. REM sleep was clearly present in two patients and probably present in most. Impaired REM sleep and lack of sleep spindles were independent, as the two patients showing the strongest REM sleep did not present any sleep spindles.

Slow activity dominates the EEG of CLIS patients during sleep and wakefulness. The slow waves of SWS have their typical frequency in some patients, in others they appear to be distinctly slower. However, all patients have slow waves in the range below 1 Hz, which can be easily detected by visual scoring or automatic analysis in the EEG. The timing of this activity, which occurs mainly after midnight and before 6:00 am in the morning, and which represents the slowest activity for each patient, leaves little doubt, that this activity actually represents SWS. All patients thus showed one or more periods of clear S3 or S4 sleep. Consistent with expectations, in both patients for which heart rate data was available, heart rate was decreasing or minimal during periods scored as SWS. During the 12-hour section of the circadian rhythm that we have recorded, we found longer stretches with slow-wave activity, which were mostly split into several consecutive periods. Night-time periods with and without slow-wave activity did not differ systematically with regard to light or other stimulation, except that sometimes a period of slow-wave activity ended with EMG activation (patient being moved). Our findings speak to an astonishingly well-conserved circadian rhythm, at least within our period of observation. It is, however, possible that there are additional periods of sleep during daytime that we did not record in the present study. Moreover, there might be periods of light S2 sleep, which we have not detected because of the lack of sleep spindles in most patients.

There is, however, another type of slow activity, which can be confounded with SWS in more than half of the patients. Most of the recordings are dominated by a regular oscillation in the upper delta/lower theta range (2–7 Hz). Several reasons speak against this activity being sleep-related. First, it appears at all times of day throughout the recordings: more strongly in the evenings, but also in the mornings. It often continues throughout periods of interaction with the patient. Second, it is distinct from the slower <1 Hz oscillations, which occur during the night, and mostly disappear during these periods. Third, this oscillation has a regular, sinusoidal shape, occurs in 5- to 20-second bursts, and has a waxing and waning amplitude during these bursts. Its shape clearly distinguishes it from theta and delta activity, which is usually more sawtooth or rectangular shaped. In most patients, it is also reflected by a single, pronounced peak in the power spectrum. Apart from the lower frequency, it is therefore strongly reminiscent of periods of alpha, which occur during resting wakefulness with eyes closed in healthy participants.

CLIS patients have their eyes closed most of the time to prevent drying of the eyeballs. It could, therefore, be expected to see strong alpha oscillations, but none are found in the 8–12 Hz range in any patient. Previous studies in locked-in ALS patients also showed a significant reduction in the alpha band over the central electrodes [32]. Moreover, our observations confirm the observations of Hohmann et al. [33], who showed in two CLIS patients that alpha frequency activity has completely disappeared and shifted towards lower frequencies. We, therefore,

hypothesize that the continuous alpha activity is gradually slowing in frequency throughout the progression of the disease, may be due to lack of sensory stimulation or overuse of alpha-generating circuitry. This, however, remains open for further investigation.

In fact, there are reports of "alpha coma" and dominant alpha-theta activity in locked-in patients that are not completely locked-in [34, 35]. The alpha-like theta/delta oscillation might, therefore, serve as an indicator of absence of slow-wave sleep. In healthy participants, alpha activity serves, together with rolling eye movements, as an indicator of falling asleep (S1). No CLIS patient showed rolling eye movements. Because of the persistence of alpha-like activity, the impossibility to describe consistent and distinct features of wake EEG in these patients, and the lack of light S2 sleep in most patients, it was impossible to distinguish a transitory S1 sleep stage in CLIS patients. We have therefore described the state of continuous (>50% of an epoch) alpha-like activity as inactive wakefulness (W|I). During most parts of the day, this stage alternates with periods of active wakefulness, which has faster more irregular activity with lower amplitudes.

Sleep spindles (11–17 Hz), are the hallmark of light S2 sleep. These were completely absent in four out of eight patients. The lack of sleep spindles mirrors the findings by Pavlov *et al.* [36], who also found few or no spindles in most of their non-responsive (vegetative state) patients. It is yet unclear when and why sleep spindles cease to occur in these patients. As spindles have been linked to the reprocessing of new memories during sleep [37], one might speculate that the daily routine of the patients with lack of change or new information renders sleep spindles superfluous. It is conceivable that the frequency of spindle oscillations also slows with the progression of the disease, but we have not found any indication of such a slowing. In fact, in those patients with spindles, these had all typical characteristics of sleep spindles in healthy participants. K-complexes, which often have a higher frequency than full slow-waves, were difficult to delineate. The presence of high-amplitude delta and theta band activity during wakefulness prevents the clear definition of individual K-complexes. However, no periods resembling S2 sleep (low-amplitude activity with a few, clearly delineated high-amplitude waves) were found in patients that did not also show sleep spindles.

Scoring of REM sleep according to standard rules relies largely on eye movements and muscle tone changes. Although patients in CLIS cannot produce any voluntary eye movements or muscle contractions, we found strong REMs during sleep in two patients and rudimentary eye movements during sleep in another four patients. This finding indicates that voluntary and autonomous eye movement control can be independent in CLIS patients. REM sleep-like irregular theta activity with medium amplitude was present during these REM periods. Scoring of REM sleep by EEG alone, which is feasible by experienced scorers in healthy patients, was impossible in our patients. The EEG could only be used in conjunction with the eye movement signal, and confident judgments of REM sleep were only possible in a few patients. Heart rate, which was unfortunately available only in patients 1 and 5, might be an additional helpful parameter for scoring REM sleep. In both patients, heart rate during periods scored as REM sleep or potential REM sleep was higher than during periods scored as sleep, and variability of the heart

rate was greater. Further studies should consider placing explicit ECG electrodes.

Although we did not find any increase in spectral power during REM sleep, we noticed a distinctive decline in 2–3 Hz activity in the spectrograms of those patients with strong REMs. We found similar periods of distinctly decreased power in this frequency band in most patients. Visual inspection of the EEG during these periods visually confirmed REM sleep-like theta activity with small deflections in the EOG trace that could not be accounted for other than by eye movements (e.g. no corresponding activity in the EEG traces, no movement artifacts). These eye movements are much smaller and fewer than those habitually seen in healthy participants, but still, as there are no other sources of artifacts in CLIS patients, they can be taken as signs of autonomous eye movement activity. We can thus confirm the presence of REM sleep in some CLIS patients and the presence of possible REM sleep in most. However, new rules for scoring REM sleep, perhaps based on spectral EEG power, should be developed to increase sleep scoring accuracy in these patients. The present data indicates that REM sleep seems to be uncoupled from the typical NREM-REM cycle and to occur at different times of the day. This pattern might be related to the lack of movement and structure in the daily routine of the patients or to an uncoupling of circadian and ultradian cycles. Comparison with other bed-ridden patients might illuminate this aspect of CLIS sleep.

The analysis of the nighttime EEG demonstrates that patients in CLIS with ALS show slow-wave sleep episodes comparable to the healthy aged population. The two younger patients (9 and 10), suffering from a genetically determined ALS, do not substantially differ from the older ALS patients. Overall, sleep is fragmented, as already noticed [27], in these completely inactive patients, which spend most of their time, some of them since more than 5 years, in a completely paralyzed state in their bed, with only some transfer to the wheelchair during daytime. This constant, mostly bedridden routine and closed eyes, weakening the influence of light as the most potent zeitgeber, might be one reason for the disruption of the NREM-REM cycle and the absence of some of the typical sleep signs. Further studies should include neuroimaging to allow a more mechanistic investigation of the relation between pathologic changes in the brain and in sleep. Still, the maintenance of SWS in all patients might be an important factor contributing to preserve the quality of life in patients in an advanced locked-in state. Undisturbed nighttime sleep should, therefore, be aimed at in CLIS patient care.

Supplementary material

Supplementary material is available at SLEEP online.

Funding

The work of the authors is supported by the Deutsche Forschungsgemeinschaft (DFG, Kosellek) DFG BI 195/77-1, BMBF (German Ministry of Education and Research) 16SV7701 CoMiCon, LUMINOUS-H2020-FETOPEN-2014-2015-RIA (686764), and Wyss Center for Bio and Neuroengineering, Geneva.

Conflict of interest statement. None declared.

References

- Jennett B, et al. Persistent vegetative state after brain damage. A syndrome in search of a name. *Lancet*. 1972;1(7753):734-737.
- Boivin DB, et al. Dose-response relationships for resetting of human circadian clock by light. *Nature*. 1996;379(6565):540-542.
- Hastings MH, et al. A clockwork web: circadian timing in brain and periphery, in health and disease. *Nat Rev Neurosci*. 2003;4(8):649-661.
- Challet E, et al. Synchronization of the molecular clockwork by light- and food-related cues in mammals. *Biol Chem*. 2003;384(5):711-719.
- Mistlberger RE, et al. Social influences on mammalian circadian rhythms: animal and human studies. *Biol Rev Camb Philos Soc*. 2004;79(3):533-556.
- Bell-Pedersen D, et al. Circadian rhythms from multiple oscillators: lessons from diverse organisms. *Nat Rev Genet*. 2005;6(7):544-556.
- Golombek DA, et al. Physiology of circadian entrainment. *Physiol Rev*. 2010;90(3):1063-1102.
- Bauer G, et al. Varieties of the locked-in syndrome. *J Neurol*. 1979;221(2):77-91.
- Birbaumer N. Breaking the silence: brain-computer interfaces (BCI) for communication and motor control. *Psychophysiology*. 2006;43(6):517-532.
- Chaudhary U, et al. Brain-computer interfaces for communication and rehabilitation. *Nat Rev Neurol*. 2016;12(9):513-525.
- Chaudhary U, et al. Brain-Computer Interface-Based Communication in the Completely Locked-In State. *PLoS Biol*. 2017;15(1):e1002593.
- Chaudhary U, et al. Brain-computer interfaces in the completely locked-in state and chronic stroke. *Prog Brain Res*. 2016;228:131-161.
- Blatter K, et al. Circadian rhythms in cognitive performance: methodological constraints, protocols, theoretical underpinnings. *Physiol Behav*. 2007;90(2-3):196-208.
- Cologan V, et al. Sleep in disorders of consciousness. *Sleep Med Rev*. 2010;14(2):97-105.
- Czeisler CA, et al. Human sleep: its duration and organization depend on its circadian phase. *Science*. 1980;210(4475):1264-1267.
- Czeisler CA, et al. Stability, precision, and near-24-hour period of the human circadian pacemaker. *Science*. 1999;284(5423):2177-2181.
- Van Someren EJ. Circadian rhythms and sleep in human aging. *Chronobiol Int*. 2000;17(3):233-243.
- Dijk DJ, Lockley SW. Integration of human sleep-wake regulation and circadian rhythmicity. *J Appl Physiol* (1985). 2002;92(2):852-862. doi:10.1152/japplphysiol.00924.2001.
- Saper CB, et al. Hypothalamic regulation of sleep and circadian rhythms. *Nature*. 2005;437(7063):1257-1263.
- Hulihan JF Jr, et al. Electroencephalographic sleep patterns in post-anoxic stupor and coma. *Neurology*. 1994;44(4):758-760.
- Isono M, et al. Sleep cycle in patients in a state of permanent unconsciousness. *Brain Inj*. 2002;16(8):705-712. doi:10.1080/02699050210127303.
- Germain A, et al. Circadian rhythm disturbances in depression. *Hum Psychopharmacol*. 2008;23(7):571-585.
- Wulff K, et al. Sleep and circadian rhythm disruption in psychiatric and neurodegenerative disease. *Nat Rev Neurosci*. 2010;11(8):589-599.
- Videnovic A, et al. Circadian and sleep disorders in Parkinson's disease. *Exp Neurol*. 2013;243:45-56.
- Musiek ES, et al. Sleep, circadian rhythms, and the pathogenesis of Alzheimer disease. *Exp Mol Med*. 2015;47:e148.
- De Massari D, et al. Brain communication in the locked-in state. *Brain*. 2013;136(Pt 6):1989-2000.
- Soekadar SR, et al. Fragmentation of slow wave sleep after onset of complete locked-in state. *J Clin Sleep Med*. 2013;9(9):951-953.
- Riemann D, et al. Sleep and depression—results from psychobiological studies: an overview. *Biol Psychol*. 2001;57(1-3):67-103.
- Chiò A, et al.; Eurals Consortium. Prognostic factors in ALS: a critical review. *Amyotroph Lateral Scler*. 2009;10(5-6):310-323.
- Raymond J, et al. Clinical characteristics of a large cohort of US participants enrolled in the National Amyotrophic Lateral Sclerosis (ALS) Registry, 2010-2015. *Amyotroph Lateral Scler Frontotemporal Degener*. 2019;20(5-6):413-420. doi:10.1080/21678421.2019.1612435.
- Rechtschaffen A, Kales A. *A manual of standardized terminology, techniques and scoring system for sleep stages of human subjects*. Los Angeles, CA: Brain Information Service/Brain Research Institute, UCLA; 1968.
- Mai R, et al. Quantitative electroencephalography in amyotrophic lateral sclerosis. *Electroencephalogr Clin Neurophysiol*. 1998;106(4):383-386.
- Hohmann MR, et al. Case series: slowing alpha rhythm in late-stage ALS patients. *Clin Neurophysiol*. 2018;129(2):406-408.
- Jacome DE, et al. Unreactive EEG: pattern in locked-in syndrome. *Clin Electroencephalogr*. 1990;21(1):31-36.
- Bragatti JA, et al. Alpha coma and locked-in syndrome. *J Clin Neurophysiol*. 2007;24(3):308. doi:10.1097/WNP.0b013e31803bb72c.
- Pavlov YG, et al. Night sleep in patients with vegetative state. *J Sleep Res*. 2017;26(5):629-640.
- Gais S, et al. Sleep after learning aids memory recall. *Learn Mem*. 2006;13(3):259-262.

B

Manuscripts ready for submission

In this appendix is reported the manuscript ready for submission.

1
2
3
4
5
6
7
8
9
10
11
12
13
14
15
16
17
18
19
20
21
22
23
24
25

A General-Purpose Framework for a Hybrid EEG-NIRS-BCI

Majid Khalili-Ardali^{1,*}, Jayro Martínez-Cerveró¹, Alessandro Tonin^{1,2}, Andres Jaramillo-Gonzalez¹, Shizhe Wu¹, Giovanni Zanella³, Giulia Corniani^{1,3}, Alberto Montoya-Soderberg¹,
Niels Birbaumer¹, Ujwal Chaudhary^{1,2,*}

¹Institute of Medical Psychology and Behavioral Neurobiology, University of Tübingen, Tübingen, Germany

²Wyss Center for Bio and Neuroengineering, Geneva, Switzerland

³Department of Information Engineering, University of Padua, Padua, Italy

Correspondence to:

Dr. Ujwal Chaudhary,

Wyss-Center for Bio- and Neuro-Engineering, Chemin de Mines 9, CH 1202, Geneva

Or,

Institute of Medical Psychology and Behavioral Neurobiology, University of Tübingen, Germany

Email: chaudharyujwal@gmail.com

Majid Khalili-Ardali,

Institute of Medical Psychology and Behavioral Neurobiology, University of Tübingen, Germany

Email: majidkhalili89@aim.com

26 **Current code version**

27

Nr	Code metadata description	Please fill in this column
C1	Current Code version	V 1.5.5
C2	Permanent link to code / repository used of this code version	https://github.com/majidkhalili/HybridBCI
C3	Legal Code License	MIT license (MIT)
C4	Code Versioning system used	Git on Github.
C5	Software Code Language used	Matlab
C6	Compilation requirements, Operating environments & dependencies	Matlab R2018a, PsychoToolbox , DSP System Toolbox (Only for EEG), TextAnalytics Toolbox (Only for speller)
C7	If available Link to developer documentation / manual	https://github.com/majidkhalili/HybridBCI
C8	Support email for questions	Majidkhalili89@aim.com

28 **Abstract**

29 Brain-computer interfaces (BCI), use brain signals to generate a control signal to control external
30 devices to assist paralyzed people in movement and communication. Electroencephalography
31 (EEG) and functional near-infrared spectroscopy (fNIRS) are the two most widely non-invasive
32 brain recording techniques to develop BCIs. This article describes a software tool called
33 “HybridBCI with an open-source framework for NIRS and EEG for a Hybrid BCI” application.
34 This HybridBCI has been successfully used to enable brain communication in patients without any
35 means of voluntary communication and has been recently reported by the authors. This software
36 tool is Matlab based, using modular object-oriented programming principles, and experimenters
37 can use it with different platforms and hardware to perform their BCI experiments and integrate
38 their custom modules according to their needs.

39 **Keywords**

40 Brain-computer interface (BCI), EEG, fNIRS, HybridBCI, Locked-in syndrome (LIS),
41 Completely locked-in syndrome (CLIS)

42 **Introduction**

43 Several research labs have developed versions of BCIs to enable communication with the ALS-
44 patients and other patients with paralysis with heterogeneous results[1–6]. Recently Tonin et al.
45 reported the successful use of an eye-movement based BCI for communication with four patients
46 with amyotrophic lateral sclerosis (ALS) in the transition from locked-in state (LIS) to completely
47 locked-in state (CLIS) [7] and the data set was published by Jaramilo-Gonzalez et. al. [8]. Despite
48 the residual oculomotor activity, these patients could not use assistive and augmentative
49 communication devices for communication. An electrooculogram (EOG) based communication
50 system was developed using which the patients employed their remnant eye-movement activity to
51 spell freely and communicate expressing their desires. The study was performed using a software
52 tool, designed by the authors for the BCI application, called HybridBCI. HybridBCI is the result
53 of extensive development of BCI application for communication purposes in LIS and CLIS
54 patients using electroencephalography (EEG), and functional near-infrared spectroscopy (fNIRS)
55 signals [7–9]. With this report, we provide the source code for HybridBCI, which can be used for
56 human-computer interface (HCI) applications in patients, including but not limited to LIS and
57 CLIS.

58 HybridBCI is not just a programming toolbox but also consists of an experimental paradigm
59 allowing the user to implement any type of BCI using EEG, electrooculography (EOG),
60 electromyography (EMG), or fNIRS. HybridBCI benefits from a modular pattern; therefore, if the
61 user wants to implement a particular algorithm, s/he can add only that particular segment without
62 the need to know how the whole system works. HybridBCI is implemented in Matlab [10] widely
63 used by neuroscientists, and due to the interpreting nature of the Matlab, once a new functionality
64 is added, there is no need to recompile the code. Besides, in clinical applications, data organization
65 and experiment logging is crucial, and HybridBCI manages the file organization and properly logs
66 recording sessions. Although several platforms have already been proposed for BCI applications
67 [1,3,4], we are introducing HybridBCI because the primary goal of the HybridBCI is to be used in
68 ALS-CLIS patients with the possibility to be used in other disorders of consciousness. In ALS-
69 CLIS patients, the vision is impaired [7] and visual paradigms cannot be used. Therefore, the
70 experimental paradigm used in HybridBCI is completely auditory based and does not require intact
71 visual perception. In these patients, the EEG is significantly altered, and common EEG biomarkers
72 are missing in some patients [11,12], and even in patients with the same syndrome, a unique pattern

73 cannot be found within a patient over time in different stages of the disease [13]. Therefore, the
74 analysis pipeline should be applicable and modified for each patient individually, and HybridBCI
75 gives us this flexibility in the analysis pipeline, as described below.

76 This paper proposes an experimental paradigm with an open-source framework of a BCI with a
77 clear and straightforward pipeline from data acquisition to signal analysis and classification with
78 a separate implementation of each part. New features at any step of the pipeline can be added to
79 the software by placing newly implemented .m files in the correct folders.

80 **Paradigm**

81 In the HybridBCI, regardless of the cognitive task used (e.g., mental calculation, the imagination
82 of hand/foot movement, covert thinking, etc.), a list of questions/sentences with answers known
83 by the experimenters is presented auditorily to the BCI user, and the user is asked to perform two
84 different tasks i.e., responding mentally “yes” or” no” (i.e., true/false or 1/0). The auditory channel
85 is used because many severely ill chronic patients suffer from impaired vision. HybridBCI uses
86 Psychotolbox [14] in presenting auditory stimuli to minimize the software delay. Questions are
87 repeated to the user with an equal, but random distribution of questions with Yes and No answer
88 (i.e. Your name is Majid. Your name is Ujwal) in an experimental block, and blocks are repeated
89 to acquire enough data for classification. The initial experimental blocks are called training blocks
90 since the user is familiarizing with the paradigm, and the data is collected to train a classifier. Once
91 enough trials are acquired, a classifier is trained to classify yes and no answers. If the classification
92 accuracy reaches above chance level, a feedback block is performed in which the user receives
93 feedback on what has been classified, which also serves as a reward. If the feedback accuracy in a
94 feedback block is also higher than chance, the model can be used for other applications with
95 unknown answers. The chance can be calculated as proposed by Müller-Putz et al.[15] based on
96 the number of trials in each block. The proposed block diagram paradigm is depicted in Figure 1.
97 The number of blocks is dependent on the selected task, the number of trials in each block, and the
98 users' condition. The rule of thumb would be to have twenty trials per block in four training blocks
99 and one feedback block, which approximately takes one hour.

100 **Implementation**

101 HybridBCI is implemented in Matlab based on object-oriented programming (OOP) principles,
102 and new features can be added by placing the user implemented .m file in the correct path to
103 guarantee the scalability [5] of the system. As depicted in Figure 2, the core structure of HybridBCI
104 is based on the two main modules named “HybridBCI.mlapp” and “ModelBuilder.mlapp”, which
105 do not need to be modified by users and are implemented using the Matlab App Designer[16].

106 **1) Hybrid BCI**

107 This module runs and controls the running experiment’s sequence, controls data acquisition
108 functions, handles the triggering, runs “ModelBuilder” and log the experimental report.
109 HybridBCI has three tabs, 'Configuration', 'Experiments', and 'Applications', which are used in an
110 experiment, respectively. In the first tab, the brain signal measuring techniques and their
111 corresponding recording handlers are selected, and the timing of the experiment is set (Figure 3A).
112 These pieces of information and other experimental information, such as the name of
113 experimenters, date and time of the experiment, and auditory stimuli list, are saved for each
114 experimental block in a single .mat file.

115 *a. Trigger*

116 The HybridBCI system's functioning relies on precise labeling and saving the paradigm's events
117 synchronized with the raw data recording. The correct timing is delivered by the HybridBCI
118 module to the acquisition devices through a set of symbols, named triggers. The proper sequence
119 of triggering values for blocks and trials is presented in Table 1. Any triggering device is an
120 instance of a class derived from ‘Device.m’ and needs to implement its’ abstract functions. With
121 this code, implementation of hardware triggering over the LPT port and the software triggering
122 through a TCP/IP protocol for Brain Products GmbH (Germany) for EEG recording and file-based
123 triggering for NIRx Medical Technologies (USA) for NIRS recording are implemented.
124 HybridBCI is designed not to have any cumulative error between blocks and trials.

125 *b. Data acquisition*

126 HybridBCI can run and handles two recording devices simultaneously as needed for NIRS and
127 EEG data acquisition, and it sends triggers to both of them at the same time. For each recording
128 device, a new instance of Matlab is loaded by clicking on the corresponding ‘RUN’ button in the
129 Experiment tab of the HybridBCI module (Figure 3B). New recording devices can be added by

130 placing their .mlapp file in the “..\lib\Devices\EEGINIRSDevices\”. With this code, data
131 acquisition and/or triggering for BrainVision, StarStim, and NIRx are also implemented and can
132 be provided upon a request.

133 *c. File Management*

134 For each day of recording, a new folder is created in ‘..\Subjects\XX\’, in which the XX denotes
135 the date of recording (e.g. ‘22-Nov-2019’), and for each block, a configuration file is saved in it,
136 containing parameters of the performed experiment. Subjects’ audio files are stored with .wav
137 extension in ‘..\Subjects\XX\Audios\Questions\’, which is very helpful in experiments with
138 (C) LIS patients, in which audios needed to be recorded by the individuals’ family members. Audio
139 question files with yes answers are labeled as ‘001_FileName.wav’ while questions with no answer
140 are labeled as ‘002_FileName.wav’. The files are optional but are recommended to be named with
141 valid identifiers since they will be stored in each block’s configuration file. A sample of 20 audio
142 files with yes and no answers are provided with this code.

143 *d. Applications*

144 Once a classification accuracy above the chance level is achieved, the same model can be used to
145 run different applications in which the intention of the user is not priory known for experimenters.
146 HybridBCI can automatically run and control the state transitions for any application that derives
147 from ‘Paradigm.m’. ‘Paradigm.m’ is a class with abstract methods that are needed for their
148 functionality in HybridBCI. Once a new paradigm class is defined, it can be accessed and run from
149 the ‘Application’ tab in the ‘HybridBCI’ module (Figure 3C). With this code, two primary
150 examples of such applications are provided, including OpenQuestion, in which the user can answer
151 the questions that the answers are unknown to the experimenters, and Speller in which the user
152 can freely spell what she/he has in mind [7].

153 **2) Model Builder**

154 “ModelBuilder” handles the analysis processing pipeline for NIRS and EEG in six steps (Figure
155 4) and stores it in a .mat file in the ‘Models’ folder for each subject to be used for giving feedback,
156 running applications, or to perform offline analysis. Each analysis step has a dedicated tab in the
157 GUI and is described below.

158 *a. Data Selection*

159 This tab enables users to select data and reject noisy channels before performing any analysis,
160 which may arise due to displaced EEG electrodes or noisy NIRS channels, or other recording
161 issues (Figure 5A).

162 *b. EEG Preprocessing*

163 EEG preprocessing fulfills the purpose of cleaning the recorded signal from noise and artifacts
164 (such as eye blinking or movement) and performing transformations or reorganizations of the
165 recorded data or any other condition necessary for further analysis [1–3]. Following what is
166 suggested by the quoted references, for a basic EEG pipeline, we include preprocessing
167 functions commonly used in EEG preprocessing, that is, selection of the frequency bands and
168 filtering, simple linear transformations (normalization and baseline correction) and re-
169 referencing operations (common-average reference) (Figure 5).

170 It is important to note that the application of preprocessing steps depends on several aspects,
171 as the study’s goal, the experimental design, the physiological phenomena being investigated
172 and the searched features in the signal, or other custom analysis necessary for the experiment.
173 Therefore, there is no standard sequence of steps for preprocessing the EEG since each
174 preprocessing sequence is tailored depending on the aforementioned variables [3,4]. For
175 example, a survey for optimizing the work with event-related potentials (ERP) in the frame of
176 BCI [5], concludes that the best-practice guidelines for preprocessing are 1) use as many EEG
177 electrodes as is practical to record, avoiding the use of sub-montages or sub-sets of electrodes,
178 2) spectral filter to remove obvious noise components, with a close to the optimal passband of
179 0.5-12 Hz, 3) apply spatial filtering for “whitening” [6], for a final stage with a classification
180 method. Naturally, for different experimental designs, the guidelines change as verified in
181 other developed platforms (e.g., [7–10]).

182 With this requirement in mind, the preprocessing pipeline of this software allows us to select the
183 order in which the preprocessing functions are applied and include other additional functions
184 necessary for a custom EEG preprocessing (e.g., spatial filtering, re-referencing, temporal
185 windowing). Thus, the particular preprocessing pipeline of this software consist – as it can be
186 configured in the EEG Preprocessing tab of the ModelBuilder (Figure 5B) – of the following steps:

187

I. Filtering

188 Previous to the filtering, two sets of options are provided for the user: First, *Source Selection*, in
189 which the user can select the types of signals to be considered in the analysis, either EEG, EOG,
190 or EMG channels. Second, *Bands Selections*, in which a group of traditional ranges of oscillations
191 commonly used in EEG analysis [27], Wideband (0.5-30 Hz), Delta (1-4 Hz), Theta (4-7 Hz),
192 Alpha (7-13 Hz) and Beta (13-30Hz), are offered to the user, with the possibility of using the
193 default given ranges, or manually introducing modifications to each range. Then we apply a
194 second-order Infinite Impulse Response (IIR) notch filter at 50 Hz, and after that, we included two
195 options for filtering: Finite impulse response (FIR) filter and Butterworth IIR filter design. Both
196 filters are applied so that the phase of the signal is not affected by [28]. We propose these two
197 types of filters to allow the user to consider each according to her/his needs and their particular
198 benefits or drawbacks applied to EEG signals [29].

199

II. Processing Functions

200 With this code, three of the most common amplitude correction methods are provided. First,
201 Normalization [30], by applying the z-score to the epoch (that is, subtraction of mean of each
202 window and division by the standard deviation [31]). Second, Baseline Correction, which in our
203 case is the simple subtraction of a pre-stimulus value (a predefined baseline) from the epoch, under
204 the assumption that any physiological effect recorded post-stimulus can be highlighted if compared
205 with a pre-stimulus "base" [32]. For this, it must be considered that the definition of a baseline
206 period varies depending on the physiological and analytical nature of the study [33]. Finally, the
207 Common Average Reference (CAR), to approach the recordings to an "inactive reference" – if all
208 the channels were recorded respective to the same physical reference – by subtracting to each
209 amplitude value the average of the amplitude values of all the channels at the same instant [33].
210 The user can choose the order in which they will be applied from the list of all available functions.
211 User implemented EEG processing functions can be added to the pipeline by placing the .m file in
212 in `.\lib\EEG\Preprocessing\`.

213

c. EEG Feature Extraction

214 With this code, an initial set of features used in the analysis of EEG in the field of BCI in the time
215 and frequency domain are included [34], including a series of range features for EEG time-series
216 (Figure 5C). Details on the implemented EEG features can be found on supplementary data. User

217 implemented EEG feature can be added to the pipeline by placing the .m file in
218 ‘.\Lib\EEG\Features’.

219 *d. NIRS Preprocessing*

220 HybridBCI develops the pipeline for the NIRS pre-processing in two steps: first wavelength
221 conversion, second filtering. In the first step, a basic default function is developed to convert the
222 wavelength signal to hemodynamic concentration using the Modified Beer-Lambert Law (MBLL)
223 [35], while in the second group, the systemic components can be filtered using a bandpass filter
224 function [36].

225 The NIRS signal is acquired as a pair of wavelengths belonging to the near-infrared spectral range
226 between 650 nm to 950 nm [37]. To get a physiological signal, the most commonly used technique
227 is the MBLL [35] to convert the wavelength to optical density and the hemodynamic
228 concentrations: oxyhemoglobin (HbO), deoxyhemoglobin (HbR), and total hemoglobin
229 concentration (HbT) [38]. In the MBLL, two terms of the equation are the molar extinction
230 coefficient and the differential path length factor that accounts for the real distance the light travels
231 due to the scattering [35]; these two terms depend on many factors (e.g., age and gender of the
232 subject), and their values can be found on the literature [36,39]. The observed hemodynamic signal
233 is the result of the sum of neuronal and systemic components, thus to analyze functional changes,
234 many techniques have been developed to separate the different components and remove external
235 noise (see [40] for an extensive review). With this code, an implementation to convert wavelength
236 data to hemodynamic response is provided, and proper filters are designed to filter hemodynamic
237 responses (Figure 5B). User implemented functionalities can be added to the processing pipeline
238 by placing the .m file in ‘.\Lib\NIRS\PreProcessing’.

239 *e. NIRS features*

240 Once the HbO, HbR, and HbT are pre-processed, it is possible to extract features to describe the
241 signal using only the data's relevant characteristics. The developed functions extract the features
242 for each of the three hemodynamic signals working on a single channel level, i.e., without
243 averaging or grouping different channels or different signal types. With this code, preliminary
244 features mostly used for NIRS signals are provided and listed in supplementary data. Any new
245 feature can be added to the pipeline by placing a related m file in ‘.\Lib\NIRS\Features’.

246 *f. Dimensionality*

247 Once the pre-processing and feature extraction steps are concluded, the dataset's size in the feature
248 space increases significantly. At this point, we incorporated two steps to reduce the dataset size
249 keeping only those features that have a more significant influence on the final result (Figure 5D).

250 *I. Features consistency*

251 This step is used to test the homogeneity of the features' distribution across the different trials used
252 to train the classifier and results in a training sample with equal or fewer features than initially.
253 This process keeps only those features that are consistent over time and discards the rest. It also
254 reduces the calculations in future stages. For details, see [41–43].

255 *II. Dimension reduction*

256 This step is used to reduce the training data's dimensionality by selecting an ordered set of the most
257 relevant features for classification [44–47]. Given a training sample with m features and a
258 percentage K specified by the user, a variable selection method is implemented, resulting in a
259 training sample with a number k percent of features. The implemented function is a variation on
260 the popular minimum redundancy maximum relevance (mRMR) method, originally created by
261 *Ding and Peng* [44] and *Peng et al.* [45] but using another association measure instead of “mutual
262 information”, as proposed by *Berrendero et al.* [46]. Their approach, which appears to work better
263 on small samples [46] and is thus relevant for BCI applications, consists of using squared “distance
264 correlation”, which measures dependency between variables and was introduced by *Székely et al.*
265 [47].

266 *g. Classification*

267 HybridBCI can use any classifier that is derived from the abstract class ‘Classifier.m’ in
268 ‘..\Lib\Classifiers\’. Classes inheriting from this class need to implement two abstract functions,
269 including training the model with given features as input and predicting a single trial using the
270 same model. With this code, two well-known classification algorithms are provided: Support
271 Vector Machines (SVM's) and k-Nearest Neighbours (k-NN) [48,49] (Figure 5E). For a review of
272 classification methods for EEG based BCI, see [50], and for hybrid EEG and NIRS see, [51].

273 *h. Validation*

274 One of the known issues in machine learning is the problem of overfitting the data, and it refers to
275 the problem that due to the incorrect tuning of the classifier, the model overfits the features space.
276 Therefore, it is necessary to check the classifier's performance on the data other than the data that
277 has been used for training (simulating the online feedback in the BCI experiment). For this reason,
278 the Validation tab in the 'ModelBuilder' is provided to check the performance of each model on
279 other datasets (Figure 5F).

280 **Discussion and conclusion**

281 During several years of research and development in the field of BCI for communication in DoC
282 patients, several versions of this software have been used to perform studies. This version of
283 HybridBCI is the outcome of this process in our lab. A version of HybridBCI was used to enable
284 communication with ALS patients on the verge from LIS to CLIS when all other communication
285 means failed and reported a yes-no communication of more than chance level, and the possibility
286 for free spelling. Details for analysis pipeline and classification results can be found in Tonin et
287 al. (2020) [7]. The code is provided in the Matlab that most of the scientists in cognitive science
288 are already familiar with and easy to develop. HybridBCI has an OOP software design, and due to
289 the interpreting nature of the Matlab programming language, as opposed to compiling based
290 programming languages, new features and functionalities can be added to the system by placing
291 new .m files in the proper path without the need to know the whole system or recompiling the
292 project. The current version of the developed software enables simultaneous interfacing and data
293 acquisition from Brain Products' EEG and NIRX's NIRS device. The software provides a user-
294 friendly interface to enable experimenters to select an appropriate EEG and NIRS data processing
295 pipeline. The experimenters can select the corresponding feature extraction method and machine
296 learning algorithm to classify the brain states. This software only has the functionality to select
297 features from EEG and NIRS signal separately, i.e., it does not have the functionality for hybrid
298 EEG and NIRS feature selection. However, an experimenter can easily implement their desired
299 hybrid feature selection method and integrate it with the HybridBCI software. An experimenter
300 can also implement his/her machine-learning algorithm as per need beyond what has been provided
301 in the current version of the software and integrate it with the HybridBCI, thereby further

302 expanding the HybridBCI software's functionality. Thus, the modular design of the software
303 enables experimenters to further expand on what has been provided in the software.

304 The HybridBCI software, through its six years of the developmental process, has been used to
305 enable communication with patients in LIS, in the transition from LIS to CLIS, and finally in CLIS.
306 During its development process, we encountered several challenges, such as lack of vigilance
307 markers in patients in CLIS, lack of clear sleep- cycle markers in CLIS, patients' cognitive status,
308 and patient's engagement in the experiment. We performed extensive studies to elucidate a sleep-
309 cycle marker in CLIS [11], resting-state state EEG in LIS and CLIS[12–14], performed a
310 preliminary study on the cognitive state of patients in CLIS [14,15] and attempted transcranial
311 direct current stimulation (tDCS) technique to target the vigilance network in CLIS. We found
312 that spontaneous brain activity in ALS-CLIS patients is significantly altered. Thus, commonly
313 used indexes of arousal state in healthy people do not necessarily serve the same purpose in these
314 patients' populations, and newly defined indexes should be introduced and validated. As we
315 continue further with our study with patients in LIS, in the transition from LIS to CLIS and finally
316 in CLIS, we aim to implement modules in the software to detect the vigilance and sleep stage of
317 the patient automatically so that the BCI communication sessions will be performed only if the
318 patient is vigilant and not sleeping. Thus, the present HybridBCI software is the first step towards
319 developing a tool to solve the challenge of enabling communication in patients who have none.

320 **Acknowledgments**

321 Deutsche Forschungsgemeinschaft (DFG), Kosellek and DFG BI 195/77-1, BMBF (German
322 Ministry of Education and Research) 16SV7701 CoMiCon, and LUMINOUS-H2020-FETOPEN-
323 2014-2015-RIA (686764).

324 **Author contributions**

325 MKH designed the software, implemented the core structure, and wrote the first draft of the paper.
326 JMC improved the core structure and combined different software modules. AT implemented
327 NIRS pipeline, presenting paradigm and classification methods, implemented speller, and wrote
328 the NIRS section. AJG implemented the EEG pipeline and wrote the EEG section. SW improved
329 EEG pipeline and test and debug the system. GZ test and reported the triggering, and improved
330 NIRS pipeline. GC implemented range features. AMS implemented and reported feature

331 consistency and dimension reduction. NB designed the paradigm and provided resources. UC
332 initiated the HybridBCI software, conceptualized, implemented initial paradigms and signal
333 processing pipeline, supervised, acquired fundings and manuscript writing.

334 **Competing interests**

335 The author(s) declare no competing interests.

336 **Code availability**

337 Source code and sample data are available at <https://github.com/majidkhalili/HybridBCI>.

338 **Ethical Approval**

339 The Internal Review Board of the Medical Faculty of the University of Tübingen approved the
340 experiment reported in this study. The study was performed per the guideline established by the
341 Medical Faculty of the University of Tübingen. The patient or the patients' legal representative
342 gave informed consent with permission to publish the data. The clinical trial registration number
343 is: ClinicalTrials.gov - Identifier: NCT02980380.

344 **References**

- 345 [1] G. Schalk, D.J. McFarland, T. Hinterberger, N. Birbaumer, J.R. Wolpaw, *IEEE Trans.*
346 *Biomed. Eng.* 51 (2004) 1034–1043.
- 347 [2] A. Schlögl, C. Brunner, *Computer* (Long. Beach. Calif.) 41 (2008) 44–50.
- 348 [3] Y. Renard, F. Lotte, G. Gibert, M. Congedo, E. Maby, V. Delannoy, O. Bertrand, A.
349 Lécuyer, *Presence Teleoperators Virtual Environ.* 19 (2010) 35–53.
- 350 [4] V. Bastian, B. Benjamin, *Front. Hum. Neurosci.* 9 (2015).
- 351 [5] M.H. Lee, S. Fazli, K.T. Kim, S.W. Lee, in: 4th Int. Winter Conf. Brain-Computer
352 Interface, BCI 2016, Institute of Electrical and Electronics Engineers Inc., 2016.
- 353 [6] M. Chiesi, M. Guermandi, S. Placati, E.F. Scarselli, R. Guerrieri, *IEEE Trans. Biomed.*
354 *Eng.* 66 (2019) 900–909.
- 355 [7] A. Tonin, Jaramillo-Gonzalez A., A. Rana, M. Khalili-Ardali, A. Birbaumer, U.
356 Chaudhary, *Sci. Rep. Manuscript* (2020).
- 357 [8] A. Jaramillo-Gonzalez, A. Tonin, A. Rana, M. Khalili-Ardali, A. Birbaumer, U.
358 Chaudhary, *Sci. Data* [Submitted] (2020).
- 359 [9] U. Chaudhary, B. Xia, S. Silvoni, L.G. Cohen, N. Birbaumer, *PLOS Biol.* [Retracted] 15
360 (2017) e1002593.
- 361 [10] MATLAB, (2018).
- 362 [11] Y. Maruyama, N. Yoshimura, A. Rana, A. Malekshahi, A. Tonin, A. Jaramillo-Gonzalez,
363 N. Birbaumer, U. Chaudhary, *Neurosci. Res.* (2020).
- 364 [12] M.R. Hohmann, T. Fomina, V. Jayaram, T. Emde, J. Just, M. Synofzik, B. Schölkopf, L.
365 Schöls, M. Grosse-Wentrup, *Clin. Neurophysiol.* 129 (2018) 406–408.
- 366 [13] A. Secco, A. Tonin, A. Rana, A. Jaramillo-Gonzalez, M. Khalili-Ardali, N. Birbaumer, U.
367 Chaudhary, *Cogn Neurodyn* (2020). <https://doi.org/10.1007/s11571-020-09639-w>
- 368 [14] M. Kleiner, D.H. Brainard, D. Pelli, A. Ingling, R. Murray, C. Broussard, *Perception* 36
369 (2007) 1–16.

- 370 [15] G.R. Müller-Putz, R. Scherer, C. Brunner, R. Leeb, G. Pfurtscheller, *Int. J.*
371 *Bioelectromagn.* 10 (2008) 52–55.
- 372 [16] The MathWorks Inc, (2019).
- 373 [17] G. Dornhege, J. del R. Millán, T. Hinterberger, D.J. McFarland, K.-R. Müller, in: *Towar.*
374 *Brain-Computer Interfacing*, MITP, 2007, pp. 207–233.
- 375 [18] Y. Li, K.K. Ang, C. Guan, in: B. Graimann, B. Allison, G. Pfurtscheller (Eds.), *Springer-*
376 *Verlag Berlin Heidelberg*, 2010, pp. 305–330.
- 377 [19] W. Peng, in: *EEG Signal Process. Featur. Extr.*, Springer Singapore, 2019, pp. 71–87.
- 378 [20] S.J. (Steven J. Luck, *An Introduction to the Event-Related Potential Technique*, n.d.
- 379 [21] J. Farquhar, N.J. Hill, *Neuroinformatics* 11 (2013) 175–192.
- 380 [22] M. Asuncion Vicente, P.O. Hoyer, A. Hyvarinen, *IEEE Trans. Pattern Anal. Mach. Intell.*
381 29 (2007) 896–900.
- 382 [23] C. Vidaurre, T.H. Sander, A. Schlögl, *Comput. Intell. Neurosci.* 2011 (2011) 935364.
- 383 [24] G. Schalk, in: *Proc. 31st Annu. Int. Conf. IEEE Eng. Med. Biol. Soc. Eng. Futur. Biomed.*
384 *EMBC 2009*, IEEE Computer Society, 2009, pp. 5498–5501.
- 385 [25] C.A. Kothe, S. Makeig, *J. Neural Eng.* 10 (2013) 056014.
- 386 [26] B. Blankertz, K.R. Müller, D.J. Krusienski, G. Schalk, J.R. Wolpaw, A. Schlögl, G.
387 Pfurtscheller, J.D.R. Millán, M. Schröder, N. Birbaumer, in: *IEEE Trans. Neural Syst.*
388 *Rehabil. Eng.*, 2006, pp. 153–159.
- 389 [27] E. Niedermeyer, F.H.L. da Silva, 1 (2005) 17–31.
- 390 [28] F. Gustafsson, *IEEE Trans. Signal Process.* 44 (1996) 988–992.
- 391 [29] A. Widmann, E. Schröger, *Front. Psychol.* 3 (2012) 233.
- 392 [30] EEGLAB, (2012).
- 393 [31] Matlab, (n.d.).

- 394 [32] T.P. Urbach, M. Kutas, *Biol. Psychol.* 72 (2006) 333–343.
- 395 [33] M.X. Cohen, *Analyzing Neural Time Series Data: Theory and Practice*, 2014.
- 396 [34] K.S. Hong, M.J. Khan, M.J. Hong, *Front. Hum. Neurosci.* 12 (2018) 246.
- 397 [35] D.T. Delpy, M. Cope, P. van der Zee, S. Arridge, S. Wray, J. Wyatt, *Phys. Med. Biol.* 33
398 (1988) 1433–1442.
- 399 [36] M.A. Franceschini, S. Fantini, J.H. Thompson, J.P. Culver, D.A. Boas, *Psychophysiology*
400 40 (2003) 548–560.
- 401 [37] W.G. (Willem G. Zijlstra, A. Buursma, O.W. van. Assendelft, *Visible and near Infrared*
402 *Absorption Spectra of Human and Animal Haemoglobin : Determination and Application,*
403 *VSP, 2000.*
- 404 [38] U. Chaudhary, M. Hall, J. DeCerce, G. Rey, A. Godavarty, *Brain Res. Bull.* 84 (2011)
405 197–205.
- 406 [39] S.J. Matcher, C.E. Elwell, C.E. Cooper, M. Cope, D.T. Delpy, *Anal. Biochem.* 227 (1995)
407 54–68.
- 408 [40] F. Scholkman, S. Kleiser, A.J. Metz, R. Zimmermann, J. Mata Pavia, U. Wolf, M. Wolf,
409 *Neuroimage* 85 (2014) 6–27.
- 410 [41] J.L. Devore, K.N. Berk, *Goodness-of-Fit Tests and Categorical Data Analysis.* In: *Modern*
411 *Mathematical Statistics with Applications,* Springer, New Yorkm Ny, 2012.
- 412 [42] Y. Benjamini, Y. Hochberg, *J. R. Stat. Soc. Ser. B* 57 (1995) 289–300.
- 413 [43] K. Pearson, London, Edinburgh, Dublin *Philos. Mag. J. Sci.* 50 (1900) 157–175.
- 414 [44] C. Ding, H. Peng, *J. Bioinform. Comput. Biol.* 3 (2005) 185–205.
- 415 [45] H. Peng, F. Long, C. Ding, *IEEE Trans. Pattern Anal. Mach. Intell.* 27 (2005) 1226–1238.
- 416 [46] J.R. Berrendero, A. Cuevas, J.L. Torrecilla, *J. Stat. Comput. Simul.* 86 (2016) 891–907.
- 417 [47] G.J. Székely, M.L. Rizzo, N.K. Bakirov, *Ann. Stat.* 35 (2007) 2769–2794.
- 418 [48] V. Vapnik, S.E. Golowich, *Support Vector Method for Function Approximation,*

- 419 Regression Estimation, and Signal Processing, 1997.
- 420 [49] B.E. Boser, I.M. Guyon, V.N. Vapnik, in: Proc. Fifth Annu. ACM Work. Comput. Learn.
421 Theory, Publ by ACM, New York, New York, USA, 1992, pp. 144–152.
- 422 [50] F. Lotte, M. Congedo, A. Lécuyer, F. Lamarche, B. Arnaldi, *J. Neural Eng.* 4 (2007).
- 423 [51] K.S. Hong, M.J. Khan, *Front. Neurorobot.* 11 (2017) 35.
- 424 [52] A. Malekshahi, U. Chaudhary, A. Jaramillo-Gonzalez, A. Lucas Luna, A. Rana, A. Tonin,
425 N. Birbaumer, S. Gais, *Sleep* 42 (2019).
- 426 [53] M. Khalili-Ardali, S. Wu, A. Tonin, N. Birbaumer, U. Chaudhary, *Clin. Neurophysiol.*
427 (2020).
- 428 [54] M. Khalili Ardali, A. Rana, M. Purmohammad, N. Birbaumer, U. Chaudhary, *Brain Lang.*
429 194 (2019) 93–97.
- 430

431 **List of Tables**

432 **Table 1:** The table represents the 14 different triggers used by the HybridBCI for managing the
 433 different events. These values are sent to the acquisition systems during the experiment and used
 434 to keep track of the timing of the different events.

435

Table1

Event	Trigger values		
	Yes Question	No Question	Open Question
Block Start	9		
Baseline	10	11	12
Question	5	6	7
Thinking	4	8	13
Feedback	1	2	3
Block End	15		

436 **List of Figures**

437 **Figure 1:** Block diagram for HybridBCI paradigm for training (yellow), feedback (blue), and any
438 application (green) blocks. If the offline or online classification accuracy of the built model is more
439 than the chance level in each block, the next block can be performed. The ultimate goal is for the
440 patient to use his/her brain signal to freely spell what s/he has in mind.

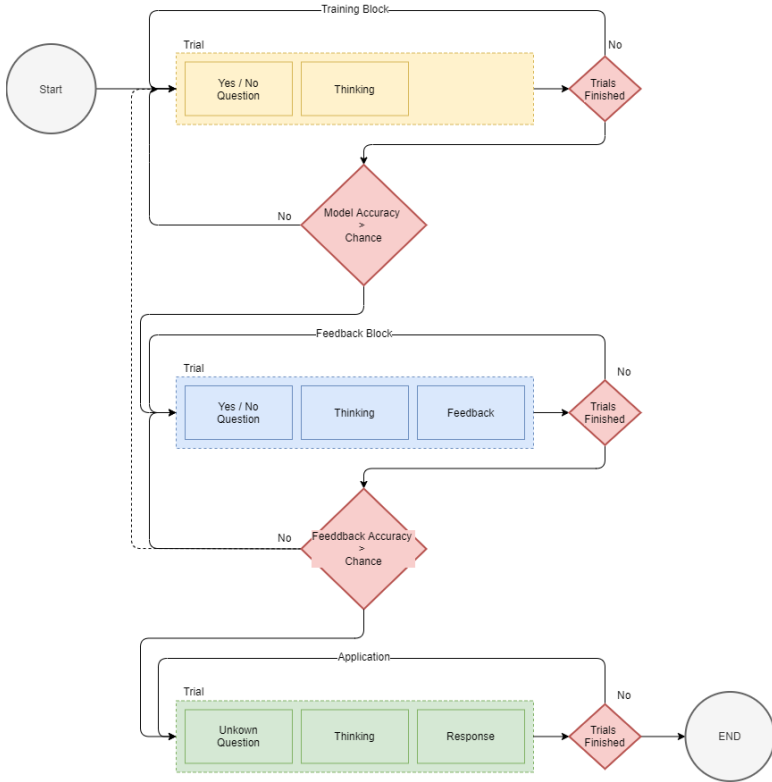
441 **Figure 2:** HybridBCI System Design and file organization. Two main software modules,
442 ModelBulder.mlapp and HybridBCI.mlapp (White boxes), and three Matlab instances (Matlab
443 Icons) control the experimental procedure and online data acquisitions. For each functionality of
444 the system, a folder is dedicated (Yello boxes) and the HybridBCI automatically recognizes new
445 .m files in these folders and extends its' functionality accordingly.

446 **Figure 3:** HybridBCI Module - A. Configuration tab for Selecting recording devices, setting the
447 timing of the experiment, selecting a list of experimenters, and controlling trigger devices. B.
448 Experiment tab for selecting patients, choosing a task, controlling the number of trials in each
449 block, running data acquisition Matlab instances, and running training and feedback blocks. C.
450 Application tab for selecting the desired application and the model to perform the task.

451 **Figure 4:** Six steps of the analysis pipeline used in ModelBuilder. Step 1 is for loading the data
452 and select/deselect channels. Step 2 is designed for the preprocessing of the NIRS and EEG signals
453 based. Step 3 is used to select the desired features to be extracted from NIRS and EEG. In step 4
454 before passing the features to classifiers in step 5, the dimension of the feature space is reduced.
455 Finally, in step 6 the acquired model is validated on the data that has not been used for training the
456 classifier.

457 **Figure 5:** ModelBuilder Module – A. Data tab for selecting data to be used for analysis and
458 rejecting noisy channels. B. Preprocessing pipeline for EEG (top) and NIRS (bottom). C. Selecting
459 features to be extracted from the signal. D. Dimensionality tab for reducing the size of the dataset
460 in features spaces. E. Classifier tab for choosing a classifier to build the model. F. Validation tab
461 for simulating online results and validating a model on previously recorded data.

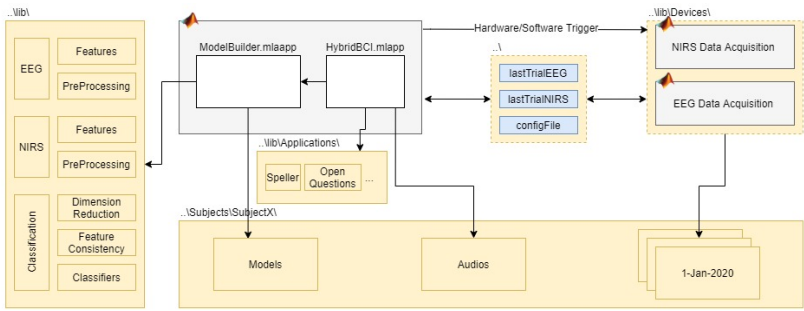
Figure 1



463

Figure 2

464



465

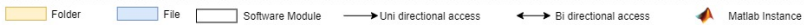


Figure 3

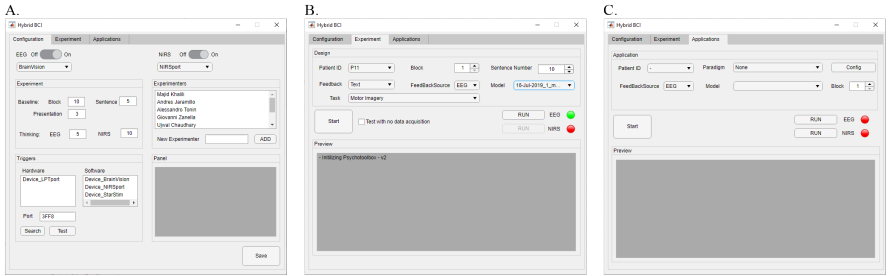


Figure 4

